UNIVERSITI TEKNOLOGI MARA

SYSTEMATIC STRUCTURAL EVALUATION OF CSM-STRENGTHENED MODULAR TIMBER BEAMS FOR PORTABLE FOREST BRIDGES

MOHD RIZUWAN BIN MAMAT

PhD

March 2026

UNIVERSITI TEKNOLOGI MARA

SYSTEMATIC STRUCTURAL EVALUATION OF CSM-STRENGTHENED MODULAR TIMBER BEAMS FOR PORTABLE FOREST BRIDGES

MOHD RIZUWAN BIN MAMAT

Thesis submitted in fulfilment
of the requirements for the degree of
Doctor of Philosophy
(Civil Engineering)

Faculty of Civil Engineering

March 2026

CONFIRMATION BY PANEL OF EXAMINERS

I certify that a Panel of Examiners has met on 28 November 2025 to conduct the final examination of Mohd. Rizuwan Bin Mamat on his Doctors of Philosophy thesis entitled "Systematic Structural Evaluation of CSM-Strengthened Modular Timber Beams for Portable Forest Bridges" in accordance with Universiti Teknologi MARA Act 1976 (Akta 173). The Panel of Examiners recommends that the student be awarded the relevant degree. The Panel of Examiners was as follows:

Jazuri Abdullah, PhD
Associate Professor
Faculty of Civil Engineering
Universiti Teknologi MARA
(Chairman)

Rohana Hassan, PhD
Professor
Faculty of Civil Engineering
Universiti Teknologi MARA
(Internal Examiner)

Abdul Rahman Mohd Sam, PhD
Associate Professor
Faculty of Civil Engineering
Universiti Teknologi Malaysia (UTM)
(External Examiner)

PROFESSOR DR HJH ZURAEDA IBRAHIM
Dean
Institute of Postgraduates Studies
Universiti Teknologi MARA

Date: 26 March 2026

AUTHOR'S DECLARATION

I declare that the work in this thesis was carried out in accordance with the regulations of Universiti Teknologi MARA. It is original and is the results of my own work, unless otherwise indicated or acknowledged as referenced work. This thesis has not been submitted to any other academic institution or non-academic institution for any degree or qualification.

I, hereby, acknowledge that I have been supplied with the Academic Rules and Regulations for Post Graduate, Universiti Teknologi MARA, regulating the conduct of my study and research.

Name of Student	:	Mohd Rizuwan Bin Mamat
Student ID. No.	:	2020999379
Programme	:	Doctor of Philosophy (Civil Engineering) – EC950
Faculty	:	Civil Engineering
Thesis Title	:	Systematic Structural Evaluation of CSM-Strengthened Modular Timber Beams for Portable Forest Bridges
Signature of Student	:	……..
Date	:	March 2026

ABSTRACT

Modular timber beam systems strengthened with chopped strand mat (CSM) present a sustainable alternative for portable forest bridge applications in remote environments, where conventional temporary log bridges frequently experience serviceability reduction due to environmental exposure and limited maintenance. While modular construction offers logistical and sustainability advantages, the introduction of beam segmentation and mechanical connections fundamentally alters structural continuity, significantly influencing stiffness response and dynamic behaviour. Despite increasing adoption of modular timber systems, the combined effects of segmentation and composite strengthening on static–dynamic stiffness characteristics and connection behaviour remain insufficiently quantified, particularly under integrated experimental and numerical evaluation frameworks. This study evaluated the static–dynamic stiffness behaviour of segmented modular timber beams strengthened with CSM, with emphasis on stiffness response, connection load transfer, and performance evolution across varying segmentation configurations. An integrated experimental–numerical approach was employed, comprising Experimental Modal Analysis (EMA) to determine dynamic characteristics, flexural bending tests to evaluate static stiffness, and finite element modelling using ANSYS to validate stress distribution and connection behaviour. Full-scale structural-grade timber beams with a 3.0 m span were tested in continuous and segmented configurations ranging from two to five segments, with and without CSM reinforcement applied to the tension flange. Standardised steel plate and bolt assemblies were used as mechanical connectors, while strain measurements quantified connection-level response under controlled loading conditions. The results demonstrate a strong inverse relationship between static flexural modulus of elasticity and EMA-derived dynamic modulus, attributed to mass augmentation and increased damping effects introduced by composite reinforcement. CSM strengthening improved stiffness retention and modified load transfer mechanisms at mechanical connections, with pronounced load concentration observed at central connectors relative to end connections. Among the investigated configurations, the three-segment system exhibited the most balanced performance, maintaining favourable stiffness response and stable dynamic characteristics, whereas segmentation beyond three segments resulted in pronounced stiffness reduction and increased stress concentration at connection interfaces. The findings confirm the applicability of EMA as a non-destructive evaluation tool for comparative assessment of modular timber systems and establish performance thresholds for segmentation in CSM-strengthened beams. The introduction of the Stiffness Reduction Index (SRI) and Segmentation Performance Index (SPI) provides a systematic framework for configuration-specific performance evaluation, indicating that segmentation should be limited to three segments per 3.0 m span with CSM reinforcement within the investigated scope of portable forest bridge applications.

ACKNOWLEDGEMENT

Firstly, I wish to thank God Almighty for granting me the strength, patience, and perseverance to embark on and complete this long and challenging PhD journey. Alhamdulillah.

I am deeply grateful to my main supervisor, Prof. Ir. Ts. Dr. Mohd Hisbany Mohd Hashim, for his invaluable guidance, continuous encouragement, and steadfast support throughout this research. My sincere thanks also go to my co-supervisor, Assoc. Prof. Dr. Noorsuhada Binti Md Nor, for her thoughtful insights, technical advice, and constructive feedback that greatly enhanced the quality of this thesis.

Special appreciation is extended to Dr. Ong Chee Beng, my FRIM-based supervisor and Head of the Wood Engineering Laboratory at the Forest Research Institute Malaysia (FRIM), for his expert guidance, laboratory supervision, and unwavering support during the experimental work. I also wish to thank the technical staff and research assistants at FRIM for their kind assistance throughout the laboratory setup, testing procedures, and data collection.

Sincere thanks are also due to the academic and administrative staff at UiTM, whose support enabled me to manage my part-time study commitments effectively. I am grateful to my colleagues and friends for their motivation, encouragement, and collaborative spirit throughout this journey.

Most importantly, I express my heartfelt gratitude to my beloved wife, Fareha Anis Mohd Taib, for her endless patience, understanding, and unwavering support throughout every stage of this journey. To my children, Nur Qurratun Radhiah, Muhammad Fadhil Abdullah, Aisyah Nur Jannah, and Ahmad Furqan Abdullah, thank you for being my source of joy, strength, and inspiration.

Finally, this thesis is dedicated to the loving memory of my late father and mother. Their sacrifices, vision, and determination to ensure I received a good education have been the foundation of this success. This piece of victory belongs to both of you. May Allah grant you the highest place in Jannah. Ameen.

TABLE OF CONTENTS

LIST OF TABLES

LIST OF FIGURES

LIST OF PLATES

LIST OF SYMBOLS

Symbols

A	Cross-sectional area (mm^2 or m^2)
E	Modulus of Elasticity (MOE) (GPa or MPa)
f	Natural frequency (Hz)
G	Shear Modulus (MPa)
I	Moment of Inertia (mm^4 or m^4)
k	Stiffness (N/m)
L	Span Length of the beam (m)
M	Bending Moment (N.m)
m	Mass (kg)
P	Applied Load (N)
SPI	Segmentation Performance Index (%)
SRI	Stiffness Reduction Index (%)
v	Poisson's ratio
ε	Strain (μm/m or mm/m)
δ	Deflection at mid-span (mm or m)
ρ	Material density (kg/m^3)
σ	Stress (MPa)

LIST OF ABBREVIATIONS

Abbreviations

ANSYS	Analysis System Software
ASTM	American Society for Testing and Materials
CFRP	Carbon Fibre Reinforced Polymer
CSM	Chopped Strand Mat
EMA	Experimental Modal Analysis
FEA	Finite Element Analysis
SFM	Sustainable Forest Management
SPI	Segmentation Performance Index
SRI	Stiffness Reduction Index
UiTM	Universiti Teknologi MARA

LIST OF NOMENCLATURES

Nomenclatures

f	Natural frequency (Hz)
k	Stiffness (N/m)
m	Mass (kg)
MOE	Modulus of Elasticity
MOR	Modulus of Rupture
SRI	Stiffness Reduction Index
SPI	Segmentation Performance Index

CHAPTER 1
INTRODUCTION

1.1 Research Background

Stream crossings are essential components of forest road networks that facilitate timber harvesting and post-harvesting operations in Malaysia. Temporary log bridges commonly used for these crossings frequently deteriorate due to high water flow, sedimentation, and insufficient maintenance, restricting access for critical post-logging activities such as replanting, soil treatment, and forest health monitoring required by Sustainable Forest Management guidelines. Modular and portable bridge designs provide a practical approach to addressing these challenges, as they can be transported, assembled, dismantled, and reused across multiple sites, reducing ecological impacts compared to traditional bridge systems. Timber provides a practical combination of structural efficiency, workability, and sustainability for modular bridge systems. Its exceptional strength-to-weight ratio enables long spans with reduced member weights, minimizing handling requirements during field deployment. The material's workability allows precise fabrication and rapid connector installation, while its natural damping properties reduce vibration effects from dynamic loading, enhancing serviceability for forest road applications.

The integration of advanced materials like fibre-reinforced polymers enhances durability and environmental resistance, while improved design methodologies strengthen performance under dynamic loads. Critical to this advancement is the development of mechanical connection systems with adequate load-bearing capacity to ensure safe load transfer between modular segments. The performance of these connectors directly determines the overall structural integrity and safety of modular timber bridge systems, making connection design optimization a fundamental requirement for practical implementation. These innovations not only address accessibility challenges but also align with contemporary environmental management practices, ensuring more efficient and sustainable forestry operations that balance operational efficiency and environmental protection.

In recent decades, modular construction has been widely adopted for its versatility, swift deployment capabilities, and cost-effectiveness across diverse sectors,

including emergency infrastructure, military applications, and rural development initiatives. Particularly, modular bridge designs have evolved significantly to cater to the growing demand for sustainable and mobile infrastructure solutions. Their design principles emphasizes prefabrication, standardization of components, and ease of transportation and installation, rendering them highly suitable for remote or ecologically sensitive areas. These bridges can be rapidly deployed to restore access in disaster-affected zones or remote forest regions, making them particularly relevant for developing countries where infrastructure gaps persist (Chordà-Monsonís et al., 2024).

The development of portable bridge systems, pioneered by the Bailey bridge during World War II with its prefabricated steel truss panels enabling rapid field assembly and disassembly, has significantly influenced modern modular bridge designs (Ambroziak et al., 2024). Contemporary innovations have incorporated lightweight materials including aluminium and fibre-reinforced polymers (FRP), enhancing efficiency under varying environmental conditions. Modern modular girder systems have improved design flexibility for diverse applications across forestry, logging, and rural transportation sectors (Kang et al., 2023). Carbon fibre-reinforced polymers (CFRP) have demonstrated substantial performance benefits when used with traditional materials, reducing deflections and extending bridge system functionality. Research increasingly emphasizes sustainability indicators, making resource consumption and environmental performance central to engineering decisions. These advancements reflect a shifting focus toward enhancing structural performance, deployment efficiency, and environmental adaptability while maintaining the Bailey bridge's foundational engineering principles of adaptability and rapid assembly.

Forest operations in Malaysia are governed by the Selective Management System, a key strategy implemented since 1978 for Permanent Reserved Forests. The SMS emphasizes minimizing environmental disruption while ensuring sustainable timber extraction (Ghazali et al., 2023). In this context, stream crossings play a critical role, providing access to logging areas and enabling post-harvest interventions such as site rehabilitation, replanting, and ecological monitoring. However, current practices predominantly utilize temporary log stringer bridges, which are often dismantled or abandoned after harvesting. These structures present significant risks of collapse, erosion, and sedimentation, particularly during the monsoon seasons when rainfall and runoff intensity increase (Halim et al., 2024). Plate 1.1 shows a typical forest bridge located in a tropical forestry operation. These access structures are vital for maintaining

connectivity in remote compartments, but their vulnerability to environmental degradation and limited maintainability during monsoon seasons highlights the need for more adaptable, durable, and sustainable alternatives.

Plate 1.1 Timber Bridge with Log Girder Construction Typical of Temporary Forest Access Infrastructure

Sustainable Forest Management principles require infrastructure solutions that minimize ecological impacts while supporting operational efficiency, particularly at sensitive stream crossings where bridge structures must be resilient, removable, and reusable (Milani et al., 2020). Modular timber bridge systems address these requirements through designs that reduce soil compaction and sedimentation while enabling component reuse across multiple sites, aligning infrastructure investment with resource efficiency objectives in forest operations.

This study employs the GT-24 lightweight lattice-web timber girder (PERI Formwork Malaysia Sdn. Bhd.) as the primary structural element for modular beam investigation. The GT-24 system is purpose-engineered to minimize self-weight (5.9 kg/m) while maintaining high flexural stiffness (800 kNm²), enabling manual handling, rapid transport, and repeated deployment in temporary and modular construction

applications which are design characteristics directly aligned with portable forest bridge requirements in remote tropical environments. The girder features solid Western White Pine (Pinus monticola) top and bottom flanges with an open lattice-web configuration that reduces mass while preserving structural efficiency. Manufactured under ISO 9001 certified quality control systems with factory-controlled geometry and material consistency, the GT-24 provides standardized structural performance verified through manufacturer testing protocols. The use of a pre-engineered beam system with consistent section properties across specimens is essential for isolating the effects of segmentation topology, mechanical connection behaviour, and reinforcement interaction mechanisms without confounding variability arising from natural timber heterogeneity. This experimental approach enables rigorous investigation of configuration-driven structural reduction phenomena, specifically segmentation-induced stiffness losses, joint flexibility accumulation, and reinforcement engagement patterns that are fundamentally governed by structural topology rather than timber species identity. The normalized performance indices developed in this research (Stiffness Reduction Index, Segmentation Performance Index) quantify relative stiffness evolution as dimensionless metrics, establishing transferable analytical frameworks applicable across timber species and engineered wood products once material property adjustments are incorporated.

The integration of mechanical connectors and advanced reinforcement materials in modular girder bridge systems presents challenges in load transfer efficiency, stress concentration management, and overall beam component performance, necessitating comprehensive experimental investigations and simulations to assess structural element interactions under flexural and vibrational loading. Research demonstrates that Fibre Reinforced Polymer (FRP) integration significantly enhances load-bearing capacity and structural integrity, particularly under dynamic conditions, while helping mitigate stress concentrations. Although modular designs with bolted connections offer flexibility, they may introduce constraints affecting system performance, with connection optimization dependent on parameters like bolt arrangement and spacing that influence composite beam bending behaviour. Achieving balance between structural stiffness and portability remains critical, with reinforcement materials proving effective in improving mechanical performance while addressing long-term behavioural characteristics under various loading scenarios. Therefore, successful modular girder bridge design requires integrated evaluation of mechanical behaviour and reinforcement effectiveness to

ensure optimal structural response while maintaining essential portability, stiffness, and resilience.

1.2 Problem Statement

Modular timber bridge systems (Figure 1.1) address critical forestry infrastructure needs in Malaysia's remote forest operations, yet their structural implementation faces significant engineering challenges including segmentation-induced discontinuities, unpredictable mechanical joint behaviour, and complex dynamic response characteristics (Chordà-Monsonís et al., 2024; Cepelka et al., 2023).

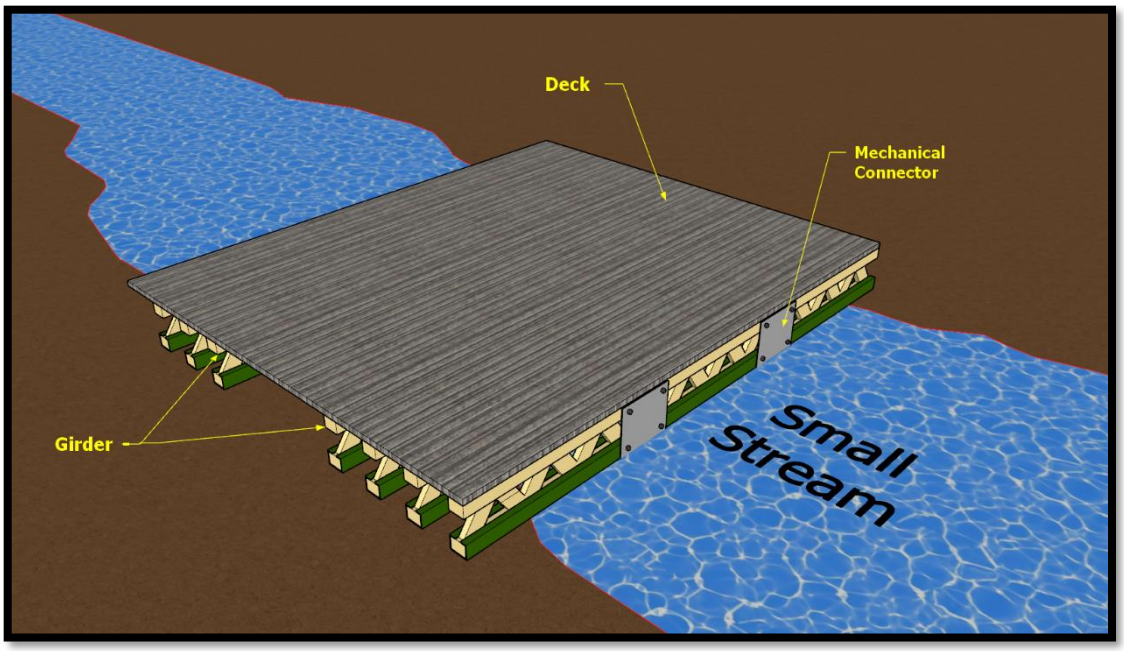

Figure 1.1 Modular timber bridge system showing beam segmentation, mechanical bolted connectors, and CSM reinforcement on tension flange.

Beam segmentation fundamentally disrupts structural continuity by introducing multiple discontinuity points that cause significant stiffness reduction and complex load redistribution patterns (Chordà-Monsonís et al., 2024; Hussein & Razzaq, 2021; Ro et al., 2021). Mechanical connections represent critical vulnerability zones where timber-bolt interfaces experience unpredictable stress concentrations and localized failure initiation under realistic loading conditions (Dobeš et al., 2022; Chen et al., 2020; Song et al., 2024). Dynamic loading conditions further complicate system performance by creating frequency interaction effects that vary significantly with segmentation patterns,

where altered structural configurations influence vibrational characteristics and energy dissipation mechanisms essential for service performance (Hassan, 2024; Bessa et al., 2022).

These engineering challenges manifest as five critical research gaps that constrain practical deployment of modular timber bridge systems, as systematically identified in Section 2.8:

Gap 1: Unvalidated Static-Dynamic Property Correlations in Modular Systems

Assessment methodologies for modular timber systems rely on destructive flexural testing, with no validated correlations enabling non-destructive dynamic evaluation of structural properties under field conditions. While relationships between static and dynamic modulus exist for continuous timber (Opazo-Vega et al., 2021; Olsson et al., 2024), whether correlations remain valid in modular configurations, where mechanical joints, segmentation patterns, and reinforcement materials fundamentally alter load transfer mechanisms that requires systematic investigation. The absence of configuration-specific correlation frameworks prevents reliable condition assessment during operational service, limiting practical deployment where non-destructive evaluation is essential. Without validated relationships between modal properties and structural capacity, engineers cannot confidently predict load-bearing performance from vibrational measurements in segmented timber assemblies.

Gap 2: Unknown Connection Load Redistribution and Governing Failure Modes

Mechanical connection performance in modular timber beams remains inadequately quantified under realistic loading conditions, particularly regarding how loads redistribute among multiple connectors and which failure mode governs design limits. While studies document stress concentrations reaching 2.5-4.0 times nominal levels at timber-bolt interfaces (Dobeš et al., 2022; Song et al., 2024), systematic characterization of load concentration patterns, progressive failure mechanisms, and governing capacity limits (timber bearing versus bolt shear versus plate bearing) across segmentation configurations remains undeveloped. This knowledge gap prevents engineers from determining whether connection adequacy is limited by hardware specifications or timber material properties, and whether reinforcement strategies can transform failure progression from brittle to ductile mechanisms. Without quantitative understanding of load-sharing behaviour among multiple mechanical joints, designers

cannot reliably predict which connectors reach critical states under service loads or establish appropriate safety factors for modular timber applications.

Gap 3: Unexplored Dynamic Response Patterns in Segmented Reinforced Systems

Dynamic behaviour of segmented timber beams, particularly how reinforcement and joint configurations influence frequency response, mode shapes, and energy dissipation characteristics, remains poorly understood. While continuous timber demonstrates established frequency-stiffness relationships, whether these patterns hold for modular configurations where mechanical joints introduce compliance and reinforcement materials alter mass-damping-stiffness interactions requires systematic investigation (Hassan, 2024; Bessa et al., 2022). The influence of segmentation frequency on natural frequency evolution, optimal wave-reinforcement interaction lengths, and component-level damping mechanisms remains uncharacterized. Without comprehensive dynamic property characterization across segmentation and reinforcement configurations, engineers cannot predict vibrational performance, assess resonance risks, or validate computational models against experimental measurements which is a critical requirement for implementing modular timber systems in dynamic service environments.

Gap 4: Unknown Reinforcement Influence on Segmented Beam Performance Evolution

Fibre-reinforced polymer effectiveness in segmented timber configurations, particularly how reinforcement influences progressive structural performance and connection behaviour during loading, remains inadequately characterized. While continuous FRP-timber systems demonstrate strength increases of 17.7-77.3% (Lee et al., 2020; Wdowiak-Postulak et al., 2023; He et al., 2022), whether these benefits translate to segmented assemblies, in which reinforcement discontinuities at mechanical joints disrupt composite action that requires systematic investigation. Critical unknowns include: whether reinforcement alters stiffness evolution during service-level loading progression, how reinforcement modifies connection failure mechanisms and load redistribution patterns, and whether optimal segmentation geometries exist where reinforcement effectiveness is maximized. Without understanding how externally-bonded reinforcement interacts with segmentation patterns to influence both global structural response and localized connection performance, designers cannot determine

appropriate reinforcement strategies for modular timber systems or predict performance transformation beyond simple capacity enhancement.

Gap 5: Absent Quantitative Performance Indices for Segmentation Effects

Current evaluation methodologies lack standardized analytical indices capable of quantifying cumulative stiffness reduction as segmentation frequency increases or establishing evidence-based configuration limits for modular timber systems. While research demonstrates that reduction occurs through multiple mechanisms because of bearing deformation, joint compliance accumulation, and progressive stress concentration, but lack of validated performance metrics exist to measure these cumulative effects systematically (Wang et al., 2022; Reynolds et al., 2015). Without quantitative tools that distinguish between baseline stiffness penalties (segmentation effects) and progressive stiffness evolution during loading (reinforcement engagement), designers cannot systematically evaluate trade-offs between transportability requirements and structural integrity demands. The absence of convergent validation frameworks integrating experimental, computational, and statistical evidence prevents establishment of optimal segmentation thresholds supported by multiple independent analytical methods rather than single-criterion empirical observations.

These five interconnected research gaps collectively prevent development of comprehensive evaluation frameworks essential for reliable field implementation of modular timber bridge systems. The absence of validated static-dynamic correlations (Gap 1) limits non-destructive assessment capabilities, while inadequate connection performance characterization (Gap 2) prevents reliable capacity prediction. Unknown dynamic behaviour patterns (Gap 3) constrain vibration performance evaluation, incomplete reinforcement effectiveness understanding (Gap 4) limits design optimization strategies, and missing quantitative performance indices (Gap 5) prevent systematic configuration threshold establishment.

The interconnected nature of these challenges necessitates integrated methodologies that capture complex synergistic interactions governing modular timber system behaviour (Caprio & Jockwer, 2023). Addressing Gap 1 requires understanding connection mechanisms from Gap 2 that govern dynamic response patterns in Gap 3. Evaluating reinforcement strategies (Gap 4) depends on quantification frameworks from Gap 5 that integrate static, dynamic, and connection performance metrics. Without such comprehensive analytical frameworks incorporating quantitative performance

indices, validated configuration thresholds, and non-destructive correlation protocols, safe and scalable deployment of modular timber bridge systems remains fundamentally uncertain, limiting acceptance in structural engineering practice and constraining potential to address critical infrastructure needs in remote forest environments (Sist et al., 2021).

This research directly supports Malaysia's Sustainable Forest Management objectives by developing validated engineering frameworks that enable infrastructure solutions balancing ecological integrity with operational efficiency (Ghazali et al., 2023; Svatoš-Ražnjević et al., 2022).

Research Gap–Objective Linkage:

- Gap 1 (Static-dynamic correlations) → Objective 1
- Gap 2 (Connection load redistribution) → Objective 2
- Gap 3 (Dynamic behaviour characterization) → Objective 3
- Gap 4 (Reinforcement effectiveness) → Objective 4
- Gap 5 (Performance quantification) → Objective 5

1.3 Research Objectives

This research aims to develop a modular girder bridge system for short-span forest road applications. The system will utilize segmented timber beams reinforced with carbon fibre materials and connected by mechanical fasteners. The design should be structurally efficient, easily transported, rapidly deployable, and aligned with the principles of Sustainable Forest Management. To systematically address this research aim, this study will examine timber beams with varying degrees of segmentation (two, three, and four segments) to determine the optimal configuration that balances portability with structural performance. Through comparative analysis of these configurations, the research aims to establish practical guidelines for identifying the ideal number of segments for modular timber bridge applications in forest environments. These findings will directly inform design recommendations that optimize the trade-off between structural integrity and field transportability.

The five objectives follow a systematic progression from baseline characterization through mechanistic understanding to design optimization. Objective 1 establishes fundamental dynamic-static property correlations, providing the non-

destructive assessment framework necessary for evaluating segmented system behaviour. Objective 2 identifies the physical mechanisms governing these correlations by quantifying connection load redistribution and stress concentration patterns that determine global system response. The connection behaviour characterized in Objective 2 directly explains the dynamic response patterns examined in Objective 3, where mechanical joint compliance and reinforcement-induced damping govern frequency evolution, mode shapes, and energy dissipation characteristics. The dynamic performance limitations revealed in Objective 3 establish the need for Objective 4, which evaluates CSM reinforcement as a mitigation strategy through progressive stiffness evolution and connection behaviour transformation analysis. Finally, Objective 5 integrates findings from Objectives 1-4 through novel analytical indices (SRI, SPI) and multi-method validation to establish evidence-based segmentation limits that balance structural integrity with modular deployment requirements. Collectively, the objectives progress from baseline characterization to mechanism identification, global behaviour assessment, reinforcement evaluation, and ultimately system optimization.

To accomplish this, the study establishes the following research objectives:

Objective 1: To establish and validate correlations between static flexural stiffness and dynamic modal response, enabling configuration-specific non-destructive assessment of modular timber systems.

Objective 2: To analyse mechanical connection performance, quantifying load redistribution, stress concentrations, and failure mechanisms governing modular timber beam behaviour.

Objective 3: To characterize dynamic properties of segmented and continuous timber beams through comparative experimental modal analysis and finite element validation.

Objective 4: To evaluate CSM reinforcement influence on structural performance evolution, connection behaviour, and optimal configuration identification in segmented beams.

Objective 5: To develop stiffness reduction indices and establish optimal segmentation limits through convergent experimental, statistical, and computational validation.

The proposed objectives collectively address critical structural aspects of modular timber girder systems, with the aim of facilitating the development of lightweight, reusable bridge structures. This would support improved forest accessibility and contribute to the advancement of sustainable infrastructure initiatives.

1.4 Scope and Limitation of Study

This study focused on the design, testing, and analysis of a modular girder bridge system intended for short-span forest road applications that align with Sustainable Forest Management principles in Malaysia. The research specifically examines the structural behaviour of segmented timber beams reinforced with Chopped Strand Mat (CSM) and connected using mechanical bolt-type fasteners. The scope encompasses both experimental and numerical investigations aimed at characterizing the stiffness performance of the system under static and dynamic loading conditions.

The structural configuration investigated in this study comprises beams fabricated from engineered timber with orthotropic mechanical properties. These beams are segmented into lengths ranging from 0.6 to 3.0 m and connected using bolt-fastened steel plate connectors. Selected beams are reinforced with CSM applied to the tension flange. The modular design reflects the practical constraints of mobility and reusability in remote forest environments, where bridge relocation or repeated deployment is necessary.

1.4.1 Scope of Analysis

Flexural Testing: Controlled laboratory experiments utilizing three-point bending tests are performed to assess the deflection, Modulus of Elasticity, and load-carrying performance of both segmented and continuous timber beam configurations.

Experimental Modal Analysis (EMA): Experimental Modal Analysis is conducted to non-destructively determine the natural frequencies and mode shapes of the specimens. These dynamic characteristics are then utilized to estimate the overall stiffness and vibrational behaviour of the system.

Finite Element Analysis (FEA): Complementary numerical simulations are conducted in ANSYS software to emulate the static bending and modal (vibrational) characteristics of the system. The timber components are modelled using orthotropic

material definitions, while the connectors and Chopped Strand Mat (CSM) reinforcement are represented with isotropic material properties.

Strain Monitoring: Strain monitoring at key locations, including the top flange, mid-span, bottom flange, and web near the support, provides insights into the localized stress behaviour and potential failure mechanisms within the system.

Statistical Analysis: Statistical analysis is employed as a validation layer to evaluate whether observed differences in stiffness evolution, dynamic response, and reinforcement effectiveness represent systematic structural behaviour rather than experimental variability across different segmentation and reinforcement configurations.

1.4.2 Scope of Materials:

Timber: GT-24 lightweight lattice-web timber girder system (PERI Formwork Malaysia Sdn. Bhd.) incorporating solid Western White Pine (Pinus monticola) flanges. The system is manufactured under ISO 9001 certified quality control with a nominal flexural stiffness of 800 kNm² and a linear weight of 5.9 kg/m. The timber component is treated as a non-homogeneous orthotropic material, with mechanical properties adopted from manufacturer specifications and established reference values reported in the Forest Products Laboratory (2010) handbook to ensure consistency and repeatability across specimens.

Connector: Steel plate with bolt-fastening mechanism representing mechanical joints.

Reinforcement: Chopped Strand Mat (CSM) bonded to the tension flange.

1.4.3 Limitations of the Study

Engineered Girder System – This study utilizes the GT-24 lightweight lattice-web timber girder (PERI Formwork Malaysia Sdn. Bhd.) rather than sawn Malaysian tropical hardwood sections. The system was intentionally selected for its low self-weight (5.9 kg/m), manual portability, and factory-controlled consistency under ISO 9001 quality certification, enabling isolation of segmentation and reinforcement effects with minimal material variability. Accordingly, the absolute stiffness values reported correspond specifically to the GT-24 system tested (nominal flexural stiffness 800

kNm²) and may not directly translate to heavier tropical hardwoods. However, the reduction mechanisms and normalized performance indices (SRI, SPI) are governed primarily by structural topology rather than species identity, and are therefore transferable across timber types. Validation using local Malaysian hardwoods is recommended for future application.

Span Constraint – The experimental investigations were constrained to beam spans up to 3.0 m due to the limitations of the laboratory facilities and test equipment. While this range aligns with the practical dimensions of modular bridge units, the study did not encompass the evaluation of full-scale bridge spans.

Boundary Conditions – The study focused on specimens under idealized simply-supported boundary conditions, without investigating the effects of continuous support, fixed ends, or real-world field conditions.

Reinforcement Continuity – The study is limited in that the CSM reinforcement is applied only to the tension face of individual beam segments, and does not extend continuously across the joints. This discontinuity in the reinforcement may impact the relevance of the results to systems with fully bonded, uninterrupted CSM reinforcement.

Environmental Effects – This study does not investigate the impact of environmental factors, such as moisture, decay, temperature, and weathering, on the timber components and their bonded interfaces. All experiments were conducted in a controlled indoor laboratory setting.

Connector Type – This study is limited to the analysis of a single type of bolted steel plate connector. The structural performance of alternative joint configurations, such as those utilizing dowels, notches, or adhesive bonding, is not within the scope of this investigation.

1.5 Significance of Study

This research addresses critical gaps in modular timber bridge engineering and makes substantial contributions across academic, national policy, and practical engineering domains. The significance of this study extends from advancing fundamental understanding of segmented timber structural behaviour to providing implementable solutions for Malaysia's sustainable forest management challenges.

1.5.1 Academic and Research Contributions

This research makes several key academic contributions that advance the field of timber structural engineering. The study establishes a novel experimental framework that integrates Experimental Modal Analysis with conventional flexural testing methodologies for segmented timber systems, addressing a significant methodological gap where dynamic and static properties are typically evaluated independently. The development of quantitative correlation models between static modulus of elasticity and dynamic frequency response provides a foundation for non-destructive assessment protocols.

The introduction of the Stiffness Reduction Index (SRI) and Segmentation Performance Index (SPI) represents an analytical innovation that quantifies performance losses associated with modular configurations, providing standardized metrics for evaluating trade-offs between structural integrity and modularity. The systematic investigation of CSM reinforcement effects on segmented timber beams contributes new knowledge to timber-composite systems, particularly addressing how reinforcement strategies must be adapted for discontinuous structural elements.

From a methodological perspective, this study advances UiTM's capabilities in structural dynamics and computational modelling by validating finite element approaches against comprehensive experimental data. The hybrid experimental-numerical framework establishes protocols for future investigations of modular structural systems, enhancing UiTM's research profile in sustainable infrastructure and positioning the institution as a leader in timber engineering research within the Southeast Asian context.

1.5.2 National Policy and Strategic Relevance

This research directly supports Malaysia's national commitments to sustainable development and responsible natural resource management. The study aligns with Malaysia's implementation of UN Sustainable Development Goals, particularly SDG 15 (Life on Land) and SDG 9 (Industry, Innovation and Infrastructure), by developing infrastructure solutions that minimize environmental impact while maintaining operational effectiveness for forest management activities.

The research addresses critical needs within Malaysia's Selective Management

System by providing technical solutions for post-harvest forest access that reduce soil compaction, erosion, and stream sedimentation. These environmental benefits directly support Malaysia's National Forestry Policy objectives and enable more effective implementation of silvicultural treatments, reforestation programs, and ecological monitoring activities essential for maintaining Malaysia's forest certification standards.

From an economic perspective, the reusable nature of the proposed modular system optimizes infrastructure investment efficiency within Malaysia's forestry sector. The ability to redeploy bridge assets across multiple sites maximizes return on investment while reducing material waste, supporting circular economy principles in forest operations. The research contributes to Malaysia's technological self-reliance in forest infrastructure by developing locally-appropriate solutions, reducing dependence on imported bridge technologies while informing national policy development for forest infrastructure standards.

1.5.3 Practical Engineering Applications

This research delivers tangible outcomes with immediate application value for engineering practitioners working in forest infrastructure, rural bridge design, and modular construction. The correlation relationships established between static and dynamic properties enable field engineers to conduct rapid structural assessments using portable modal analysis equipment, eliminating the need for destructive testing in operational environments. This capability is particularly valuable for remote forest sites where traditional testing infrastructure is unavailable.

The design guidelines developed through this research provide civil engineers and forest engineers with quantitative parameters for optimizing modular timber bridge configurations. These guidelines address critical design decisions including optimal segmentation patterns, connection specifications, and reinforcement strategies that balance structural performance with portability requirements. The research findings enable practitioners to make evidence-based design decisions rather than relying on conservative assumptions that may result in over-designed or inefficient systems.

The validated finite element modelling approaches developed in this study provide engineering consultants with reliable computational tools for predicting modular timber bridge performance. These modelling capabilities reduce design iteration time and enable parametric optimization of bridge configurations for specific

site conditions and loading requirements. The computational frameworks established through this research can be implemented in commercial finite element software, making the findings accessible to practicing engineers.

The study provides practical solutions for addressing the growing demand for sustainable infrastructure in remote and environmentally sensitive areas. Beyond forest applications, the modular bridge concepts developed in this research have potential applications in rural infrastructure development, emergency response scenarios, and temporary construction access where rapid deployment and environmental sensitivity are priorities.

CHAPTER 2
LITERATURE REVIEW

2.1 Modular Timber Bridges in Forestry Applications

Stream crossings represent critical infrastructure bottlenecks in Malaysia's tropical forest management systems, where traditional bridge solutions systematically fail to reconcile operational demands with environmental constraints. Temporary log bridges deteriorate rapidly under aggressive monsoon conditions and biological degradation, while permanent concrete structures create lasting access corridors that undermine conservation security (Morais et al., 2023; Mamat & Ahmad, 2020). This fundamental inadequacy of conventional approaches has catalysed interest in modular timber bridge systems that offer controlled deploy ability, environmental reversibility, and alignment with Sustainable Forest Management (SFM) protocols. This section examines the operational context driving modular bridge adoption in Malaysian forestry, reviews the limitations of conventional temporary and permanent crossing solutions, and establishes the material and sustainability considerations that inform contemporary modular system design before transitioning to detailed engineering analysis of structural performance requirements.

2.1.1 Structural Performance Constraints of Conventional Forest Bridge Systems

Forest bridge systems in tropical environments face combined exposure to high humidity (>80%), thermal cycling (15-20°C daily fluctuations), and biological attack that accelerate material degradation (Acosta et al., 2022). These conditions create moisture-induced dimensional instability, progressive stiffness reduction, and time-dependent material property variation. Under repetitive dynamic loading from heavy forestry equipment, these degradation mechanisms produce unpredictable structural responses and premature failures that conventional design methodologies cannot reliably anticipate.

Temporary log bridges comprise discontinuous round timber members in non-engineered bearing configurations relying on natural friction and contact forces for load

transfer. This structural system exhibits fundamental mechanical deficiencies precluding reliable performance prediction. Non-uniform stiffness distribution arises from variable log diameters, inconsistent material properties, and uncontrolled bearing interface conditions (Aust et al., 2011; Morais et al., 2023). Without defined load paths or engineered connections, load transfer occurs through localized crushing at bearing interfaces rather than distributed structural action. This bearing-dominated mechanism creates critical deficiencies: variable log geometries produce non-uniform deflection patterns, material property variations prevent reliable capacity predictions, progressive bearing deformation reduces member engagement, and sudden load redistribution following localized failure triggers catastrophic collapse (Morais et al., 2023). The combination of high structural variability and unpredictable failure characteristics renders these systems unsuitable for applications requiring consistent performance across repeated operational cycles.

Service life assessment reveals moisture penetration initiates dimensional instability within months, followed by biological degradation compromising load-bearing capacity within 2-3 years which is significantly shorter than the 10–15-year operational planning cycles required for sustainable forest management programs (Morais et al., 2023). Plate 2.1 illustrates typical structural failure demonstrating the unpredictable collapse patterns characteristic of non-engineered bearing systems. This durability-demand mismatch creates fundamental incompatibility between temporary bridge structural characteristics and forestry operational requirements, necessitating frequent replacement cycles that compound economic costs and operational disruption (Mamat & Ahmad, 2020).

Permanent concrete bridges achieve superior structural performance through monolithic reinforced construction providing continuous flexural action and predictable load transfer mechanisms (Arias et al., 2022). Plate 2.2 shows a representative permanent log girder bridge installation, highlighting heavy equipment requirements limiting deployment flexibility. Structural advantages include high global stiffness, controlled deformation response, consistent material properties, and well-established design methodologies enabling reliable capacity prediction. However, permanent infrastructure proves incompatible with rotational forest management systems where access requirements shift across different compartments over multi-year operational cycles.

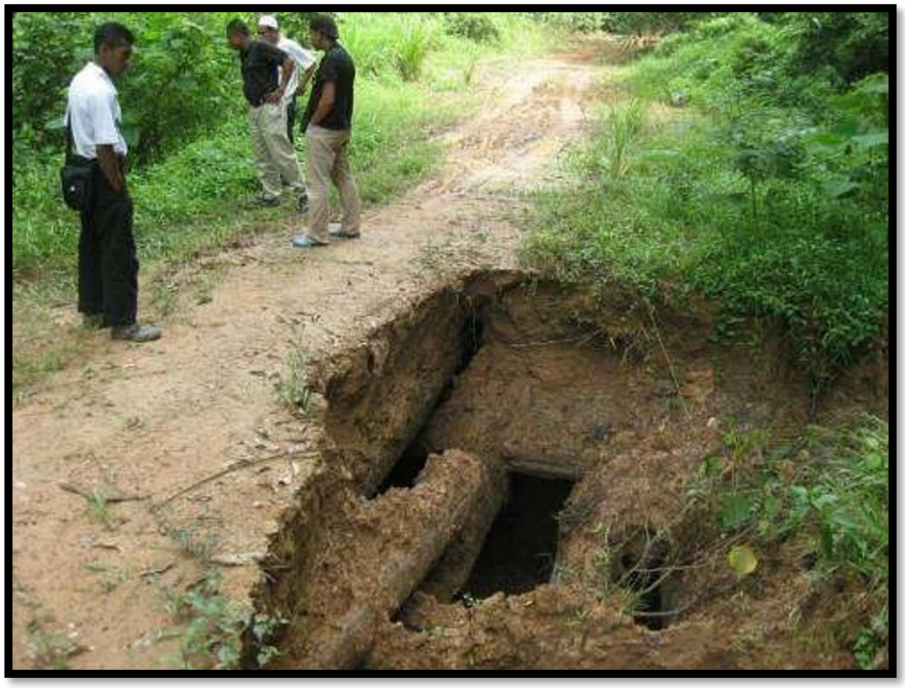

Plate 2.1 Structural failure of temporary log bridge demonstrating unpredictable collapse mechanisms characteristic.

Engineering limitations in forestry contexts manifest through three mechanisms. First, structural over-capacity designed for continuous traffic loading proves economically inefficient for temporary crossing demands where intermittent access patterns do not justify permanent installation investment (Arias et al., 2022). Second, fixed geometry cannot accommodate stream channel evolution during high-flow hydrological events, with inadequate foundation design triggering cascading failures through progressive erosion and streambank destabilization (Pacheco et al., 2021). Third, deployment inflexibility prevents relocation or span adjustment without complete structural reconstruction, creating operational constraints incompatible with compartmentalized harvesting schedules requiring infrastructure mobility.

This comparative analysis reveals a dual inadequacy: temporary log bridges provide insufficient structural durability and unpredictable performance characteristics, while permanent concrete bridges offer excessive permanence and deployment inflexibility. This dichotomy establishes a fundamental engineering gap requiring bridge systems that combine predictable structural behaviour with controlled deploy ability where precisely the performance characteristics that modular timber bridge systems are designed to provide. The challenge lies in achieving this combination without compromising either structural reliability or operational versatility, creating the

motivating framework for the systematic investigation of modular timber beam performance presented in this research.

Plate 2.2 Permanent log girder bridge requiring heavy installation equipment, illustrating deployment inflexibility inherent to fixed infrastructure solutions.

2.1.2 Modular Timber Bridge Systems

Modular timber bridge systems address the limitations of conventional approaches through prefabricated timber segments connected via mechanical joints enabling controlled assembly and disassembly while maintaining predictable structural performance. Rather than relying on material properties alone, these systems achieve their performance characteristics through engineered interaction between segment stiffness and connection behaviour, positioning them as segmented beam systems where global structural response emerges from component-level mechanics.

Table 2.1 provides systematic engineering comparison focusing on parameters directly governing mechanical performance. The structural advantages stem from factory-controlled fabrication processes ensuring dimensional consistency and reduced material property variability compared to field-assembled temporary structures. Off-site manufacturing enables precise member tolerances, standardized connection interfaces,

and quality assurance protocols producing predictable component-level performance (Aust et al., 2011). Connection behaviour becomes quantifiable through bolt-timber-steel interfaces with defined load-displacement characteristics, enabling explicit consideration of joint stiffness in system-level analysis rather than relying on empirical friction coefficients characteristic of bearing-only systems (Saad & Lengyel, 2022).

Table 2.1
Structural Performance Comparison of Bridge Systems for Forest Applications

Engineering Aspect	Temporary Log Bridge	Permanent Concrete Bridge	Modular Timber Bridge
Structural System	Discontinuous round logs, non-engineered arrangement (Aust et al., 2011; Morais et al., 2023)	Monolithic reinforced concrete (Arias et al., 2022)	Engineered segmented timber girders (Saad & Lengyel, 2022)
Structural Consistency	Highly variable (log quality, geometry) (Morais et al., 2023)	Highly consistent (Arias et al., 2022)	Consistent, factory-controlled members (Saad & Lengyel, 2022)
Load Transfer Mechanism	Bearing between logs (Aust et al., 2011)	Continuous flexural action (Arias et al., 2022)	Flexural action with mechanical joints (Saad & Lengyel, 2022)
Connection Behaviour	Natural bearing and friction (Aust et al., 2011)	Cast-in reinforcement (Arias et al., 2022)	Bolt–timber–steel plate interfaces (Muthumala et al., 2022)
Flexural Performance Control	Poor due to non-uniform stiffness (Morais et al., 2023)	Excellent (Arias et al., 2022)	Good–Excellent, design-dependent (Saad & Lengyel, 2022)
Dynamic Behaviour	Uncontrolled, high variability (Aust et al., 2011)	Low vibration response (Arias et al., 2022)	Moderate vibration, damping-dependent (Saad & Lengyel, 2022)
Portability / Deploy ability	Low (Morais et al., 2023)	Very low (Arias et al., 2022)	High, modular and demountable (Saad & Lengyel, 2022)
Suitability for Temporary Forest Roads	Limited durability (Aust et al., 2011)	Over-designed for temporary access (Arias et al., 2022)	High suitability (Saad & Lengyel, 2022)

System-level benefits include component replaceability where damaged segments can be exchanged without full system reconstruction, span adaptability through standardized connection patterns, and repeatable performance across multiple deployment cycles. Critically, structural performance becomes system-dominated rather than material-dominated, with global behaviour determined by the interaction between segment properties and connection characteristics. This transition from

material-limited to system-limited performance enables optimization strategies unavailable to conventional bridge types.

However, mechanical joints introduce structural discontinuities that reduce global flexural stiffness relative to continuous members where the central engineering challenge governing modular timber bridge performance. At each connection interface, load transfer occurs through discrete bearing contacts and fastener deformation rather than material continuity, creating compliance zones that contribute to system-level deflection beyond member flexure alone. The mechanical consequences include reduced flexural rigidity (decreased effective EI), increased mid-span deflection under equivalent loading, altered vibration characteristics through modified stiffness-to-mass relationships, and connection-governed failure modes where joint capacity may limit system performance below member strength capacity.

This discontinuity effect creates a fundamental design trade-off: increasing segment numbers enhances portability but systematically degrades structural stiffness through cumulative connection compliance. Understanding how this stiffness reduction scales with segment number, how connection detailing influences reduction magnitude, and how reinforcement strategies can mitigate discontinuity effects forms the core technical motivation for this research. The relationship between segmentation strategy and structural performance cannot be predicted from continuous beam theory, necessitating systematic experimental investigation of connection testing (Objective 2), stiffness reduction quantification (Objective 5), and segmentation limit determination that comprise the primary research objectives.

Fibre-reinforced polymer (FRP) integration addresses multiple performance requirements simultaneously: improved durability through moisture-resistant polymer matrices, enhanced stiffness retention under sustained loading, and modified energy dissipation characteristics affecting dynamic response (Wdowiak-Postulak et al., 2023). Documented strength improvements of 40-60% in bending capacity demonstrate how composite reinforcement transforms timber into high-performance structural components suitable for demanding forestry applications (Lee et al., 2023). However, reinforcement effectiveness in modular configurations depends critically on bond condition at timber-FRP interfaces, segment length relative to reinforcement extent, and connection interaction where reinforcement must be interrupted at joint locations. Unlike continuous reinforced beams where FRP can extend the full member length, segmented systems create discontinuous reinforcement patterns that alter composite

action and stress distribution. This reinforcement-connection interaction requires experimental validation to establish whether localized reinforcement within segments can effectively restore stiffness losses introduced by joint discontinuities.

The fundamental characteristics of modular timber systems with segmented geometry, mechanical connections, potential reinforcement, and operational deployment requirements that create a complex structural problem requiring systematic investigation. The subsequent sections develop the theoretical foundation for understanding how these characteristics influence performance through examination of timber orthotropic behaviour (Section 2.2), connection stiffness and slip mechanisms (Section 2.4), segmentation effects on flexural behaviour (Section 2.5), reinforcement strategies (Section 2.6), and dynamic response characteristics (Section 2.7).

2.1.3 Operational Requirements for Forestry Applications

Modular timber bridge systems in forestry contexts must satisfy distinct operational requirements that directly influence structural design parameters. The primary operational demand is rapid deployment capability, where construction timelines measured in days rather than weeks minimize operational disruption and equipment mobilization costs in remote locations (Chordà-Monsonís et al., 2024). This deployment speed requirement translates into engineering constraints including: (1) component weights enabling manual or light-equipment handling, (2) connection systems facilitating assembly without specialized tools, and (3) standardized interfaces ensuring interchangeability across deployment sites.

Rotational forest management systems impose additional structural requirements through compartmentalized harvesting schedules. Malaysian forestry operations following Selective Management Systems divide production forests into discrete management units accessed sequentially over 25–30-year cutting cycles, consistent with selective logging frameworks in tropical production forests governed by minimum cutting cycle regulations (Putz et al., 2022). This operational pattern creates two critical engineering requirements: (1) bridge service life matching compartment access duration (5-15 years between relocations), and (2) disassembly capability enabling infrastructure relocation without component degradation. The structural challenge lies in achieving adequate fatigue resistance for repeated assembly-disassembly cycles while maintaining connection integrity under operational loading.

Redeploy ability across multiple sites introduces standardization requirements affecting structural design. Components must accommodate variable span lengths, loading conditions, and site geometries without requiring custom engineering for each installation (Cepelka et al., 2023; Ambroziak et al., 2024). This operational flexibility translates into engineering requirements for: (1) modular span adjustment through standardized segment lengths, (2) connection tolerance ranges accommodating site-specific variations, and (3) predictable structural performance across deployment configurations. These operational requirements directly inform the segmentation strategies, connection design parameters, and reinforcement approaches investigated in this research, establishing the functional constraints within which structural optimization must occur.

2.1.4 Summary: Context to Engineering Transition

The preceding sections establish that both temporary and permanent bridge solutions present fundamental limitations in Malaysian tropical forestry contexts. Temporary log bridges deteriorate rapidly under monsoon conditions and aggressive biological degradation, generating replacement cycles of 2 to 3 years that substantially conflict with the 10-to-15-year operational timeframes characteristic of sustainable forest management programs (Morais et al., 2023; Acosta et al., 2022). Conversely, permanent concrete and reinforced structures, while addressing durability concerns, inadvertently create lasting access corridors that facilitate unauthorized resource extraction long after legitimate operations conclude, undermining conservation security in remote forest zones (Mamat & Ahmad, 2020). This dual inadequacy (insufficient longevity in temporary systems and excessive permanence in conventional infrastructure) establishes the operational context from which modular timber bridge systems emerge as responsive solutions.

Modular systems reconcile these competing demands through rapid deployment capabilities, environmental reversibility, and adaptability across compartmentalized management units operating on 25-to-30-year rotation cycles (Cepelka et al., 2023). The capacity for controlled access through removable infrastructure addresses illegal logging concerns while maintaining operational flexibility, and the reduced ecological footprint aligns with Sustainable Forest Management (SFM) and Selective Management System (SMS) requirements. However, successful implementation depends

fundamentally on the structural performance of constituent elements and assemblies. The operational advantages (portability, reusability, minimal ecological footprint) translate into engineering requirements that must be rigorously addressed through comprehensive analysis of timber's structural behaviour as an orthotropic material, the mechanical performance of connector systems governing load transfer between segments, the dynamic response characteristics of jointed beam assemblies under operational loading, and the influence of reinforcement strategies on overall system stiffness and durability (Wdowiak-Postulak et al., 2023). These engineering considerations establish the technical foundation upon which modular bridge performance ultimately depends, necessitating detailed examination of the structural and mechanical principles that govern timber system behaviour in segmented configurations.

2.2 Structural Behaviour of Timber & Engineered Timber Systems

Building on the operational context of modular forest bridge systems, this section examines timber as a structural material from a mechanical and dynamic behaviour perspective. Emphasis is placed on the fundamental material characteristics that govern stiffness, deformation, and vibration response, including orthotropic elasticity, inherent variability, moisture sensitivity, and time-dependent behaviour. These properties directly influence the static and dynamic performance of timber beams, particularly when structural continuity is disrupted through segmentation and mechanical connections. The section further reviews engineered timber systems as reference benchmarks for stiffness control and material consistency, providing a theoretical foundation for subsequent evaluation of stiffness reduction, dynamic response, and reinforcement effects in modular timber beam configurations investigated in this study.

2.2.1 Orthotropic Behaviour of Timber

Timber exhibits complex orthotropic mechanical properties characterized by distinct elastic behaviour along three mutually perpendicular axes corresponding to its natural growth structure. These principal material directions that are longitudinal (L, parallel to grain), radial (R, perpendicular to growth rings), and tangential (T, tangent

to growth rings) which reflect timber's cellular anatomy where fibre orientation governs directional stiffness and strength characteristics (Dobeš et al., 2022). Unlike isotropic materials such as steel or concrete, timber's orthotropic nature means structural performance depends critically on load orientation relative to grain direction, with the longitudinal elastic modulus (EL) typically exceeding radial (ER) and tangential (ET) moduli by an order of magnitude (Kurzinski & Crovella, 2023).

This pronounced directional variation reflects timber's cellular architecture where longitudinally-oriented cellulose fibres provide primary load resistance parallel to grain while transverse properties depend on weaker cell wall interactions. For structural softwoods, EL typically ranges from 10 to 20 GPa, substantially exceeding ER and ET which range from 1.0 to 4.0 GPa (Güntekin, 2023). Western White Pine (Pinus monticola) which the material employed in this investigation that reports EL values near 10.6 GPa, ER approximately 1.8 GPa, and ET around 1.5 GPa, yielding an approximate orthotropy ratio of 11:1.7:1 (Arzola-Villegas et al., 2025). This order-of-magnitude difference demonstrates that longitudinal stiffness exceeds tangential stiffness by approximately ten-fold, directly influencing segmented beam behaviour where load paths must traverse connection interfaces.

Shear behaviour and Poisson's ratios similarly exhibit directional dependency, with longitudinal-radial shear modulus (GLR) typically measuring approximately 1100 MPa while radial-tangential values (GRT) approach only 100 MPa (Güntekin, 2023). Poisson's ratios range from 0.1 to 0.4 for longitudinal-radial coupling, influencing both connection design where bolt hole deformation depends on local stress states and dimensional stability predictions where moisture-induced swelling creates internal stresses at connection interfaces (Kurzinski & Crovella, 2023).

Load orientation relative to grain direction critically governs structural capacity and failure mechanisms. Timber loaded parallel to grain exhibits substantially higher strength and stiffness compared to perpendicular loading, with compression strength perpendicular to grain typically measuring only 10% of parallel capacity (Muñoz et al., 2022). This dramatic reduction necessitates careful load path analysis in timber structures, with optimal designs aligning primary loads parallel to grain wherever possible. Opazo-Vega et al. (2021) demonstrated that moisture content and grain orientation interact synergistically, with moisture-induced property reductions becoming more pronounced under perpendicular loading, compounding the challenges inherent to connection design in variable environmental conditions.

In modular timber bridge systems comprising mechanically-connected segments, orthotropic behaviour becomes critically important as both material anisotropy and connection discontinuities compound to influence overall structural performance. Research demonstrates that forces aligned parallel to grain in bolted connections achieve substantially higher stiffness and load capacity than perpendicular loading configurations, with grain misalignment causing uneven load distribution and premature connection failure (Zhang et al., 2021). Segmentation introduces additional stiffness reduction beyond material orthotropy alone, as discontinuities at connection interfaces prevent smooth stress flow characteristic of continuous members. Experimental investigations on multi-segment timber beams reveal that five-segment configurations experience 49.5% load capacity reduction compared to continuous beams of identical cross-section, attributed to cumulative stiffness losses at connection interfaces where stress concentrations develop (Mamat et al., 2025). This segmentation effect becomes particularly significant when combined with orthotropic grain behaviour, as each connection represents a location where directional stiffness variations influence local deformation patterns and load redistribution mechanisms. These compound effects which material anisotropy and geometric discontinuity that necessitate careful consideration in modular timber bridge design, with connection detailing requiring explicit attention to grain orientation, fastener configuration, and load path continuity. The orthotropic characteristics governing both static elastic modulus (MOE) and dynamic elastic modulus measurements directly inform the structural performance indices and dynamic behaviour investigations central to the current research.

2.2.2 Variability, Defects, and Grading

Timber's mechanical properties including modulus of elasticity (MOE), modulus of rupture (MOR), tensile strength, and shear resistance are vary considerably across species, creating fundamental challenges for structural design that demand significantly more conservative approaches than homogeneous engineered materials like steel or concrete. These properties are influenced by moisture content, grain orientation, growth conditions, and natural defects, creating a complex matrix where changes in one parameter cascade through the entire performance profile (Muthumala et al., 2022). This inherent variability becomes particularly problematic in modular

timber bridge applications where inconsistent material properties between segments can lead to disproportionate load distribution and premature localized failures.

For structural timber used in bridge applications, MOE typically exhibits coefficient of variation (COV) ranging from 15-25%, while MOR shows greater variability with COV often exceeding 25-30% depending on species and grading quality (Grześkiewicz et al., 2023). Machine strength grading effectively classifies timber into higher strength classes with improved predictability, though inherent biological variability remains a fundamental characteristic that cannot be eliminated. Directional property variations compound this uncertainty, with compression strength perpendicular to grain typically measuring only 10-20% of parallel capacity, creating stress concentrations at connection interfaces where load paths necessarily traverse weak grain directions (Mishra et al., 2025).

Natural defects including knots, grain deviation, splits, and density variations that create additional variability sources requiring careful management through grading protocols. Knots represent discontinuities where branch growth interrupted normal grain patterns, creating localized zones of reduced tensile strength and stress concentrations that can reduce mechanical properties by 40-196% depending on location and orientation relative to loading (Cherry et al., 2022). These defect-induced property reductions prove particularly problematic at connection interfaces where stress concentrations already exist, potentially creating failure initiation sites that govern system capacity despite adequate average material properties.

For modular timber systems, material variability propagates through connection interfaces affecting global structural behaviour in ways continuous beams do not exhibit. When adjacent segments possess different elastic moduli, non-uniform EI distribution causes preferential load attraction to stiffer segments, potentially overloading these members while under-utilizing capacity in flexible segments. Mamat et al. (2025) concluded segmentation inherently reduces structural integrity with connections representing weakest elements where stiffness discontinuities concentrate stress and amplify material property variation effects. Jaramillo and Fischer (2023) demonstrated intermodular connection stiffness critically influences load distribution patterns, with connection rigidity variations directly affecting load transfer mechanisms. This creates a multiplicative rather than additive effect: material variability combines with connection compliance to produce system-level uncertainty exceeding that predictable from either factor alone. Vogiatzis et al. (2022) revealed

material property mismatches at component interfaces redirect load paths unpredictably, while Offerman and Bompa (2023) identified excessive connection quantities can degrade rather than enhance performance suggesting connection design must account for cumulative material variability effects across multiple interfaces.

Grading systems control material variability through standardized assessment protocols, with machine strength grading employing mechanical or optical sensors that measure properties with objective consistency, eliminating the subjective interpretation inherent to visual grading methods (Grześkiewicz et al., 2023). For modular applications, machine grading provides superior control over material variability, though even optimally graded timber retains inherent biological variation requiring appropriate design factors and system-level validation. In segmented beam systems where multiple timber pieces interact through mechanical connections, material variability amplifies stiffness uncertainty, with property variations across segments compounding connection flexibility effects to create unpredictable global structural response patterns that demand the quantitative performance assessment frameworks developed in this investigation.

2.2.3 Moisture Effects on Mechanical Behaviour

Moisture content fundamentally alters timber's mechanical properties through two primary mechanisms: cell wall plasticization that reduces elastic modulus, and water mass addition that affects density and dynamic response characteristics. Standards such as BS 5268 and Eurocode 5 specify maximum moisture content limits of 20% for structural applications to maintain adequate mechanical performance (Azmi et al., 2022), though timber MOE decreases progressively with moisture content variations above fibre saturation point through weakening of hydrogen bonds within the cellulose-hemicellulose matrix (D'Alvia et al., 2022). Experimental investigations on structural softwoods report MOE reductions ranging from 30-70% relative to baseline handbook values, reflecting combined effects of moisture content, material grade variation, and actual loading conditions (Forest Products Laboratory, 2010).

In modular timber systems, moisture-induced dimensional changes create critical challenges for connection performance. Western White Pine exhibits tangential shrinkage of approximately 7.4% and radial shrinkage of 4.1% from green to oven-dry conditions, with dimensional changes approximately proportional to moisture content

variations below fibre saturation point (Fu et al., 2023). Standards for bolted timber connections typically recommend clearance allowances of 1-2mm for bolt holes to accommodate dimensional movement while maintaining adequate bearing contact (Rajanayagam et al., 2023). Cyclic moisture exposure creates continuous stress cycling regimes that contribute to joint failures through mechanical mechanisms where inducing fatigue in connection hardware through repeated loading imposed by timber's dimensional instability on rigid connection elements. Connection systems must simultaneously provide structural reliability, accommodate movement, and maintain performance through multiple assembly cycles characteristic of modular applications (Yaghoubzadehfard et al., 2024). In segmented beams, differential moisture-induced swelling between adjacent segments exacerbates stress concentrations at connection interfaces, potentially causing bolt-hole deformation and progressive joint slip under sustained loading.

Dynamic response characteristics exhibit complex relationships with moisture content through multiple interactive mechanisms. Classical vibration theory predicts natural frequency according to $f = (1/2\pi)\sqrt{(k/m)}$, where moisture absorption increases timber mass through water uptake while simultaneously reducing elastic modulus. When MOE reductions of 30-70% occur simultaneously with mass increases of 10-15%, compound effects on vibrational characteristics require careful interpretation in structural analysis, particularly for modular segmented systems where multiple timber pieces with potentially different moisture equilibrium states interact through mechanical connections (Bahtiar et al., 2022).

Moisture content significantly influences damping characteristics through viscous energy dissipation mechanisms and enhanced viscoelastic effects, with damping ratios increasing 50-150% and natural frequencies decreasing 15-30% as moisture content rises from oven-dry to fibre saturation conditions (Cai et al., 2023; Hu et al., 2021). Dynamic modulus of elasticity demonstrates heightened sensitivity to moisture variations compared to static measurements, attributed to time-dependent viscoelastic effects more pronounced under rapid loading scenarios (Carreira et al., 2022).

For segmented timber bridge systems, moisture variation influences interpretation of both static and dynamic stiffness measurements. Static flexural testing determines MOE through load-deflection relationships under sustained loading where viscoelastic effects reach equilibrium, while dynamic modal analysis extracts MOE

from frequency measurements reflecting instantaneous elastic response. These measurement approaches capture different aspects of timber's time-dependent mechanical behaviour, with moisture content modulating the magnitude of discrepancy between static and dynamic values. In modular configurations where multiple segments interact through mechanical connections, differential moisture states between segments compound measurement uncertainty, affecting both global system stiffness calculations and local connection behaviour predictions essential for structural performance index development.

2.2.4 Dynamic Behaviour of Timber Beams

The dynamic response characteristics of timber structural systems represent critical performance parameters governed by frequency-stiffness relationships, damping characteristics, and material variability. Understanding these dynamic properties becomes essential for developing comprehensive performance evaluation frameworks, as timber's natural heterogeneity and moisture sensitivity introduce variability in both static and dynamic mechanical properties that must be systematically characterized to ensure reliable structural predictions.

The relationship between structural stiffness and natural frequency in timber beams follows fundamental vibration theory, where frequency provides a non-destructive indicator of structural condition and material properties. Opazo-Vega et al. (2021) demonstrate that the natural frequency of timber beams correlates directly with the modulus of elasticity through the classical relationship derived from Euler-Bernoulli beam theory, enabling calculation of dynamic modulus of elasticity (MOE *d*) from measured frequency data as a rapid assessment technique complementing traditional static testing methods. However, the practical application of frequency-based stiffness evaluation in modular timber systems introduces complexity beyond simple beam theory, as segmented configurations create discontinuities that alter mode shapes and frequency distributions compared to monolithic beams. Liu et al. (2019) note that multi-segment timber structures exhibit frequency characteristics influenced by both individual segment properties and connection stiffness, suggesting that modular systems may display frequency responses that cannot be predicted solely from component-level testing.

The frequency-stiffness relationship in timber structures demonstrates sensitivity to multiple factors including moisture content, temperature, and material defects, creating challenges for reliable MOE determination from dynamic measurements. Wang et al. (2022) report that timber's orthotropic nature results in directional dependency of dynamic properties, while natural defects introduce local stiffness variations that affect global frequency response. For modular systems specifically, Cepelka & Malo (2018) emphasize that connection details between segments act as semi-rigid joints that modify effective boundary conditions, potentially reducing natural frequencies compared to equivalent continuous beams even when individual segments possess identical material properties. This connection-induced frequency reduction becomes particularly significant when evaluating strengthened systems, as composite reinforcement may increase local stiffness while introducing material interface discontinuities that complicate dynamic response predictions.

Damping characteristics represent a second critical aspect of timber's dynamic behaviour, influencing vibration amplitude decay and energy dissipation capacity under cyclic loading conditions. Damping in timber structures arises from multiple sources including internal material damping, connection damping at bolted or adhesive joints, and structural damping from relative motion between components in assembled systems. Srikanth et al. (2022) quantify damping through the damping ratio (ζ), with reported values for solid sawn timber typically ranging from 1% to 10% depending on species, moisture content, and grain orientation. Comparative studies reveal systematic differences between solid timber and engineered wood products attributable to manufacturing processes and adhesive presence, with moisture content emerging as a dominant factor affecting damping characteristics through enhanced viscoelastic behaviour as absorbed water acts as a plasticizer (Wang et al., 2022).

The correlation between static and dynamic modulus of elasticity represents a critical validation parameter for timber structural assessment. Theoretical considerations suggest that MOE dynamic typically exceeds MOE static by 4% to 40% for sound timber, with this difference attributed to strain-rate dependent mechanical behaviour and the elimination of localized crushing effects present in static loading but absent in vibrational response (Olsson et al., 2024). However, this relationship exhibits considerable scatter influenced by moisture content, grain orientation, defect distribution, and testing methodology. Material variability compounds the challenge of establishing reliable static-dynamic MOE correlations, as natural variation in wood

properties introduces uncertainty that propagates differently through static versus dynamic testing protocols. Zhang et al. (2020) demonstrate that coefficient of variation (COV) values for MOE dynamic measurements are typically lower than those for MOE static in comparable specimen populations, attributed to the averaging effect inherent in global frequency measurements compared to localized stress-strain relationships in static bending. For modular timber systems specifically, Liu et al. (2019) emphasize that segment-to-segment property variation creates system-level uncertainty where the weakest component may govern static capacity while dynamic response reflects composite properties of all segments, potentially masking localized deficiencies that static testing would reveal.

For segmented timber beam systems, these dynamic characteristics where frequency-stiffness relationships, damping mechanisms, and static-dynamic MOE correlations that interact with connection discontinuities and material variability to create complex structural behaviour requiring systematic evaluation. The theoretical principles governing frequency response and damping in timber structures form the basis for experimental modal analysis (EMA) techniques, where measured vibration characteristics enable non-destructive assessment of structural stiffness and energy dissipation properties. These dynamic behaviour fundamentals provide the theoretical foundation for EMA-based stiffness evaluation methodologies applied in the current investigation of modular timber bridge systems.

2.2.5 Engineered Timber Systems

Engineered timber products which specifically glued laminated timber (Glulam), laminated veneer lumber (LVL) and cross-laminated timber (CLT) serve as important reference materials for understanding mechanical property variability and stiffness consistency in timber structural systems. This comparison is necessary because engineered products represent the upper bound of achievable material uniformity through controlled manufacturing, against which the inherent variability of solid timber can be contextualized. For modular beam systems where stiffness degradation and load distribution depend critically on material consistency, understanding this performance differential provides essential baseline expectations for experimental analysis and design optimization.

Glulam achieves reduced property variability through lamination of multiple timber layers with grain oriented parallel to the member length, strategically positioning higher-grade laminations in critical stress zones while accommodating lower grades in less-stressed regions (Yang et al., 2023). This controlled layering disperses natural defects throughout the cross-section rather than concentrating them in critical load paths, fundamentally altering stress concentration patterns that govern solid timber failure modes. LVL extends this principle through thin wood veneers arranged in parallel orientations, creating highly uniform products with exceptional modulus of elasticity (MOE) consistency (Duriot et al., 2021).

The fundamental mechanical advantage of engineered timber manifests through dramatic reduction in coefficient of variation (COV) for stiffness properties, creating design reliability essential when multiple prefabricated components must function cohesively within integrated assemblies. Solid timber exhibits large performance variability due to natural inconsistencies including growth conditions, defect distribution, and anisotropic behaviour (Fan et al., 2024). Conversely, engineered products achieve controlled variability through adhesive bonding quality, moisture content management during manufacturing, and strategic density distribution across laminae (Oliveira et al., 2025). This uniformity enables specification of narrow property ranges that facilitate more aggressive design optimization than possible with solid timber's wide performance bands. For stiffness-based analysis in modular systems, engineered timber products effectively establish an upper-bound reference for stiffness stability, against which solid timber modular beams are expected to deviate due to inherent material heterogeneity and natural defect presence. The stiffness degradation observed in segmented solid timber beams can thus be contextualized using engineered timber behaviour as the theoretical maximum achievable through material uniformity alone, isolating segmentation effects from material variability effects in experimental analysis.

Wood's hygroscopic nature introduces mechanical property fluctuations when exposed to moisture. In engineered products, moisture influences adhesive bond stiffness and introduces delamination risk that can compromise load transfer continuity across lamination interfaces, fundamentally altering the continuous stress distribution that defines engineered timber's mechanical advantage (Shirmohammadi, 2023). This moisture-stiffness relationship proves particularly relevant when comparing dynamic and static MOE measurements, as moisture content variations between testing

conditions can introduce systematic discrepancies in observed stiffness values independent of structural configuration effects.

Mechanical connections interrupt lamination continuity in engineered timber, creating stress concentrations at bolt holes that propagate differently than in solid timber due to adhesive interface presence. These connections introduce semi-rigid behaviour that reduces the stiffness benefits achieved through controlled lamination, demonstrating that engineered timber is not immune to stiffness loss at joints despite superior base material consistency. The interaction between connection compliance and lamination architecture represents a critical consideration for modular systems employing engineered timber, where the mechanical advantages of uniform material properties can be systematically negated by inadequate connection detailing.

This investigation employs solid timber that specifically Western White Pine rather than engineered products for modular beam construction, reflecting both practical deployment constraints and research objectives focused on material systems typical of field-deployed forest bridge applications. Engineered timber's established mechanical behaviour provides the theoretical benchmark for interpreting stiffness degradation observed in solid timber modular configurations, enabling quantification of how material variability compounds with segmentation effects to influence overall structural performance. The performance differential between engineered and solid timber thus contextualizes experimental findings, establishing whether observed stiffness reductions result primarily from joint compliance, material heterogeneity, or synergistic interaction between both factors where a distinction essential for developing design strategies that appropriately balance material selection against segmentation requirements in practical modular bridge systems.

2.2.6 Implications for Modular/Segmented Beams

The transition from continuous timber members to segmented modular configurations fundamentally alters structural behaviour through three mechanisms: (1) segmentation converts material behaviour into system-level performance where component interactions govern capacity, (2) mechanical connections act as amplification points that magnify material uncertainties, and (3) discontinuity effects create multiplicative rather than additive degradation pathways. Understanding these

mechanisms proves essential for developing design methodologies that account for fundamental differences between monolithic and segmented timber structures.

Timber's orthotropic nature creates directional dependency in load transfer that becomes critically problematic at connection interfaces. While continuous beams efficiently transfer loads along favourable longitudinal grain directions, segmented configurations force mechanical fasteners to accommodate perpendicular-to-grain loading that exploits timber's weakest directional properties. Dobeš et al. (2022) demonstrate that bolted connections create stress concentrations where local grain orientation relative to fastener placement determines load transfer efficiency. In multi-segment assemblies, each connection introduces potential grain misalignments that cannot be systematically controlled in solid timber procurement, creating cumulative uncertainty in load path efficiency that increases with segment quantity. Orthotropy becomes critical only when joints redirect load paths across weak grain directions where a condition absent in continuous beams but unavoidable in segmented systems.

Natural variability in timber properties introduces performance uncertainty that multiplies when multiple segments must function as integrated systems. Liu et al. (2019) demonstrate that segment-to-segment variation creates system-level uncertainty where component properties combine probabilistically rather than deterministically. A five-segment beam does not average the properties of five segments where it creates five potential weak links where the lowest-performing segment may disproportionately govern system capacity. The coefficient of variation (COV) for system stiffness thus exceeds individual material COV because segmentation introduces additional uncertainty sources: connection tolerance variations, assembly precision limitations, and load distribution asymmetries that compound material heterogeneity (Zhang et al., 2020). This behaviour invalidates the assumption that average material properties govern modular beam performance where system design must instead account for probabilistic worst-case combinations that continuous members do not exhibit.

Timber's hygroscopic behaviour generates particularly problematic consequences in mechanically connected assemblies where differential movement between segments introduces concentrated stress at joint interfaces. Differential moisture absorption rates between segments create relative dimensional changes that fasteners must accommodate through bearing deformation, potentially inducing progressive bolt loosening that reduces connection stiffness (Gong et al., 2022). Wang et al. (2022) demonstrate that moisture-damping relationships introduce systematic

inconsistencies in frequency response between segments, complicating structural health monitoring. Moisture effects drive: (1) connection slip through differential swelling, (2) stiffness degradation through bolt-hole deformation, and (3) dynamic inconsistency through segment-specific damping variations.

Continuous-beam vibration theory fails for segmented timber beams because connection compliance introduces frequency-dependent stiffness characteristics that conventional analysis cannot capture. While Opazo-Vega et al. (2021) demonstrate that natural frequency measurements provide stiffness assessment in continuous beams, Liu et al. (2019) reveal that multi-segment structures exhibit frequency characteristics influenced by both material properties and connection stiffness in ways preventing direct application of continuous beam theory. Cepelka & Malo (2018) establish that mechanical joints act as semi-rigid interfaces creating mode shapes fundamentally different from equivalent continuous members even when timber segments possess identical material properties. Connection compliance contributes differently to static deflection (through bearing deformation under sustained load) versus dynamic response (through inertial effects and vibration-induced microslip). The MOE dynamic/MOE static correlation factors established for continuous timber cannot be reliably applied to segmented systems, demanding integrated experimental validation capturing static-dynamic relationships specific to segmented configurations.

Engineered timber products quantify how much observed stiffness reduction originates from material variability versus segmentation effects. The dramatic COV reduction in engineered products compared to solid timber (Oliveira et al., 2025) isolates material heterogeneity as a quantifiable factor that, when minimized, reveals irreducible stiffness loss attributable purely to segmentation and connection compliance. However, segmentation effects persist even under ideal material uniformity that connections interrupt continuity creating stress concentrations regardless of material quality (Fan et al., 2024). For this investigation employing solid timber, the engineered timber benchmark confirms that observed stiffness reduction reflects synergistic interaction between connection compliance and material heterogeneity.

Three fundamental claims characterize segmented timber behaviour which the first where the segmentation amplifies stiffness loss through multiple simultaneous mechanisms: Each connection reduces effective continuity through fastener bearing deformation (Dobeš et al., 2022), stress concentration-induced microcracking around

bolt holes (Gong et al., 2022), and progressive loosening under cyclic loading. These mechanisms operate concurrently, creating cumulative stiffness reduction that increases non-linearly with segment quantity. Design implication: Stiffness prediction cannot simply multiply segment properties by connection efficiency factors that is non-linear interaction effects require experimental calibration.

Second, segmentation amplifies uncertainty through probabilistic property combination: System performance reflects statistical distribution of segment properties rather than average characteristics, with lowest-performing segments potentially governing capacity (Zhang et al., 2020). Connection tolerance variations introduce assembly-dependent behaviour absent in continuous members. Design implication: Confidence intervals for capacity predictions widen with each segment interface, requiring either conservative design negating modularity benefits or acceptance of higher failure probabilities.

Third, the segmentation invalidates static-dynamic assumptions through rate-dependent connection behaviour: Connection compliance contributes differently across loading regimes where quasi-static bearing deformation behaves fundamentally differently than dynamic response governed by inertial effects (Cepelka & Malo, 2018). Frequency-stiffness relationships established for continuous timber cannot be directly applied where mode shapes reflect composite material-connection behaviour. Design implication: Dynamic property prediction requires separate characterization rather than correlation factor application.

2.3 Modular Bridge Systems and Structural Implications of Segmentation

Building This section examines modular bridge systems from a structural mechanics perspective, focusing on how segmentation fundamentally alters load transfer behaviour and system-level performance characteristics. The analysis progresses systematically from historical military engineering origins that established modular construction principles, through the structural characteristics that distinguish segmented systems from continuous bridges, to the specific discontinuity mechanisms where joint slip, localized rotation, and stress concentration that govern performance. Particular emphasis is placed on how these localized phenomena accumulate across multiple connection points to produce system-level consequences including global stiffness reduction, deflection amplification, and altered dynamic response. The section

identifies critical knowledge gaps in current modular bridge literature, which emphasizes deployment logistics and environmental benefits while providing limited quantitative frameworks for predicting structural performance penalties inherent to segmentation. Understanding these structural mechanics challenges provides essential context for the detailed investigations of connection systems, flexural behaviour, and dynamic characterization methodologies that follow.

2.3.1 Evolution of Modular Bridge Systems

Modular bridge systems originated in military engineering, where operational demands necessitated rapid deployment, prefabrication, and field assembly under constrained conditions. The Bailey Bridge, developed during World War II, established the foundational principle of modular construction through standardized, interchangeable panels that could be assembled without heavy machinery (Ostrowska & Chmielewski, 2023). This innovation demonstrated that structural systems composed of discrete, prefabricated segments could provide comparable load-carrying capacity to conventional bridges while offering tactical advantages through transportability and reversibility. Post-war civilian adaptation revealed broader applicability in temporary access and logistically constrained deployment scenarios

The transition from military to civilian applications maintained the core advantages of modular design where lightweight construction, prefabrication, and reusability, while addressing additional serviceability requirements including durability under repeated deployment and adaptability to variable site conditions (Shabaev, 2021). In forestry contexts specifically, these characteristics aligned with operational needs for temporary crossing infrastructure that could be deployed across challenging terrain without extensive site preparation. Modern modular bridge systems, exemplified by the Lessard Logging Bridge and Yard King Portable Bridge, combine prefabricated steel and timber components to balance structural performance with field deployment constraints. Recent developments have focused on optimizing load configurations and enhancing assembly mechanisms to reduce deployment time while maintaining structural integrity (Chordà-Monsonís et al., 2024).

The engineering significance of modular bridge systems lies not merely in their operational advantages but in their fundamental structural characteristic: segmentation. Unlike monolithic continuous bridges where load paths remain uninterrupted

throughout the span, modular systems achieve their transportability and assembly advantages through division into discrete segments connected via mechanical interfaces. This segmentation introduces structural discontinuities at connection points, fundamentally altering how forces are transmitted through the structure. While prefabrication enables quality control and rapid assembly, the resulting segmented configuration creates a structural system where behaviour is governed by interface mechanics rather than member properties alone. These advantages are achieved structurally through segmentation, which fundamentally alters load paths and stiffness continuity compared to continuous bridge designs.

2.3.2 Structural Characteristics of Modular Bridge Systems

Modular bridge systems represent a fundamental departure from conventional continuous bridge designs, distinguished by their intrinsic structural behaviour rather than merely assembly methodology. While continuous bridges achieve load-carrying capacity through uninterrupted material continuity, modular systems derive performance from coordinated action of discrete segments connected through mechanical interfaces. The presence of joints fundamentally alters force propagation, transforming the design problem from member sizing to interface mechanics and system-level integration (Zhang et al., 2024). Unlike continuous bridges where structural analysis can assume perfect displacement and rotation continuity, modular systems require explicit consideration of connection behaviour, as discrete joints introduce discontinuities that govern overall structural response (Ferrara et al., 2022).

Classical Euler-Bernoulli beam theory which assumes continuous members with perfect displacement compatibility and negligible joint effects that provides the foundational framework for analysing timber structural behaviour. However, modular bridge systems fundamentally violate these assumptions through discrete joints that interrupt structural continuity, creating a critical conceptual shift where interface characteristics rather than member properties alone govern behaviour. Modular systems must achieve load transfer across discrete connections where bending moments and shear forces cannot be transmitted through material continuity but must instead be managed through bearing contact, friction, and mechanical fastening at joint interfaces (Khan et al., 2021; Lakshmidevi et al., 2025). The efficiency of this load transfer depends critically on joint stiffness, which directly influences moment-rotation

response of individual segments and consequently determines global structural behaviour (Ferrara et al., 2022). This dependency means modular bridge behaviour cannot be predicted through simple scaling of continuous bridge theory where joints introduce fundamentally different structural characteristics requiring specialized analysis approaches.

The loss of continuity creates localized compliance at connection points that disrupts ideal load paths assumed in classical beam theory. Where continuous bridges transmit forces smoothly through uninterrupted material following predictable equilibrium trajectories, joints create discontinuity points where load paths must redirect through connection mechanisms, inducing stress concentrations and localized deformations that continuous beam theory fails to capture (Romaniuk et al., 2021). This localized compliance manifests as relative displacement and rotation between adjacent segments which phenomena that accumulate across multiple joints to produce system-level effects on deflection and stiffness exceeding predictions based solely on member properties. Research on segmented bridge systems reveals that shear deformation at joint interfaces contributes significantly to overall deflection, with joint compliance effects becoming increasingly dominant as segment numbers increase (Liu et al., 2023). Furthermore, under dynamic loading conditions, joint characteristics influence energy dissipation mechanisms and vibrational response in ways that have no direct analog in continuous systems, as interfaces provide additional degrees of freedom for relative motion between segments (Salehi et al., 2021).

The governing role of joint stiffness in modular systems establishes connection design as the primary determinant of structural performance, shifting analytical focus from member capacity to interface mechanics. Unlike continuous bridges where connection design is secondary to member sizing, modular systems require joints to provide sufficient rotational and translational stiffness for system-level structural integrity while simultaneously accommodating assembly tolerances and enabling prefabrication advantages. Experimental investigations demonstrate that joint stiffness directly influences global structural characteristics including load distribution, deflection patterns, and failure modes (Duanmu et al., 2025). For timber-based modular bridges specifically, mechanical joints typically represent the weakest points in load paths, with joint capacity often governing overall system capacity rather than individual timber member load-bearing capability (Mamat et al., 2025). The design challenge lies in achieving adequate joint stiffness to prevent excessive relative motion between

segments while avoiding overly rigid connections that compromise assembly advantages justifying modular construction. Research on various connection types reveals substantial variation in stiffness characteristics and corresponding effects on structural behaviour , indicating that connection selection and detailing fundamentally determine whether modular systems can achieve performance comparable to continuous alternatives (Lakshmidevi et al., 2025; Farajian et al., 2024).

Structural implications of segmentation extend beyond static load considerations to encompass dynamic response characteristics, serviceability performance, and progressive failure mechanisms distinguishing modular systems from continuous counterparts. Inter-module connections determine both stiffness under gravity loading and lateral behaviour during seismic events, with connection rotational capacity directly affecting energy dissipation and force redistribution capabilities (Khan & Yan, 2021; Vedyakov et al., 2023). The discrete nature introduces progressive joint failure possibilities, where inadequate connection capacity at one interface can trigger load redistribution overloading adjacent joints that creating failure propagation mechanisms absent in continuous bridges (Pan et al., 2024). Additionally, multiple joints increase sensitivity to construction tolerances and long-term effects such as connection loosening, requiring explicit consideration in serviceability limit state design. Understanding these distinctions is essential for recognizing that modular bridges cannot be designed as simply scaled-down continuous bridges with added connections where they represent fundamentally different structural systems where interface mechanics dominate performance characteristics and design methodology must explicitly account for multiple discrete connections throughout the span.

2.3.3 Segmentation- Segmentation-Induced Structural Discontinuities

The division of modular bridge systems into discrete segments introduces structural discontinuities at connection points that fundamentally violate core Euler-Bernoulli beam theory assumptions which particularly perfect continuity and uniform stiffness distribution, thereby altering mechanical behaviour through three primary mechanisms: joint slip, localized rotation, and stress concentration. In segmented configurations, mechanical fasteners and bearing interfaces create discrete zones where displacement compatibility and force transmission occur through fundamentally different mechanisms than material continuity. Understanding these discontinuity

effects is essential for predicting system-level performance, as localized phenomena at individual joints accumulate across multiple segments to produce global effects on stiffness, deflection, and load distribution that cannot be captured through isolated member analysis alone.

Joint slip represents the first critical discontinuity mechanism, manifesting as relative displacement between connected segments under shear loading despite mechanical fasteners intended to prevent such movement. This phenomenon occurs because even properly tightened bolted connections exhibit compliance due to bearing deformation in timber surrounding fastener holes, elastic deformation of fasteners themselves, and microscopic irregularities at contact surfaces preventing perfect load transfer (Wang et al., 2023). The magnitude of slip depends critically on interface characteristics, with variations in material properties across connection interfaces generating substantial localized slip, particularly where harder fastener materials bear against softer timber substrates (Gu et al., 2021). This slip introduces fundamental departure from continuous beam assumptions: while continuous structures maintain perfect shear transfer along their length, segmented systems experience incremental relative displacements at each joint that accumulate to produce system-level effects exceeding those predicted by member deformation alone. The structural significance lies in recognizing that joint slip effectively reduces the structure's ability to resist shear forces, as energy that would contribute to elastic deformation in continuous systems is instead dissipated through frictional sliding and bearing deformation at interfaces. Segmentation creates stress concentration zones at joint boundaries where load paths must redirect through fastener bearing, inducing localized stress states that can exceed average section stresses by substantial factors (Evans et al., 2022). These concentrated stress zones become potential initiation sites for progressive damage, as material yielding or fastener bearing failure at one joint can trigger load redistribution increasing demands on adjacent connections.

Localized rotation at connections constitutes the second critical discontinuity mechanism, arising from semi-rigid rotational behaviour of mechanical fastener joints under bending moments. Unlike idealized rigid connections maintaining zero relative rotation between members, or perfectly pinned connections transmitting no moment, timber joints fastened with bolts or dowels exhibit intermediate semi-rigid behaviour characterized by finite rotational stiffness and corresponding moment-rotation relationships (Gauthier-Turcotte et al., 2022). This semi-rigid response occurs because

fastener-based connections allow small relative rotations through combined effects of bearing deformation in timber around fasteners, bending deformation of fasteners themselves, and geometric rearrangement of connection components under load. Experimental investigations demonstrate that these semi-rigid joints accommodate moderate rotational deformations while maintaining load-carrying capacity, with rotational stiffness depending strongly on fastener configuration, timber density, and connection geometry (Kasal et al., 2025). The structural implications are profound: each joint effectively introduces an additional degree of freedom in the structural system, allowing relative rotation between segments that increases overall deflection beyond that predicted by member flexibility alone. Research on lattice structures with semi-rigid joints reveals that rotational flexibility at connections reduces effective flexural stiffness of assembled systems, with magnitude of reduction increasing as joint rotational stiffness decreases (Yoshino & Kimura, 2025). This stiffness reduction occurs because rotational deformation at joints contributes directly to member end rotations without requiring curvature-induced strain energy in members themselves, essentially providing a "softer" load path than would exist in rigidly connected systems. Segmented beams consequently experience greater deflections under equivalent loading compared to continuous beams of identical member properties, with differences attributable entirely to joint rotation effects. Furthermore, rotational behaviour influences force distribution across structures, as semi-rigid connections partially release bending moments rather than fully transmitting them between segments, altering internal moment distribution from that assumed in rigid-connection analysis (Taheripour et al., 2022).

Stress concentrations at fastener locations represent the third fundamental discontinuity mechanism, arising from geometric discontinuities introduced by bolt holes and local intensification of bearing stresses where fasteners contact timber. Drilling holes for mechanical fasteners necessarily interrupts continuity of load-bearing fibres in timber members, creating geometric stress raisers where applied loads must redistribute around voids. The severity of these stress concentrations depends on hole diameter relative to member dimensions, with larger fastener holes producing more pronounced stress intensification effects that can reduce local load-carrying capacity and accelerate damage initiation (Yu et al., 2025). Additionally, the bearing mechanism through which loads transfer from fasteners to timber creates highly localized compression zones where contact stresses significantly exceed average stresses in

connected members, with peak stresses occurring at fastener-timber interfaces where load concentration is most severe (Wu et al., 2023). These elevated stress states become critical because they can induce localized yielding, fibre crushing, or crack initiation at stress levels well below member nominal strength capacity. The implications extend beyond local damage concerns to affect overall structural stiffness, as localized damage accumulation around fastener zones progressively reduces connection stiffness and increases compliance, contributing to system-level stiffness degradation over time (Yang et al., 2025). Under cyclic loading conditions, stress concentration effects become particularly significant, with repeated loading causing progressive bearing damage, hole elongation, and connection loosening that incrementally degrades joint performance (Durão et al., 2023). Geometric arrangement and fibre orientation around fastener holes also influence stress concentration severity, with certain configurations either mitigating or exacerbating stress intensification depending on how load paths interact with material grain direction and connection geometry (Mohamed et al., 2024).

The cumulative effects of multiple joints introduce non-linear stiffness degradation that represents perhaps the most critical characteristic distinguishing segmented systems from continuous structures. The stiffness reduction produced by multiple joints is not simply additive rather, it exhibits multiplicative or compounding characteristics where each additional joint reduces system stiffness by a percentage depending on the degraded state created by previous joints (Cai et al., 2021). This non-linear behaviour occurs because joint-induced discontinuities affect not only local compliance at connection points but also alter global load distribution and deformation patterns throughout structures. Research on multi-segment systems demonstrates that stiffness reduction accelerates with increasing numbers of joints, with five-segment configurations showing disproportionately greater stiffness reductions than would be predicted by linearly scaling effects observed in two-segment systems (Zhou et al., 2024). The physical mechanism underlying this non-linearity involves complex interactions between joint compliance, load redistribution, and progressive damage accumulation: as joints deform, they redistribute loads to adjacent connections in ways that increase local demands, which in turn accelerates damage accumulation and further compliance increases in a self-reinforcing cycle. The combined effects of slip, rotation, and stress concentration at multiple joints produce system-level flexibility that fundamentally alters the structure's effective flexural rigidity (EI), manifesting through increased deflections, modified natural frequencies, and altered load distribution

patterns (Liu et al., 2023). Environmental factors such as moisture exposure can accelerate joint degradation through mechanisms that interact non-linearly with mechanical loading effects, producing failure mode transitions and accelerated performance deterioration in aged connections (Niu et al., 2023). Understanding these non-linear cumulative phenomena is essential for recognizing that the structural challenge in modular bridge design lies not in optimizing individual joints but in managing system-level consequences of multiple interacting discontinuities distributed throughout the span.

2.3.4 System-Level Consequences of Segmentation

The localized discontinuities at individual joints manifest at the system level through three primary consequences that fundamentally distinguish segmented bridge behaviour from continuous beam performance: global flexural stiffness reduction, deflection amplification, and altered dynamic response characteristics. These system-level effects emerge from cumulative influence of multiple connection points distributed throughout the span, where combined impact of joint slip, rotational flexibility, and stress concentration produces structural behaviour that cannot be predicted through simple scaling of single-joint properties or linear superposition of local effects. Understanding these system-level phenomena is essential for recognizing that modular bridge design requires fundamentally different analytical approaches than continuous structures.

Global flexural stiffness reduction represents the most fundamental system-level consequence of segmentation, occurring because segmentation introduces effective flexural hinges at connection points that allow independent movement between adjacent segments. Research demonstrates that this stiffness reduction is attributable to discontinuous nature of load transfer across joints, where rotational compliance at connections effectively reduces the structure's resistance to bending deformation (Hannard et al., 2021). The physical mechanism underlying this reduction lies in how segmentation alters deformation response: whereas continuous beams resist bending through material strain distributed along the entire length, segmented systems must accommodate additional deformation arising from relative rotation and slip at each joint, effectively introducing "soft spots" in otherwise stiff members. Studies on composite and precast segmental beams reveal that these internal discontinuities

produce flexibility and resultant stiffness reductions more pronounced than anticipated from member properties alone, with presence of mechanical joints complicating flexural behaviour compared to monolithic construction (Yan et al., 2022). Any discontinuities or variations in sectional stiffness attributed to segmentation must be explicitly accounted for in limit-state analysis, as they directly influence deflection characteristics and overall performance in ways that homogeneous beam theory does not capture (Tao et al., 2021). Experimental evidence from segmental reinforced concrete structures demonstrates that reduced stiffness occurs progressively as joints open under shear and bending loads, with stiffness degradation compromising structural integrity in ways that manifest only at the system level rather than through isolated joint testing (He et al., 2024). This progressive nature highlights a critical characteristic: the effective flexural rigidity (EI) is not a constant material property but rather a system-level parameter depending on joint configuration, load level, and interaction between multiple connection points throughout the span.

Deflection amplification represents the direct consequence of reduced system stiffness, with increased joint flexibility contributing to mid-span deflections that exceed predictions based on member properties and standard deflection formulas for continuous beams. Research on built-up steel beams reveals that slippage within bolted connections leads to notable mid-span deflection increases even when global beam rigidity remains nominally unchanged, indicating that flexible connections amplify deformations under service loads through mechanisms not captured in rigid-connection analysis (Both et al., 2022). This deflection amplification becomes particularly pronounced in systems with multiple connection interfaces, where cumulative compliance of distributed joints produces mid-span displacements significantly greater than would occur in continuous equivalents. Studies on bridge structures with multiple connections confirm that variations in connection stiffness substantially affect mid-span deflection, establishing a direct causal relationship between connection characteristics and system-level deformation response (Guan et al., 2024). The physical mechanism involves how additional flexibility at joints creates effective "hinges" allowing greater rotation under bending loads, with each connection point contributing incremental rotation that accumulates to produce larger mid-span displacements than would occur from member flexure alone. Research on composite timber-concrete systems demonstrates that slip behaviour at joint interfaces critically impacts both load distribution and resultant deflection, underscoring the importance of connection design

in managing deflection responses in segmented structures (Zhao, 2025). The practical significance for modular bridge serviceability is substantial: deflection limits established for continuous beam designs become inadequate when applied to segmented configurations, as additional compliance introduced by multiple joints can push deflections beyond acceptable thresholds even when member properties satisfy conventional design criteria. Experimental investigations confirm that increased joint flexibility under impact or dynamic loading conditions leads to even greater mid-span deflection amplification (Hunegnaw et al., 2024).

Altered dynamic response characteristics through stiffness degradation constitutes the third critical system-level consequence, with reduced flexural rigidity increasing the structure's sensitivity to vibrations and modifying natural frequencies in ways that affect both serviceability and resonance behaviour. The fundamental relationship between stiffness and dynamic properties means that any reduction in system stiffness necessarily shifts natural frequencies downward, potentially bringing them closer to excitation frequencies from traffic loads or environmental sources and thereby increasing vibration amplitudes through resonance effects. Research on structures with segmented stiffness distributions demonstrates that modifications to stiffness characteristics alter vibration modes and dynamic responses, with systems exhibiting increased sensitivity to dynamic instabilities that manifest as resonance and vibrational amplification when stiffness is reduced (Sheng et al., 2024). This sensitivity becomes particularly significant for modular bridges, where vehicle passage generates dynamic loads at frequencies that may coincide with the structure's modified natural frequencies, creating conditions for resonance that would not occur in stiffer continuous designs. Studies on mechanical systems with varying stiffness configurations reveal that nonlinear dynamic behaviour accentuates sensitivity to vibration at critical operational frequencies, with segmented stiffness models showing that systems become more susceptible to coupled vibrations when overall rigidity is reduced (Wang et al., 2024). The implications extend to vibration comfort considerations, as dynamic responses that satisfy acceptability criteria for continuous bridges may produce unacceptable vibration levels in segmented equivalents due to reduced damping and increased flexibility introduced by multiple joints. For modular bridge design, these dynamic considerations introduce serviceability criteria beyond static deflection limits: vibration amplitudes, frequency response, and resonance avoidance must be explicitly evaluated with

recognition that segmented configurations exhibit fundamentally different dynamic characteristics than continuous designs of equivalent member properties.

The system-level performance of segmented bridges is highly sensitive to variations in joint quality, assembly precision, and connector detailing, introducing sources of performance variability that are absent in continuous structural systems. Joint quality variations affect structural performance through their influence on connection stiffness and load transfer efficiency, with high-quality joints ensuring effective force transmission while poor-quality connections introduce additional compliance that compounds stiffness reduction inherent to segmentation (An et al., 2024). Assembly precision introduces another source of performance variability, with dimensional errors or improper tightening of mechanical fasteners reducing connection stiffness below design values and creating unpredictable variations in system behaviour (Chu et al., 2022). These sensitivities to construction quality and detailing mean that segmented bridge performance exhibits inherent variability that must be addressed through appropriate design margins, quality control procedures, and serviceability criteria explicitly accounting for potential deviations from ideal connection behaviour.

2.3.5 Limitations of Existing Modular Bridge Design Approaches

The existing body of literature on modular and portable bridge systems demonstrates pronounced emphasis on operational advantages, deployment logistics, and environmental sustainability, while systematically underrepresenting fundamental structural mechanics challenges governing actual field performance. Contemporary studies direct substantial attention toward assembly methodologies, material selection for transportability, constructability optimization, and life-cycle environmental impacts which all critical considerations for modular system viability, while providing comparatively limited investigation into how segmentation fundamentally alters structural behaviour through mechanisms of joint slip, rotational compliance, stress concentration, and cumulative stiffness reduction. The consequence of this research emphasis is that designers possess extensive guidance on maximizing deployment efficiency and minimizing environmental footprint, but lack quantitative frameworks for predicting structural performance penalties inherent to segmented configurations or systematically evaluating how joint numbers and characteristics influence system-level stiffness, deflection, and dynamic response.

Deployment efficiency and constructability emphasis reflects genuine practical concerns but leaves critical structural behaviour questions inadequately addressed. Research extensively documents how prefabrication, standardized components, and simplified assembly procedures enable rapid installation with minimal specialized equipment requirements (Robin et al., 2025). This deployment-centric perspective extends to investigations of operational versatility achieved through efficient packing, storage, and transportation characteristics (Akhtar & Ramkumar, 2023). Constructability studies concentrate on optimizing material combinations for structural efficiency while reducing construction waste, employing life cycle assessment tools to support sustainable material selections (Gulo & Aulia, 2025). While these contributions advance important dimensions of modular bridge design particularly regarding rapid deployment capabilities and environmental responsibility that they systematically avoid quantifying structural performance trade-offs that segmentation introduces. The literature establishes that modular bridges can be deployed quickly and assembled efficiently, but provides limited guidance on predicting how these operationally optimized designs will actually perform structurally under service loads, or how designers might systematically balance deployment advantages against stiffness penalties and deflection amplification effects inherent to segmented configurations.

Material selection research exhibits similar patterns, emphasizing logistics optimization, sustainability metrics, and supply chain efficiency while providing limited structural performance quantification specifically attributed to segmentation effects. Studies on cross-laminated timber and mixed-grade lumber applications focus predominantly on optimizing costs and mechanical properties within manufacturing constraints (Bayramoğlu et al., 2025). Emphasis on embodied energy comparisons between timber and conventional materials demonstrates sustainability advantages, with analyses showing timber structures exhibiting substantially lower embodied energy (Schenk & Amiri, 2022). While these material-focused investigations provide valuable insights into sustainable sourcing, manufacturing efficiency, and supply chain management which all essential for modular bridge viability that they do not systematically address how material selection interacts with segmentation to influence system-level structural performance. The literature establishes which materials optimize sustainability and logistics metrics, but offers limited guidance on selecting materials specifically to mitigate stiffness degradation, deflection amplification, or stress concentration effects that segmentation inherently introduces, leaving designers

without quantitative frameworks for material selection decisions accounting for unique structural challenges of segmented configurations.

Quantitative stiffness characterization represents perhaps the most critical gap, with existing literature providing limited characterization of how stiffness reduction due to segmentation manifests across different joint numbers and configurations, despite acknowledging that such reduction occurs. Studies reference stiffness reductions in segmented concrete beams during destructive testing, noting substantial percentage drops as damage progresses (Hu et al., 2024). Research on segment number effects demonstrates that reducing segments within precast columns improves structural integrity and energy dissipation capacity, confirming that segment count influences performance (Wang et al., 2025). However, these investigations typically examine specific configurations under particular loading conditions without developing generalized quantitative relationships between number of segments, joint characteristics, and resulting system stiffness that would enable designers to predict performance across varying configurations. The literature confirms that segmentation causes stiffness reduction and that joint flexibility affects global response, but lacks systematic frameworks quantifying how stiffness reduction scales with increasing segment numbers or how joint properties should be specified to achieve target system-level performance. This gap becomes particularly significant when considering that structural consequences discussed in Section 2.3.4 that including global stiffness reduction, deflection amplification, and altered dynamic characteristics which depend fundamentally on cumulative effects of multiple joints, yet designers lack quantitative tools to predict these cumulative effects during the design phase.

Static-dynamic correlation represents another critical knowledge gap that existing literature acknowledges but inadequately addresses. While research confirms that modular expansion joints influence both static and dynamic bridge performance under vehicular loads, and that stiffness variations complicate dynamic responses during traffic or seismic loading (Zhang et al., 2024), explicit quantitative relationships linking static stiffness degradation to dynamic property changes remain poorly characterized. Studies emphasize that dynamic effects become paramount in designing modular steel bridges as span lengths increase, with stiffer structures better absorbing dynamic impacts and reducing vehicle-induced vibrations (Chordà-Monsonís et al., 2024). However, the literature explicitly acknowledges that explicit correlations between static stiffness degradation and dynamic response in modular bridge systems

are infrequently addressed, with most studies examining these phenomena separately rather than establishing quantitative predictive relationships between them. This represents a fundamental limitation for modular bridge design: while designers understand that segmentation reduces static stiffness and that this reduction affects dynamic behaviour, they lack systematic methods to predict dynamic properties from static measurements or to design for acceptable dynamic performance given known static stiffness characteristics. The practical consequence is that dynamic serviceability criteria including vibration comfort limits and resonance avoidance that cannot be systematically evaluated during design based on static stiffness properties that are more readily measured or predicted.

2.3.6 Synthesis: Modular Bridges as a Structural Mechanics Problem

The preceding analysis establishes that modular bridge systems represent fundamentally a structural mechanics problem governed by segmentation-induced discontinuities rather than merely an operational logistics challenge or material selection exercise. While the literature's emphasis on deployment efficiency, environmental sustainability, and constructability optimization addresses important practical considerations that justify modular approaches in specific applications, actual performance under service loads is determined primarily by how segmentation alters load paths, introduces compliance at joints, and produces cumulative stiffness reduction through multiple connection points. The structural behaviour of modular bridges cannot be adequately characterized through frameworks developed for continuous structures supplemented with connection design provisions rather, segmentation fundamentally transforms the analytical problem from one of member sizing under idealized boundary conditions to one of system-level response prediction accounting for discrete discontinuities whose cumulative effects dominate performance characteristics. This distinction has profound implications for design methodology: whereas continuous bridge design can proceed from material properties and section geometry to predict stiffness and deflection with reasonable accuracy, modular bridge design requires explicit quantification of how joint slip, rotational flexibility, and stress concentration at multiple interfaces combine to produce system-level behaviour that diverges substantially from predictions based on member properties alone.

The mechanisms through which segmentation alters structural behaviour where joint slip, localized rotation, and stress concentration that manifest through well-understood physical principles, yet their cumulative effects across multiple segments produce system-level responses exhibiting non-linear characteristics requiring specialized analytical frameworks. Joint slip occurs because mechanical connections cannot achieve perfect shear transfer assumed in continuous beam theory, with bearing deformation and interface compliance allowing incremental relative displacements that accumulate across multiple joints (Wang et al., 2023; Evans et al., 2022). Rotational compliance at semi-rigid timber connections introduces flexibility beyond that attributable to member curvature, with each joint effectively adding a rotational degree of freedom that increases deflections and alters moment distributions (Gauthier-Turcotte et al., 2022; Yoshino & Kimura, 2025). Stress concentrations at fastener locations create zones of elevated local stress and progressive damage that gradually reduce connection stiffness, contributing to time-dependent performance degradation (Wu et al., 2023). Most significantly, cumulative effects of multiple joints exhibit non-linear rather than additive behaviour , with stiffness reduction accelerating as segment numbers increase due to complex interactions between joint compliance, load redistribution, and progressive damage accumulation (Cai et al., 2021; Zhou et al., 2024). These phenomena collectively establish that modular bridge performance depends fundamentally on managing discontinuities distributed throughout the span rather than optimizing individual component properties.

The system-level consequences of segmentation which global stiffness reduction, deflection amplification, and altered dynamic response that distinguish modular bridges from continuous structures in ways that necessitate different design approaches and acceptance criteria. Segmentation reduces effective flexural rigidity by introducing compliance beyond that arising from material strain, with this stiffness reduction manifesting as a system-level parameter influenced by joint configuration and load level rather than a constant material property (Hannard et al., 2021; He et al., 2024). Deflections in segmented systems consequently exceed predictions from standard beam formulas by margins that increase with joint numbers, rendering deflection limits calibrated for continuous bridges inadequate for segmented equivalents (Both et al., 2022; Guan et al., 2024). Dynamic characteristics similarly diverge from continuous bridge behaviour , with reduced stiffness shifting natural frequencies and increasing vibration sensitivity in ways that affect serviceability but remain poorly characterized

in design guidance (Sheng et al., 2024; Wang et al., 2024). These system-level effects underscore that modular bridges require performance evaluation frameworks addressing cumulative discontinuity effects rather than member-level capacity checks, yet existing literature provides limited quantitative tools for such evaluation.

Addressing the structural mechanics challenges of modular bridges necessitates developing quantitative frameworks that explicitly account for segmentation effects on system-level performance rather than treating connections as supplementary considerations to member design. The critical knowledge gaps identified in Section 2.3.5 including limited quantification of stiffness reduction across varying segment configurations, absent systematic frameworks relating joint numbers to system performance, and poorly characterized correlations between static and dynamic properties that represent fundamental limitations in current design methodology that force reliance on conservative assumptions or empirical adjustments lacking theoretical foundation. Advancing modular bridge technology beyond its current applications requires establishing systematic relationships between design parameters (segment numbers, joint configurations, material properties) and performance outcomes (stiffness, deflection, dynamic response) that enable prediction rather than merely documentation of behaviour. The subsequent sections of this chapter address specific aspects of this structural mechanics problem: Section 2.4 examines connection systems and their influence on load transfer efficiency, Section 2.5 investigates flexural behaviour of timber members and segmented configurations, and Section 2.7 explores dynamic characterization methodologies. Understanding modular bridges as structural mechanics problems governed by segmentation-induced discontinuities rather than operational logistics challenges provides the conceptual foundation for these detailed investigations into how discrete connections and member properties combine to produce system-level performance in ways that continuous bridge theory cannot adequately represent.

2.4 Timber Mechanical Connections and Joint Behaviour

While modular bridge systems offer compelling sustainability and adaptability advantages, their structural reliability ultimately depends on mechanical connection integrity. This section examines critical vulnerability points where timber's anisotropic behaviour intersects with stress concentrations and environmental degradation

pathways. The analysis explores connection design strategies, fibre-reinforced polymer reinforcement approaches, moisture protection treatments, and dynamic performance under cyclic loading. By investigating established engineering practices alongside emerging joint innovations, this section identifies critical research gaps in integrated connector performance that limit system-level optimization, positioning mechanical connections as fundamental determinants of modular timber bridge reliability in demanding forest applications.

2.4.1 Role and Vulnerability of Mechanical Connections in Modular Timber Bridges

The mechanical performance of modular timber bridges fundamentally depends on their most critical vulnerability: the mechanical connections that enable modular functionality (Wdowiak-Postulak et al., 2023). These joints present an inherent engineering paradox, requiring simultaneous rigid load transfer and flexible assembly/disassembly capabilities while creating unavoidable stress concentration points that interrupt structural continuity and serve as natural failure initiation sites. Bolted connections exemplify this complexity by offering installation convenience and reusability while introducing multiple interdependent failure pathways through timber's anisotropic behaviour, where loading perpendicular to grain orientation triggers catastrophic splitting and group tear-out failures, particularly with inadequate edge distances or insufficient reinforcement. Moisture-induced dimensional changes intensify these vulnerabilities by altering load distribution patterns and creating additional stress concentrations at bolt interfaces, while improper bolt spacing geometry creates cascade effects leading to uneven load sharing that amplifies local stresses and accelerates fatigue damage under repeated loading (Rebouças et al., 2022). Installation precision becomes equally critical, as over-tightening or misalignment compounds inherent vulnerabilities through residual stresses that reduce connection capacity to withstand service-level cyclic loading.

However, current research reveals significant limitations in understanding mechanical connector behaviour, as studies primarily examine bolted connection performance under isolated rather than integrated system conditions. While Dobeš et al., (2022) identify timber-bolt interfaces as critical vulnerability points where stress concentrations and stiffness discontinuities emerge, and Guo & Shu, (2019)

demonstrate that bolt arrangement and joint configuration significantly influence load-carrying capacity and moment resistance in timber assemblies, comprehensive investigations addressing how connector configurations influence global beam behaviour under combined flexural and dynamic loading remain limited. Liu et al., (2022) established that variations in bolt spacing and quantity substantially affect bending performance, yet translating these insights to fully integrated modular timber systems represent a critical knowledge gap that impedes optimal connector design for forest bridge applications where system-level performance integration determines structural reliability and operational success.

A critical limitation in current mechanical connection research is the insufficient emphasis on quantitative load-bearing capacity verification under realistic service conditions. While numerous studies examine connection performance through ultimate load testing, few provide comprehensive analysis of safety factors, stress distribution patterns, and load transfer efficiency that are essential for practical design implementation. Dobeš et al. (2022) demonstrate that stress concentrations at timber-bolt interfaces can reach 2.5-4.0 times nominal design values, yet systematic methodologies for incorporating these amplification factors into load-bearing capacity calculations remain underdeveloped. This knowledge gap creates uncertainty in connection design, where engineers must rely on conservative assumptions that may result in over-designed systems or, conversely, inadequate safety margins. Furthermore, the interaction between load-bearing capacity and connection compliance presents complex design challenges that current literature inadequately addresses. Song et al. (2024) establish that bolted connection performance varies significantly with joint configuration, but comprehensive frameworks linking experimental capacity measurements to theoretical design models remain limited. This limitation is particularly pronounced in modular systems where multiple connections must operate collectively, requiring understanding of load redistribution mechanisms and capacity sharing among connection points that extends beyond individual joint analysis.

2.4.2 Reinforcement Strategies and Hybrid Joint Configurations

Strategic reinforcement of timber joints represents a fundamental shift from managing inevitable brittle failures to engineering controlled plastic deformation mechanisms through fibre-reinforced polymers, self-tapping screws, and toothed

connectors that create alternative load paths redistributing stress concentrations away from critical timber fibres (Gubana et al., 2023; Wdowiak-Postulak et al., 2023). This approach transforms failure progression from catastrophic crack propagation to gradual yielding, where reinforcement materials absorb and dissipate energy through controlled deformation, with self-tapping screws exemplifying this principle through high tensile strength and withdrawal resistance that creates secondary load-bearing networks maintaining joint integrity after initial timber yielding. Joint configuration optimization extends beyond material selection to encompass geometric arrangement of load transfer mechanisms, where moment-resisting designs incorporating aluminium or steel plates fundamentally alter modular connection behaviour, with Rebouças et al., (2022) demonstrating that properly engineered beam-column connections achieve enhanced ductility through controlled stress distribution preventing localized overloading while maintaining structural continuity across modular segments.

However, long-term performance faces critical challenges from environmental degradation mechanisms operating on multiple interconnected levels, where moisture cycling creates cascading deterioration through timber shrinkage generating contact pressure gaps while simultaneous thermal expansion of metal fasteners introduces differential movement accelerating bolt loosening and joint reduction that particularly pronounced in forestry operations where dynamic loading and humidity fluctuations create accelerated degradation pathways. Despite these strategic advancements, the literature reveals limited empirical data on how connector design parameters influence joint integrity and energy dissipation in fully integrated modular timber systems, with Liu & Xiong, (2018) establishing that bolt arrangement significantly impacts load capacity and ductility in timber connections while comprehensive investigations within complete modular assemblies remain scarce. Shi et al., (2023) demonstrated through cyclic testing that connection configuration significantly affects hysteretic behaviour and energy dissipation characteristics critical for modular applications exposed to dynamic loading, yet these findings have not been extended to understand how various fastening strategies perform within complete modular timber bridge systems where joint integrity directly impacts overall structural performance.

The design of adequate load-bearing capacity in modular timber connections requires systematic integration of material properties, geometric constraints, and load distribution mechanisms that current design methodologies insufficiently address. Traditional connection design approaches, developed for monolithic structures, often

inadequately account for the unique stress redistribution patterns and load sharing mechanisms inherent in segmented systems where multiple connections must function as an integrated load transfer network. Rebouças et al. (2022) demonstrate that connection capacity in timber assemblies depends not only on individual bolt capacity but on the complex interaction between connection spacing, load path geometry, and material compliance, suggesting that modular system capacity design requires systems-level analysis rather than component-level verification. The challenge intensifies when considering the probabilistic nature of timber material properties and the precision limitations of field assembly conditions, where connection capacity must account for variability in both material performance and installation quality. This necessitates robust safety factor determination based on experimental validation of actual load-bearing performance rather than theoretical calculations alone, particularly for applications like forest bridges where maintenance access limitations and reliability requirements create unforgiving operational environments.

2.4.3 Predictive Modelling of Joint Behaviour Using FEA

Finite element analysis has emerged as a valuable computational tool for predicting failure modes and optimizing joint configurations in timber structures. Simulation-based studies have demonstrated that FEA can effectively model the anisotropic and nonlinear behaviour of timber joints, enabling engineers to assess load transfer paths, joint stiffness, and potential crack initiation zones before physical testing (Miao et al., 2022; Wang & Wang, 2023). This predictive capability is further enhanced through advanced techniques, such as the Extended Finite Element Method, which allows for the modelling of crack propagation without requiring predefined paths or extensive mesh refinement near crack tips (Berkouch et al., 2020). By simulating discontinuities and stress concentrations under multi-axial loading, these computational tools provide critical insights into failure mechanisms, particularly in hybrid or bolted-glued timber connections subjected to cyclic and environmental loading. When integrated into the early design phase, such advanced models improve the accuracy of mechanical assessments and support long-term performance planning. This is especially relevant for tropical deployments, where timber joints encounter complex combinations of mechanical stress, moisture fluctuations, and biological degradation that demand highly informed design interventions.

2.4.4 Protective Treatments and Environmental Resistance

Protective treatment strategies represent a critical analytical framework where multi-barrier defence systems must balance comprehensive environmental resistance against the practical constraints of modular assembly requirements. Integrated protection approaches combining coatings, sealants, and corrosion-resistant fasteners create redundant defence mechanisms that address distinct but interconnected degradation pathways from biological attack, electrochemical corrosion, and moisture-induced dimensional instability while requiring careful analysis of material compatibility to prevent unintended galvanic interactions between protective layers. Galvanized and stainless steel fasteners exemplify this strategic approach by providing inherent corrosion resistance, while zinc or aluminium-based protective systems extend joint lifespan through sacrificial protection mechanisms that must be optimized for specific environmental stressors such as UV exposure, temperature cycling, and humidity fluctuations (Chen et al., 2021). The analytical challenge lies in developing composite coating systems that maintain protective effectiveness while accommodating the repeated assembly-disassembly cycles inherent to modular bridge deployment, where Lin et al., (2019) demonstrated that properly engineered composite coatings can improve corrosion resistance even in demanding environments. This integrated protection principles, confirmed by (Chung et al., 2019) to reduce maintenance requirements and extend service life, ultimately requires cost-benefit optimization analysis to justify upfront protection investments against long-term maintenance savings, particularly in forest applications where accessibility constraints make remedial interventions both expensive and logistically challenging.

2.4.5 Dynamic Performance and Structural Health Monitoring of Joint

The design of modular joints must consider how joint stiffness continuity affects the dynamic behaviour of bridge systems. Poorly stiffened joints can act as pseudo-hinges, reduce the overall girder stiffness and alter the structure's natural frequency response, thereby impacting dynamic performance (Zhang et al., 2024). Joint flexibility can introduce unintended vibration modes and increase the risk of resonance under vehicular or environmental loads. The stiffness characteristics of joints directly influence force transmission paths and the system's ability to dissipate energy during

dynamic events. To address these challenges, joint stiffness calibration and structural health monitoring are recommended to detect potential stiffness degradation over time (Dogra et al., 2020). Through such monitoring and adaptive maintenance, modular systems can sustain their intended performance and mitigate the effects of dynamic excitation on long-span or repetitive-use timber bridges. In summary, mechanical joints are central to the performance of modular timber bridge systems. Their effectiveness relies on a combination of appropriate material selection, precise geometric detailing, reinforcement approaches, protective measures, and advanced computational modelling. By integrating these elements, modular bridge designs can attain the durability, adaptability, and reliability necessary for sustainable forestry applications. The subsequent section will investigate the flexural and stiffness characteristics of modular timber beams, further emphasizing the significance of joint integrity for overall structural behaviour.

2.4.6 Knowledge Gaps in Integrated Connector Performance

Mechanical connector behaviour in modular timber systems reveals fundamental research limitations that fail to address the integrated nature of these structural elements, where understanding timber's dynamic properties is essential for predicting modular system responses to bridge application forces Opazo-Vega et al., (2021). While recent advancements show promising developments in bio-based laminated structures with bolted connections Ataei et al., (2022), research addressing complex interactions between bolted connections and overall beam behaviour in modular timber bridge applications remains insufficient. This creates a critical knowledge gap where connector design optimization cannot be achieved without understanding system-level performance implications, as current studies explore mechanical behaviour of various connection types but lack integrated testing methodologies that capture both static and dynamic performances. To address these research limitations, this study develops innovative evaluation methods including the Stiffness Reduction Index (SRI) to assess performance of reinforced materials and the Segmentation Performance Index (SPI) to quantify segmentation effects in modular beam assemblies, providing quantitative frameworks for optimizing both reinforcement strategies and modular configuration design in timber bridge applications.

2.5 Flexural Behaviour and Stiffness in Modular Timber Beams

Building upon the mechanical connection analysis, this section validates theoretical insights through experimental flexural testing that translates computational predictions into practical design outcomes. The investigation examines how segmentation patterns, reinforcement strategies, and connector configurations affect global flexural performance and stiffness characteristics of modular timber beams. Through integrated analysis of strain behaviour, mid-span deflection patterns, and stiffness reduction using both three-point bending tests and finite element modelling, this section provides comprehensive understanding of structural responses under realistic loading conditions. The analysis introduces quantitative metrics including the Stiffness Reduction Index to characterize performance variations across modular configurations, delivering essential validation data for design optimization in forest bridge applications where reliability, portability, and structural performance must be balanced in demanding field environments.

2.5.1 Significance of Flexural Testing in Modular Bridge Design

The flexural behaviour and stiffness performance of modular timber beams represent fundamental design considerations for portable bridge systems in forestry applications, where the convergence of repetitive vehicular loading and harsh environmental conditions creates a particularly demanding structural challenge. This operational reality, as demonstrated by Gao et al., (2019), necessitates exceptional reliability and durability standards that extend beyond conventional timber applications, particularly when these systems must function independently in remote settings where maintenance access is severely limited. The performance characteristics of segmented timber beams joined through mechanical connectors emerge from a complex interplay of timber material properties, joint configuration precision, and assembly quality standards (Wdowiak-Postulak et al., 2023), suggesting that optimization requires a systems-level approach rather than isolated component improvements. While three-point and four-point bending tests provide the essential empirical foundation for understanding load-bearing capacity, deflection characteristics, and strain distribution patterns (Liu et al., 2020), the real analytical value lies in how these testing protocols validate not merely material selection but the effectiveness of integrated reinforcement

strategies under realistic loading scenarios. The substantial enhancement in bending strength and load capacity achieved through externally bonded CFRP reinforcement, as confirmed by Mansour et al., (2024), reveals a critical pathway for addressing the inherent limitations of timber in high-stress applications, while optimized connector designs demonstrate measurable improvements in mechanical performance for multi-layer composite configurations Han et al., (2021). Most significantly, the strategic positioning of fibre-reinforced polymers has yielded bending stiffness increases of up to 60% (Yeoh et al., 2023), indicating that the future viability of modular timber bridges in demanding forestry environments depends not simply on material strength, but on the sophisticated integration of reinforcement placement, connection optimization, and load distribution strategies that collectively transform individual timber segments into cohesive structural systems capable of sustained performance under operational stress.

2.5.2 Influence of Beam Segmentation on Stiffness Reduction

Modular beam configurations represent a fundamental engineering trade-off where operational advantages of portability and field assembly compromise structural integrity through discontinuous load paths and localized stress concentrations at joint interfaces. Rather than functioning as continuous structural elements, segmented beams create weak zones that alter load distribution mechanics and require connection design to compensate for inherent material limitations. As Ro et al., (2021) demonstrated, increasing segment numbers produces compounding effects on joint flexibility, where each additional interface disproportionately contributes to structural vulnerability through shear slippage, joint rotation, and progressive load transfer inefficiencies that cannot be predicted from single-joint testing. Lacey et al., (2019) confirmed this through experimental studies revealing not only reduced flexural stiffness in modular configurations compared to continuous beams, but progressive degradation patterns under cyclic loading that suggest assembly tolerances and connection imperfections exponentially amplify weaknesses under repeated deployment conditions typical of portable forestry bridges. Furthermore, Gong et al., (2022) demonstrated that inadequate connector detailing including bolt placement precision, spacing optimization, and interface friction management that triggers progressive failure modes such as longitudinal cracking and fatigue deterioration that become particularly problematic in field environments where temporary installation practices may

compromise connection quality.

However, this emerging understanding reveals a critical knowledge gap in current research methodologies that predominantly address monolithic timber structures while neglecting the cumulative stiffness reduction essential for optimizing modular bridge portability. While studies demonstrate that stiffness reduction occurs, the field lacks comprehensive quantitative models that can systematically predict performance across different segmentation strategies, significantly impeding design methodologies that must balance transportability requirements with structural integrity demands Reynolds et al., (2015). Wang et al., (2022) emphasize that advancing beyond current limitations requires sophisticated understanding of shear dynamics across various connector configurations, suggesting that optimization must address not only individual joint performance but the complex interaction between connection behaviour, cumulative flexibility effects, and realistic field assembly constraints. This research gap represents a critical barrier to developing modular timber bridge designs that can maintain structural resilience in forestry applications where maintenance access limitations and reliability demands create unforgiving operational environments.

2.5.3 Strain Distribution and Mid-span Deflection

Strain behaviour across beam sections reveals fundamental insights into flexural performance that extend beyond load-bearing capacity to illuminate complex stress redistribution mechanisms governing structural integrity, with mid-span deflection serving as a critical indicator of how effectively modular systems maintain global stiffness under realistic loading scenarios. The asymmetrical or non-linear strain profiles that Radhakrishnan et al., (2023) demonstrated in modular beams signal a fundamental breakdown in conventional beam theory assumptions, where joint flexibility creates discontinuities forcing structures to accommodate stress through complex three-dimensional deformation patterns rather than predictable linear responses expected in continuous members. This phenomenon becomes particularly critical in shorter spans where joint behaviour overwhelms inherent structural properties, creating stress concentrations that disproportionately impact deflection behaviour and suggest traditional design approaches may systematically underestimate real-world performance limitations. The effectiveness of externally bonded reinforcements like CSM in counteracting these deficiencies reveals sophisticated

interactions between material properties and application methodology, with Guo et al., (2022) demonstrating that CFRP application achieves significant enhancement in flexural capacity and stiffness by fundamentally altering strain distribution patterns to reduce peak tensile strains and mid-span deflections. However, Zhang & Li, (2023) emphasized that reinforcement efficiency depends critically on bonding quality, fibre alignment precision, and application extent across joint interfaces, where inadequate execution can transform strengthening interventions into premature failure sources under fatigue loading conditions.

However, comprehensive strain distribution documentation across modular beam systems remains notably lacking in current literature, especially at critical locations such as segment interfaces and around mechanical fasteners where understanding localized stress concentrations is essential for predicting failure modes and optimizing structural configurations. Ro et al., (2021) highlight that joint interfaces in precast concrete modular beams with bolted connecting plates often experience significant stress concentrations representing weak points in modular systems, while Liu et al., (2022) reveal that bolt arrangement parameters significantly influence load distribution and failure risk in timber-steel composite beams. He et al., (2022) demonstrate how finite element modelling can predict stress distributions in CFRP-reinforced glulam beams, and Wdowiak-Postulak et al., (2023) show that FRP reinforcement alters failure modes and enhances load-bearing capacity, emphasizing the importance of understanding local strain responses in modular configurations. Li et al., (2023) reveals that material property nonuniformities and interface slip phenomena can introduce systematic weaknesses persisting as residual strain concentrations when bonding applications are incomplete or improperly aligned across segments, suggesting that successful reinforced modular timber structures depend not only on material selection and design optimization, but on developing construction methodologies that consistently achieve precision required to realize theoretical performance improvements in field applications.

2.5.4 Quantifying Stiffness: Modulus of Elasticity and Stiffness Reduction Index (SRI)

The Modulus of Elasticity (MOE) serves as the primary indicator of material resistance to flexural deformation, yet in modular configurations its significance

extends beyond material characterization to represent the effectiveness with which segmented systems maintain structural continuity despite joint discontinuities, with values from bending tests providing critical insights into how connection strategies and reinforcement approaches fundamentally alter load distribution mechanisms. The Stiffness Reduction Index (SRI) becomes particularly valuable in this context, as Huang et al., (2024) demonstrate that this metric effectively captures stiffness retention patterns after repeated or sustained loading cycles revealing progressive failure modes inherent to modular systems by making SRI invaluable for distinguishing between immediate reinforcement benefits and long-term durability under operational stress. The methodological breakthrough achieved by Zhang et al., (2020) in combining modal analysis with static flexural testing produces more reliable stiffness parameters because modular systems exhibit complex dynamic behaviours that static testing alone cannot characterize, with Tata, (2024) confirming that complementary approaches reveal both elastic and degraded states across beam configurations. Li et al., (2024) established that this combined methodology enhances assessment accuracy by capturing multi-modal nature of modular beam behaviour, while Mao et al., (2021) demonstrated that specific reinforcement strategies achieve measurable performance improvements across different loading cycles.

The limited empirical data on strain distribution in modular timber systems represents a critical knowledge gap hindering reliable design guideline development, where Pupsys et al., (2017) establish that mechanical attachment methods for GFRP-reinforced timber beams modify failure modes and strain distributions under load. Dobeš et al., (2022) emphasize the necessity of robust connections for sufficient load-bearing capability, while Liu & Xiong, (2018) show that understanding joint behaviour helps mitigate structural deficiencies. This study addresses these gaps through systematic strain monitoring across specimen configurations, revealing how deformation propagates through segmented structures and identifying failure-prone regions, with Opazo-Vega et al., (2021) validating non-destructive methods for assessing structural integrity and dynamic properties under load to enable early identification of weaknesses.

Recent advances in early-stage stiffness assessment emphasize the critical importance of monitoring structural performance during initial loading phases, where joint slip behaviour serves as a potential precursor to failure in timber structures. Research demonstrates that detection of initial composite reinforcement engagement

and stiffness variations at early loading conditions (approximately 20-40% of maximum load) provides essential indicators for structural health assessment without requiring destructive testing protocols (Buka-Vaivade et al., 2022; Corradi et al., 2017). This approach enables continuous operational monitoring while maintaining bridge functionality, with studies showing that FRP reinforcement actively participates in structural recovery during early loading phases by minimizing deflection and improving load response characteristics (Wdowiak-Postulak & Świt, 2021; KILINÇARSLAN et al., 2023). These findings prove particularly significant for modular timber bridges where progressive stiffness reduction from mechanical connections represents the primary factor determining service life and maintenance requirements in field applications.

2.5.5 Comparative Performance of Continuous vs. Modular Beams

While modular timber systems offer significant constructional advantages, their structural performance consistently demonstrates the fundamental engineering trade-off between assembly flexibility and structural integrity, where interrupted material continuity and connector-induced flexibility create systematic rather than incidental performance limitations that manifest as higher mid-span deflections and reduced flexural stiffness regardless of material quality or construction precision. The persistence of these disparities even when both modular and continuous beam types are fabricated from identical materials under equivalent load conditions, as confirmed by Li et al., (2023), reveals that the performance gap stems from inherent discontinuity effects rather than material or workmanship deficiencies, suggesting that optimization strategies must address fundamental system behaviour rather than seeking incremental improvements in component quality. Finite Element Analysis (FEA), when properly calibrated against empirical data as demonstrated by Ormarsson et al., (2019), has proven invaluable not merely for predicting these performance differences but for visualizing the complex stress redistribution mechanisms that occur around joint interfaces, particularly how segment length, joint detailing, and reinforcement strategies interact to influence stress concentration patterns and failure zone development in ways that cannot be fully understood through experimental testing alone.

The partial mitigation achieved through CFRP or hybrid reinforcement systems, as shown by Saad & Lengyel, (2020), represents both a promising intervention and a

limitation indicator, since even sophisticated reinforcement approaches cannot fully eliminate the fundamental discontinuity effects, with Premrov & Leskovar, (2023) emphasizing that recovery degrees remain contingent upon specific configurations and bonding effectiveness in ways that suggest current reinforcement strategies may be approaching their theoretical limits. These persistent disparities highlight a fundamental limitation in current analytical frameworks, which were primarily developed for continuous structures and fail to adequately account for the complex interplay between segment length, connector type, and reinforcement strategy in modular systems. The sophisticated integration of advanced materials and computational tools cannot fully compensate for this methodological gap, where the cumulative effects of multiple interfaces create stress distribution patterns that existing design approaches struggle to predict accurately. The broader implications become evident when considering Jaramillo & Fischer, (2023)'s findings that intermodular connection quality significantly affects overall structural behaviour under lateral loads, revealing that modular systems must simultaneously address not only primary flexural performance but multi-directional loading scenarios that expose connection vulnerabilities, thereby underscoring the need for innovative connection designs that can optimize structural performance while preserving the inherent constructional advantages that justify modular approaches in applications where material efficiency and assembly flexibility remain paramount considerations.

2.5.6 Advanced Reinforcement Strategies and Hybrid Systems

Beyond conventional FRP applications, recent developments in hybrid reinforcement systems that strategically combine CSM, and metallic components represent a fundamental shift from single-material optimization toward synergistic material integration, where the remarkable strength increases of up to 319% and load-bearing capacity enhancements of 2.5 to 4.2 times demonstrated by Hashemi & Ayoub, (2024) suggest that hybrid approaches can transcend the individual limitations of component materials by exploiting complementary mechanical properties that address different aspects of structural performance simultaneously. These systems achieve improved flexural capacity, enhanced ductility, and superior load redistribution across modular interfaces through what amounts to engineered redundancy, where multiple reinforcement mechanisms provide backup pathways for stress transfer which a

characteristic particularly critical for meeting the stringent serviceability criteria established in design standards like AASHTO LRFD Bridge Design Specifications, as emphasized by Medhlom & Abed, (2023), since modular systems inherently lack the robustness margins available in continuous structures. The promising potential of natural fibres such as jute demonstrated by Jagadeesh et al., (2022) in resource-limited regions reveals an intriguing convergence between sustainability imperatives and structural innovation, where eco-friendly reinforcement alternatives can significantly improve flexural behaviour in lightweight applications while introducing an entirely different paradigm that prioritizes local resource utilization and environmental compatibility without compromising structural integrity. Nazari et al., (2024) confirmed that hybrid reinforcement approaches more effectively meet stringent performance criteria through optimal reinforcement placement and joint detailing precisely because they can be tailored to address the specific failure modes and stress concentration patterns inherent to modular configurations, while Sreekanth & Balamurugan, (2022) demonstrated that their cost-efficiency and sustainability advantages over single-material strategies make them particularly valuable for modular timber bridge applications where the intersection of structural performance requirements and environmental considerations demands solutions that can simultaneously optimize technical effectiveness and ecological responsibility.

2.5.7 Modelling Flexural Behaviour Using Finite Element Analysis (FEA)

Finite Element Analysis (FEA) has proven invaluable for understanding the complex behaviour of modular timber beams precisely because these systems exhibit multi-scale interactions between local joint behaviour and global structural response that cannot be fully characterized through experimental testing alone, with Liu et al., (2024) demonstrating FEA's ability to capture strain evolution, stress propagation, and reinforcement layout effects with high resolution that reveals the intricate stress redistribution mechanisms occurring around discontinuous interfaces where traditional analytical methods fail to provide adequate insight. The remarkable consistency between predicted and experimental results confirmed by Zhang et al., (2022) in their study of load-displacement behaviour at beam mid-spans represents more than mere validation and it indicates that properly calibrated simulation models can effectively bridge the gap between idealized design assumptions and the complex reality of

modular system behaviour, where multiple failure modes and load paths interact in ways that would be prohibitively expensive to explore experimentally across all relevant parameter combinations. Parametric modelling enables predictive design optimization that becomes particularly powerful when estimating critical performance metrics under various loading scenarios, as Effendi & Awaludin, (2022) established by demonstrating how geometric parameters influence structural performance in laminated veneer lumber beams revealing design sensitivities that would require extensive physical testing to uncover but can be systematically explored through computational analysis. Duong et al., (2023) further demonstrated FEA's unique capability in addressing structural complexities like non-uniform cross-sections and large deflections that are characteristic of modular systems under service loads, where the nonlinear interactions between components create analytical challenges that exceed the scope of simplified design methods. The integration of experimental data with FEA provides robust validation frameworks that extend beyond simple correlation checking to enable the development of reliable reinforcement strategies and joint behaviour predictions, as confirmed by Xu et al., (2021) when assessing lateral force performance in modular designs, establishing FEA as an essential component of performance-based design approaches for modular timber bridges where the ability to predict structural reliability under variable loading conditions determines whether these innovative systems can transition from experimental concepts to practical engineering solutions.

2.5.8 Summary and Transition

In summary, the flexural behaviour and stiffness of modular timber beams are governed by a complex interplay of material selection, segment configuration, connector performance, and reinforcement design that represents far more than simple additive effects which these factors interact synergistically to create emergent structural behaviours where optimization in one area can either amplify or negate improvements in others, making system-level understanding essential for advancing beyond current performance limitations. Modular systems fundamentally introduce structural discontinuities that degrade flexural performance through mechanisms that cannot be eliminated but only managed, yet the significant advancements in reinforcement materials and design optimization tools such as FEA offer viable pathways for performance recovery that transform what were once insurmountable limitations into

engineering challenges with quantifiable solutions. The critical insight emerging from this analysis is that successful modular timber bridge design requires abandoning traditional continuous beam assumptions in favour of discontinuity-aware approaches that explicitly account for joint behaviour, stress redistribution patterns, and the progressive nature of performance reduction under service conditions. This section has established the fundamental understanding of how structural flexibility, joint detailing, and reinforcement strategies collectively influence stiffness and load-bearing behaviour, revealing that modular beams represent a distinct structural category requiring specialized analysis methods rather than modified applications of conventional beam theory. Despite these advances, a significant knowledge gap persists in understanding how segmentation strategies fundamentally alter structural behaviour compared to monolithic timber systems. While FEA modelling has improved understanding of individual connection behaviour, quantitative models predicting performance across different segmentation configurations remain underdeveloped. This research gap represents a critical barrier to optimizing modular timber bridge designs, where the complex interaction between transportability requirements and load-bearing capacity demands sophisticated analytical frameworks that current methodologies cannot adequately provide.

2.6 Reinforcement Strategies in Timber Beams

Having established the fundamental influence of segmentation, joint detailing, and reinforcement strategies on flexural performance, this section examines advanced reinforcement technologies that enable performance recovery in modular timber systems. The analysis focuses on Chopped Strand Mat, exploring their tensile behaviour, bonding mechanisms, and compatibility with segmented configurations. Through systematic evaluation of material properties, application techniques, and environmental durability, this section investigates how this reinforcement strategies mitigate stiffness reduction, control deflection patterns, and restore structural continuity across mechanical joints. The discussion addresses critical implementation challenges including surface preparation, adhesive selection, and reinforcement continuity in segmented systems, providing essential insights for optimizing composite timber bridge performance in demanding field environments.

2.6.1 Overview of CSM Materials

The strategic integration of advanced reinforcement materials into timber construction represents a paradigm shift in addressing the fundamental mechanical limitations that have historically constrained wood's structural applications, particularly in modular and portable bridge systems where performance reliability is paramount. This investigation focuses specifically on Chopped Strand Mat (CSM), a Glass Fibre Reinforced Polymer (GFRP) consisting of randomly oriented E-glass fibres bonded with resin matrix, selected for its cost-effectiveness and field-practical application in modular timber systems. CSM function as engineered solutions that systematically target timber's inherent weaknesses such as limited tensile capacity, crack propagation susceptibility, progressive stiffness reduction, and environmental vulnerability by creating composite behaviour that leverages each material's optimal characteristics (Harrach & Rad, 2021). This composite approach proves particularly effective because it addresses the fundamental disconnect between timber's excellent compressive strength and its comparatively poor tensile performance, with CFRP's exceptional tensile properties (high strength-to-weight ratio, corrosion resistance, and fatigue durability) strategically positioned on the tension side to create a more balanced structural response. When bonded to timber beams, CFRP laminates not only significantly reduce mid-span deflection and delay crack propagation by efficiently absorbing tensile loads that would otherwise cause premature failure, but they also redistribute stress concentrations more uniformly throughout the cross-section, fundamentally altering the failure progression from brittle wood fracture to more predictable composite behaviour (Mansour et al., 2024). The analytical significance extends beyond immediate performance gains, as research by (KILINÇARSLAN et al., 2023) demonstrates that these reinforcements can effectively restore and even enhance the long-term mechanical properties of timber that may deteriorate due to biological attacks or environmental exposure, suggesting that composite timber systems may actually improve with age when properly designed. Furthermore, experimental evidence reveals that CFRP's effectiveness scales predictably with reinforcement ratio, showing consistent improvements in both flexural stiffness and ultimate strength with incremental CFRP layers, which provides engineers with quantifiable design parameters for optimizing performance while controlling material costs (Harrach & Rad, 2021) - a critical consideration for modular bridge systems where standardization

and economic viability directly influence adoption rates in challenging service environments.

2.6.2 Tensile Strength, Fatigue Resistance, and Ductility Properties

Research demonstrates that CFRP reinforcement substantially enhances timber beam performance with ultimate flexural strength increases ranging from 17.7% to 77.3% (Mansour et al., 2024) - a notably wide performance spectrum that analytically suggests significant optimization potential exists through careful consideration of application technique, fibre orientation, bond quality, and beam geometry interactions. This variability, rather than representing inconsistency, actually reveals the sophisticated nature of composite timber behaviour where reinforcement effectiveness becomes highly sensitive to design parameters, indicating that engineers can strategically tune performance outcomes to match specific structural requirements. When applied to glued laminated beams, CFRP not only significantly improves both stiffness and strength but critically transforms the failure mechanism from unpredictable brittle fracture to more favourable ductile failure patterns under bending forces (İşleyen et al., 2021), which represents a fundamental shift in structural reliability since ductile failures provide visible warning signs and redistribute loads more gradually, enhancing overall system safety. Complementing CFRP's directional strength advantages, Chopped Strand Mat (CSM) introduces a strategically different reinforcement principles through its superior ductility and energy absorption characteristics, where the randomly oriented glass fibres create isotropic reinforcement that proves especially beneficial for timber elements with irregular grain patterns or inherent material variability (Wdowiak-Postulak et al., 2023). This isotropic behaviour analytically represents a crucial design advantage because natural timber's anisotropic properties create stress concentrations and failure initiation points, making CSM's multidirectional reinforcement particularly valuable for creating more homogeneous composite behaviour. Applied as external laminate or wrap to tension surfaces, CSM enhances stress distribution and inhibits crack development during both static and dynamic loading (Halicka & Ślósarz, 2021), functioning essentially as a crack arrestor that prevents localized failures from propagating catastrophically and becomes strategically critical for mitigating brittle failures in segmented timber components exposed to environmental and mechanical stresses, particularly in modular timber

bridges where joints represent inherent discontinuities and potential failure initiation sites that could compromise entire structural systems (Harrach & Rad, 2021).

2.6.3 Bonding Challenges and Segmental Reinforcement Limitations

CFRP reinforcement performance depends critically on surface preparation, adhesive selection, bond coverage, and joint detailing, with Glišović et al., (2017) emphasizing that insufficient bonding or discontinuous application leads to stress concentrations, inconsistent stiffness gradients, and premature failure at modular segment interfaces. Ensuring CFRP sheets extend into critical stress zones particularly joint interfaces and mid-span areas becomes essential for reliable reinforcement outcomes in modular timber systems where structural discontinuities already present challenges. Environmental durability remains problematic, as moisture ingress and temperature fluctuations degrade CFRP-timber interfaces, affecting adhesive strength and increasing delamination risks (Islam et al., 2019), with prolonged exposure leading to brittle fracture and weakened fibre-matrix bonding particularly critical in modular bridge systems requiring repeated transport, assembly, and vibration exposure. Recent studies confirm that adhesive cohesive stiffness significantly improves elasticity of CFRP-strengthened timber beams (Saad & Lengyel, 2022), while increasing CFRP sheet numbers enhances both bending strength and reinforcement effectiveness (İşleyen et al., 2021; Mansour et al., 2024).

These bonding challenges intensify when considering that CFRP reinforcement research has predominantly focused on continuous members rather than segmented configurations with mechanical joints. While Lee et al., (2020) and Wdowiak-Postulak et al., (2023) demonstrate CFRP's enhanced strength and various reinforcement patterns in timber elements, they primarily address continuous systems where reinforcement continuity can be maintained. He et al., (2022) explored CFRP-reinforced glulam beams indicating that joint configurations and application methods significantly influence outcomes, while Corradi et al., (2015) documented increased capacity in solid timber beams with CFRP bars, yet translation of these benefits to jointed systems remains underexplored. The distinct challenges of segmented timber designs including variable load distributions across interfaces that represent a critical gap in current literature warranting focused research on long-term durability and effectiveness of CFRP reinforcement in modular applications.

2.6.4 Hybrid Systems with Bolts, Plates and CSM

Hybrid reinforcement systems incorporating CSM, and metallic components such as steel plates or bolts are increasingly favoured in modular timber bridge applications, with Mansour et al., (2024) demonstrating how these composite strategies effectively leverage the distinct mechanical properties of each material: CFRP provides superior tensile reinforcement, CSM improves ductility and toughness, while steel elements ensure rigidity and reliable anchorage. In this study's hybrid approach, CSM provides the primary reinforcement enhancement while steel connectors ensure mechanical joint integrity. İşleyen et al., (2021) confirmed through experimental research that such hybrid systems significantly outperform single-material reinforcement by offering a more balanced response to complex stress states, particularly in modular applications where joints create discontinuities. Halicka & Ślósarz, (2021) emphasized that system effectiveness depends on precise material placement, compatibility, and detailing to enable effective load transfer and minimize interface failures. The weaknesses at material interfaces can lead to debonding issues that compromise structural integrity, while the importance of proper anchoring systems to mitigate potential bond failures between CSM and timber substrates for considerations particularly crucial for forest bridge applications subject to environmental exposure and variable loading conditions. The comprehensive review of reinforcement strategies reveals significant advances in timber enhancement technologies, yet exposes a critical limitation in current research approaches. While numerous studies demonstrate substantial performance improvements through CSM, and hybrid reinforcement systems, the overwhelming focus on continuous structural members creates a fundamental knowledge gap for modular timber applications. Table 2.2 systematically summarizes key research findings in timber reinforcement, highlighting both the achievements and limitations of existing approaches.

The literature synthesis reveals that despite documented performance improvements ranging from 17% to 77% in continuous systems, no systematic investigation has evaluated reinforcement effectiveness across segmented configurations where mechanical joints create discontinuities that fundamentally alter stress distribution and load transfer mechanisms. This research gap becomes particularly critical when considering that modular timber bridges require segmentation for transportability, yet existing design guidelines are based entirely on continuous

member behaviour.

The absence of quantitative frameworks for evaluating reinforcement performance in segmented systems represents a significant barrier to optimizing modular timber bridge designs, where the complex interaction between reinforcement continuity, joint compliance, and segmentation strategy demands specialized analytical approaches that current literature cannot provide. This systematic limitation directly motivates the integrated experimental methodology presented in Chapter 3, which addresses these knowledge gaps through novel performance indices and comprehensive evaluation of reinforcement effectiveness across controlled segmentation variables.

Table 2.2
Summary of Literature Findings on Modular Timber Reinforcement

Study	Reinforcement Type	Beam Condition	Performance Improvement	Key Findings
Mansour et al. (2024)	CFRP	Continuous timber	↑ Flexural strength 17.7-77.3%	Wide performance spectrum; optimization potential through application technique
Wdowiak-Postulak et al. (2023)	FRP	Continuous timber	↑ MOE by ~ 32%	Reinforcement improved stiffness; maintained strength-to-weight ratios
İşleyen et al. (2021)	Hybrid CFRP	Glued laminated beams	Transforms failure mode	Brittle to ductile failure; enhanced system safety
He et al. (2022)	CFRP	Glulam beams	Variable	Joint configurations significantly influence outcomes
Corradi et al. (2015)	CFRP bars	Solid timber beams	↑ Load capacity	Increased capacity but limited to continuous systems
Current Study	CSM	Segmented (1-5 parts)	↑ 27.1% (continuous) Novel SRI/SPI indices	First systematic evaluation of segmentation effects on reinforcement effectiveness

2.6.5 Experimental Evidence of Stiffness Recovery and Deflection Reduction

Building on these reinforcement strategies, this study investigates the structural performance of modularly constructed timber beams with mechanical joints and CSM reinforcement, using static flexural testing and Experimental Modal Analysis (EMA) to assess stiffness characteristics, natural frequency variations, and reduction patterns. Wdowiak-Postulak et al. (2023) highlight CFRP's ability to enhance timber structural integrity while maintaining favourable strength-to-weight ratios, while Zhu et al. (2023)

demonstrate improvements in stiffness and flexural behaviour when incorporating CFRP into timber beamsCheng et al. (2020) emphasizes the necessity of rigorous modal analysis to determine natural frequency characteristics and minimize resonance effects in reinforced modular timber designs, principles directly applicable to the CSM-reinforced systems investigated in this study. In the Malaysian context, utilizing renewable timber resources with enhanced structural resilience aligns with global sustainability goals, while non-destructive assessment methods support evaluations of structural integrity without compromising wood's inherent properties. The findings aim to guide the design of modular girder bridges tailored for sustainable forestry operations in Malaysia and similar ecological settings.

The use of FEA and EMA in this study is supported by numerous findings across recent literature. Finite Element Analysis (FEA) has emerged as an indispensable computational tool for evaluating reinforced timber systems, fundamentally transforming the design paradigm from empirical trial-and-error approaches to predictive optimization strategies that can systematically explore complex material interactions before physical testing, with Saad & Lengyel, (2022) demonstrating its sophisticated capability to simulate strain development, failure progression, and the intricate stress transfer mechanisms between reinforcement materials and timber substrates which interactions are analytically critical because they determine whether composite action is achieved or whether delamination and premature failure occur. The analytical power of properly calibrated FEA extends beyond simple stress analysis to enable engineers to systematically evaluate thousands of potential reinforcement configurations, determining optimal layouts, fibre orientations, and bond patterns with remarkable accuracy while significantly reducing the experimental burden and associated costs that would otherwise make comprehensive parametric studies prohibitively expensive. Glišović et al., (2017) demonstrated this optimization potential by using FEA to systematically enhance structural performance of glulam beams reinforced with CFRP plates, while KILINÇARSLAN et al., (2023) provided crucial validation evidence showing that simulated deformation profiles closely matched experimental testing of reinforced modular beams, thereby confirming FEA's reliability in both predictive design and performance assessment applications by a validation loop that is analytically essential because timber's inherent variability and anisotropic properties create modelling challenges that require empirical calibration to ensure simulation accuracy.

The analytical sophistication of modern FEA becomes particularly evident in heterogeneous timber compositions, where Wdowiak-Postulak et al., (2023) established its versatility in modelling complex stress distributions under both static and dynamic loads, highlighting the computational framework's critical value for analysing hybrid reinforcement configurations where understanding multi-material interactions, bond behaviour, and failure mode transitions becomes essential to long-term design viability and structural reliability. This integration of computational modelling with empirical validation, as concluded by Islam et al., (2019) offers the most robust and analytically comprehensive framework for developing innovative reinforcement strategies in modular timber bridge applications, creating a synergistic approach where simulation guides experimental design and experimental results continuously refine computational models, ultimately enabling the development of optimized composite timber systems that would be impossible to achieve through purely experimental or purely theoretical approaches.

In summary, the integration of CSM reinforcements into modular timber bridge systems offers a viable solution to many of the structural limitations inherent in unreinforced timber. CSM enhances tensile strength and stiffness and improves ductility and stress dispersion, particularly in segmented configurations. Hybrid systems further extend these benefits by balancing strength, flexibility, and anchorage capacity. However, reinforcement effectiveness is strongly influenced by bonding quality, material compatibility, and environmental resilience. The use of FEA alongside experimental testing provides a robust framework for optimizing reinforcement strategies and validating their performance under practical conditions. These insights are foundational for designing modular bridge systems that are not only structurally efficient but also adaptable to the dynamic and environmental demands of forestry operations. The next section will explore how dynamic and modal analyses are employed to evaluate the vibrational behaviour of these reinforced timber systems.

2.7 Dynamic and Modal Analysis in Structural Timber Design

While reinforcement strategies such as CSM effectively enhance flexural strength and stiffness, understanding their influence on dynamic behaviour is equally critical for evaluating long-term performance and serviceability of modular timber bridges. This section examines how segmentation, joint detailing, and reinforcement

collectively affect vibrational characteristics including natural frequency, damping ratios, and mode shapes. These dynamic parameters serve as indicators of structural integrity while enabling predictive maintenance and health monitoring strategies, particularly vital for timber systems deployed in variable field conditions where visual inspection may be limited. Through integration of Experimental Modal Analysis, finite element simulations, and structural health monitoring frameworks, this section establishes comprehensive methodologies for evaluating dynamic performance and correlating non-destructive assessment techniques with conventional static testing methods in modular timber systems.

2.7.1 Fundamentals of Natural Frequency and Mode Shapes

Dynamic and modal analyses serve as critical diagnostic tools for modular timber bridges, where the inherent complexity of segmented systems demands sophisticated understanding of vibrational behaviour beyond conventional structural assessment. Srikanth et al., (2022) demonstrated that evaluating natural frequencies, mode shapes, and damping ratios provides essential insights into resonance susceptibility and user safety, yet the analytical challenge intensifies when considering how Yu et al., (2014) observed that mechanical joints and material heterogeneity fundamentally alter load transfer mechanisms and create discontinuous stiffness distributions throughout the structure. This discontinuity suggests that traditional dynamic analysis approaches may inadequately capture the unique response characteristics of modular systems, where localized joint behaviour can disproportionately influence global dynamic properties. Timber's comparatively low stiffness-to-mass ratio naturally produces lower fundamental frequencies than steel or concrete alternatives, making these structures particularly vulnerable to pedestrian-induced vibrations and wind loading which vulnerability that becomes amplified in modular configurations where Museros et al., (2012) identified the first vertical bending mode as the primary indicator of flexural integrity and serviceability performance. The practical significance emerges through Li & Zhang, (2020)'s correlation between frequency measurements and structural degradation, enabling real-time monitoring capabilities where frequency shifts can quantitatively indicate joint loosening or material deterioration, thereby transforming dynamic analysis from a design verification tool into a predictive maintenance strategy for modular timber bridge

systems.

2.7.2 Role of Joint Flexibility and Beam Configuration

Modularization fundamentally alters the dynamic characteristics of timber bridges through a cascading effect where segmentation introduces compliance at mechanical joints, creating a system where Cepelka & Malo, (2018) demonstrated that global stiffness reduction occurs not merely as an additive effect of individual joint flexibilities, but through complex load redistribution patterns that concentrate stress at connection points while reducing overall structural continuity. This stiffness degradation manifests as decreased natural frequencies, which positions modular systems dangerously closer to excitation frequencies from typical operational loads such as traffic, wind, and seismic forces and thereby creating resonance conditions that extend beyond user discomfort to accelerate fatigue accumulation and compromise long-term structural integrity. The critical insight emerges from understanding that Han et al., (2019) observed failures predominantly originating from connection inadequacy rather than timber material limits, suggesting that modular bridge performance hinges on the weakest link principle where joint behaviour governs system-wide dynamic response and reliability. Cepelka & Malo, (2018) revealed that mechanically coupled threaded rods achieving high rotational stiffness can effectively counteract segmentation-induced frequency reductions, indicating that joint design represents a powerful tool for tuning dynamic performance rather than merely accommodating structural assembly requirements. This relationship between joint stiffness and natural frequency elevation implies that optimal modular bridge design requires balancing connection rigidity against practical assembly constraints, while recognizing that timber's inherent material variability demands probabilistic design approaches to ensure that connection performance remains adequate across the full spectrum of possible wood properties and environmental conditions, ultimately transforming joint monitoring from routine maintenance into a critical component of structural resilience strategy.

2.7.3 Use of Experimental Modal Analysis (EMA)

Experimental Modal Analysis (EMA) represents a sophisticated diagnostic

approach crucial for modular timber systems, where traditional static testing cannot capture complex dynamic interactions between segments, joints, and reinforcement elements governing real-world performance under operational loading. The methodology employs controlled excitation through impact hammers or electromagnetic shakers coupled with accelerometer or microphone response measurement, enabling Pasca et al., (2021) to extract modal parameters which natural frequency, damping ratio, and mode shape that reveal how joint flexibility, segment configuration, and reinforcement placement collectively influence structural dynamics in ways unpredictable through analytical modelling alone. This approach proves essential because Wang et al., (2022) established that timber structures exhibit configuration-dependent dynamic properties varying significantly with loading characteristics, requiring understanding of how modular assembly affects load transfer mechanisms and energy dissipation patterns throughout the structure. Opazo-Vega et al., (2021)'s Operational Modal Analysis demonstrates practical value by extracting dynamic properties from ambient vibration responses, transforming bridges into self-monitoring systems where operational loads provide excitation for continuous structural assessment. The first vertical bending mode identification becomes critical due to its direct correlation with flexural stiffness and sensitivity to joint reduction, making frequency shifts reliable indicators of structural health changes preceding visible damage or serviceability failures. Amaddeo & Dorn, (2023) emphasized that long-term modal monitoring creates comprehensive structural biographies where systematic frequency and damping changes enable predictive maintenance strategies, transforming EMA from one-time verification into continuous structural intelligence systems.

However, a significant methodological gap exists in correlating non-destructive dynamic assessment techniques with conventional static testing methods for modular timber structures, where relationships between EMA-derived stiffness indicators and traditional flexural properties remain insufficiently established, particularly for segmented timber systems with mechanical joints. While Opazo-Vega et al., (2021) demonstrated that dynamic modulus measurements can effectively predict static bending properties, and Liu & Xiong, (2018) associated semi-rigid timber connections with both dynamic and static performance, quantitative relationships between modal parameters and static flexural characteristics in modular configurations require systematic investigation to establish reliable assessment protocols.

2.7.4 Simulation Approaches Using Finite Element Analysis (FEA)

Simulation-based modal analysis through finite element platforms like ANSYS and Abaqus provides indispensable computational capabilities that extend beyond experimental limitations by enabling systematic exploration of parameter spaces impossible to achieve through physical testing, particularly valuable for modular timber systems where the interaction matrix between segments, joints, reinforcement, and boundary conditions creates exponentially complex design scenarios that demand virtual prototyping before costly physical implementation. These computational models excel at capturing the nuanced mechanics where Liu et al., (2019) demonstrated that increasing segment numbers or lengths systematically reduces natural frequencies through cumulative stiffness degradation, revealing the fundamental trade-off between modular flexibility for construction convenience and structural performance under dynamic loading that create a relationship that suggests optimal modular design requires balancing assembly practicality against frequency requirements to avoid resonance zones. The strategic implementation of CSM reinforcement emerges as a sophisticated countermeasure that operates by selectively enhancing flexural rigidity in critical stress regions, effectively compensating for joint-induced stiffness losses while maintaining the modular assembly advantages that justify segmented construction approaches. Xu et al., (2021) confirmed that intelligent joint strengthening transcends simple stiffness enhancement by simultaneously improving ductility and energy dissipation characteristics, indicating that modern connection design must optimize multiple performance criteria rather than pursuing maximum rigidity that could lead to brittle failure modes under extreme dynamic loading. Dersch et al., (2021) revealed that contemporary fastening systems achieve this delicate equilibrium between adequate stiffness for frequency control and sufficient flexibility for load redistribution and fatigue resistance, demonstrating that successful modular bridge design requires understanding joints as sophisticated mechanical devices rather than simple structural connections. The integration of advanced analytical techniques which covariance-driven stochastic subspace identification, empirical mode decomposition, and frequency domain decomposition and create comprehensive modelling frameworks that can predict complex structural behaviour across multiple loading scenarios and environmental conditions, ultimately enabling optimization of hybrid reinforcement configurations that maximize both structural performance and economic viability in

modular timber bridge applications.

2.7.5 Implications for Structural Health Monitoring and Resonance Avoidance

Dynamic analysis plays a pivotal role in structural health monitoring (SHM) for modular timber bridges, with Finite Element Model Updating (FEMU) combined with ambient vibration testing can detect early signs of joint loosening and stiffness reduction in timber structures exposed to repetitive loading and environmental variability. Zinno et al., (2022) established that continuous modal tracking effectively identifies subtle shifts in vibration response over time, particularly in lightweight and joint-sensitive structures where connection performance directly influences global stiffness. Oliveira et al., (2015) confirmed that Operational Modal Analysis allows for real-time monitoring without artificial loading, and this approach enables predictive maintenance strategies that enhance both safety and reliability. International standards such as AASHTO LRFD emphasize that a bridge's fundamental frequency should not align with traffic excitation frequencies (typically 2–5 Hz), with reinforcing the critical importance of accurate dynamic analysis in design validation. Gao et al., (2020) and Verstrynge et al., (2020) further highlighted how advancements in sensor technology and computational analysis have significantly enhanced SHM practices for timber structures, allowing engineers to identify potential vulnerabilities before catastrophic failures occur.

In summary, dynamic and modal analyses are central to the design, evaluation, and maintenance of modular timber bridge systems. By integrating Experimental Modal Analysis (EMA), Finite Element Analysis (FEA), and Structural Health Monitoring (SHM) strategies, engineers can assess the impact of segmentation, joint detailing, and reinforcement on vibrational performance. These methods help ensure compliance with serviceability standards, enable early detection of damage, and guide improvements in material selection and connector detailing. The integration of dynamic and static assessment methodologies represents a critical advancement in structural evaluation, where non-destructive techniques like ultrasonic pulse velocity and resonance frequency measurements provide valuable insights without compromising structural integrity. Amaddeo & Dorn, (2023) confirmed modal dynamics as significant predictors of overall stiffness and ductility in timber systems, while He et al., (2022) established the viability of enhancing FRP-reinforced glulam beam performance while maintaining

non-destructive assessment approaches. These integrated methodologies, supported by predictive modelling techniques (Virgen-Cobos et al., 2022), create more reliable evaluations and establish foundations for robust assessment protocols specifically tailored for modular timber bridges.

2.7.6 Synthesis: Need for Integrated Systems Analysis

A significant limitation pervading existing research is the systematic tendency to examine structural parameters such as connector design, reinforcement type, and segmentation strategy in isolation rather than as interconnected components within a unified system, creating a fragmented analytical approach that fundamentally fails to capture the complex, synergistic interactions that collectively determine modular timber bridge performance in real-world applications. This reductionist methodology, while valuable for understanding individual component behaviour, creates critical blind spots where the emergent properties of integrated systems remain unexplored, potentially leading to optimization strategies that enhance isolated parameters while inadvertently compromising overall structural integrity. Dobeš et al., (2022) demonstrate how steel-plate connection methods significantly affect load-carrying capacity, while Wdowiak-Postulak et al., (2023) show that fibre-reinforced polymers enhance timber reinforcement with improved strength-to-weight ratios, yet these studies examine components independently without considering how connection performance interacts with reinforcement effectiveness or how both parameters collectively influence segmentation viability.

The analytical challenge deepens when recognizing that modular timber bridges represent complex structural ecosystems where component-level optimizations can create system-level vulnerabilities through unintended interaction effects that traditional isolated testing cannot reveal. He et al., (2022) emphasize that interaction between CFRP reinforcement and timber substrate significantly influences overall performance, underscoring the critical need to address material properties and structural connections concurrently rather than sequentially, while Liu et al., (2022) highlight the necessity of numerical simulations to understand interactions between structural components that extend beyond simple load transfer mechanisms to encompass dynamic coupling, fatigue interactions, and progressive failure propagation. Furthermore, Caprio & Jockwer, (2023) challenge fundamental assumptions of linear

behaviour in timber structures, advocating for sophisticated modelling approaches that consider combined load interactions and material responses where connector flexibility influences reinforcement effectiveness, segmentation patterns affect dynamic characteristics, and environmental factors simultaneously impact multiple system components in ways that cannot be predicted from individual parameter studies.

This fragmented research landscape becomes particularly problematic when considering that practical modular timber bridge deployment requires simultaneous optimization across multiple performance criteria which structural adequacy, assembly efficiency, transportation constraints, environmental durability, and maintenance accessibility in where trade-offs between competing demands can only be understood through comprehensive systems analysis that captures the multi-dimensional nature of design optimization. The absence of integrated analytical frameworks creates a critical knowledge gap where engineers must extrapolate from isolated component studies to predict integrated system behaviour, introducing significant uncertainty into design decisions and potentially compromising reliability and cost-effectiveness of modular timber bridge solutions in demanding forestry applications. The present research addresses this substantial gap by implementing a holistic experimental framework that simultaneously evaluates multiple interdependent variables across various beam configurations, integrating static flexural testing, dynamic modal analysis, comprehensive strain monitoring, and comparative reinforcement assessment within a single cohesive study design to provide unprecedented systems-level understanding of modular timber bridge behaviour. This integrated methodology enables identification of synergistic effects, optimization trade-offs, and failure mode interactions that more accurately reflect practical deployment conditions, while simultaneously developing quantitative metrics including the Stiffness Reduction Index (SRI) and Segmentation Performance Index (SPI) that provide engineers with reliable tools for systems-level design optimization accounting for complex interdependencies governing modular timber bridge performance in real-world forestry applications.

2.8 Research Gaps and Methodological Rationale

The preceding analysis reveals urgent need for integrated frameworks capturing complex interactions among segmentation, reinforcement, and dynamic performance in modular timber systems. This section synthesizes critical limitations including

unresolved joint behaviour, reinforcement continuity, and static-dynamic performance correlation that impede real-world design optimization. Through systematic identification of four fundamental knowledge deficiencies, the analysis connects structural deficiencies in existing literature to novel analytical tools including the Stiffness Reduction Index and Segmentation Performance Index. This establishes compelling justification for the integrated experimental and computational methodology developed in this study, transitioning from conceptual insights toward evidence-based design solutions for modular timber bridge applications.

2.8.1 Critical Analysis and Knowledge Gaps in Modular Timber Bridge Research

The literature demonstrates increasing interest in modular timber bridge systems for forest applications, where timber's renewability, favorable strength-to-weight ratio, and alignment with Sustainable Forest Management (SFM) principles make it an attractive structural material. However, timber's natural durability presents significant challenges, particularly in tropical climates where biological degradation, moisture absorption, and inherent strength variability accelerate deterioration (Fortino et al., 2020). This creates a fundamental design paradox where timber bridges are most needed in precisely the environments where they perform worst structurally by remote tropical forest locations with high operational demands but harsh environmental conditions. The convergence of operational necessity and material vulnerability suggests that successful modular timber bridge systems must transcend traditional material limitations through integrated engineering approaches rather than relying solely on material selection. While comprehensive timber bridge management programs incorporating reliability and risk analysis tools can assess and mitigate deterioration risks, and structural health monitoring technologies facilitate early detection of moisture levels and potential damage Björngrim et al., (2016), current research predominantly addresses monolithic timber structures, neglecting the cumulative stiffness reduction in segmented configurations essential for modular bridge portability.

Mechanical joints, particularly bolted connections, represent the critical vulnerability where modular timber systems transition from material-limited to connection-limited performance. These connections are indispensable for enabling segmentation and facilitating assembly, yet introduce significant structural challenges

including stress concentrations, shear slippage, and localized crushing, especially under dynamic loading conditions (Chen et al., 2020; Zhang et al., 2018). This reveals that connection failure modes in modular systems can trigger progressive collapse mechanisms that wouldn't exist in continuous timber structures, where the structural bottleneck shifts from timber capacity to joint performance. Despite their widespread application, these connections remain incompletely understood, with substantial research gaps in their shear performance and long-term mechanical behaviour under cyclic loading (Song et al., 2024). Current research primarily examines bolted connection performance under isolated rather than integrated conditions, while timber-bolt interfaces represent critical vulnerability points where stress concentrations and stiffness discontinuities emerge (Dobeš et al., 2022). Studies indicate that bolt arrangement and joint configuration significantly influence load-carrying capacity and moment resistance in timber assemblies (Guo & Shu, 2019), with variations in bolt spacing and quantity substantially affecting bending performance (Liu et al., 2022), yet research addressing how connector configurations influence global beam behaviour under combined flexural and dynamic loading remains limited.

Specifically, the quantification of connection load-bearing capacity under realistic loading conditions represents a fundamental research gap that impedes practical implementation of modular timber bridge systems. Current literature predominantly focuses on ultimate capacity determination through standard testing protocols, but provides insufficient guidance on safety factor establishment, stress concentration quantification, and load redistribution analysis essential for reliable design practice. The absence of validated methodologies for incorporating experimentally-observed stress concentration factors (typically 2.5-4.0x nominal levels) into design calculations creates uncertainty in connection adequacy assessment, while limited understanding of load sharing mechanisms among multiple connections in segmented systems restricts optimization of connection spacing and sizing strategies. This knowledge gap creates uncertainty in connection design, where engineers must rely on conservative assumptions that may result in over-designed systems or, conversely, inadequate safety margins, particularly problematic in modular systems where multiple connections must operate collectively as an integrated load transfer network.

The comprehensive literature analysis reveals four critical knowledge deficiencies that this research addresses through novel methodological contributions.

Table 2.3 systematically links these identified gaps to the original research innovations developed in this study and addressing these gaps through novel analytical frameworks represents a fundamental advancement from existing approaches, providing the foundation for the integrated experimental methodology. Reinforcement techniques using Chopped Strand Mat (CSM) have demonstrated promising improvements in tensile capacity, stiffness retention, and fatigue resistance of timber connections (Cepelka & Malo, 2018).

Table 2.3
Summary of Knowledge Gaps and Novel Research Contributions

Knowledge Gap Identified	Novel Research Contribution
Inadequate quantification of cumulative stiffness reduction in segmented assemblies	FIRST introduction of Stiffness Reduciton Index (SRI) - a novel quantitative tool that captures progressive stiffness changes during loading (previously no systematic reduction assessment existed)
Insufficient understanding of mechanical connection performance under realistic loading	FIRST comprehensive Segmentation Performance Index (SPI) - novel quantitative framework comparing segmented vs. continuous performance (existing research lacked systematic comparison methodology)
Limited characterization of reinforcement continuity effects across segment interfaces	FIRST systematic evaluation of CSM reinforcement effectiveness across 1-5 segment configurations with quantified discontinuity effects (previous studies only examined continuous reinforcement)
Absence of validated correlations between static and dynamic response characteristics	FIRST triangulated validation framework integrating EMA-Flexural-FEA with validated correlation equations (no previous research systematically correlated these three methods)

However, persistent integration challenges include discontinuity of reinforcement across segment joints and achieving consistent high-quality bonding between dissimilar materials (Ceraldi et al., 2021; Wang et al., 2022). While studies by Lee et al., (2020) and Wdowiak-Postulak et al., (2023) demonstrate CFRP's enhanced strength and various reinforcement patterns in timber elements, they primarily address continuous systems rather than segmented configurations with mechanical joints. He et al., (2022) explored CFRP-reinforced glulam beams, indicating that joint configurations and application methods significantly influence outcomes, yet in modular bridge applications, reinforcement effectiveness is compromised by discontinuities at segment junctions, creating challenges in stress transfer and reinforcement anchoring that are not present in monolithic systems. Despite these advancements, ensuring uniform stress distribution across interfaces without compromising timber integrity remains

problematic, necessitating an integrated approach that addresses both material reinforcement techniques and the complex behaviour of timber joints under various loading conditions (Silva & Liyanage, 2019).

Dynamic behaviour represents a critical concern for short-span modular bridges in forestry operations, where segment joints significantly reduce system stiffness and lower natural frequencies, heightening resonance risks under traffic-induced vibrations (Yan et al., 2018). However, current dynamic analysis approaches treat segmentation effects as secondary perturbations rather than fundamental system characteristics, suggesting that conventional bridge dynamic design methods may be inadequate for modular timber systems where joint flexibility and segment interactions create entirely different vibration modes. Comprehensive analysis methodologies, including Experimental Modal Analysis (EMA) and Finite Element Analysis (FEA), have proven essential for quantifying these dynamic effects and developing more resilient modular systems (Miyamoto et al., 2018), yet a significant methodological gap exists in correlating non-destructive dynamic assessment techniques with conventional static testing methods for modular timber structures. The relationship between EMA-derived stiffness indicators and traditional flexural properties remains insufficiently established, particularly for segmented timber systems with mechanical joints, while non-destructive techniques like ultrasonic pulse velocity and resonance frequency measurements provide valuable insights without compromising structural integrity (Opazo-Vega et al., 2021). Research has established that dynamic impacts from vehicular loading substantially contribute to bridge fatigue and significantly alter design life, necessitating the incorporation of dynamic amplification factors to ensure structural safety (Zhang et al., 2017).

The most significant limitation revealed by this literature review is the fragmented approach to modular timber bridge research, where material properties, connection behaviour, reinforcement strategies, and dynamic performance are studied in isolation despite their fundamental interdependence. This reductionist methodology fails to capture the emergent properties of modular systems, where the interaction between components often determines performance more than individual component capabilities. Comprehensive strain distribution documentation across modular beam systems is notably lacking, especially at critical locations such as segment interfaces and around mechanical fasteners, where Ro et al., (2021) highlight that joint interfaces often experience significant stress concentrations representing weak points in modular

systems. While Dobeš et al., (2022) demonstrate how steel-plate connection methods significantly affect load-carrying capacity, and Wdowiak-Postulak et al., (2023) show that fibre-reinforced polymers enhance timber reinforcement with improved strength-to-weight ratios, the tendency to examine these parameters in isolation fails to capture the complex interactions that collectively determine modular timber bridge performance in real-world applications. The absence of integrated experimental programs that simultaneously evaluate static, dynamic, and long-term performance under realistic assembly constraints represents a critical knowledge gap that limits the translation of laboratory findings to field applications, where the integration of advanced monitoring technologies and computational analysis methods could significantly enhance structural assessment practices for timber structures (Kafle et al., 2016; Maizuar et al., 2017; Xiao et al., 2019).

2.8.2 Justification for Experimental and Numerical Approach

This research employs a sophisticated three-phase integrated methodology specifically designed to address the complex, multifaceted challenges identified in modular timber bridge systems. The investigation utilizes a triangulated approach combining Experimental Modal Analysis (EMA), destructive flexural testing, and finite element analysis (FEA) to provide comprehensive characterization of structural behaviour across static and dynamic loading domains.

Phase 1: Non-destructive dynamic assessment employs EMA using controlled impact excitation and acoustic response measurement to extract natural frequencies and estimate dynamic stiffness characteristics without compromising specimen integrity. This approach addresses the critical literature gap regarding the relationship between segmentation patterns and dynamic performance by enabling systematic evaluation of how mechanical connectors and material discontinuities alter vibrational properties across different beam configurations. The fundamental relationship $k=(2\pi f)^2 m$ enables direct correlation between measured frequencies and structural stiffness, providing an independent validation pathway for subsequent static testing results.

Phase 2: Static performance quantification implements standardized three-point flexural testing using a Shimadzu AG-IS 100 kN Universal Testing Machine to systematically evaluate load-deflection behaviour, stiffness characteristics, and failure progression under controlled loading conditions. This phase addresses identified

limitations in understanding how CSM reinforcement effectiveness varies across segmented configurations while simultaneously providing comprehensive load-bearing capacity verification of mechanical connections through systematic safety factor analysis, stress concentration quantification, and load redistribution assessment. The methodology incorporates precise strain measurement at critical locations, implements novel denting correction protocols to ensure accurate deflection quantification despite steel-timber contact effects, and establishes validated relationships between experimental connector performance and theoretical design capacity predictions essential for practical implementation.

Phase 3: Computational validation and extension utilize ANSYS finite element analysis to simulate both static and dynamic responses under equivalent boundary conditions, enabling detailed stress-strain analysis at connector interfaces and reinforcement regions that are experimentally inaccessible. The computational framework extends experimental findings beyond laboratory constraints while providing critical validation of the relationship between measured performance and predicted behaviour under variable loading scenarios.

The study introduces two novel performance indices which are the Stiffness Reduction Index (SRI) and Segmentation Performance Index (SPI) that quantify distinct reduction mechanisms and enable systematic optimization of modular configurations. SRI captures progressive stiffness changes within individual beams during loading, while SPI evaluates performance reduction relative to continuous control specimens, collectively providing a comprehensive framework for assessing the trade-offs between modular practicality and structural integrity.

This integrated approach creates a synergistic investigative framework where experimental findings validate computational models, dynamic measurements corroborate static performance assessments, and novel analytical indices enable quantitative design optimization and directly addressing the complex interactions between segmentation, reinforcement, and connection design that existing literature has identified but inadequately characterized.

2.8.3 Methodological Framework Derived from Literature Review

The comprehensive literature analysis has directly informed the development of a systematic experimental matrix comprising ten full-scale specimens strategically

configured to address the most significant knowledge gaps through controlled parametric evaluation. The research methodology detailed in Chapter 3 represents a direct response to the specific limitations identified in current modular timber bridge research.

Recognizing the critical need to quantify cumulative stiffness reduction in modular configurations, the experimental design implements a controlled segmentation matrix ranging from continuous single-segment beams to highly segmented five-segment assemblies (segment lengths from 3.0 m to 0.6 m). This approach enables precise measurement of how increasing connector frequency affects global structural behaviour while maintaining consistent total beam length (3.0 m) and standardized U-shaped steel connector geometry across all configurations, effectively isolating segmentation effects from geometric variables.

Addressing the documented uncertainty regarding the relationship between dynamic properties and static performance in segmented timber systems, the methodology integrates EMA frequency measurements with flexural stiffness quantification to establish empirical correlations between modal characteristics and load-bearing capacity. This dual-domain approach provides complementary perspectives on how modularization affects both serviceability (through dynamic response) and ultimate capacity (through static testing), filling a critical gap where existing studies typically address only one performance domain.

The identified limitations in understanding CSM reinforcement effectiveness across mechanical joints has shaped the development of a parallel ETN/ETR specimen series that enables direct comparison of reinforced and non-reinforced configurations at equivalent segmentation levels. The 5 mm thick CSM bottom-flange reinforcement protocol, deliberately excluding connector interfaces to prevent bonding interference, allows systematic evaluation of how tension-zone strengthening influences both global stiffness retention and local stress distribution patterns across modular assemblies.

Acknowledging the significant performance uncertainties associated with mechanical joint behaviour, the methodology employs a single standardized U-shaped steel connector design (300 mm × 250 mm × 100 mm with four-bolt pattern) across all segmented specimens. This approach eliminates joint geometry as a variable, enabling definitive attribution of performance differences to reinforcement presence and segmentation frequency rather than connection design variations which a critical methodological refinement absents from existing comparative studies.

Recognizing the significant challenges facing timber structures in tropical forestry environments, the experimental protocol incorporates full-scale specimens (3.0 m span) tested under realistic moisture conditions, addressing the common limitation where laboratory studies using small-scale specimens may not accurately represent field performance. The Western White Pine material selection, based on established forestry applications and favourable strength-to-weight characteristics, ensures practical relevance for portable bridge deployment scenarios.

The integrated FEA approach using ANSYS addresses the documented gap between theoretical design models and actual modular system behaviour by implementing detailed contact modelling, orthotropic timber properties, and explicit representation of mechanical connections under realistic boundary conditions. This computational framework enables validation of experimental findings while extending analysis to stress concentrations and failure mechanisms not directly measurable through physical testing. The methodological integration of novel performance indices (SRI and SPI) with established testing protocols creates a comprehensive analytical framework that directly addresses the most significant research gaps identified in the literature review, providing both immediate practical insights for modular timber bridge design and a robust foundation for future optimization studies in sustainable forest infrastructure applications.

2.8.4 Conclusion

This chapter has established a comprehensive scientific foundation for understanding modular timber bridge systems through systematic analysis of structural performance, environmental compatibility, and operational versatility in forest management contexts. The literature review demonstrates significant evolutionary progress from traditional timber construction practices toward sophisticated modular configurations that strategically balance structural integrity with ecological responsibility and deployment flexibility, yet reveals critical knowledge deficiencies that constrain practical implementation and optimization.

The analysis identifies four fundamental research limitations that collectively impede advancement in modular timber bridge technology: (1) inadequate quantification of cumulative stiffness reduction mechanisms in segmented assemblies, particularly how connector frequency and placement patterns influence global structural

behaviour; (2) insufficient understanding of mechanical connection performance under realistic loading conditions, especially the interaction between joint flexibility and overall system reliability; (3) limited characterization of reinforcement continuity effects across segment interfaces, particularly how fibre-reinforced polymer applications perform when interrupted by mechanical connections; and (4) absence of validated correlations between static load-bearing capacity and dynamic response characteristics essential for serviceability assessment and resonance avoidance in operational environments.

Building on this foundation, Chapter 3 introduces an innovative three-phase experimental methodology specifically designed to address these identified research gaps through systematic parametric evaluation. The framework integrates non-destructive dynamic assessment via Experimental Modal Analysis, controlled static performance quantification through standardized flexural testing, and comprehensive computational validation using finite element analysis creating a triangulated approach that provides unprecedented insight into the complex interactions between segmentation patterns, reinforcement strategies, and connection design in modular timber systems.

The methodology introduces novel performance indices which are Stiffness Reduction Index (SRI) and Segmentation Performance Index (SPI), that quantify distinct reduction mechanisms and enable systematic optimization of modular configurations. These indices address the literature's documented inability to consistently evaluate trade-offs between modular practicality and structural integrity, providing quantitative frameworks for design decision-making that existing research approaches have been unable to achieve.

The comprehensive experimental matrix comprising ten full-scale specimens across controlled segmentation and reinforcement variables, combined with sophisticated analytical protocols and computational validation frameworks, establishes a robust investigative platform that extends significantly beyond current research capabilities. This approach provides the methodological structure for the systematic data analysis, performance evaluation, and practical design recommendations presented in Chapter 4, ultimately contributing to more resilient and field-adaptable timber bridge solutions that can advance sustainable forest management practices while meeting demanding structural performance requirements.

The transition from this foundational analysis to the detailed methodology

represents a critical evolution from identifying research limitations to developing comprehensive solutions that address the complex, multifaceted challenges facing modular timber bridge implementation in contemporary forestry applications.

CHAPTER 3
RESEARCH METHODOLOGY

3.1 Introduction

The methodological framework is explicitly structured to address the five research objectives, encompassing static–dynamic property correlation (Objective 1), mechanical connection behaviour (Objective 2), dynamic response characterization (Objective 3), reinforcement performance evaluation (Objective 4), and the development of stiffness reduction indices and segmentation limits (Objective 5). Modular timber systems offer key advantages in terms of transportability and ease of on-site assembly, making them highly suitable for remote and temporary infrastructure. However, segmentation introduces mechanical joint interfaces that interrupt stiffness continuity and modify stress transfer, creating joint compliance and localized stress concentrations that can reduce global beam integrity.

The integration of CSM reinforcement with segmented timber systems introduces complex dynamic interactions that challenge conventional frequency–stiffness relationships established in classical vibration theory under idealised continuous-member assumptions. While traditional structural dynamics predicts positive correlations between system stiffness and natural frequency, composite timber systems can exhibit counterintuitive behaviour where mass addition effects, enhanced damping mechanisms, and fibre-matrix interface dynamics fundamentally alter these relationships. This necessitates comprehensive experimental validation to establish reliable correlations between static and dynamic properties, particularly in modular configurations where mechanical discontinuities create additional complexity. Accordingly, this chapter defines the experimental and numerical procedures used to quantify frequency, mode shapes, and stiffness evolution across segmentation–reinforcement configurations to validate (or refute) the expected frequency–stiffness trend under modular conditions.

This study employs a hybrid methodology integrating Experimental Modal Analysis (EMA), flexural bending tests, and Finite Element Analysis (FEA) to assess dynamic and static responses of modular timber beams. Figure 3.1 illustrates this integrated framework, where EMA and flexural testing provide experimental data while

FEA validates findings and extends analysis capabilities. This experimental-numerical approach systematically captures complex static-dynamic relationships in segmented systems, focusing on how segmentation, bolted connectors, and Chopped Strand Mat (CSM) reinforcement influence stiffness reduction and natural frequency shifts, which are critical serviceability indicators for timber bridge safety for timber bridge serviceability assessment and structural performance evaluation.

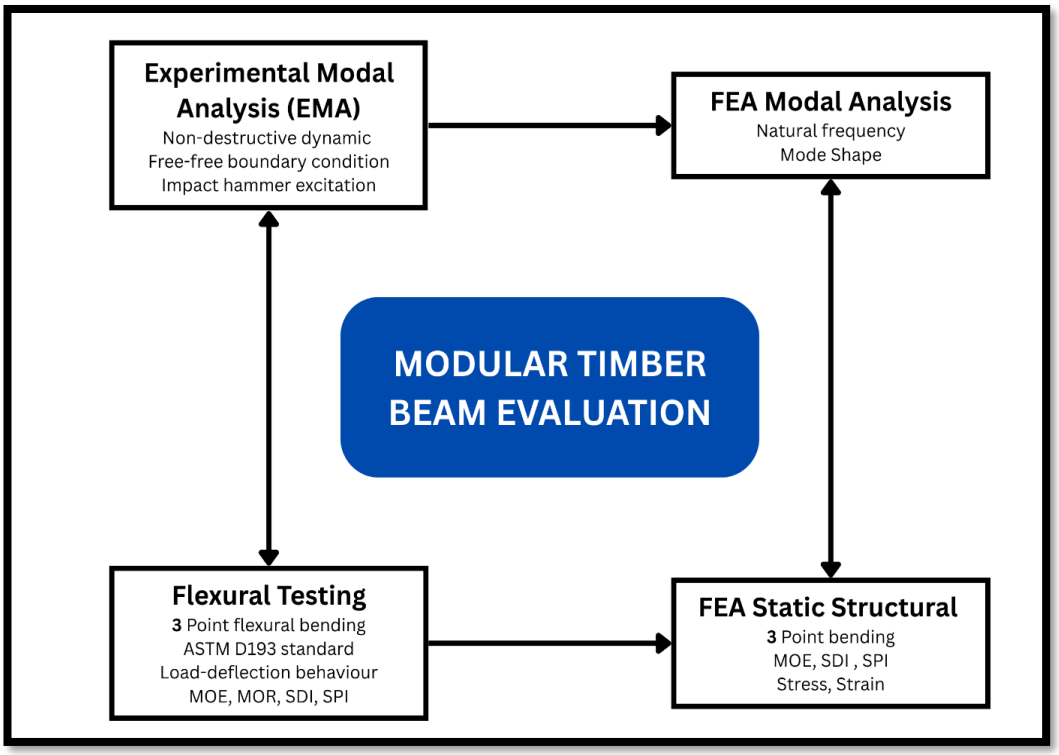

Figure 3.1 Methodological framework correlating EMA, flexural testing, and FEA

The fundamental relationship equation between natural frequency (f), stiffness (k), and mass (m) is expressed as in equation (3.1). In segmented timber systems, this idealization requires validation because joint compliance and damping mechanisms can decouple frequency response from static stiffness.

$$f = \frac{1}{2\pi}\sqrt{\frac{k}{m}} \tag{3.1}$$

This multi-method approach was structured to ensure reproducibility, comparative reliability, and triangulated validation across physical and virtual domains. However, the application of this classical relationship to composite segmented systems requires careful validation, as the assumptions of uniform material properties and continuous stiffness distribution do not hold. The methodology specifically investigates

scenarios where traditional frequency–stiffness correlations may deviate from classical assumptions, requiring experimental validation across segmented and reinforced configurations. The integrated approach enables comprehensive characterization of complex static-dynamic relationships in composite segmented systems, where single-method assessments inadequately capture system behaviour. By analysing reinforced and non-reinforced specimens with varying segment lengths and connector configurations, this methodology provides a systematic pathway for optimizing modular timber bridge strategies while establishing evidence-based design guidelines for field deployment.

The research design encompasses three integrated phases providing comprehensive structural characterization. Figure 3.2 illustrates the research design framework that integrates experimental and simulation approaches for systematic performance evaluation.

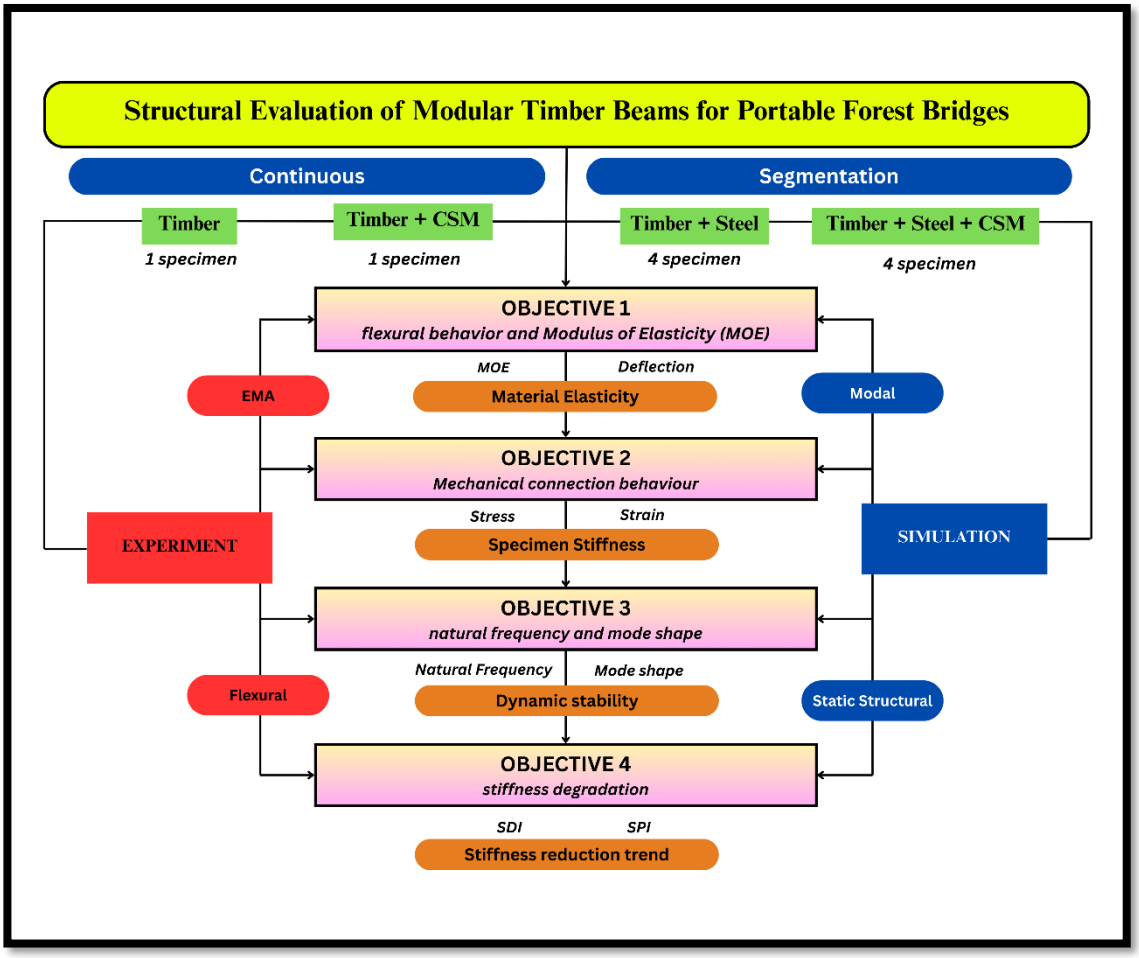

Figure 3.2 Research Design Framework that Integrate Experimental and Simulation Approaches

Phase 1 (Objectives 1 and 3): EMA employs non-destructive dynamic assessment using controlled impact excitation and acoustic response measurement to extract natural frequencies and estimate dynamic stiffness characteristics without compromising specimen integrity. This approach addresses critical literature gaps regarding the relationship between segmentation patterns and dynamic performance, enabling systematic evaluation of how mechanical connectors and material discontinuities alter vibrational properties across different beam configurations.

Phase 2 (Objectives 1, 2, and 4): Static Performance Quantification implements standardized three-point flexural testing using a Shimadzu AG-IS 100 kN Universal Testing Machine to systematically evaluate load-deflection behaviour, stiffness characteristics, and failure progression under controlled loading conditions. This phase addresses identified limitations in understanding how CSM reinforcement effectiveness varies across segmented configurations while simultaneously providing comprehensive load-bearing capacity verification of mechanical connections through systematic safety factor analysis, stress concentration quantification, and load redistribution assessment.

Phase 3 (Objectives 2, 3, and 5): Computational Validation and Extension utilize ANSYS 2019 R3 FEA to simulate both static and dynamic responses under equivalent boundary conditions, enabling detailed stress-strain analysis at connector interfaces and reinforcement regions that are experimentally inaccessible. The computational framework extends experimental findings beyond laboratory constraints while providing critical validation of the relationship between measured performance and predicted behaviour under variable loading scenarios.

A critical component of this methodology is the systematic verification of mechanical connector load-bearing capacity under realistic loading conditions. The experimental design incorporates comprehensive safety factor analysis, stress concentration quantification, and load redistribution assessment essential for practical implementation. This integrated approach ensures connector performance validation through multiple independent assessment methods, providing robust confidence in connection adequacy for forest bridge applications.

This investigation introduces two novel indices developed in this study to quantify performance reduction: the Stiffness Reduction Index (SRI) and the Segmentation Performance Index (SPI), which quantitatively assess the trade-offs between modular constructability and structural performance. These systematic

analytical tools address existing knowledge gaps in the evaluation of modular timber systems by facilitating the identification of configurations that achieve an effective balance between transportation efficiency and structural integrity. The methodology is deliberately structured to determine critical performance thresholds, including the maximum permissible segmentation and the most effective reinforcement strategies, derived through comprehensive evaluation of modular timber bridge systems.

3.2 Specimen Design and Preparation

This This section defines the specimen matrix, material specifications, and fabrication procedures for the modular timber beam configurations used in the experimental programme and FEA validation. Ten full-scale specimens were systematically designed to evaluate the effects of segmentation and reinforcement on structural performance in portable forest bridge applications.

3.2.1 Specimen Configuration Matrix

A systematic specimen matrix was developed to evaluate the independent and combined effects of reinforcement and segmentation on modular timber beam performance. The experimental design employed a two-factor approach with reinforcement status and segment configuration as primary variables.

Specimens were categorized into two series based on reinforcement status. The ETN series (Experimental Timber Non-reinforced) comprised control specimens without bottom-flange reinforcement, establishing baseline performance for evaluating segmentation effects without reinforcement influence (as shown in Figure 3.3). The ETR series (Experimental Timber Reinforced) comprised identical specimens reinforced with a 5 mm CSM layer bonded to the bottom flange using epoxy resin, enabling evaluation of tension-zone strengthening in mitigating segmentation-induced stiffness reduction (as shown in Figure 3.4).

Each series included a continuous control specimen and segmented configurations spanning 2–5 segments, where 2–4 segments represent the primary design space aligned with the study objectives, and the 5-segment case provides an upper-bound limit condition for stiffness reduction quantification:

a) **Continuous Configuration (1 segment):** Single 3000 mm timber beam serving as control specimen for each series (ETN131, ETR136). These specimens provided baseline stiffness and strength values for comparison with segmented configurations.
b) **Two-Segment Configuration:** 1500 mm segment length with single mid-span steel connector, representing minimal segmentation for modular assembly while maintaining structural continuity.
c) **Three-Segment Configuration:** 1000 mm segment length with two steel connectors positioned at third-points, providing moderate segmentation for enhanced transportability.
d) **Four-Segment Configuration:** 750 mm segment length with three steel connectors, approaching optimal balance between modularity and structural performance.
e) **Five-Segment Configuration:** 600 mm segment length with four steel connectors, representing maximum segmentation for ultimate portability with corresponding structural trade-offs.

The specimen identification follows a structured alphanumeric coding system to ensure consistency and traceability across experimental testing, FEA and data processing. Each code begins with “ET”, denoting Experimental Timber, followed by “R” for Reinforced or “N” for Non-reinforced configurations. This is then followed by numerical identifiers that indicate the segmentation configuration (e.g., number of segments and segment length), and a final digit sequence that serves as a unique specimen number. For example, ETR313 denotes a reinforced specimen with 3 segments of 1.0 m, while ETN21.52 denotes a non-reinforced specimen with 2 segments of 1.5 m.

Non-Reinforced Specimens (ETN) Comprised timber segments and steel connector plates (for segmented configurations), focusing evaluation on fundamental timber behaviour and connector effectiveness. Reinforced Specimens (ETR**)** Integrated timber, CSM reinforcement, and steel connectors (for segmented configurations), enabling assessment of reinforcement continuity effects across mechanical joints.

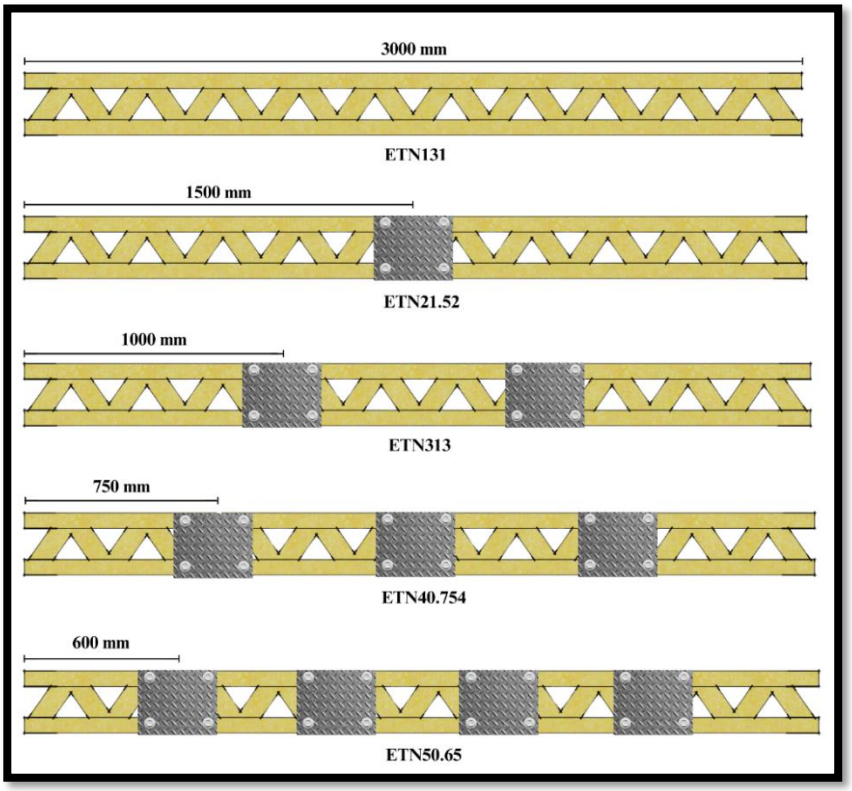

Figure 3.3 Non-reinforced Specimen for Continuous and Segmented Configuration

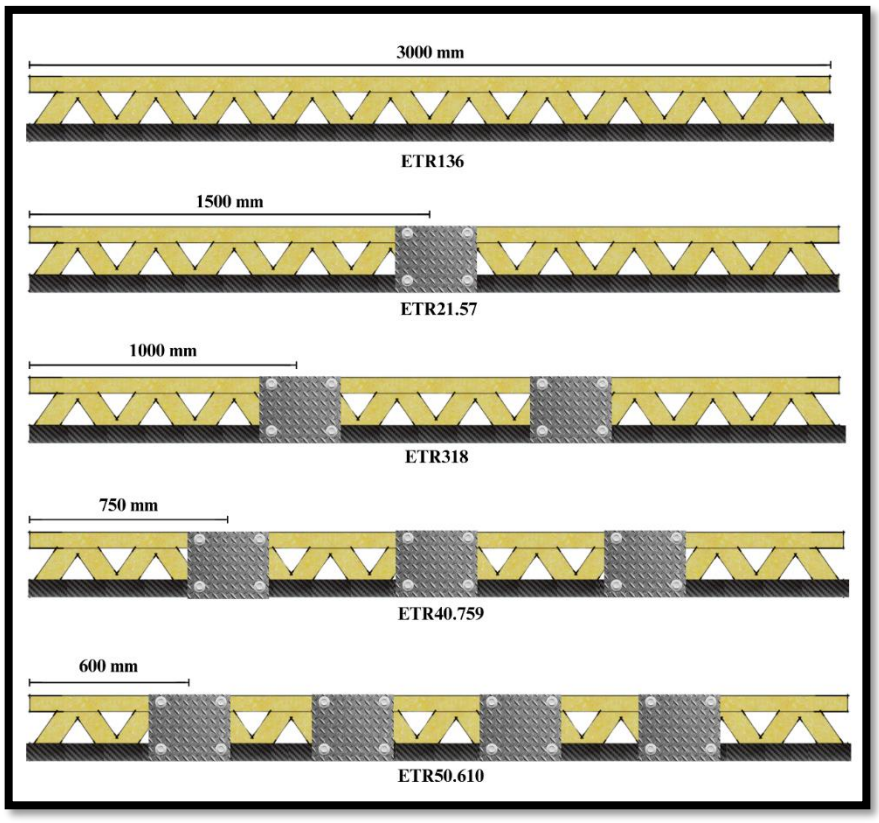

Figure 3.4 Reinforced Specimen for Continuous and Segmented Configuration

All segmented specimens utilized identical steel connector plates and high-tensile bolts to ensure consistent joint behaviour across configurations. The connector placement strategy maintained structural symmetry while enabling systematic evaluation of joint frequency effects on global beam performance. In the specimen identification code, the first number denotes the number of segments, the decimal value denotes the segment length in metres, and the final digit represents the specimen tracking number (1–10). The complete specimen matrix detailing identification codes and configuration specifics is presented in Table 3.1.

Table 3.1
Complete Specimen Matrix with Identification Codes and Configuration Details

Specimen ID	Series	Segment Length (mm)	Number of Segments	Reinforcement Type	Material	Notes
ETN131	ETN	3000	1	None	Timber	Continuous, Control
ETN21.52	ETN	1500	2	None	Timber + Steel	1 Connector, Connector at midspan
ETN313	ETN	1000	3	None	Timber + Steel	2 Connector
ETN40.754	ETN	750	4	None	Timber + Steel	3 Connector, Connector at midspan
ETN50.65	ETN	600	5	None	Timber + Steel	4 Connector
ETR136	ETR	3000	1	CSM Reinforced	Timber + CSM	Reinforced continuous, Control
ETR21.52	ETR	1500	2	CSM Reinforced	Timber + CSM + Steel	1 Connector, Connector at midspan
ETR313	ETR	1000	3	CSM Reinforced	Timber + CSM + Steel	2 Connector
ETR40.759	ETR	750	4	CSM Reinforced	Timber + CSM + Steel	3 Connector, Connector at midspan
ETR50.610	ETR	600	5	CSM Reinforced	Timber + CSM + Steel	4 Connector

3.2.2 Material Properties and Selection

The modular timber beam system comprised four primary materials selected based on structural performance requirements, field deployment constraints, and commercial availability for portable bridge applications. The baseline material properties for all system components are comprehensively detailed in Table 3.2,

establishing the foundation for experimental testing and computational modelling. All specimens utilized standardized GT-24 cross-sectional geometry with material-specific properties determined through literature review and experimental calibration.

3.2.2.1 Specimen Geometry and Baseline Material Properties

All timber specimens were fabricated to replicate the standardized GT-24 Lattice Girder Cross-Section (PERI), which features I-beam geometry with triangular lattice web configuration. The GT-24 designation refers to the standardized timber formwork beam specification with 240 mm overall depth, commonly used in temporary bridge applications. The cross-sectional dimensions include web depth of 240 mm, flange width of 80 mm, and flange thickness of 60 mm. The lattice web configuration optimizes structural efficiency by concentrating material at maximum distances from the neutral axis while minimizing weight compared to solid web alternatives. This standardized geometry facilitated consistent cross-sectional properties across all configurations and enabled direct performance comparisons between segmentation and reinforcement conditions. Figure 3.5 illustrates the detailed cross-sectional geometry.

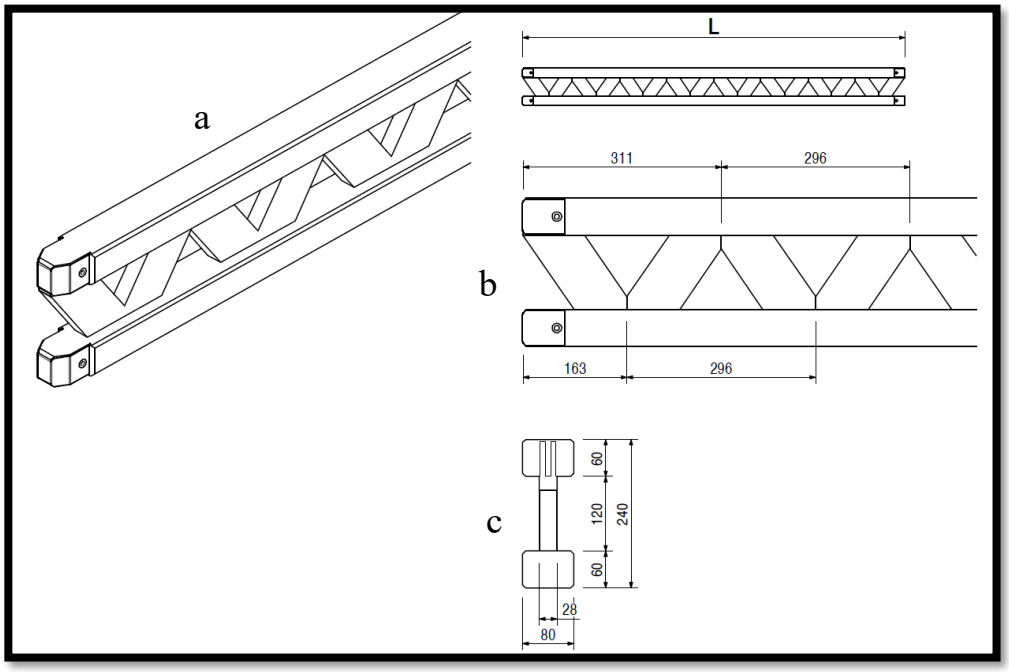

Figure 3.5 Cross-sectional Geometry Specifications (a) Isometric View , (b) Side Elevation View and (c) Cross-Sectional Front View (dimension in mm)

Table 3.2
Baseline Material Properties used for this study

Material	Property	Parameter	Remarks
Western White Pine	Modulus of Elasticity	11,100.559 MPa	Orthotropic; based on Forest Products Laboratory (2010)
	Mass Density	425.338 kg/m³	Kiln-dried and planed for consistency
	Shear Modulus	577.091 MPa	Orthotropic behaviour considered
	Poisson's Ratio	0.329	
	Notes	Orthotropic relationships applied	Favourable strength-to-weight ratio
CSM	Young's Modulus	9,760 MPa	E-glass fibre with epoxy resin
	Poisson's Ratio	0.2	Isotropic material assumption
	Density	2,540 kg/m³	Applied as 5 mm thick reinforcement layer
	Curing	24-hour at room temperature	Clamping pressure applied during curing
Steel Connectors	Young's Modulus	145,000 MPa	Custom-fabricated 5 mm thick plates
	Poisson's Ratio	0.3	Galvanized for corrosion resistance
	Density	7,850 kg/m³	Designed for modular field compatibility
Steel Fasteners	Young's Modulus	170,000 MPa	High-tensile bolts and nuts (typically Ø10 mm)
	Poisson's Ratio	0.3	Installed with calibrated torque wrenches
	Application	Mechanical assembly of beam segments	Ensures standardized connection integrity

Note: The steel connector modulus (145,000 MPa) represents an effective stiffness adopted for calibrated FEA modelling of joint compliance, not the nominal elastic modulus of structural steel.

3.2.2.2 FEA Calibration Methodology

Material properties were iteratively calibrated through FEA validation to account for specimen-specific behaviour, joint interactions, and modelling assumptions not captured by baseline literature values. The systematic calibration process involved:

a) **Control Specimen Selection:** ETN131 (non-reinforced continuous), ETR136 (reinforced continuous), and ETN21.52 (segmented configuration)
b) **Iterative Property Adjustment:** Material parameters systematically refined until FEA deflection predictions matched experimental results within ±5% error tolerance
c) **Validation Metrics:** Mid-span deflection under identical loading conditions, with cross-validation using modal frequency predictions

d) **Convergence Criteria:** Consistent model behaviour across multiple load levels and boundary conditions.

This calibration approach ensured simulation accuracy reflected physical test behaviour rather than theoretical material properties alone, accounting for timber variability, reinforcement bonding efficiency, and connector flexibility under actual loading conditions.

3.2.2.3 Calibrated FEA Properties

The final calibrated material properties demonstrated significant deviations from Maloney's baseline values and manufacturer specifications, highlighting the importance of experimental validation in modular timber system modelling are detailed in Table 3.3.

Table 3.3
Calibrated FEA Material Properties

Property	Property	Value	Remarks
Western White Pine (Calibrated)	Longitudinal Modulus	3,650 MPa	Reduced to 33%
	Radial Modulus	868.74 MPa	Maintained from baseline
	Tangential Modulus (Continuous)	420.58 MPa	Used for continuous specimens
	Tangential Modulus (Segmented)	145 MPa	Effective calibrated parameter representing joint compliance
	Density	466.84 kg/m³	Increased to 110% of baseline
CSM Reinforcement (Calibrated)	Young's Modulus	13,000 MPa	Increased to 133% of baseline
	Poisson's Ratio	0.2	Maintained from baseline
	Density	2,540 kg/m³	Maintained from baseline
Steel Connectors (Calibrated)	Young's Modulus	145,000 MPa	Maintained baseline
	Poisson's Ratio	0.3	Maintained baseline
	Density	7,850 kg/m³	Maintained baseline

The calibrated material properties matrix reveals substantial differences from the baseline Western White Pine characterization, particularly the reduced effective longitudinal stiffness (33% of the baseline 11,100.559 MPa) and the enhanced CSM modulus (133% of baseline). Steel connector properties remained consistent with baseline values, indicating accurate initial characterization. For segmented configurations, calibrated orthotropic parameters represent an equivalent system-level response introduced to achieve agreement between numerical predictions and experimental measurements, with stiffness reduction originating from joint and

interface compliance rather than intrinsic changes in timber material properties. These adjustments were essential for achieving accurate deflection predictions within acceptable engineering tolerances, confirming the necessity of experimental calibration for complex modular timber systems with mechanical connections.

3.2.3 Beam Geometry and Cross-Sectional Design

The detailed cross-sectional geometry is illustrated in Figure 3.6. The lattice (zig-zag) web design improves structural efficiency by maximizing material distribution from the neutral axis while reducing self-weight compared to solid web alternatives. Total beam lengths were standardized at 3000 mm to enable systematic comparison across segmentation levels. The I-beam profile mirrors commercial PERI GT24 sections commonly used in temporary bridge applications, ensuring practical relevance for field deployment. The effective cross-sectional properties were determined through computational analysis to account for the complex lattice web geometry. Under normal conditions, the cross-section maintains consistent geometry throughout the beam length, allowing for uniform structural properties along the span.

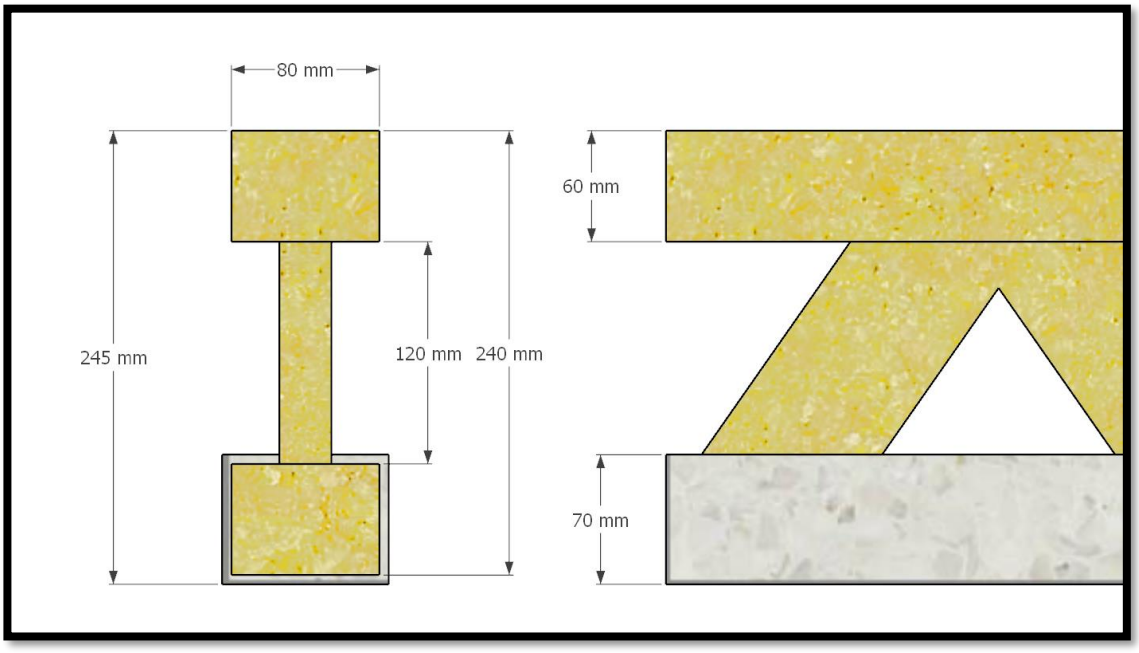

Figure 3.6 Cross-sectional Geometry of I-beam Specimens with Lattice Web Configuration

The theoretical solid web cross-sectional area was calculated as 0.01296 m², representing the equivalent area if the I-beam utilized a continuous solid web instead of the lattice configuration. This baseline provided the reference for comparing the

material efficiency of the lattice design. The actual cross-sectional area of the lattice (zig-zag) web design was determined using Computer-Aided Design (CAD) volume analysis. For control specimen ETN131 with a total volume of 0.0351 m^3 over a 3.0m length, the effective cross-sectional area was calculated as: Cross-sectional Area = Volume ÷ Length = 0.0351 m^3 ÷ 3.0m = 0.0117 m^2. The lattice web configuration resulted in a cross-sectional area reduction of 9.72% compared to the equivalent solid web design. Area Reduction = (0.01296 - 0.0117) ÷ 0.01296 × 100 = 9.72%. The calculated lattice web cross-sectional area of 0.0117 m^2 was consistently used throughout all experimental testing, FEA, and structural calculations in this study. This approach focused the investigation on the actual timber material behaviour rather than theoretical solid web properties, providing realistic assessment of modular timber beam performance under field conditions.

The 9.72% material reduction compared to solid web design demonstrates the efficiency of the lattice configuration while maintaining the study's focus on understanding the fundamental mechanical behaviour of the actual timber cross-section used in portable bridge applications. All geometric properties including moment of inertia, section modulus, and cross-sectional area incorporated the actual lattice geometry rather than simplified solid web assumptions. This approach ensured that simulation results accurately reflected the mechanical behaviour of the fabricated specimens under loading conditions.

3.2.4 U-Shaped Steel Connector Design and Assembly Procedures

Mechanical connectors constitute the critical interface elements in modular timber bridge systems, representing the primary vulnerability points where continuous beam behaviour transitions to segmented performance. As established in Chapter 2, connections introduce structural discontinuities that fundamentally alter load transfer mechanisms and create stiffness reduction patterns unique to modular configurations (Chen et al., 2020; Zhang et al., 2018). This section establishes the standardized U-shaped steel connector (as shown in Figure 3.7) specifications that enable systematic evaluation of modular connection performance in support of Objective 2.

3.2.4.1 Rationale for Standardized Connector Design

This study aims to promote modular connection technology by accurately quantifying stiffness reduction in modular timber beams, where connections represent the weakest point in the structural system. The implementation of identical U-shaped connector configurations across all segmented specimens is essential for precise characterization of modular-induced performance reduction.

The research specifically targets stiffness reduction patterns that result from beam segmentation, where mechanical connections inherently compromise continuous beam performance. To identify these reduction effects and develop exact predictive models, all connection variables must remain constant across specimen configurations. Using identical connector designs ensures that observed performance differences directly reflect the fundamental effects of modular segmentation rather than variations in connection hardware.

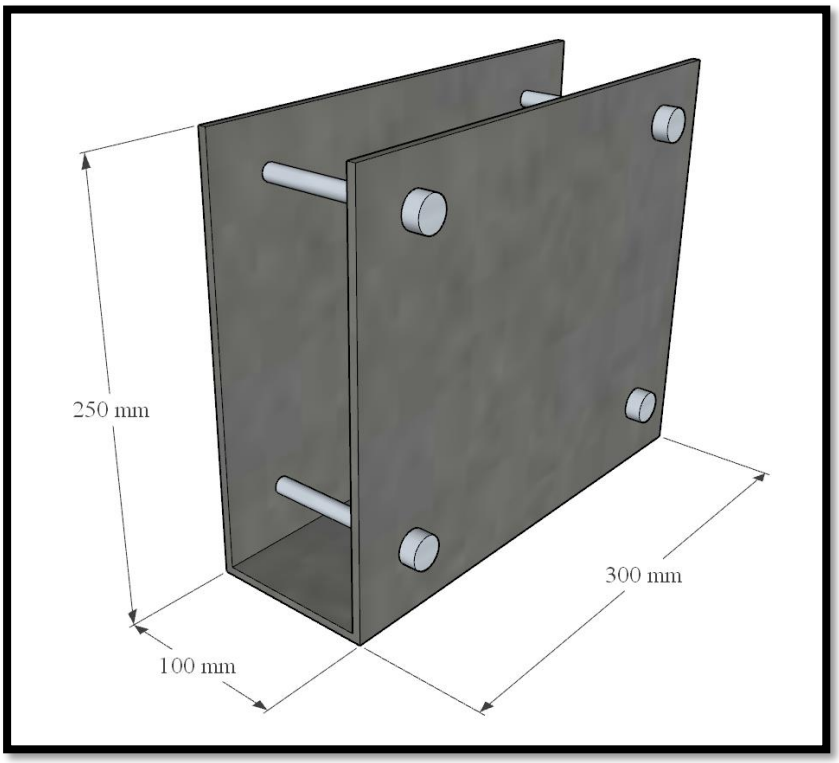

Figure 3.7 U-shaped Steel Connector that Used to Join the Segmented Beam.

Since connections constitute the weakest point in modular systems, standardizing connector design eliminates hardware variability as a confounding factor. While two connector sizes are employed (90 mm outer width for ETN specimens and 100 mm for ETR specimens to accommodate CSM reinforcement), both maintain

identical structural characteristics, load transfer mechanisms, and material properties. This controlled variation ensures optimal bearing contact for each specimen type while preserving experimental validity. The approach enables systematic evaluation of how segmentation frequency and reinforcement strategies affect structural performance, providing the quantitative relationships essential for evidence-based modular design guidelines.

3.2.4.2 U-Shaped Steel Connector Specifications

A standardized U-shaped steel connector configuration was developed using appropriate structural design standards to provide consistent mechanical interfaces across all segmented specimens. The design balances adequate load transfer capacity, uniform experimental conditions, and practical field assembly requirements for portable forest bridge applications.

The U-shaped connector used in this study is fabricated from structural steel and was designed in accordance with Eurocode 3 (EN 1993-1-8), which governs steel joint configurations, bolt spacing, edge distances, and net section performance (British Standards Institution (BSI), 2005). This standard was used to ensure the connector plate's structural adequacy based on established criteria for bolted steel connections.

In contrast, the bolt interaction with the timber flange, particularly the risk of splitting or edge tear-out, was evaluated in Chapter 4 using BS 5268-2:2002, which provides edge distance and spacing requirements specific to timber bearing and connection design (BSI, 2002). The use of both standards reflects the hybrid nature of the steel-to-timber connection system and ensures that each material is assessed using the appropriate regulatory framework consistent with accepted structural engineering practice.

The U-channel configuration provides complete wraparound engagement with the I-beam cross-section through precise dimensional control. Each connector is fabricated from 5 mm thick mild steel and configured as a three-plate channel assembly comprising two side plates and a base plate, forming a rigid U-shaped connector. The assembled connector has an overall length of 300 mm along the beam axis and an overall height of approximately 245 mm, fully enclosing the timber flanges while providing adequate material distribution for load transfer and structural continuity across segmented interfaces.

Two connector variants were fabricated to accommodate the different cross-sectional requirements of non-reinforced (ETN) and reinforced (ETR) specimens, as illustrated in Figure 3.8. The ETN connector features an outer envelope width of 90 mm, providing an internal channel width of 80 mm precisely sized for the timber beam cross-section. The ETR connector incorporates a larger outer envelope width of 100 mm, creating an internal channel width of 90 mm to accommodate the additional 5 mm CSM reinforcement thickness applied to the bottom flange of reinforced specimens. This dimensional variation ensures optimal fit and consistent bearing contact for both specimen types while maintaining identical load transfer mechanisms and structural performance characteristics across all configurations.

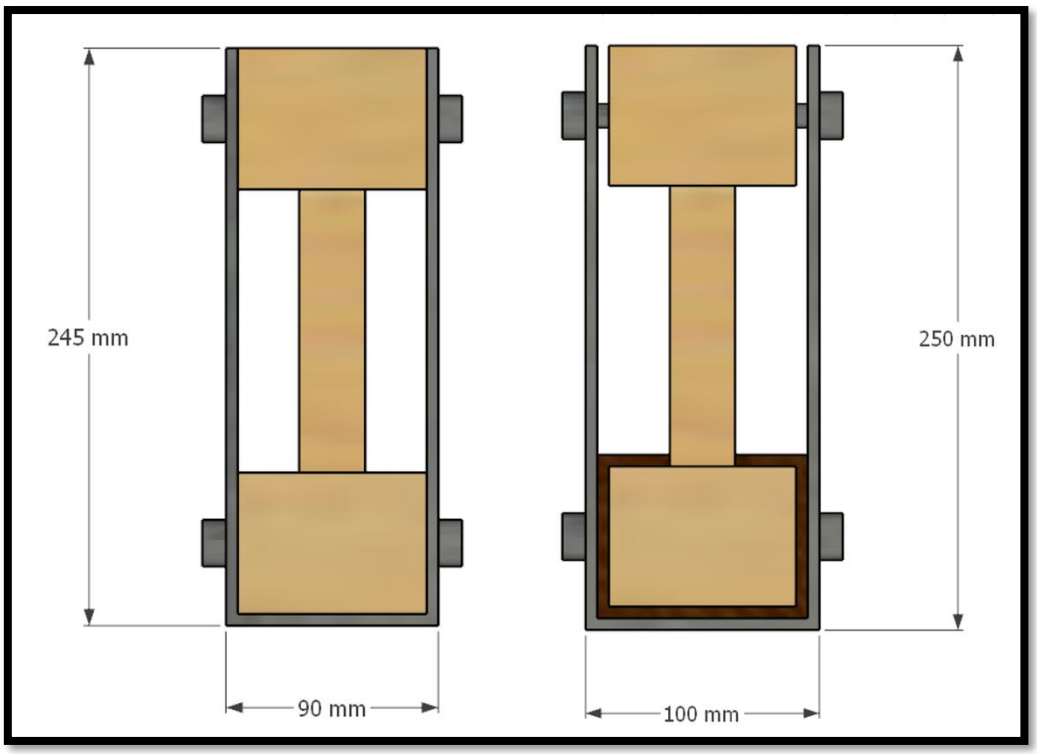

Figure 3.8 Steel Connector Front View of U-Shaped Steel Connector Configurations (Left: ETN, Right: ETR)

Material and Fabrication Standards: High-precision cutting and drilling processes ensure consistent dimensions across all connectors, with smooth edges and accurate positioning essential for uniform assembly and load distribution. The 5 mm plate thickness provides adequate structural capacity while maintaining practical handling characteristics for field operations. Both connector variants (ETN and ETR) are fabricated to identical quality standards, with the only difference being the internal

channel width accommodation for reinforcement thickness. Steel component parameters comply with EN 1993-1-8 requirements (as shown in Figure 3.9), with edge distances of 40 mm substantially exceeding minimum requirements to ensure adequate stress distribution and prevent localized failures. Timber-specific performance criteria including bearing capacity and connection adequacy are evaluated using BS 5268-2:2002 standards as presented in Chapter 4.

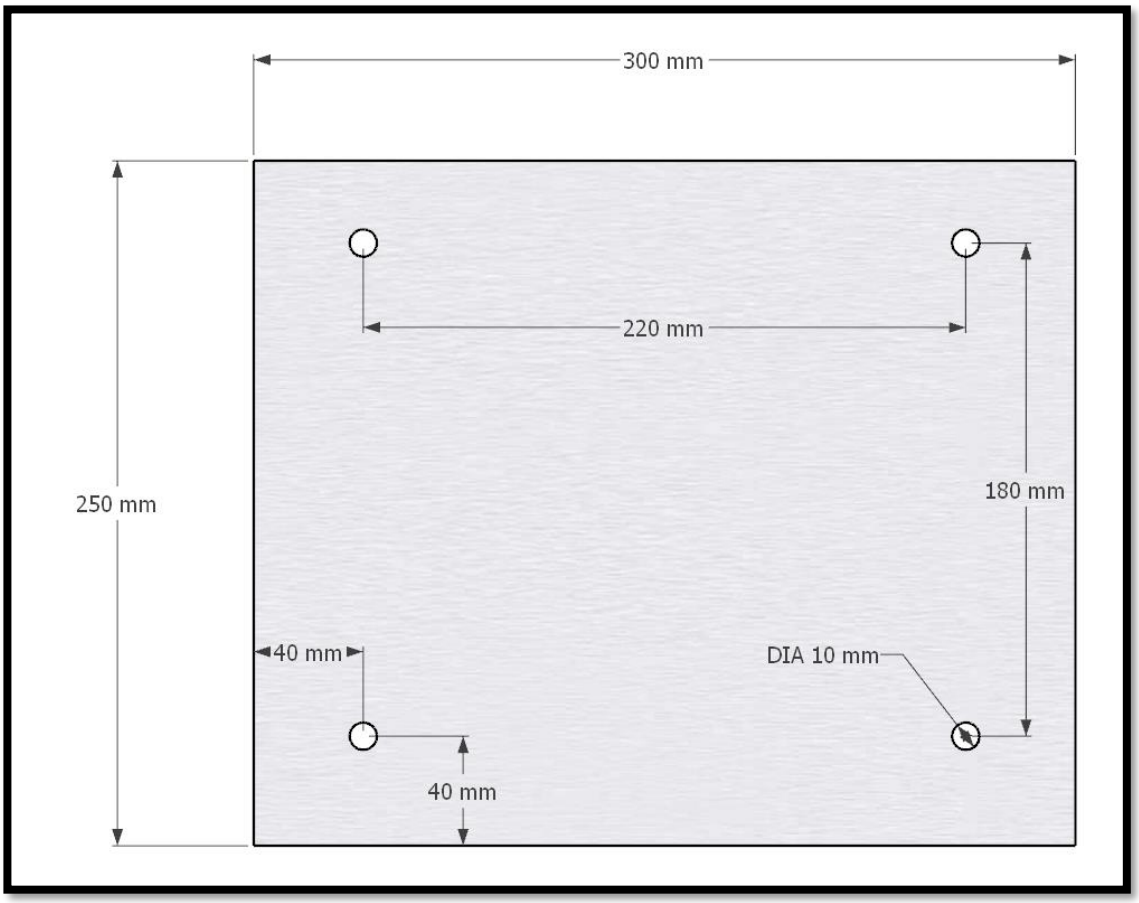

Figure 3.9 Side View of Steel Connector Showing Layout of Bolt Location

3.2.4.3 Load Transfer and Structural Performance

The U-shaped connector design facilitates comprehensive load transfer through multiple interface mechanisms: direct bearing contact between steel plates and timber flanges, shear transfer through wraparound geometry, and moment resistance through rigid channel configuration. This approach eliminates load transfer inefficiencies associated with partial engagement designs.

The steel connector geometry provides complete cross-sectional interaction with both upper and lower timber flanges while maintaining direct web interface contact.

The wraparound design distributes bearing loads uniformly across the timber surface, minimizing stress concentrations at timber-steel contact points and reducing potential for localized crushing or splitting. For reinforced specimens, the larger outer envelope (100 mm vs 90 mm) provides an internal channel width of 90 mm to accommodate the CSM reinforcement layer while maintaining identical contact pressure and load distribution characteristics. The symmetric geometry eliminates eccentricity effects while providing balanced load paths for both tension and compression forces across both specimen types.

The mild steel construction provides adequate strength and ductility characteristics for anticipated loading conditions while maintaining cost-effectiveness and fabrication simplicity. The material properties enable reliable performance under both static and dynamic loading conditions typical of portable forest bridge applications, with sufficient flexural rigidity to prevent local buckling under concentrated loads.

3.2.4.4 Assembly Procedures and Quality Control

Standardized assembly procedures incorporate precision alignment and comprehensive quality control protocols to ensure consistent connector behaviour across all specimen configurations. The methodology encompasses connector placement verification, alignment assessment, and systematic assembly sequencing to maintain structural integrity and reproducible performance.

U-shaped connectors are positioned using precision alignment fixtures to ensure consistent placement relative to timber segment interfaces. Assembly procedures employ systematic positioning sequences documented in Appendix 3, maintaining consistent connector orientation and timber engagement across all specimen configurations. This approach minimizes installation-induced variability while ensuring reproducible connection performance essential for accurate reduction analysis.

Connector performance is systematically integrated with global beam performance indices (SRI and SPI), enabling evaluation of connection behaviour effects on overall structural system performance. Cross-validation between experimental measurements and FEA ensures reliability of connector performance conclusions while maintaining focus on the steel connector's role in modular system behaviour.

3.2.4.5 Experimental Integration and Validation

The standardized U-shaped steel connector design provides the controlled foundation necessary for systematic investigation of modular timber system performance. This approach ensures experimental findings reflect fundamental modular behaviour rather than connection design variables, supporting development of evidence-based guidelines for modular timber bridge applications.

Connector performance metrics are integrated throughout the experimental framework: Phase 1 (EMA) establishes baseline dynamic response with consistent connector mass and stiffness properties; Phase 2 (Flexural) provides direct assessment of connector load transfer effectiveness; Phase 3 (FEA) enables detailed stress analysis of connector performance under various loading conditions. This integration ensures comprehensive understanding of connector adequacy while generating essential data for Objective 2 analysis.

The conservative connector geometry and material specifications ensure reliable performance under anticipated loading conditions while providing the experimental control necessary for accurate reduction quantification. As demonstrated in Table 3.4, the design substantially exceeds all Eurocode 3 requirements, ensuring robust structural performance that enables confident focus on modular system characteristics rather than connection adequacy concerns.

Table 3.4
Steel Connector Compliance with EN 1993-1-8

Design Criterion	Standard Requirement	ETN Design Value	ETR Design Value	Compliance
Plate thickness	≥ 4 mm (EN 1993-1-8)	5 mm mild steel	5 mm mild steel	Comply
Outer envelope width	Fit requirement	90 mm	100 mm	Comply
Internal channel width	Timber accommodation	80 mm	90 mm	Comply
Edge distance (top)	≥ 15 mm (EN 1993-1-8)	35 mm	35 mm	Comply
Edge distance (side)	≥ 15 mm (EN 1993-1-8)	40 mm	40 mm	Comply
Plate layout geometry	Symmetric recommended	Fully symmetric U-channel	Fully symmetric U-channel	Comply

3.3 Experimental Modal Analysis (EMA)

EMA was conducted as the initial phase of testing to assess the dynamic response of modular timber beam specimens, which is one of the non-destructive testing

methods. The complete EMA methodology is outlined in the experimental flowchart (Figure 3.10). The goal was to extract fundamental modal properties, namely the natural frequencies associated with the first vertical bending mode, to evaluate global stiffness and vibration sensitivity. This non-destructive testing method provided a valuable baseline for understanding how segmentation, mechanical connections, and reinforcement influence dynamic performance without causing material damage.

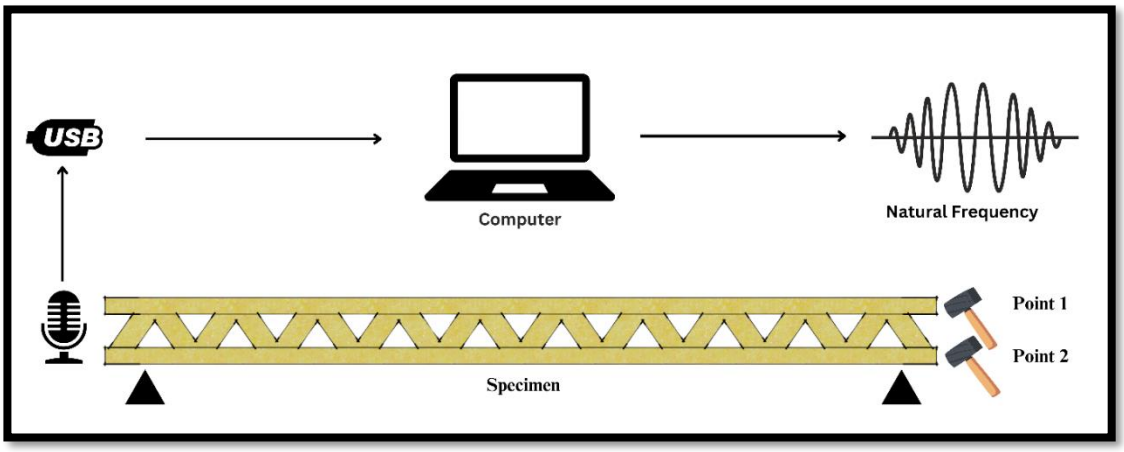

Figure 3.10 EMA Methodology Experimental Flowchart.

3.3.1 Purpose and Significance

This study employed EMA, a widely recognized diagnostic technique in structural dynamics, to support multiple objectives related to modular timber beam performance assessment, particularly suited for evaluating vibrational characteristics of lightweight and composite structures (Ahmed et al., 2019; Siva & Ramakrishna, 2020).

The first objective was to estimate the natural frequency corresponding to the first vertical bending mode, which is directly related to the beam's global stiffness and mass distribution using EMA. This study applied established structural vibration theory principles where natural frequency increases with stiffness and decreases with mass (Sarrazin & Valerio, 2022; Ahmed et al., 2019) to track frequency shifts as a practical method for evaluating structural changes due to segmentation, reinforcement variation, or joint reduction. Equation (3.2) represents the fundamental theoretical relationship governing natural frequency in beam structures; however, its direct application to segmented and reinforced timber systems requires experimental verification due to the influence of joint compliance and damping effects that may decouple frequency response from static stiffness.

$$f = \frac{1}{2\pi}\sqrt{\frac{k}{m}} \tag{3.2}$$

Where:

f = Natural frequency (Hz)

k = Structural stiffness (N/m)

m = Mass (kg)

$\frac{1}{2\pi}$ = Conversion from angular frequency ω (rad/s) to frequency $f(Hz)$, since $f = \omega/2\pi$

This relationship enables direct correlation between dynamic measurements and structural stiffness properties and it is the fundamental natural frequency equation for a single-degree-of-freedom (SDOF) system modelled as a spring-mass system. It relates the natural frequency f of a system to its stiffness k and mass m.

Second objective, EMA was enabled the differentiation of stiffness levels among beams with various configurations such as continuous vs. segmented, and reinforced vs. non-reinforced. This capability is essential for identifying mechanical weaknesses or inconsistencies in modular timber systems, particularly where mechanical connectors introduce local flexibility or discontinuity (Anwar & Hashad, 2020).

The Third objective, EMA was served as a non-destructive technique to preliminarily validate structural integrity before performing destructive flexural tests. The presence of significant frequency drops was treated as an indicator of potential damage or insufficient joint performance, consistent with observations by Yassin & Othman, (2024), who highlighted the effectiveness of modal frequency tracking for structural anomaly detection. Al-Raheimy & Hammed, (2022) similarly noted that dynamic testing methods such as EMA can reveal internal behavioural characteristics without physically compromising the specimen.

Finally, EMA was used to support the modal calibration of FEA simulations. By comparing experimentally obtained modal frequencies with those predicted numerically, the study ensured greater accuracy in simulation output and improved predictive capabilities for design evaluation. This interaction between physical and numerical data is critical in refining simulation models, as demonstrated by Ahmed et al., (2019) and reinforced by Aman et al., (2023), who stressed the importance of

aligning modal parameters to enhance simulation reliability.

These complementary applications establish EMA as an indispensable part of the methodological framework, providing a comprehensive non-destructive evaluation approach that bridges experimental validation with computational modelling for systematic assessment of modular timber beam performance.

3.3.2 Experimental Setup

EMA was conducted to investigate the dynamic response of modular timber beams under controlled boundary conditions. The complete experimental setup is illustrated in Plate 3.1. Each specimen was horizontally supported using metal tripods positioned near both ends, introducing minimal restraint and providing a near free–free boundary condition appropriate for comparative modal analysis across specimens. This support arrangement enabled assessment of fundamental vibrational modes while minimizing boundary effects that could influence natural frequency measurements.

Plate 3.1 EMA Experimental Setup.

The test protocol employed longitudinal excitation applied directly to the top and bottom flanges using a polyurethane-tipped dead blow hammer (Model 5-40), as illustrated in Plate 3.2. This provided controlled, repeatable impacts suitable for timber structures without surface damage. Dynamic excitation was applied at two specific

locations along the beam's length (Point 1 and Point 2 as shown in Figure 3.10) to assess vibrational energy transmission through continuous and segmented configurations. This setup enabled systematic evaluation of how mechanical connectors influence stiffness continuity and wave propagation characteristics. The excitation layout ensured clean longitudinal modal responses while minimizing transverse wave interference.

Plate 3.2 Hammer Used to Strike for Wave Excitation.

Dynamic response was captured using a precision omnidirectional microphone (MG M360 with MH 64 holder) mounted on a tripod and positioned approximately 30mm from the beam surface near one end. The microphone positioning and mounting arrangement is illustrated in Plate 3.3.

This non-contact acoustic method eliminated mass loading effects that could alter the structural dynamics while enabling consistent, repeatable signal capture across all specimens. The microphone positioning was standardized to maintain consistent measurement conditions and minimize environmental interference during testing.

Signal acquisition was accomplished using a National Instruments NI 9233 analog input module housed within a NI USB-9162 high-speed USB carrier, as shown in Plate 3.4. The microphone connected to the data acquisition system via BNC cable, providing reliable signal transmission with minimal noise interference. The analog signals were digitized at appropriate sampling rates to capture the frequency bandwidth of interest (0-30 Hz) while ensuring adequate resolution for accurate frequency identification. The data acquisition hardware was calibrated prior to testing to ensure measurement accuracy and consistency across all specimens.

Plate 3.3 Microphone Setting Up For EMA Testing.

Plate 3.4 National Instruments NI 9233 Analog Input Module.

A custom-built virtual instrument (VI) acquired time-domain data, performed real-time Fast Fourier Transform (FFT) analysis, and displayed natural frequency,

sound pressure spectra, and preliminary MOE within a 0-30 Hz frequency bandwidth sufficient for capturing dominant vibration characteristics. At each test point, a minimum of ten impacts were applied with real-time monitoring via LabVIEW and video recording for quality control. Five high-quality impacts per point were selected for analysis based on signal clarity and consistency, with spectral peaks manually verified to ensure reliable frequency identification. Plate 3.5 is the specimen ETN21.52 prepared for this testing, while other images of other specimens and configurations are compiled in Appendix 1 for reference.

Plate 3.5 Specimen (ETN21.52) Ready for EMA Data Collection.

3.3.3 Dynamic Stiffness and MOE Estimation

The fundamental relationship expressed in Equation (3.3) enables dynamic stiffness estimation from extracted natural frequencies and known mass values, allowing comparative evaluation of different beam configurations including reinforced versus non-reinforced and segmented versus continuous designs. For comparative purposes, the modular beam system was represented using an equivalent single-degree-of-freedom (SDOF) approximation based on the dominant first vertical bending mode, which governs the global dynamic response of the specimens. This formulation facilitates direct analysis of how design changes influence effective dynamic stiffness characteristics, while the EMA framework provides insights that directly inform structural performance assessment, reinforcement effectiveness quantification, and

numerical model validation across multiple parameters relevant to modular timber bridge applications.

To quantify structural stiffness and validate natural frequency results, dynamic stiffness (k) in Equation (3.3) was calculated for each specimen using the measured total mass and the fundamental frequency obtained from EMA. The total mass of each beam was measured individually using calibrated digital scales. The relationship between natural frequency and structural parameters therefore provides a consistent, non-destructive basis for stiffness comparison across different segmentation and reinforcement configurations.

$$k = (2\pi f)^2 \, m \tag{3.3}$$

where:

k = estimated structural stiffness (N/m),

f = first natural frequency (Hz), and

m = total mass of the beam (kg).

The frequency *f* reflects the beam's global stiffness-to-mass ratio, providing a non-destructive assessment independent of loading conditions. This formulation, commonly used in structural dynamics, provides an independent means of estimating stiffness, which can later be compared against flexural test results and finite element simulations. In addition to stiffness, the MOE was estimated using the following analytical expression derived for free-free beam vibration as in equation (3.4):

$$MOE = \frac{4}{n} L^2 f^2 \rho \tag{3.4}$$

where:

E = estimated MOE (Pa),

n = mode constant (typically n=1n = 1n=1 for the first mode),

L = span length of the beam (m),

f = fundamental natural frequency (Hz), and

ρ = average material density (kg/m³).

This MOE expression relates natural frequency to elastic modulus under the assumption of a uniform, simply vibrating beam with negligible damping. Density (ρ) was derived based on measured mass and beam volume. Although this formulation assumes negligible damping and uniformity, it is adopted in this study as an effective comparative metric for evaluating relative stiffness trends across different segmentation and reinforcement configurations rather than as an absolute material property. Together, these formulations enabled the extraction of dynamic mechanical parameters from vibration data. The stiffness and MOE estimates were used to assess consistency across test methods and to provide reference benchmarks for comparison with results obtained from flexural testing and finite element simulations in Chapter 4.

3.3.4 Analysis Framework for Segmentation Effects

The EMA analysis framework was structured to systematically evaluate the dynamic behaviour of modular timber beams across multiple design variables and their interactions. The analytical approach focused on quantifying frequency variation patterns as segment counts increased from single continuous beams (1 segment) to highly segmented configurations (5 segments), enabling identification of the relationship between modular assembly and dynamic stiffness characteristics.

Reinforcement effectiveness was assessed through systematic comparison of natural frequencies between ETN (non-reinforced) and ETR (reinforced) series specimens at equivalent segmentation levels. This paired comparison approach isolated the contribution of CSM reinforcement to dynamic stiffness while controlling for connector and segmentation variables. The analysis framework incorporated dynamic stiffness correlation with static flexural stiffness measurements to validate the relationship between modal properties and mechanical performance under loading conditions.

Modal parameter validation served as a critical component for FEA model calibration, ensuring computational models accurately reflected experimental dynamic behaviour before application to design optimization or parametric studies. Statistical analysis incorporated correlation assessment between frequency measurements and design parameters including segment count, reinforcement presence, and total beam mass to identify significant relationships governing dynamic behaviour patterns. The analytical framework examined whether increasing segment count resulted in

systematic reductions in calculated dynamic stiffness attributable to connector flexibility and discontinuities, consistent with trends reported in modular structural systems (He et al., 2022).

The comprehensive analysis framework enabled triangulation of dynamic properties with static mechanical testing and finite element predictions, providing multiple validation pathways for structural performance assessment. This multi-method approach ensured robust characterization of modular timber beam behaviour across the complete range of segmentation and reinforcement configurations investigated in the study.

3.4 Flexural Bending Test

The flexural bending test was conducted to evaluate the stiffness characteristics and load–deflection behaviour of modular timber beam specimens, both reinforced and non-reinforced. This experimental investigation aimed to simulate structural loading conditions representative of in-service performance and to assess mechanical responses under flexural stress, with particular emphasis on stiffness reduction attributed to segmentation and mechanical fastener interfaces (Hasan et al., 2024; Zhu et al., 2023). The testing methodology adhered to the three-point bending configuration outlined in ASTM D198-21a (ASTM International, 2021), a widely accepted standard for determining the flexural properties of full-size structural timber elements. This section presents the complete flexural test methodology, including experimental setup, denting correction procedures, strain measurement configuration, analytical calculations for stiffness, MOE and MOR, and the development of reduction indices (SRI and SPI) for performance assessment. Connection behaviour and quality control measures are also outlined to ensure experimental consistency and validity of results.

3.4.1 Experimental Setup

3.4.1.1 Deflection result

The flexural test was conducted using a Shimadzu AG-IS 100 kN Universal Testing Machine (Plate 3.6) fitted with a SLFL-100 kN load cell, operating in displacement control mode at 6.6 mm/min. The complete experimental setup for the

flexural bending test is illustrated in Figure 3.11. Each specimen was simply supported over a 2700 mm clear span, with central loading applied through a steel loading head. Because no LVDT was mounted under the mid-span, deflection was derived from the overhead actuator movement. Although crosshead displacement includes machine compliance effects, this approach was adopted due to experimental constraints and was systematically corrected for localized indentation to ensure consistent comparative stiffness evaluation across all specimens.

To correct for indentation caused by the contact between the steel loading head and the timber beam surface, the denting effect was quantified post-test. The effective mid-span deflection was computed by subtracting this denting displacement from the raw actuator movement. This correction enabled accurate structural stiffness and MOE calculations.

Plate 3.6 Shimadzu AG-IS 100 kN Universal Testing Machine.

During experimental loading, localized denting occurred beneath the loading head due to direct steel-to-timber contact. This surface indentation introduced non-structural deformation that inflated the displacement values recorded by the crosshead.

As a result, the total stroke measured by the Shimadzu UTM comprised both genuine beam deflection and localized surface compression, particularly in non-reinforced specimens.

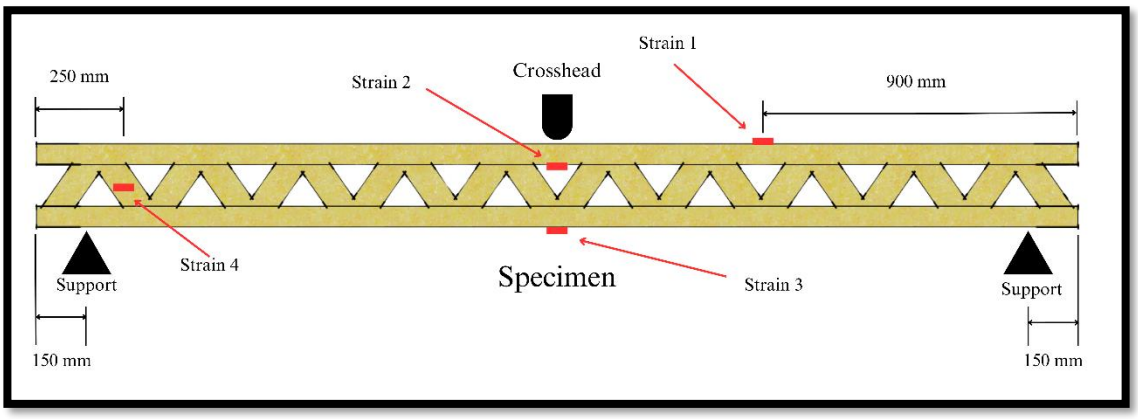

Figure 3.11 Experimental Setup for Flexural Bending Test.

To correct for this and obtain an accurate representation of flexural behaviour, a denting correction procedure was implemented. After each test, the indentation depth (δ_{dented}) at the loading point was measured and subtracted from the total recorded displacement (δ_{measured}) producing the effective deflection ($\delta_{\text{effective}}$) used in all subsequent equation (3.5).

$$\delta_{\text{effective}} = \delta_{\text{measured}} - \delta_{\text{dented}} \tag{3.5}$$

This correction improved the alignment between experimental results and theoretical stiffness predictions. It was observed that non-reinforced beams experienced greater denting due to their unprotected timber surfaces, while reinforced beams showed shallower indentation depths, suggesting that the CSM reinforcement provided additional surface resistance against localized compressive damage. Incorporating this adjustment was essential to accurately quantify the flexural stiffness and ensure valid comparisons between configurations.

3.4.1.2 Strain Data

The strain gauge system was configured separately from the bending test machine. While not electronically synchronized, it was manually triggered at the same

time as the start of loading. The Kyowa strain measurement and data acquisition system is shown in Plate 3.7. Four Kyowa KFGS-10-120-C1-11 L5M2R single-axis strain gauges were installed at specific location as illustrated in Figure 3.11.

a) **Strain 1** – Top flange (compression zone)
b) **Strain 2** – Mid-depth under loading head (neutral axis)
c) **Strain 3** – Bottom flange (tension zone)
d) **Strain 4** – Web near support (shear zone)

The strain gauges employed were Kyowa KFGS-10-120-C1-11 L5M2R (Japan), single-axis electrical resistance type with a gauge length of 10 mm (Plate 3.8). The gauges have a gauge factor of 2.05 ± 1%, nominal resistance of 120.0 ± 0.8 Ω, temperature coefficient of +0.008%/°C, and thermal expansion coefficient of 11.7 ppm/°C, which is compatible with timber substrates. Each gauge was supplied with pre-attached 5000 mm two-wire leads to facilitate instrumentation of large beam specimens. That strain gauge was installed at the mid-span bottom flange of the beam, corresponding to the region of maximum tensile strain under flexural loading. The same strain gauge type, orientation, and installation procedure were applied consistently at all designated strain measurement locations along the beam.

.

Plate 3.7 Kyowa Strain Measurement and Data Acquisition System

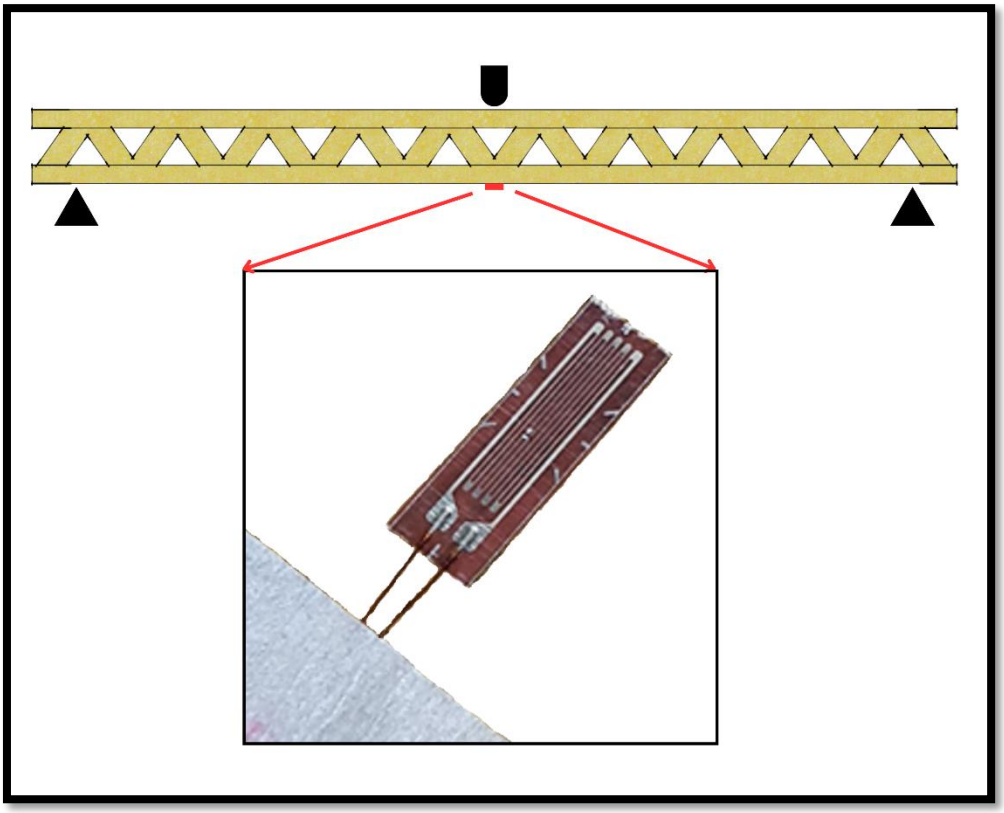

Plate 3.8 Single-axis Strain Gauge 10 mm Length at Mid-span Bottom Flange.

Installation followed a standardized procedure as recommended in the *Kyowa Strain Gauge Installation Manual* (Kyowa, 2021), whereby bonding areas were cleaned with acetone and wiped with lint-free Kimwipes, strain gauges positioned using tape alignment, Kyowa CC-33A instantaneous adhesive (Plate 3.9) applied with uniform pressure for several seconds, followed by curing at ambient laboratory conditions before testing. Lead wires were soldered to terminals with strain relief provided using adhesive tape to prevent wire pullout during testing. This standardized installation protocol ensured consistent gauge performance across all specimens and minimized installation-induced variability in strain measurements.

Plate 3.9 Kyowa CC-33A Adhesive.

Data collection was performed using the Kyowa EDX-11A/EDX-10B compact data acquisition system**,** equipped with a UI-54A-120 4-channel adapter**.** Data were recorded using DCS-100A software, configured in manual mode with a sampling rate of 10 Hz**.** Channels were balanced (zeroed) before testing, and live strain responses were visualized in real-time. Upon test completion, data were exported in Excel format for further processing.

3.4.2 Specimen Matrix and Reinforcement Strategy

The experimental matrix consisted of ten configurations divided into two series: ETN Series (five non-reinforced specimens with 1–5 segments) and ETR Series (five reinforced specimens with CSM bottom-flange reinforcement), where reinforcement was applied as 5 mm thick CSM bonded using epoxy resin through a wet lay-up process, cured for 24 hours at room temperature, and deliberately excluded from connector interfaces to prevent bonding interference. Specimen IDs followed a structured convention where ETN50.65 denotes a non-reinforced beam with 5 segments of 0.6 m segment length and ETR318 represents a reinforced beam with 3 segments of 1.0 m segment length, with each configuration maintaining a constant total length of 3.0 m while varying the number of segments and individual segment lengths. This grouping and reinforcement layout provided a controlled experimental matrix, enabling comparative analysis between beam types with and without reinforcement and across varying segment lengths and connector arrangements (Bakalarz & Kossakowski, 2022; Moawad & Fawzi, 2021). Plate 3.10 shows specimen ETN131 prepared for the flexural bending test using the Shimadzu Universal Testing Machine. Figures of other specimens with varying configurations are compiled in Appendix 2 for reference and documentation.

Plate 3.10 Specimen ETN131 Prepared for Flexural Bending Test.

3.4.3 Analytical Framework for Structural Performance Assessment

This section presents the comprehensive analytical framework employed to evaluate the structural performance of modular timber beams under flexural loading conditions. The quantitative assessment methodology integrates load-deflection analysis, strain measurements, and derived stiffness metrics to characterize material behaviour, assess reinforcement effectiveness, and quantify reduction trends specific to segmented timber systems. All calculations utilize corrected mid-span deflection data and applied loads within the elastic range to ensure measurement accuracy and enable valid comparisons across beam configurations.

3.4.3.1 Fundamental Structural Parameters

Structural stiffness serves as the primary indicator of system resistance to deformation and provides the fundamental parameter for comparative performance assessment across modular timber beam configurations. The flexural stiffness (k) characterizes the load-deflection relationship and represents the structural efficiency of both segmented and continuous beam systems. As shown in Equation (3.6), structural

stiffness is calculated from the slope of the load–deflection curve within the linear elastic region, specifically between 10–40% of the maximum load capacity (*P Maximum*), to eliminate initial non-linearity effects and avoid plastic deformation influences that could compromise measurement accuracy. Accordingly, the applied load P in Equation (3.6) represents the load within this selected linear elastic range rather than the ultimate load value. Stiffness was therefore determined from the incremental relationship between load and deflection ($\Delta P/\Delta\delta$) within the specified range rather than from a single maximum load value. This loading range ensures consistent material behaviour while providing sufficient data points for reliable stiffness determination across all beam configurations, enabling valid comparisons between reinforced and non-reinforced specimens as well as different segmentation levels.

$$k = \frac{P}{\delta} \tag{3.6}$$

Where:

$P =$ Maximum Load
$\delta =$ Effective Deflection

The Modulus of Elasticity (MOE) as in equation (3.7) serves as a effective flexural modulus for system-level performance comparison characterizing the resistance to elastic deformation under flexural stress and provides critical insight into both timber material behaviour and composite system performance. In segmented configurations, the calculated MOE represents an effective system response incorporating joint compliance rather than an intrinsic timber material constant. The MOE determination follows the standardized methodology outlined in ASTM D198-21 (2021) for simply supported beams under three-point loading configurations. This widely accepted standard for determining flexural properties of full-size structural timber elements (Puaad et al., 2024; Jahedi et al., 2024) enables consistent evaluation of material elastic properties across different beam configurations and reinforcement conditions. The MOE calculation utilizing the ASTM D198 formula quantifies the material's ability to resist deformation under stress, providing essential parameters for both individual material characterization and comparative assessment of reinforcement effectiveness in modular timber systems.

$$E = \frac{PL^3}{48I\delta} \tag{3.7}$$

Where:

P = applied load in linear region (N)

L = clear span between supports (mm)

I = moment of inertia of cross-section (mm⁴)

δ = corresponding mid-span deflection (mm)

The moment of inertia for the I-beam cross-section incorporates both flange and web contributions, calculated as a composite of rectangular profiles to accurately represent the engineered timber geometry (Carvalho et al., 2021; Costa et al., 2020). All values are converted to SI units to ensure consistency with simulation and EMA stiffness comparisons, particularly considering the material's nonlinear elastic behaviour at elevated loading levels (Kurzinski & Crovella, 2023).

The Modulus of Rupture (MOR) quantifies the ultimate bending strength and provides insight into failure mechanisms and reinforcement effectiveness. The MOR is determined using the equation (3.8).

$$MOR = \frac{P_{max}L}{bd^2/6} \tag{3.8}$$

where Pmax represents the maximum load at failure (N), b denotes beam width (mm), and d indicates beam depth (mm). This parameter enables identification of CSM reinforcement effects on load-carrying capacity and characterization of failure mode transitions from brittle timber failure to more ductile composite behaviour, consistent with established research (Lee et al., 2019; Navaratnam et al., 2022).

3.4.3.2 Advanced Reduction Assessment Framework

To comprehensively evaluate the unique performance characteristics of modular timber systems, this research introduces two novel reduction indices that capture distinct aspects of structural deterioration in segmented configurations. These indices address critical gaps in existing evaluation methodologies by providing standardized metrics specifically designed for modular structural systems.

Table 3.5 presents the definitions and purposes of the two complementary performance indices developed for this study. These indices offer systematic approaches to quantify structural efficiency and reduction mechanisms, providing essential guidance for optimal modular design decisions.

Table 3.5
Performance Indices Definitions

Index	Acronym	Purpose
Stiffness Reduction Index	SRI	Quantifies progressive stiffness changes within individual beams during loading
Segmentation Performance Index	SPI	Quantifies stiffness reduction due to segmentation relative to continuous control specimens

Stiffness Reduction Index (SRI)

Following established practices for serviceability monitoring in timber bridge systems, this study focuses on early loading phases where initial joint slip and composite reinforcement engagement provide critical indicators for structural health assessment (Buka-Vaivade et al., 2022; Corradi et al., 2017). Early-stage stiffness assessment enables non-destructive evaluation of modular systems while maintaining operational capacity, with research demonstrating that detection of stiffness variations at approximately 20–40% of maximum load provides essential indicators for field monitoring applications (Wdowiak-Postulak & Świt, 2021). Both initial k and final k are defined as the slope of the load–deflection curve $(\Delta P/\Delta \delta)$ within their respective load intervals. The Stiffness Reduction Index (SRI) quantifies progressive stiffness loss within individual beam specimens during loading cycles and is calculated using Equation (3.9).

$$SRI = \left(\frac{k_{\text{initial}} - k_{\text{final}}}{k_{\text{initial}}}\right) \times 100 \tag{3.9}$$

Where:

k_{initial} = stiffness at 10 – 20% of max load
k_{final} = stiffness at 30 – 40% of max load

A positive SRI indicates reduction due to joint slip or material damage, while negative SRI values indicate progressive reinforcement engagement, particularly

evident during CSM activation. This parameter enables assessment of joint performance and reinforcement effectiveness under realistic loading conditions, following established approaches for comparing segmented or reinforced beam stiffness to baseline continuous specimens (Gomes et al., 2019; Lu et al., 2019).

Higher SRI values typically indicate greater stiffness loss associated with mechanical joint flexibility, bolt slippage, or localized crushing (Niu et al., 2024; Li & Liu, 2024), while reinforced beams are expected to demonstrate lower SRI values through CSM reinforcement effectively mitigating these effects by improving load distribution and joint integrity (He et al., 2025; Shyamala et al., 2023).

Segmentation Performance Index (SPI)

The SPI evaluates stiffness reduction attributed to beam segmentation relative to continuous control specimens, providing direct quantification of modular assembly penalties. SPI reflects geometric and connection-induced stiffness penalties associated with segmentation and does not imply material degradation or damage. The index is calculated using Equation (3.10).

$$SPI = \left(\frac{k_{\text{continuous}} - k_{\text{segmented}}}{k_{\text{continuous}}} \right) \times 100 \tag{3.10}$$

Where:

$k_{\text{continuous}}$ = stiffness of continuous beam

$k_{\text{segmented}}$ = stiffness of segmented beam

Reference stiffnesses are established using ETN131 as the control for non-reinforced beams and ETR136 as the control for reinforced beams. The SPI values quantify the percentage loss in stiffness due to segmentation relative to these continuous control specimens, enabling systematic comparison of segmentation effects across different beam configurations.

The dual-index interpretation utilizes SRI to highlight in-test stiffness behaviour and reinforcement effectiveness while SPI compares global structural efficiency across configurations. Combined, these indices validate the optimality of specific configurations, such as the 3-segment design, by balancing stiffness retention with modular practicality.

This structured framework supports the integrity of reduction analysis presented in Chapter 4 and provides a foundation for identifying and validating optimal modular timber beam configurations. The methodology addresses the fundamental challenge of characterizing discontinuous structural systems where traditional assessment approaches may provide incomplete or misleading evaluations of modular system performance.

3.4.4 Connection Performance Assessment and Load Bearing Verification

The structural integrity of modular timber systems fundamentally depends on mechanical connection adequacy, requiring systematic verification that joint performance does not compromise the validity of segmentation and reinforcement assessments. This critical component of the experimental methodology ensures that observed performance variations reflect genuine material and system-level behaviours rather than connection inadequacies that could invalidate comparative analyses. The connection assessment protocol integrates real-time monitoring, post-test evaluation, and theoretical capacity verification to establish robust foundations for interpreting modular beam performance data.

3.4.4.1 Integrated Connection Monitoring Framework

The connection assessment methodology employs concurrent evaluation of mechanical joint components through systematic monitoring of bolt performance, timber bearing behaviour, and steel plate adequacy during flexural testing. Real-time connection zone assessment utilizes strategically positioned strain gauges to capture stress redistribution patterns at critical timber-bolt interfaces, providing direct measurement of load transfer mechanisms throughout the complete loading progression.

Strain gauge arrays positioned adjacent to connector locations operate at 10 Hz sampling rates using the Kyowa EDX-11A data acquisition system, enabling precise characterization of stress concentration effects and load distribution patterns across multiple connection points. This high-frequency monitoring approach captures transient phenomena and progressive connection behaviour changes that static post-test assessment alone cannot reveal.

Post-test quantitative assessment employs graph paper to document bolt deformation and assess connection performance reduction, providing objective evidence of joint adequacy under applied loading conditions. This dual-approach methodology ensures comprehensive evaluation of both progressive connection behaviour under increasing static load and cumulative performance effects.

3.4.4.2 Safety Factor Establishment and Capacity Verification

Connection adequacy verification follows a systematic approach comparing applied loads against theoretical capacity limits while incorporating experimentally-observed stress concentration factors into design calculations. The methodology establishes conservative safety factors through comprehensive analysis of component-level capacities:

Bolt Shear Capacity Assessment: Theoretical capacity of 18,850 N per bolt based on 10mm high-tensile steel specifications (σy = 400 MPa), with experimental validation confirming adequate performance margins under maximum applied loads.

Timber Bearing Capacity Evaluation: Western White Pine parallel-to-grain bearing stress limits of 25 MPa provide baseline capacity assessments, with strain gauge data validating that actual bearing stresses remain within acceptable limits throughout testing.

Steel Plate Bearing Verification: 5mm U-channel plate yield strength of 250 MPa establishes connection component adequacy, with systematic evaluation confirming performance margins under realistic loading scenarios.

Stress concentration factors, typically ranging from 2.5 to 4.0 times nominal stress levels, are incorporated into safety factor calculations to account for local stress amplification effects observed at timber-bolt interfaces. This conservative approach ensures connection adequacy under both service and ultimate loading conditions.

3.4.4.3 Load Distribution Analysis and Failure Mode Assessment

Strain gauge arrays enable quantitative assessment of stress amplification patterns at timber-bolt interfaces, with stress concentration factors calculated as maximum measured stress relative to nominal uniform distribution assumptions. Load distribution patterns across multiple connector positions are systematically evaluated to

identify effective load-carrying mechanisms and assess redistribution effects specific to segmented configurations.

The connection assessment protocol incorporates systematic evaluation of failure mode progression, employing standardized post-test inspection procedures to distinguish between potential failure mechanisms including bolt shear failure, timber bearing failure, and steel plate bearing failure. This comprehensive approach ensures that observed structural behaviours reflect intended system performance rather than unintended connection limitations.

3.4.4.4 Code Compliance and Standards Framework

Connection design verification follows BS 5268-2 requirements for bolted timber connections, selected as the primary design standard due to its comprehensive coverage of timber bearing capacity, bolt spacing requirements, and safety factor specifications applicable to Western White Pine applications. The standard provides minimum spacing criteria (70mm edge distance), safety factor adequacy (minimum 2.25), and geometric specifications that align with the experimental connector configuration.

While Eurocode 5 (EN 1995-1-1) offers alternative design approaches for timber connections, BS 5268-2 was selected for this research due to its well-established design methodologies and conservative safety factors that provide appropriate margins for novel modular configurations where connection behaviour may differ from conventional continuous beam applications.

Compliance verification includes:

- Minimum bolt spacing and edge distances per BS 5268-2 Section 6.6
- Load duration factors appropriate for timber bridge applications
- Safety factor validation against experimental loading data
- Connection capacity verification under realistic service conditions

3.4.4.5 Performance Integration and System Validation

Connection performance metrics are systematically correlated with global beam performance indices, specifically the SRI and SPI, enabling direct evaluation of

connection behaviour effects on overall structural system performance. This integration ensures that modular system assessments accurately reflect reinforcement and segmentation effects rather than connection-induced performance variations.

Cross-validation between strain gauge data, post-test inspection findings, and FEA predictions provides multiple verification pathways for connection assessment conclusions, ensuring reliability and supporting confidence in subsequent modular beam performance interpretations. This rigorous validation approach establishes the foundation for reliable application of research findings to practical modular timber bridge design applications.

The connection performance assessment methodology provides essential verification that mechanical joints maintain adequate capacity throughout testing, enabling valid interpretation of modular system performance data presented in Chapter 4. This systematic approach ensures that observed performance variations reflect genuine material and system-level behaviours, supporting the reliability of novel performance indices and design recommendations developed through this research.

3.4.5 Quality Control and Error Minimization

The experimental methodology incorporates comprehensive quality control measures to ensure data reliability and minimize systematic errors that could compromise the validity of comparative assessments across different beam configurations. These standardized protocols address material variability, assembly consistency, instrumentation accuracy, and measurement repeatability to establish a controlled experimental environment where observed performance differences can be confidently attributed to design variables rather than procedural inconsistencies. The quality control framework encompasses material preparation, assembly procedures, instrumentation calibration, and measurement standardization to support robust statistical analysis and meaningful interpretation of modular timber beam performance data.

a) **Material Conditioning**: All timber was from a single batch of kiln-dried Western White Pine, conditioned at 25 ± 2°C and 55–65% RH.
b) **Assembly**: Connector holes were precision-drilled; bolts were torque-tightened with visual verification of alignment.

c) **Instrumentation**: Strain gauges were calibrated and verified for baseline zero offset. Denting corrections were measured and applied.
d) **Measurement and Marking Consistency**: All specimens were measured and marked consistently for support locations and strain gauge placements to ensure test repeatability and comparability across configurations.

This protocol ensured consistency across configurations and enabled meaningful comparison of reinforcement and segmentation effects on beam stiffness and strength.

3.5 Finite Element Analysis (FEA)

Finite Element Analysis using ANSYS Workbench 2019 R3 provided computational support for experimental findings through simulation of modular timber beam behaviour under static and dynamic loading conditions. All geometric models were developed in SketchUp Pro 2019 and exported in SKP 2014 format for ANSYS compatibility, replicating experimental configurations including segmentation patterns, connector details, and CSM reinforcement applications. The analysis framework consisted of two modules: static structural analysis for mid-span deflection and stress distributions, and modal analysis for natural frequency and mode shape extraction.

All finite element simulations were conducted under idealised modelling assumptions to enable controlled comparative assessment across beam configurations. Linear elastic material behaviour was assumed for all components within the serviceability load range, and contact interactions were represented using simplified bonded or frictional formulations without progressive damage evolution. Accordingly, the finite element analysis is employed as a comparative and interpretive tool to evaluate relative stiffness trends, stress distribution patterns, and modal behaviour between configurations, rather than as a predictive model for ultimate capacity, failure mechanisms, or long-term material degradation.

3.5.1 Purpose, Computational Framework, and Software Implementation

The finite element analysis served three computational purposes: static simulation of mid-span deflection under three-point bending for correlation with experimental load-deflection data, modal analysis of natural frequencies for comparison

with EMA measurements, and stress distribution investigation at connector interfaces and critical beam sections. The computational framework employed ANSYS Workbench 2019 R3 as the primary simulation platform, with geometric models developed in SketchUp Pro 2019 and exported in SKP 2014 format. All models replicated full-scale beam geometry including dimensional specifications, segmentation layouts with connector spacing, steel U-channel connector assemblies with bolt positions, and CSM reinforcement layer applications matching experimental fabrication procedures. The unified modelling strategy shared a single geometry and material dataset between static structural and modal analysis modules, ensuring both analysis types operated on identical finite element meshes with consistent material properties, nodal connectivity, and element formulations. Primary outputs extracted included mid-span deflection (mm) from static analysis, maximum principal stress (MPa) at connector interfaces and bottom flange mid-span, maximum principal elastic strain (με) at strain gauge positions, and natural frequencies (Hz) with mode shapes from modal analysis.

Finite element analysis (FEA) was systematically implemented to support each research objective through objective-specific computational functions. As summarised in Table 3.6, a direct mapping was established between individual research objectives and corresponding FEA tasks. The ANSYS Workbench project was configured using an integrated architecture in which the Engineering Data module defined material properties that were consistently linked to the Geometry and subsequently propagated to both the Static Structural and Modal Analysis systems via a shared Model environment, as illustrated in Figure 3.12. This unified modelling framework ensured identical mass distribution, consistent stiffness assumptions, and uniform boundary condition definitions across static and dynamic simulations. Consequently, any modification to material parameters or geometric characteristics was automatically reflected in both analysis modules through the shared parameterisation system, maintaining coherence and comparability between static and modal FEA results.

Table 3.6
Research Objective Mapping to FEA Implementation

Objective	FEA Analysis Type	Outputs Extracted	Application in Chapter 4
Objective 1: Static-Dynamic Stiffness Correlation	Static structural + Modal analysis	Mid-span deflection, natural frequencies	Section 4.2: MOE correlation analysis
Objective 2: Mechanical Connection Performance	Static structural	Maximum principal stress at bolt-timber interfaces, contact status	Section 4.3: Connector stress analysis
Objective 3: Segmentation Effects on Dynamic Behaviour	Modal analysis	Natural frequencies (0-50 Hz), Mode shapes (Modes 1-6)	Section 4.4: Frequency reduction trends
Objective 4: Reinforcement Effectiveness	Static structural + Modal analysis	Deflection comparison (reinforced vs non-reinforced), stress distributions	Section 4.5: CSM performance evaluation
Objective 5: Performance Indices and Optimization	Static structural + Modal analysis	Comparative stiffness data across specimen matrix	Section 4.6: SRI and SPI calculations

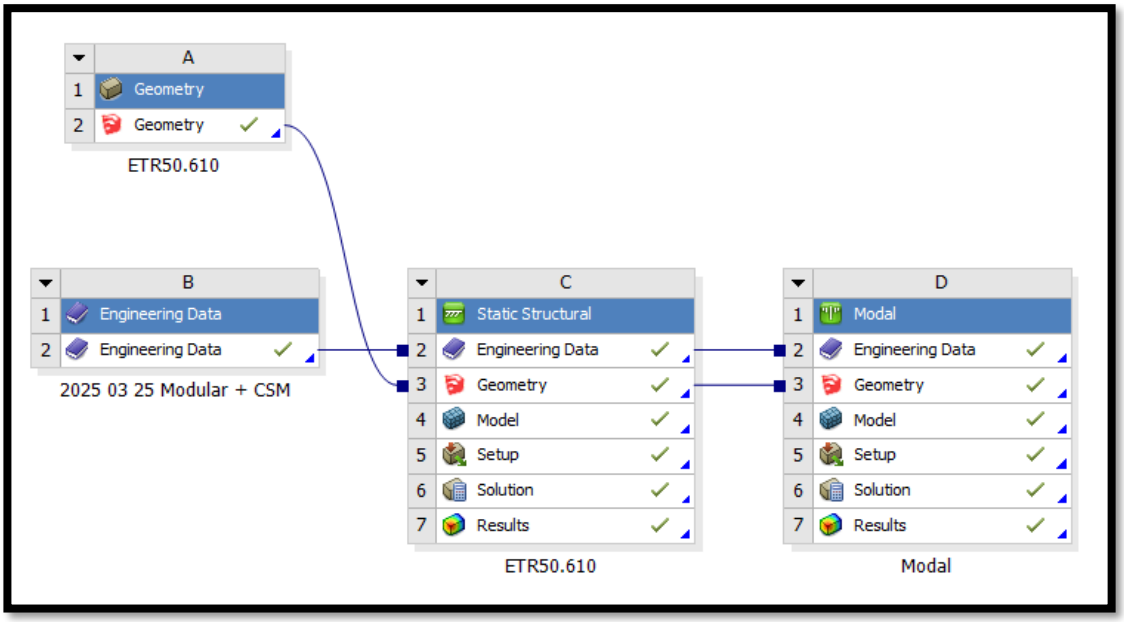

Figure 3.12 ANSYS Workbench project schematic showing integrated workflow with shared Engineering Data, Geometry, and Model components.

3.5.2 Material Properties, Contact Definitions, and Boundary Conditions

Material property assignments followed systematic calibration procedures where computational predictions were iteratively adjusted to match experimental measurements from control specimens. All material properties are documented in Table 3.3. Direct experimental testing of timber material properties was not conducted, as the

primary objective of the numerical modelling was to evaluate relative stiffness behaviour arising from segmentation, mechanical connections, and CSM reinforcement configuration rather than to characterise absolute material properties. The adopted calibration approach ensures internal consistency between experimental and numerical results while intentionally minimising material variability effects.

Timber components were modelled as orthotropic elastic materials with nine independent elastic constants defining stiffness in three principal material directions: longitudinal (L) parallel to grain, radial (R) perpendicular to growth rings, and tangential (T) perpendicular to grain. The orthotropic material orientation was assigned with the L-axis aligned along the beam longitudinal axis. Steel components (U-channel plates, bolts, nuts, washers) were modelled as homogeneous isotropic materials with Young's modulus and Poisson's ratio specifications. Linear elastic behaviour was assumed for all steel components within the serviceability load range. CSM reinforcement layers were modelled as equivalent isotropic laminates with homogenized elastic properties representing the global stiffness contribution of the CSM-epoxy composite system. The equivalent elastic modulus was calibrated to match experimentally observed stiffness enhancement in reinforced control specimens.

Contact interface definitions governed load transfer behaviour between dissimilar materials and at mechanical joints. Two contact formulations were implemented:

1. **Bonded contact** (perfect adhesion): Applied to CSM reinforcement-timber substrate interfaces along the bottom flange. This formulation prevents all relative motion including separation, sliding, and rotation.
2. **Frictional contact** ($\mu = 0.1$): Applied to all mechanical fastener interfaces including bolt shank to steel plate and steel plate to timber bearing surfaces. The friction coefficient $\mu = 0.1$ represents a conservative value for steel-timber contact under dry conditions. This formulation permits tangential sliding when interface shear stress exceeds μ times normal stress.

All contact pairs were defined explicitly using ANSYS named selections. Figure 3.13 illustrates contact definition locations.

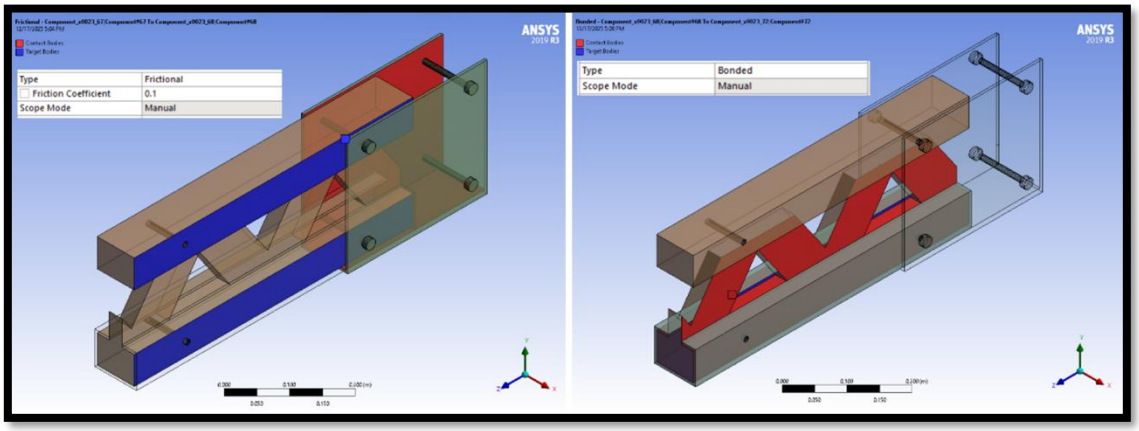

Figure 3.13 Contact interface definitions: (a) Frictional contact at mechanical fastener interfaces, (b) Bonded contact at CSM reinforcement-timber interface.

Several simplifications were implemented to maintain computational tractability while enabling parametric investigation across multiple specimen configurations. The following simplifications were implemented with their implications:

1. **Perfect bonding assumption (CSM-timber):** Neglects progressive delamination. Post-test inspection validated intact bonding under laboratory conditions. Represents upper bound on reinforcement effectiveness.
2. **Friction coefficient uncertainty:** Single-point estimate ($\mu = 0.1$) neglects variability from moisture content and surface finish. Sensitivity analysis indicated ±12% stiffness variation for $\mu = 0.05$-0.15 range.
3. **Idealized contact geometry:** Assumes perfect mating surfaces without bolt-hole clearances or surface roughness to maintain computational stability.
4. **Linear elastic material models:** Operates within small deformation framework. Excludes material plasticity, crack propagation, and progressive damage accumulation beyond serviceability load levels.
5. **Static load application:** Represents instantaneous elastic response. Excludes time-dependent effects including creep and moisture-induced property changes.

Boundary conditions and loading configurations were implemented to replicate experimental testing protocols for both static and dynamic analyses.

Static Structural Analysis:

Simply supported end conditions replicated the experimental three-point bending configuration. Vertical displacement restraint (Uy = 0) was applied at both beam ends (x = 0 and x = 3000 mm). Horizontal and rotational degrees of freedom remained unrestricted at both supports, representing a pin-roller arrangement. A vertical concentrated load (18-30 kN depending on specimen configuration) was applied at mid-span (x = 1500 mm) to the top flange centroid in the negative Y-axis direction. The applied pin–roller boundary condition represents an idealised abstraction of the experimental support system, acknowledging that minor compliance effects arising from support fixtures and contact surfaces are not explicitly modelled. This simplification is considered acceptable as the numerical analysis focuses on comparative stiffness behaviour and relative performance trends across beam configurations under serviceability-level loading rather than exact replication of local support deformation. Figure 3.14 illustrates the boundary condition implementation.

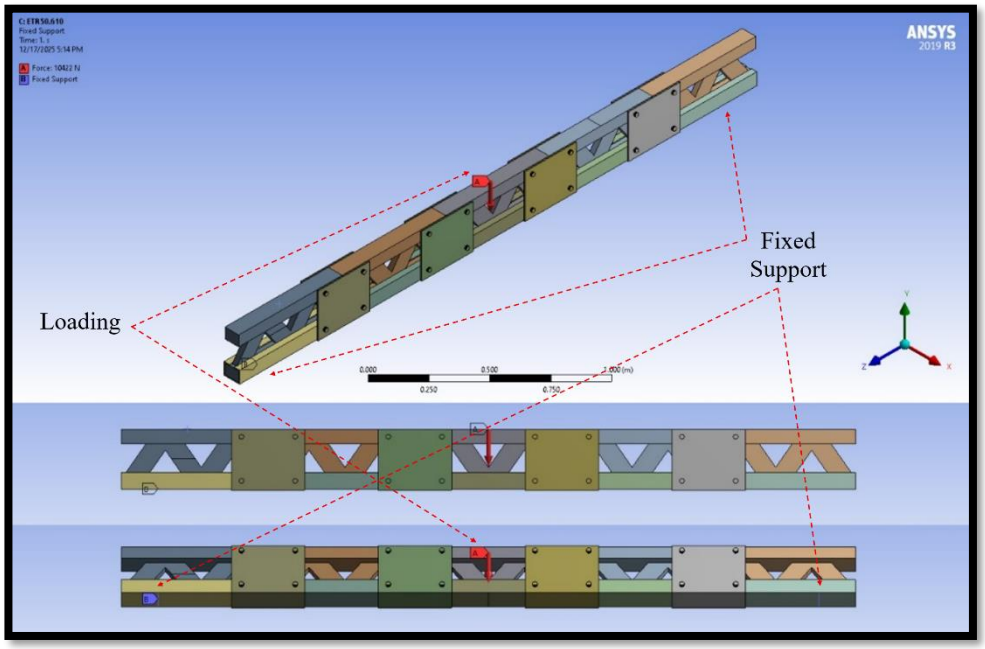

Figure 3.14 Static structural boundary conditions showing support locations and concentrated mid-span load.

Modal Analysis:

Free–free boundary conditions were implemented to replicate the Experimental Modal Analysis (EMA) configuration, in which specimens were supported on compliant foam to approximate unconstrained vibration. No vertical displacement restraints were applied. A minimal axial displacement constraint (Ux = 0) was imposed

at a single node located on the neutral axis solely to eliminate numerical rigid body motion; this constraint does not introduce artificial stiffness or alter the dynamic characteristics of the system, as all rotational degrees of freedom remained unrestricted. The analysis extracted the first six vibration modes within the frequency range of 0–50 Hz. The modal analysis formulation extracts undamped natural frequencies and corresponding mode shapes and therefore does not account for energy dissipation mechanisms such as material damping, joint friction, or boundary compliance present in experimental impact hammer testing. Consequently, modal results are interpreted for relative trend comparison across configurations rather than absolute frequency equivalence. Figure 3.15 illustrates the modal boundary condition implementation.

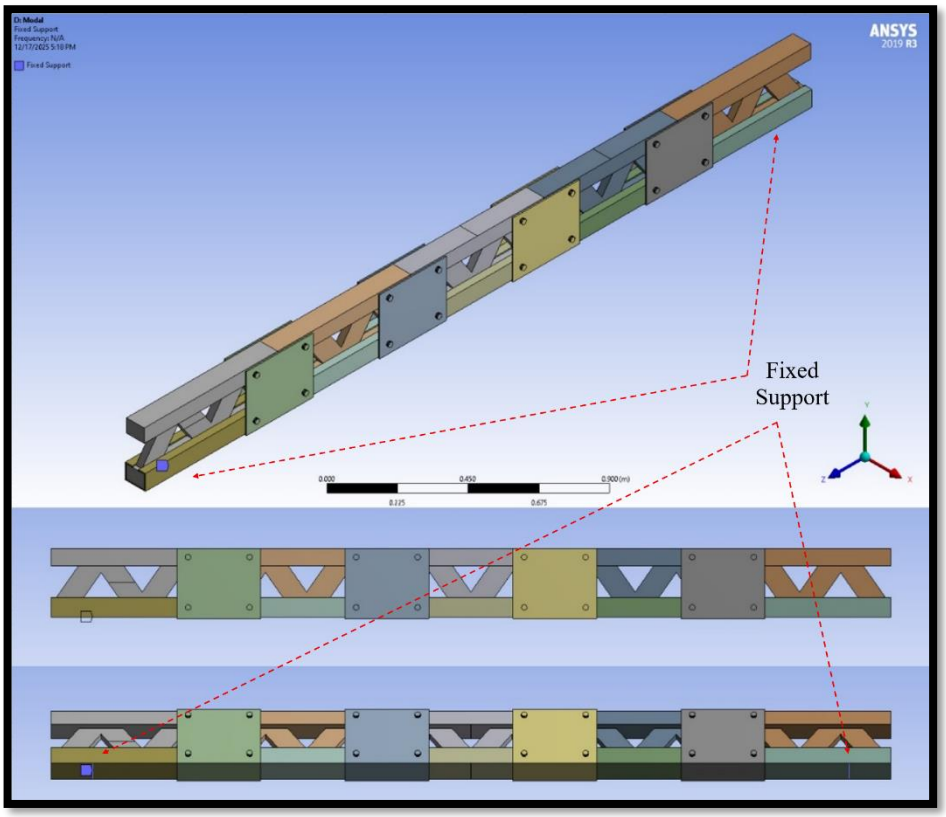

Figure 3.15 Modal analysis boundary conditions showing minimally constrained configuration for free-free vibration simulation.

3.5.3 Meshing, Solver Configuration, and Simulation Setup

SOLID186 tetrahedral elements were employed for all structural components. This 20-node quadratic element provides second-order displacement behaviour suitable for capturing stress gradients in structural analysis.

Differentiated mesh densities were applied based on geometric complexity:

- Timber components (lattice web): 20 mm element size
- Connector plates, CSM reinforcement, fasteners: 10 mm element size

Steel plates, bolts, and nuts were merged into single solid bodies in SketchUp prior to ANSYS import to reduce meshing instability at small geometric interfaces. Figure 3.16 shows the mesh refinement strategy.

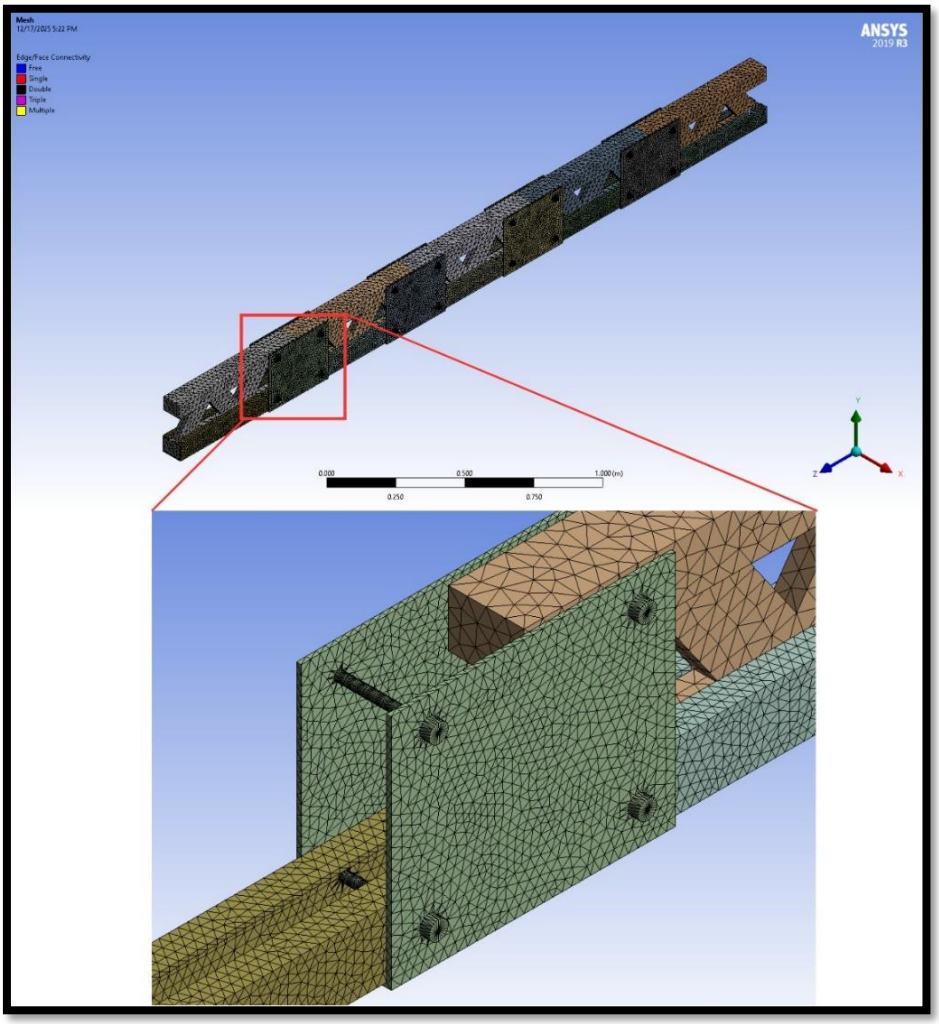

Figure 3.16 Finite element mesh showing overall beam discretization and refined connector regions.

A systematic mesh convergence study was performed on specimen ETN131 (non-reinforced continuous control) to establish optimal element size. Mesh sizes were refined from 100 mm to 5 mm, corresponding to element counts from approximately 1.5×10^3 to 2.4×10^6 elements. Mid-span deflection under 19,709 N applied load served as the convergence criterion, evaluated against the experimental reference value of 23.962 mm. Convergence was defined as achieving variation in mid-span deflection

predictions of ≤±5% between successive refinement levels. Based on this analysis, an element size of 20 mm was selected (40,755 elements), yielding simulated deflection of 23.904 mm with relative error of +0.24%. Figure 3.17 presents the convergence analysis results.

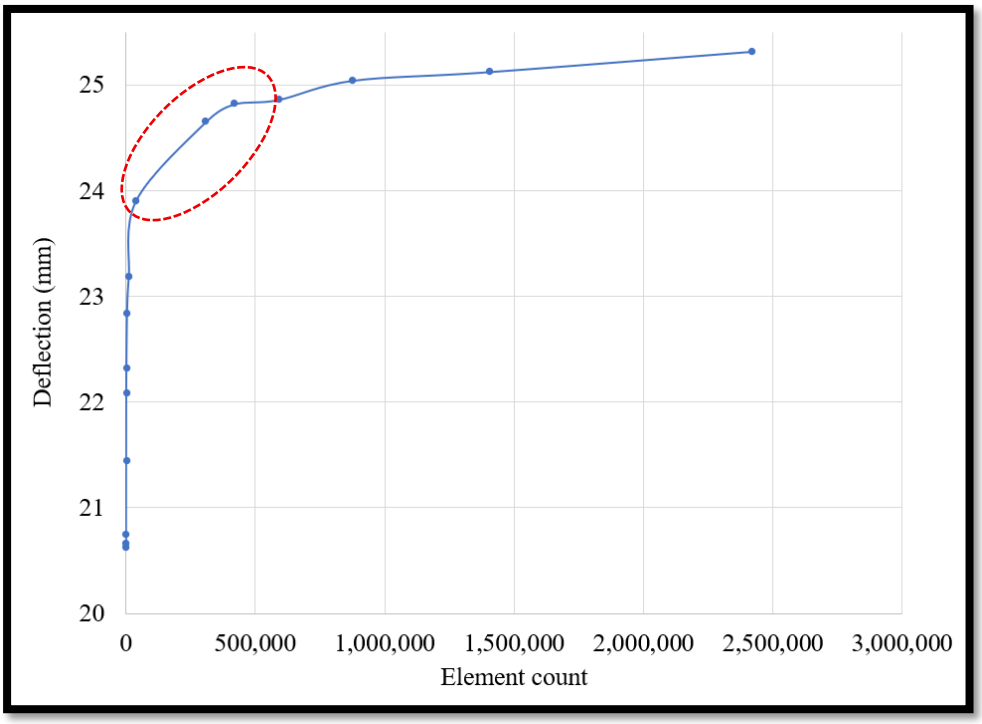

Figure 3.17 Mesh convergence analysis for ETN131 showing deflection prediction versus element count.

This validated mesh size was adopted as the standard discretization parameter for the complete specimen matrix. The 20 mm mesh size was applied uniformly across all subsequent specimen models. Table 3.7 summarizes mesh quality metrics for all analysed specimens. Specimen ETR50.610 was selected for detailed mesh quality verification as it represents the most geometrically complex configuration in the study due to maximum segmentation length (five segments), increased number of mechanical connectors (four connector assemblies), and the greatest number of contact interfaces (16 frictional contact pairs).

Table 3.7
Mesh Convergence Results for All FEA Specimens

Specimen ID	Average Mesh Metric	Nodes	Elements

ETN131	0.8396	454412	304305
ETN21.52	0.7365	102446	58612
ETN313	0.68907	136640	75568
ETN40.754	0.6558	169864	92403
ETN50.65	0.63478	205105	110170
ETR136	0.75772	169434	90806
ETR21.52	0.71546	206552	109369
ETR313	0.68438	243150	127735
ETR40.759	0.66259	278732	145407
ETR50.610	0.64856	315776	163949

Figure 3.18 presents the mesh quality metrics for this specimen, showing element quality distribution and global mesh statistics. The adopted meshing strategy achieved average element quality of 0.6486 for this configuration, with element quality histogram showing the majority of elements within acceptable quality range (>0.4). Numerical solution convergence was achieved for this worst-case configuration using the standard solver settings indicating that the same meshing approach is applicable to all specimens with simpler geometries and fewer contact interfaces.

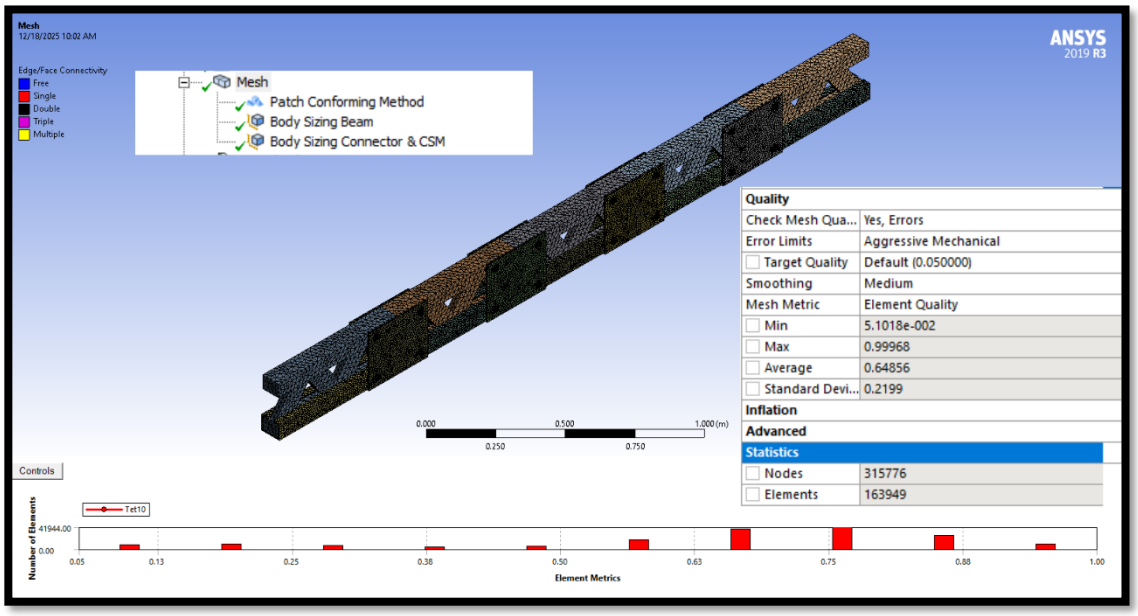

Figure 3.18 Mesh quality metrics and element statistics for specimen ETR50.610 (Tet10 elements), showing element quality distribution histogram and global mesh statistics.

Specific output parameters were extracted from each analysis module to enable systematic comparison with experimental measurements. The solver configurations comprised two primary sets of parameters: (a) static structural analysis settings and (b) modal analysis settings, as defined as in Figure 3.19

Static Structural Analysis:

The ANSYS direct sparse solver was employed with the following settings:

- Single load step matching experimental protocol (18-30 kN depending on specimen)
- Substep strategy: initial substeps = 1, minimum substeps = 1, maximum substeps = 10
- Automatic substep adjustment enabled
- Convergence criteria: force tolerance = 0.005 (0.5%), displacement tolerance = 0.05 (5%), moment tolerance = 0.005 (0.5%)

Modal Analysis:

The Block Lanczos eigenvalue solver was employed with the following settings:

- Mode extraction range: Modes 1 through 6
- Frequency range: 0-50 Hz
- Mass-normalized mode shapes
- Convergence tolerance: 1.0×10^{-6}

Specific output parameters were extracted from each analysis type to enable systematic comparison with experimental measurements.

Static Structural Analysis Outputs:

1. **Total deformation (mm):** Extracted at mid-span bottom flange node for comparison with LVDT measurements
2. **Maximum principal stress (MPa):** Extracted at connector interfaces (bolt-timber contact zones) and bottom flange mid-span
3. **Maximum principal elastic strain (με):** Extracted at bottom flange strain gauge positions matching experimental layout
4. **Contact status and sliding distance:** Extracted at all frictional contact pairs.

Modal Analysis Outputs:

1. **Natural frequencies (Hz):** Extracted for first six modes with focus on first vertical bending mode
2. **Mode shapes:** Animated visualization showing displacement magnitude distribution
3. **Modal participation factors:** Quantified contribution of each mode to overall structural response

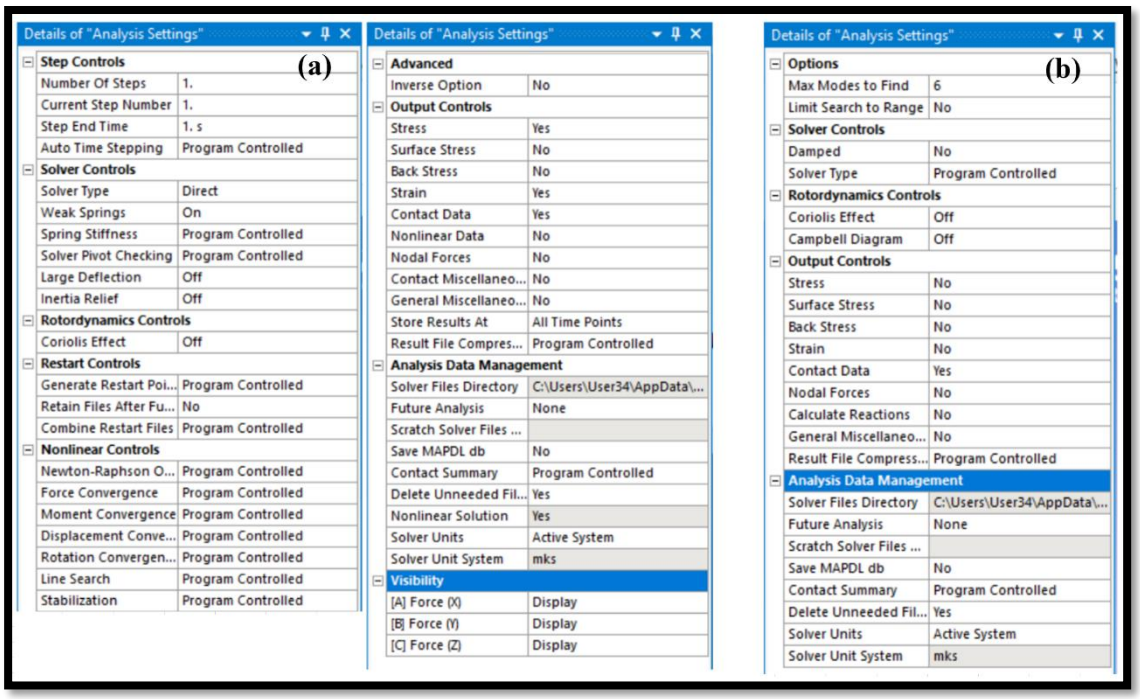

Figure 3.19 Solver configuration settings: (a) Static structural analysis parameters, (b) Modal analysis parameters.

Modal participation factors were used qualitatively to identify dominant vibration modes and to support mode shape classification, rather than to predict absolute dynamic response amplitudes or in-service vibration levels. Post-solution processing employed systematic mode shape visualization to identify the first vertical bending mode through examination of primary deformation direction (Y-axis vertical displacement dominance) and frequency ranking validation. Figure 3.20 presents representative FEA output results.

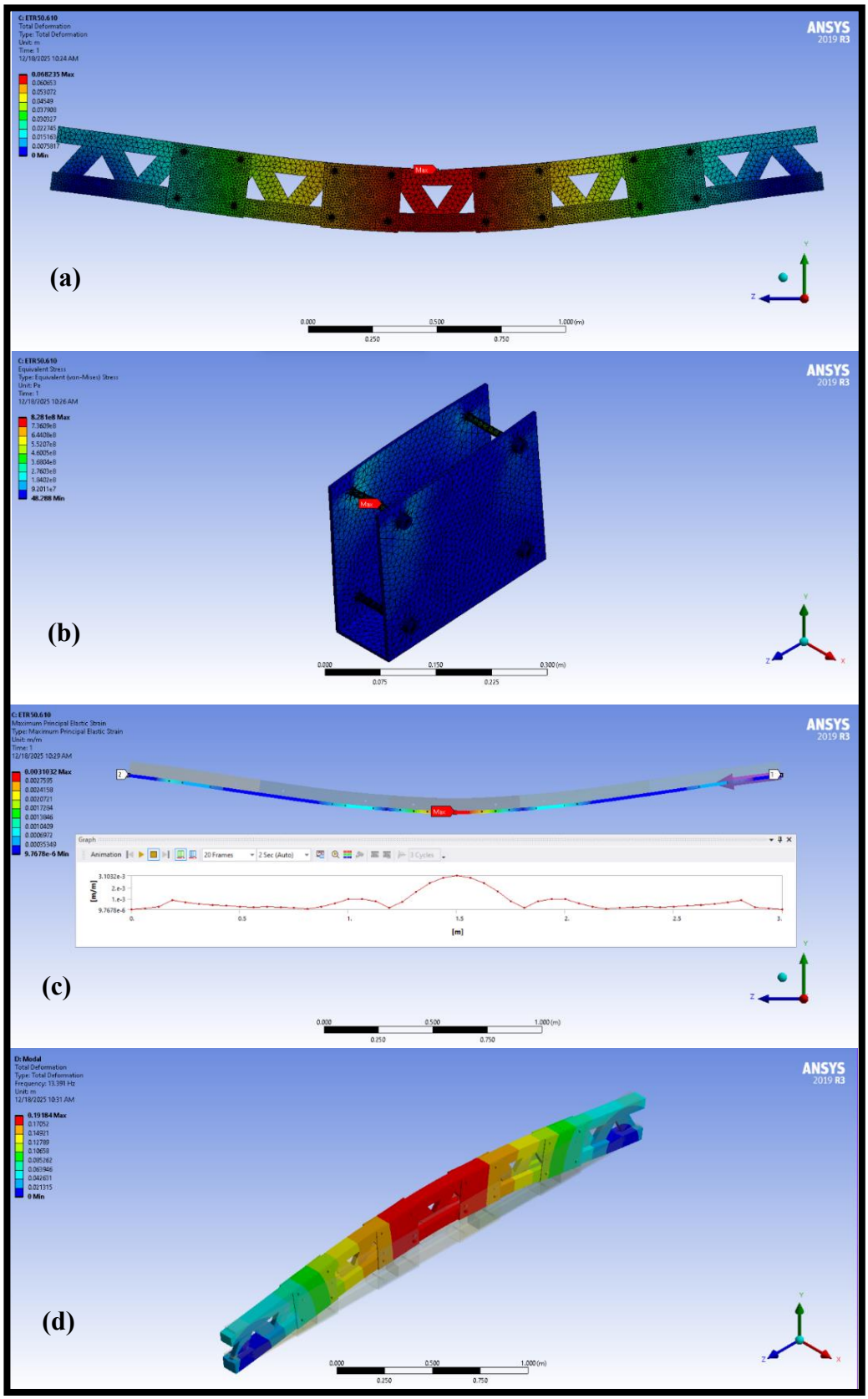

Figure 3.20 Representative FEA output results: (a) Total deformation contour, (b) von Mises stress distribution (connector), (c) Maximum principal elastic strain (path), (d) First mode shape of vertical bending.

3.5.4 Validation and Calibration Methodology

Three representative specimens were selected for FEA benchmarking:

1. **ETN131:** Continuous non-reinforced control (single-piece beam without joints or CSM reinforcement)
2. **ETR136:** Continuous reinforced control (single-piece beam with CSM bottom flange reinforcement)
3. **ETN21.52:** Two-segment assembly with single central connector without reinforcement

This selection provided calibration coverage across three modelling dimensions: material behaviour (timber only versus timber-CSM composite), structural continuity (continuous versus segmented), and contact complexity (no contacts versus frictional mechanical interfaces). Calibration employed systematic iteration of material property definitions through three sequential phases:

Phase 1: Baseline Timber Property Calibration (ETN131)

1. Establish initial material properties from Forest Products Laboratory (2010) handbook values (Table 3.3)
2. Execute static structural analysis with handbook MOE values
3. Compare predicted mid-span deflection against experimental LVDT measurement (23.962 mm)
4. Calculate MOE adjustment factor: MOE_adjusted = MOE_initial × (δ_FEA / δ_experimental)
5. Update material property definition and re-solve
6. Iterate until deflection prediction converges within ±5% acceptance criterion

Phase 2: CSM Reinforcement Calibration (ETR136)

1. Fix timber properties from Phase 1
2. Execute static analysis using handbook CSM properties
3. Compare predicted deflection against experimental measurement
4. Adjust CSM elastic modulus based on composite stiffness contribution
5. Verify stress-strain distribution patterns appear realistic
6. Iterate until deflection and strain distribution achieve acceptance

Phase 3: Contact Behaviour Verification (ETN21.52)

1. Fix material properties from Phases 1-2
2. Execute static analysis with frictional contact definitions (Section 3.5.2.2)
3. Compare predicted deflection accounting for connection compliance
4. Verify contact status output shows sliding at appropriate load levels without unwanted separation
5. Confirm stress concentration patterns at connector interfaces appear physically reasonable
6. Adjust friction coefficient within realistic range (0.05-0.15) if necessary

Acceptance criteria were established to quantify the agreement between computational predictions and experimental measurements.

Static Structural Validation:

The primary validation criterion for the static structural model was defined as a mid-span vertical deflection prediction error of ≤ ±5% relative to the experimental LVDT measurements (Figure 3.21).

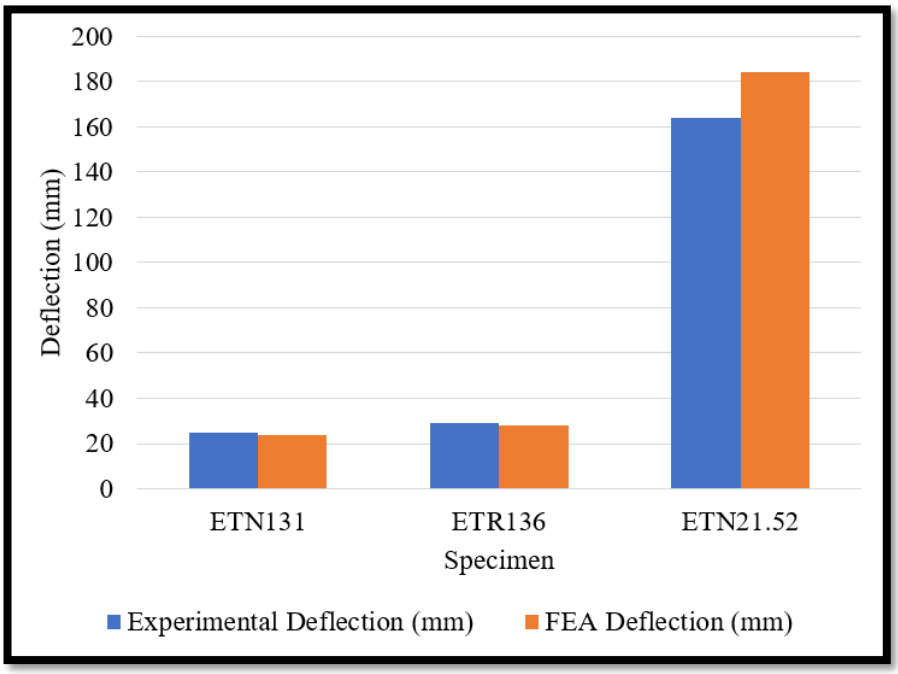

Figure 3.21 Experimental-numerical validation comparison methodology at mid-span deflection comparison protocol

This tolerance threshold accounts for cumulative uncertainties arising from experimental instrumentation (typically ±2% for LVDT systems), inherent variability in timber material properties, numerical approximation errors associated with finite element discretization, and idealization of contact behaviour at mechanical interfaces. This criterion ensured that the numerical model reproduced the global flexural response of the specimens with sufficient fidelity for comparative analysis across segmentation and reinforcement configurations.

Modal Analysis Validation:

For the modal analysis, the primary validation criterion was based on the consistency of qualitative trends in natural frequency predictions rather than strict absolute frequency matching. Specifically, the model was required to reproduce the experimentally observed directional trends, including continuous configurations exhibiting higher natural frequencies than segmented configurations and reinforcement effects remaining directionally consistent across specimen types (Figure 3.22).

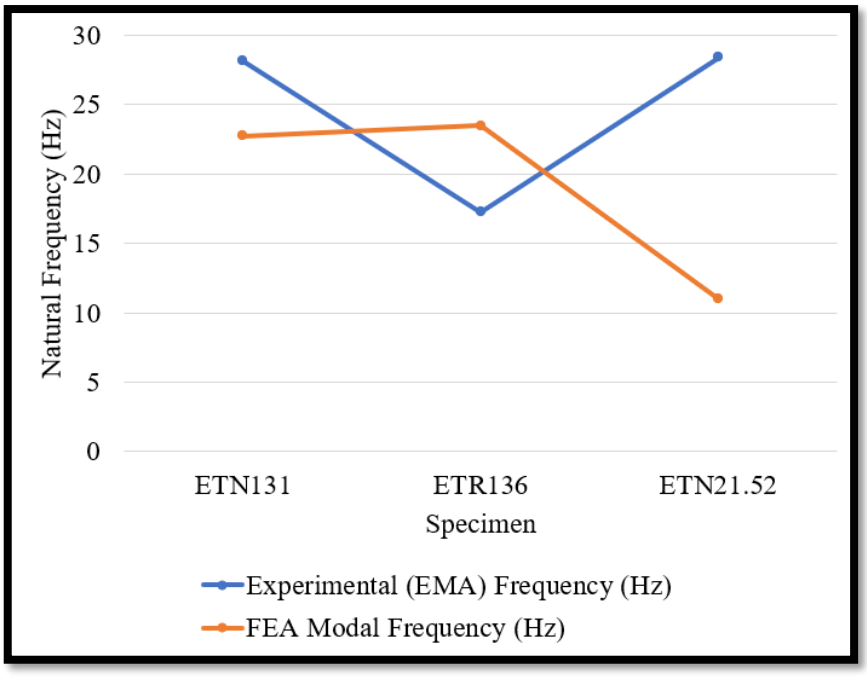

Figure 3.22 Experimental-numerical validation comparison methodology for the first natural frequency comparison protocol.

Absolute frequency matching was not enforced as a strict validation requirement due to known systematic idealizations inherent in the numerical formulation, including assumptions of perfect bonding, simplified boundary conditions, and linear elastic

behaviour. These simplifications preclude explicit representation of damping mechanisms, micro-slip, and material heterogeneity. Accordingly, the FEA validation framework was designed to establish model reliability for the following purposes:

1. **Relative performance comparison:** Predicting which configurations exhibit superior stiffness and where stress concentrations develop
2. **Trend accuracy:** Capturing directional effects of reinforcement and segmentation on structural performance
3. **Internal behaviour investigation:** Revealing stress-strain distributions not accessible through external measurements

The validation framework explicitly excluded:

1. **Absolute failure prediction:** Linear elastic formulation cannot predict ultimate load capacity or post-peak behaviour
2. **Dynamic damping effects:** Modal analysis extracts undamped natural frequencies
3. **Long-term behaviour:** Static simulations represent instantaneous elastic response without time-dependent effects.

3.6 Data Analysis and Validation Framework

The data analysis strategy employed a triangulated approach integrating results from EMA, flexural bending tests, and FEA to ensure comprehensive validation of modular timber beam performance. This multi-platform methodology provided complementary assessment capabilities, with EMA offering non-destructive dynamic stiffness evaluation through frequency analysis, flexural testing delivering direct static load–deflection measurements, and FEA providing computational validation under equivalent boundary conditions (Figure 3.23). The systematic specimen identification protocols using ETN/ETR designation combined with configuration codes ensured complete traceability across all testing platforms, enabling reliable cross-validation and confidence assessment for different beam configurations.

To comprehensively evaluate structural performance and stiffness reduction mechanisms, two novel performance indices were developed specifically for this study. The Stiffness Reduction Index (SRI) quantifies progressive changes in stiffness

response within individual beams during loading, reflecting the combined effects of joint slip, stiffness redistribution, and reinforcement interaction. Positive SRI values indicate a reduction in effective stiffness primarily associated with connection compliance and segment interaction, while negative SRI values indicate progressive stiffness engagement, particularly evident in CSM-reinforced specimens where fibre contribution becomes increasingly effective with load application.

The Segmentation Performance Index (SPI) evaluates the performance reduction of segmented beam configurations relative to continuous control specimens. Reference stiffness values were established using ETN131 as the non-reinforced control and ETR136 as the reinforced control, providing baseline performance benchmarks for comparative analysis. The combined SRI–SPI analytical framework enables identification of favourable configurations by revealing both internal stiffness reduction mechanisms (through SRI analysis) and global segmentation penalties (through SPI comparison).

The two indices serve complementary but distinct analytical roles within the study. The Stiffness Reduction Index (SRI) evaluates stiffness evolution within individual beam specimens during loading, capturing internal response changes associated with joint interaction and reinforcement engagement. In contrast, the Segmentation Performance Index (SPI) provides a comparative measure of global stiffness performance between different beam configurations relative to continuous reference specimens. Both indices are employed as analytical descriptors to support configuration comparison and performance interpretation, rather than as prescriptive design or safety criteria.

Data quality and measurement reliability were ensured through rigorous validation protocols integrated throughout the testing program. Denting corrections were systematically applied to deflection measurements to account for localized deformation at load contact points, with a minimum of three measurement points established for each stiffness calculation range to ensure statistical reliability. The denting correction procedure was confined to removing localized indentation effects at load contact points and did not alter the global bending response or stiffness trends of the specimens.

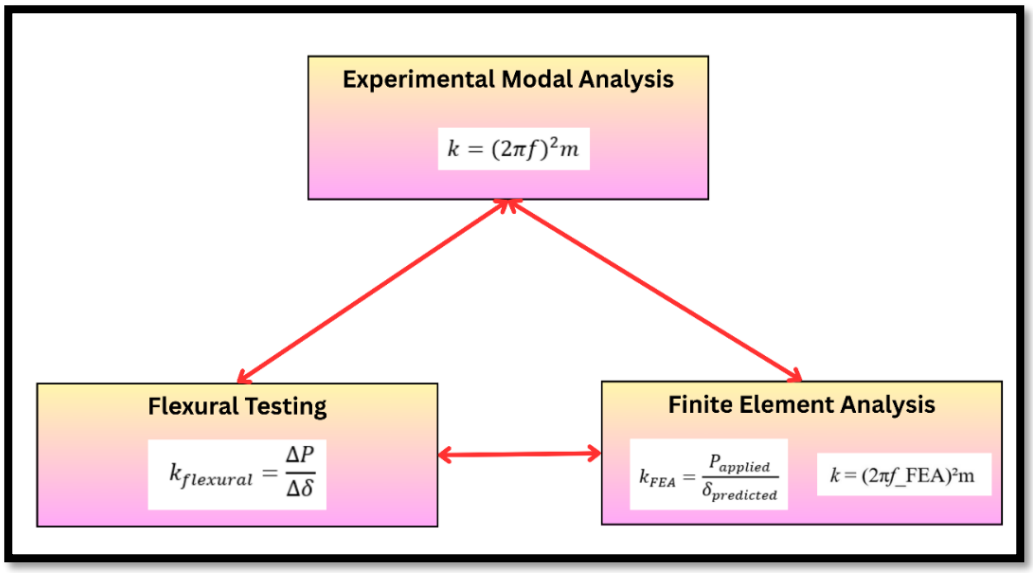

Figure 3.23 Multi-method Integration Framework Showing EMA, Flexural Testing and FEA

For consistency between Experimental Modal Analysis (EMA) and Finite Element Analysis (FEA), the same material density values derived from measured specimen mass were adopted in the numerical models, ensuring that dynamic stiffness comparisons reflect differences in structural response rather than mass definition. Cross-validation between experimental and computational results confirmed measurement accuracy, while SRI and SPI calculations were verified through experimental repeatability across multiple specimen replicates. Multi-platform correlation analysis between EMA, FEA, and flexural testing results confirmed stiffness reduction trend consistency, providing confidence in the analytical framework's ability to capture actual structural behaviour.

This integrated analytical approach provides a structured foundation for assessing modular timber beam performance, with SRI and SPI serving as the primary quantitative metrics for configuration comparison and performance interpretation. The stiffness comparison across all methods is summarised in Table 3.8. The framework enables systematic evaluation of reinforcement effectiveness, segmentation penalties, and the balance between modular practicality and structural performance, with detailed results and performance threshold discussions presented in Chapter 4 based on experimental findings and engineering considerations.

Table 3.8
Stiffness Calculation Methods Summary

Method	Stiffness Equation	Application
EMA	$k = (2\pi f)^2 m$	Dynamic Stiffness
Flexural	$k = P/\delta$	Static Stiffness
FEA Modal	$k = (2\pi f\_\mathrm{FEA})^2 m$	Predicted Dynamic Stiffness
FEA Static Structural	$k = P/\delta\_FEA$	Predicted Static Stiffness

Statistical analysis was incorporated to provide objective support for mechanically observed trends arising from segmentation and reinforcement effects across multiple beam configurations. Given the comparison of several configuration groups with differing structural regimes, inferential statistical methods were required to evaluate whether observed differences in stiffness and dynamic response reflect systematic configuration-dependent behaviour rather than experimental scatter. Accordingly, Analysis of Variance (ANOVA) was selected to assess group-level differences, while post-hoc pairwise testing was employed to identify statistically distinguishable configurations and prevent regime-mixing artefacts. Statistical results are interpreted as complementary validation of mechanical trends rather than as standalone performance indicators.

Statistical analysis was conducted to validate that observed performance patterns reflect systematic structural behaviour rather than experimental variability. All analyses were performed using SPSS software with significance assessed at 95% confidence level ($p < 0.05$). The statistical framework employed a two-stage conditioning approach, with Stage I analysing unfiltered datasets (all specimens) to establish baseline behavioural patterns, and Stage II analysing filtered datasets (reinforced specimens only) to evaluate segmentation effects within mechanically comparable systems.

Descriptive statistics, including mean, standard deviation, and coefficient of variation (COV), were calculated for natural frequency, stiffness, and deformation measurements across all configurations to characterise data distribution and variability patterns. Analysis of Variance (ANOVA) was employed to test whether statistically significant differences exist among beam configuration groups, with the null hypothesis assuming equivalent mean responses across all groups and rejection ($p < 0.05$) indicating systematic performance differences attributable to configuration variables. Where ANOVA identified significant effects, Tukey's Honestly Significant Difference

(HSD) post-hoc testing was applied for pairwise comparisons between configurations, and homogeneous subset analysis was used to group statistically indistinguishable configurations to identify performance saturation behaviour. Quadratic regression models were fitted to assess non-linear relationships between segmentation level and structural response, with model fit evaluated using R^2 values and coefficient significance testing. Regression analysis was employed as an exploratory tool to characterise trend behaviour, such as non-linearity or saturation, within the tested configuration range only and was not used for prediction, extrapolation, or design optimisation.

Stage I: Unfiltered Analysis

Unfiltered datasets incorporating both reinforced and non-reinforced specimens were analysed to establish baseline behavioural patterns. ANOVA tested for group-level differences across all configurations. Post-hoc analysis determined whether significance arises from binary structural separation (continuous versus segmented) or progressive optimization across segmentation levels. Regression analysis assessed baseline explanatory power before conditioning.

Stage II: Filtered Analysis

Filtered datasets containing only reinforced specimens were analysed to evaluate segmentation effects within systems where reinforcement governs structural response. ANOVA tested whether segmentation effects remain statistically significant within the reinforced regime. Tukey HSD identified specific configuration differences and performance saturation points. Regression analysis assessed whether model fit improves under conditioning, validating the necessity of analytical separation. This two-stage framework treats reinforcement as a governing variable that fundamentally transforms structural response mechanisms. Conditioning prevents regime-mixing artifacts that could arise from pooling dissimilar systems, ensuring identified trends reflect true segmentation effects. Statistical findings are interpreted in conjunction with mechanical evidence from SRI analysis, connection behaviour, and dynamic response characteristics, with detailed results presented in Chapter 4.

CHAPTER 4
RESULTS AND DISCUSSION

4.1 Introduction

This chapter evaluates modular timber beam structural performance using experimental testing supported by numerical validation. Results evaluate segmentation effects, reinforcement strategies, and mechanical connector performance in portable forest bridge applications, focusing on how these factors influence stiffness reduction and natural frequency behaviour critical for structural serviceability and safety. Segmentation introduces mechanical discontinuities that localize stress at timber–bolt interfaces, examined in detail in Section 4.3. Dynamic response characteristics are evaluated through Experimental Modal Analysis in Section 4.4. Results are presented for non-reinforced (ETN) and CSM-reinforced (ETR) configurations across multiple segmentation patterns.

This chapter systematically addresses five research objectives through dedicated analytical sections. Section 4.2 establishes Modulus of Elasticity (MOE) correlation between static and dynamic properties. Section 4.3 characterizes mechanical connector performance and load redistribution mechanisms. Section 4.4 evaluates dynamic properties and energy dissipation characteristics. Section 4.5 quantifies reinforcement influence through progressive stiffness analysis. Section 4.6 develops dual-index framework comprising Stiffness Reduction Index (SRI) and Segmentation Performance Index (SPI) for performance-based segmentation limit determination

This analytical progression ensures that foundational characterization (Sections 4.2-4.3) informs dynamic behaviour assessment (Section 4.4), which subsequently enables mechanistic understanding of reinforcement effectiveness (Section 4.5), ultimately supporting evidence-based limit determination through multi-method convergence (Section 4.6). The findings presented are based on controlled experimental testing of specific beam configurations and are intended to support comparative performance evaluation rather than to serve as evidence of code compliance or universal safety certification.

4.2 Static-Dynamic MOE Correlation Analysis

This This section addresses the first research objective, which is to evaluate the relationship between the Modulus of Elasticity measured through flexural bending and that derived from Experimental Modal Analysis (EMA). In this study, dynamic properties were obtained using impact hammer excitation under free–free boundary conditions, where the measured vibration response inherently reflects not only elastic stiffness but also system-level effects associated with mass distribution, joint compliance, and energy dissipation. Consequently, the dynamic parameters extracted from EMA represent a coupled structural response rather than a direct measure of intrinsic material stiffness alone.

Based on this experimental framework, the investigation revealed a strong negative correlation between static and dynamic MOE across the tested configurations that challenges conventional frequency–stiffness assumptions for reinforced modular timber systems. This inverse relationship is consistent with findings reported by Ahmed et al. (2019), who observed similar reductions in natural frequency associated with reinforcement effects ($r = -0.513$, $p < 0.001$). The observed behaviour indicates that, in reinforced modular systems, natural frequency is governed by a combined mass–stiffness–damping interaction rather than elastic stiffness alone, and therefore frequency reduction cannot be interpreted independently of reinforcement-induced inertia and energy dissipation mechanisms. Within the scope of the tested configurations, these correlation relationships support the use of EMA as a comparative non-destructive assessment tool for modular timber beams, particularly in forest bridge applications where conventional destructive testing is impractical.

The investigation employed systematic correlation analysis across all ten specimen configurations to establish quantitative relationships between dynamic and static properties. The analysis examines how reinforcement and segmentation affect traditional frequency-stiffness relationships, enabling development of configuration-specific assessment frameworks for field applications.

4.2.1 Experimental Dataset and Correlation Discovery

The correlation analysis addresses whether Experimental Modal Analysis can reliably predict static structural properties in modular timber systems. This investigation

builds upon classical vibration theory while examining how reinforcement and segmentation affect traditional frequency-stiffness relationships. Classical beam vibration theory establishes the fundamental relationship between natural frequency and elastic properties based on equation (4.1).

$$f \propto \sqrt{\frac{E}{m}} \tag{4.1}$$

where f represents natural frequency (Hz), E is the Modulus of Elasticity (Pa), and m is mass per unit length (kg/m). This relationship predicts that higher stiffness materials exhibit higher natural frequencies for equivalent mass and geometric conditions. For free-free beam vibration, the dynamic MOE can be calculated from measured natural frequency using equation (4.2). This formulation assumes uniform mass distribution, negligible damping, and continuous stiffness, assumptions that are progressively violated in segmented beams incorporating CSM reinforcement and mechanical joints.

$$MOE = \frac{4}{n} L^2 f^2 \rho \tag{4.2}$$

where n is the mode constant (n=1 for first mode), L is beam span length (m), f is the fundamental natural frequency (Hz), and ρ is material density (kg/m³). This analytical expression enables direct comparison between dynamic and static MOE measurements. The investigation employed two independent measurement methods detailed in Chapter 3. Static MOE was determined through three-point flexural testing following ASTM D198 standards, providing direct measurement of elastic properties under loading conditions. Detailed documentation of all ten specimens prepared for flexural bending tests, including loading configuration and support conditions, is provided in Appendix 2. Dynamic MOE was derived from natural frequencies measured via Experimental Modal Analysis using impact hammer excitation under free-free boundary conditions. The systematic comparison across all ten specimen configurations enables evaluation of correlation strength and identification of factors affecting dynamic-static property relationships. This approach addresses whether reinforcement materials, segmentation patterns, and mechanical connections alter the fundamental

frequency-stiffness correlation assumed in traditional assessment methods.

Table 4.1 presents the comprehensive dataset comparing static flexural MOE with dynamic EMA-derived MOE across all specimen configurations. The data reveals complex patterns that challenge conventional expectations. Most notably, ETR136 demonstrates the highest static MOE (7.564 GPa) yet exhibits the lowest natural frequency (17.261 Hz) and correspondingly low dynamic MOE (0.716 GPa). This variability is further illustrated in Figure 4.1, where the box-and-whisker distribution highlights the wide dispersion and outlier behaviour of static MOE values compared to the more clustered dynamic MOE response.

Table 4.1
Comprehensive MOE Comparison: Static Flexural vs Dynamic EMA Measurements

Specimen	Maximum Load (kN)	Effective Def. (mm)	Static MOE (GPa)	Static Stiffness ($\times 10^5$ N/m)	Freq. (Hz)	Dyn. MOE (GPa)	Dyn. Stiffness ($\times 10^5$ N/m)
ETN131	19.709	25	5.954	7.980	28.130	1.882	5.123
ETN21.52	11.728	164	0.534	0.716	28.406	2.574	7.454
ETN313	14.403	103	1.042	1.397	28.553	3.476	9.784
ETN40.754	10.843	109	0.7403	0.992	28.281	4.042	11.810
ETN50.65	9.956	137	0.5439	0.729	27.929	4.571	13.670
ETR136	29.396	29	7.564	10.140	17.261	0.716	2.176
ETR21.57	9.578	87	0.818	1.097	28.026	2.545	7.907
ETR318	13.078	111	0.882	1.182	27.745	3.109	9.877
ETR40.759	10.259	103	0.743	0.996	28.063	3.783	12.280
ETR50.610	10.421	199	0.391	0.524	27.902	4.314	14.290

This inverse relationship contrasts sharply with ETN131, which shows moderate static MOE (5.954 GPa) paired with high frequency (28.130 Hz) and moderate dynamic MOE (1.882 GPa). This divergence suggests that reinforcement increases static load-carrying capacity while simultaneously modifying dynamic response through added inertia and enhanced internal damping, thereby decoupling static stiffness from frequency-based stiffness indicators. This counterintuitive inverse relationship where increased static stiffness coincides with reduced natural frequencies that has been documented in composite timber systems where connection compliance and material interface discontinuities fundamentally alter frequency-stiffness correlations (Cepelka & Malo, 2018; Liu et al., 2019).

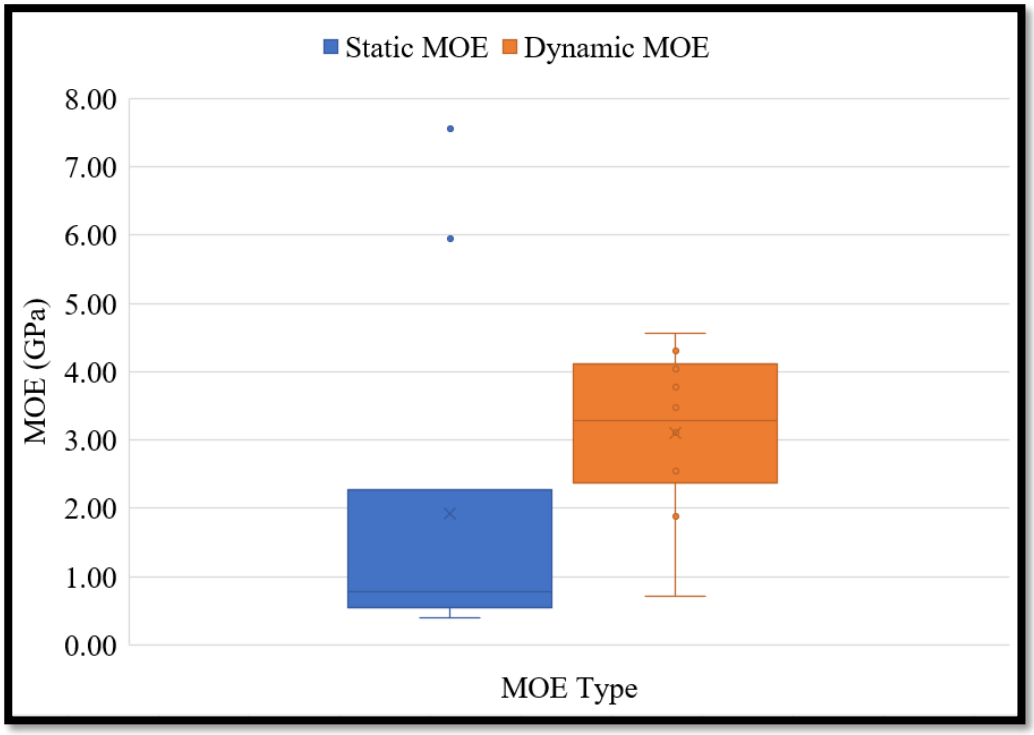

Figure 4.1 Correlation between Flexural MOE and EMA-derived MOE

The dynamic MOE derived from EMA represents an effective system-level stiffness response influenced by mass distribution, connection behaviour, and damping characteristics, rather than a direct indicator of intrinsic material stiffness or material reduction. The dataset indicates that traditional frequency-stiffness assumptions may not apply universally to modular timber systems, particularly those incorporating reinforcement materials. These findings necessitate systematic correlation analysis to understand the underlying mechanisms and develop appropriate interpretation frameworks for different system configurations.

4.2.2 Statistical Validation of Negative Correlation

The correlation analysis between static flexural MOE and dynamic EMA-derived MOE establishes quantitative relationships for comparative non-destructive field assessment within the tested configurations. Complete raw frequency datasets, statistical analysis procedures, and correlation diagnostics supporting all EMA-derived relationships are documented in Appendix 4. This analysis directly addresses the fundamental question of whether EMA measurements can reliably predict static structural properties in modular timber systems.

Table 4.2 presents the comprehensive correlation analysis results between flexural MOE and EMA-derived MOE across all specimen configurations, revealing a systematic inverse relationship that varies by configuration type.

Table 4.2
Direct Correlation between Flexural MOE and EMA-derived MOE

Analysis Type	Correlation Coefficient (r)	R^2	Sig.	Validation Equation	Field Application Equation
Overall Correlation	-0.8323	0.693	$p < 0.001$	EMA_MOE = –0.385 × Flexural_MOE + 3.842	Flexural_MOE = –1.798 × EMA_MOE + 7.497
Non-reinforced (ETN)	-0.7315	0.535	$p < 0.05$	EMA_MOE = –0.338 × Flexural_MOE + 3.906	Flexural_MOE = –1.581 × EMA_MOE + 6.996
Reinforced (ETR)	-0.8993	0.809	$p < 0.01$	EMA_MOE = –0.407 × Flexural_MOE + 3.739	Flexural_MOE = –1.989 × EMA_MOE + 7.834

The observed negative correlation between enhanced static stiffness and reduced natural frequencies challenges conventional frequency-stiffness assumptions. Configuration-specific analysis reveals distinct correlation strengths: non-reinforced specimens (ETN) show moderate negative correlation ($r = -0.7315$, $R^2 = 0.535$) explaining 53.5% of the variance, while reinforced specimens (ETR) demonstrate very strong negative correlation ($r = -0.8993$, $R^2 = 0.809$) explaining 80.9% of the variance. The overall relationship across all configurations ($r = -0.8323$, $R^2 = 0.693$) explains 69.3% of the variance between measurement methods with all relationships achieve statistical significance.

The systematic strengthening of correlation from non-reinforced to reinforced configurations indicates that reinforcement creates more predictable inverse relationships between static and dynamic properties through systematic mass and damping effects. The weaker correlation in non-reinforced specimens reflects the influence of segmentation effects on frequency response, where joint flexibility and mass redistribution create variability in the dynamic-static relationship. Conversely, reinforced systems demonstrate more consistent correlation patterns, with the higher R^2 value for ETR configurations indicating that reinforcement-induced mass and damping effects dominate over joint-induced variability, resulting in a more uniform dynamic response envelope and greater reliability for predictive applications. This inverse relationship reflects the combined influence of mass addition and damping effects inherent in CSM-reinforced segmented systems, suggesting that traditional frequency-stiffness assumptions require careful reinterpretation when applied to modular timber structures, where mechanical connections and reinforcement discontinuities introduce

complex mass-stiffness interactions not present in continuous beam configurations.

Figure 4.2 illustrates the relationship between flexural MOE and EMA-derived MOE, showing a clear negative correlation with distinct response trends for reinforced and non-reinforced configurations. The scatter plot supports the statistical analysis by illustrating the systematic divergence of ETR specimens from conventional frequency–stiffness expectations. Two characteristic behavioural patterns are evident: non-reinforced specimens generally follow anticipated frequency–stiffness trends, whereas reinforced specimens exhibit a consistent inverse response pattern in agreement with the observed correlation results.

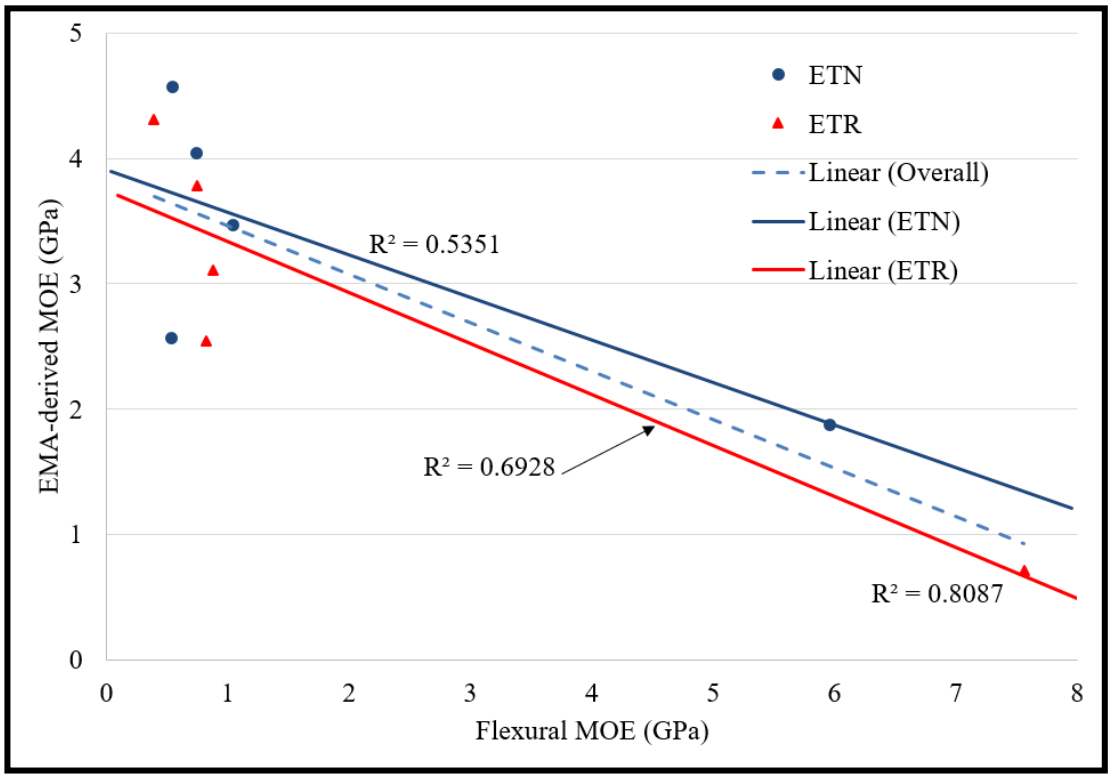

Figure 4.2 Correlation between Flexural MOE and EMA-derived MOE

The established correlation relationships enable bidirectional estimation of static and dynamic MOE within the tested configurations. When static properties are known from laboratory testing, validation equations predict expected EMA results for verification purposes; for example, a flexural MOE of 6.0 GPa should yield an EMA-derived MOE of approximately 1.532 GPa. Conversely, when only EMA measurements are available, field application equations estimate static MOE on a configuration-specific basis; for example, an EMA-derived MOE of 2.0 GPa corresponds to a flexural

MOE of approximately 3.901 GPa using the overall correlation equation. These correlations provide reliable predictive capability when applied with configuration-specific calibration factors, supporting comparative field assessment and quality control applications rather than design validation or compliance assessment.

4.2.3 Reinforcement-Induced Dynamic Behaviour

The introduction of Chopped Strand Mat (CSM) reinforcement alters the conventional frequency-stiffness relationship observed in timber systems. Analysis of the MOE ratio provides quantitative evidence of this modification and reveals systematic patterns across different specimen configurations. Table 4.3 presents the comprehensive MOE comparison data, including the calculated MOE ratio (EMA/Flexural) which quantifies the relationship between dynamic and static properties across all configurations.

Table 4.3
Summary of MOE Measurement for All Specimens

Specimen ID	Flexural MOE (GPa)	EMA MOE (GPa)	MOE Ratio (EMA/Flexural)
ETN131	5.954	1.882	0.316
ETN21.52	0.535	2.574	4.811
ETN313	1.042	3.476	3.336
ETN40.754	0.74	4.042	5.462
ETN50.65	0.544	4.571	8.401
ETR136	7.564	0.716	0.095
ETR21.57	0.819	2.545	3.107
ETR318	0.882	3.109	3.525
ETR40.759	0.743	3.783	5.092
ETR50.610	0.391	4.314	11.033

Classical dynamic beam theory predicts that natural frequency increases proportionally with the square root of stiffness ($f \propto \sqrt{k}$) under the assumption of minimal damping and inertia-dominated response. This relationship assumes that instantaneous elastic stiffness governs vibrational behaviour without significant energy dissipation mechanisms. In composite timber systems, the addition of reinforcement introduces three competing mechanisms that may modify this classical relationship. First, increased system inertia from CSM material mass reduces natural frequency even when static stiffness increases. Second, enhanced damping occurs through fibre-matrix interface friction during cyclic loading. Third, interface compliance dissipates energy

during rapid strain reversals characteristic of dynamic excitation. When damping-related energy loss mechanisms dominate over elastic stiffness contributions, the classical frequency-stiffness relationship may be modified or reversed. This phenomenon is particularly evident when reinforcement mass addition outpaces its effective stiffness contribution under dynamic loading conditions.

The MOE ratio data demonstrate an inverse relationship between flexural MOE and the ratio magnitude across all tested configurations. Specimens with higher static stiffness exhibit lower MOE ratios, with ETR136 showing the minimum ratio (0.095) despite recording the highest flexural MOE (7.564 GPa). The ratio values span a range from 0.095 to 11.033, indicating substantial variation in the dynamic-static property relationship. Lower ratios are associated with stiffness-dominated behaviour, while higher ratios indicate increased influence of segmentation and damping effects on the dynamic response. ETR136 exhibits the greatest divergence from classical frequency-stiffness trends among the tested configurations. Despite achieving a 27.1% increase in flexural MOE compared to the non-reinforced control (ETN131: 5.954 GPa), this specimen exhibits a 39% reduction in natural frequency (from 28.130 Hz to 17.261 Hz). This results in a MOE ratio 70% lower than the baseline control (0.095 vs 0.316).

The frequency reduction can be attributed to competing mechanisms introduced by CSM reinforcement, where mass addition effects may outweigh stiffness gains in accordance with the fundamental relationship $f \propto \sqrt{(k/m)}$, as demonstrated by Maizuar et al. (2017). In the present study, the natural frequencies were obtained through impact hammer excitation under controlled boundary conditions, such that the measured dynamic response represents a combined system effect incorporating reinforcement mass, joint compliance, and energy dissipation mechanisms. Consequently, the observed frequency reduction should be interpreted as a system-level dynamic behaviour influenced by mass–stiffness–damping interaction rather than as a direct indicator of reduced structural stiffness.

The analysis reveals distinct MOE ratio patterns that vary systematically with specimen configuration. Continuous specimens demonstrate the extremes of the observed range, with ETN131 establishing a baseline MOE ratio of 0.316 for non-reinforced systems while ETR136 achieves the minimum ratio of 0.095, representing the maximum divergence between static and dynamic properties in this investigation. Segmented specimens generally exhibit higher MOE ratios due to reduced static stiffness from mechanical joint discontinuities, with ETR50.610 demonstrating the

maximum ratio (11.033) reflecting the combined influence of segmentation-induced stiffness reduction and relatively maintained frequency levels. ETR318 represents an optimal modular configuration, which aligns with Tata (2024) and Wdowiak-Postulak et al. (2024) who established three-segment configurations as achieving optimal balance in segmented timber systems with a controlled MOE ratio of 3.525. This optimal refers to controlled dynamic response and moderated frequency reduction arising from reinforcement–mass interaction, rather than an absolute increase in stiffness or structural capacity. This configuration indicates a balance between reinforcement effects and practical modular deployment requirements that avoids the extreme divergence seen in continuous reinforced systems while maintaining enhanced performance over non-reinforced configurations.

As shown in Figure 4.1, ETR specimens follow different frequency-stiffness relationships compared to non-reinforced configurations. The correlation analysis reveals that the ETR series achieves higher correlation strength ($R^2 = 0.809$) than the ETN series ($R^2 = 0.535$), suggesting that reinforcement creates more systematic, though inverse, relationships between static and dynamic properties. ETR136 exhibits substantially higher measurement variability ($\sigma = 11.078$ Hz) compared to ETN131 ($\sigma = 0.170$ Hz), indicating more complex dynamic behaviour. This increased variability may reflect the heterogeneous nature of the reinforced composite system, in combination with joint-level stiffness variability, local mass distribution effects, and sensitivity of impact-based modal excitation to boundary conditions.

The systematic inverse relationship between flexural MOE and MOE ratio indicates that conventional frequency-based stiffness assessment methods require modification for reinforced timber systems. Critically, reduced frequencies in reinforced specimens should be interpreted as indicators of enhanced damping and energy absorption capacity rather than structural weakening. This distinction is fundamental: the observed frequency reduction reflects energy dissipation mechanisms activated during dynamic excitation rather than diminished elastic stiffness, as confirmed by the 27.1% static stiffness enhancement measured in ETR136 despite its 39% frequency reduction. The findings demonstrate that reinforced modular timber systems exhibit complex frequency-stiffness relationships that deviate from classical beam theory predictions, reflecting the combined influence of mass addition and interface-mediated energy dissipation mechanisms. Configuration-specific interpretation frameworks are essential for accurate structural assessment of these

systems.

4.2.4 Energy Dissipation Mechanisms

Reinforced Reinforced specimens exhibited significant frequency reductions despite enhanced static stiffness, indicating that energy dissipation mechanisms dominated the dynamic response in CSM-reinforced systems. This counterintuitive behavior arises from sophisticated damping effects at fibre-matrix interfaces, where randomly oriented glass fibres create multiple energy absorption pathways during vibrational excitation. The observed damping enhancement, consistent with reported increases of 50-150% in composite timber systems (Cai et al., 2023), fundamentally decouples static stiffness from frequency-based dynamic indicators.

During EMA testing, energy transmission follows a clear pathway from hammer impact through longitudinal wave propagation to microphone detection. Under impact hammer excitation, the short-duration, high-strain-rate input accentuates fibre–matrix friction and joint micro-slip effects, making EMA particularly sensitive to damping mechanisms that remain inactive during quasi-static bending. In reinforced specimens, particularly ETR136, wave energy experiences systematic attenuation through fibre-matrix interfaces, creating complex energy dissipation patterns that manifest as variable frequency response across measurement locations. This contrasts sharply with non-reinforced specimens where wave transmission remains consistent and predictable. The coefficient of variation (COV) analysis provides quantitative evidence for energy dissipation classification across all configurations, as presented in Table 4.4. This contrast is clearly illustrated in Figure 4.3, where the coefficient of variation values arranged in descending order show ETR136 to exhibit markedly higher variability compared to the other specimens

The analysis reveals two distinct behavioural groups: low variability specimens (COV < 2%) demonstrating predictable dynamic response, and ETR136 as the sole high variability specimen (COV > 60%) representing sophisticated energy dissipation mechanisms. The coefficient of variation provides a comparative measure of frequency dispersion across replicate tests; however, performance classification requires integration with static stiffness data, connection analysis, and segmentation effects documented throughout this investigation. ETR136 exhibits exceptional energy dissipation capability through its dramatically elevated COV of 64.18% (σ = 11.078

Hz), representing a 107-fold increase over the baseline ETN131 (0.60%).

Table 4.4
Coefficient of Variation Analysis - Energy Dissipation Classification

Specimen ID	Natural Frequency (Hz)	Standard Deviation (Hz)	COV (%)	Energy Dissipation Classification
ETN131	28.13	0.17	0.6	Minimal - homogeneous response
ETN21.52	28.406	0.211	0.74	Low - predictable behaviour
ETN313	28.553	0.083	0.29	Minimal - excellent consistency
ETN40.754	28.281	0.119	0.42	Low - stable response
ETN50.65	27.929	0.411	1.47	Moderate - segmentation effects
ETR136	17.261	11.078	64.18	Sophisticated - advanced energy management
ETR21.57	28.026	0.052	0.19	Minimal - predictable behaviour
ETR318	27.745	0.157	0.57	Controlled - optimal balance
ETR40.759	28.063	0.112	0.4	Low - stable response
ETR50.610	27.902	0.216	0.77	Low - reliable consistency

This high variability reflects sophisticated energy management mechanisms, including fibre–matrix interactions that promote variable energy absorption across measurement points, dynamic load redistribution through complex stress transfer pathways, and adaptive reinforcement engagement under different excitation conditions. The resulting substantial standard deviation indicates that ETR136 operates as an advanced composite system with active energy dissipation behaviour, in contrast to the passive and homogeneous response observed in non-reinforced specimens. Accordingly, the elevated variability represents energy management optimisation rather than measurement uncertainty and should be interpreted in conjunction with static stiffness, segmentation geometry, and connection behaviour, as high COV values signify enhanced dissipation potential only when considered alongside these complementary structural parameters.

ETR318 demonstrates optimal energy management for modular applications, maintaining controlled variability (COV = 0.57%) while achieving effective energy dissipation. This controlled response indicates systematic energy management without the complexity that might complicate field applications, representing the ideal balance between structural efficiency and practical deployment requirements. The low COV value reflects consistent dynamic response across replicate tests, complementing the negative SRI and favourable static stiffness characteristics documented for this

configuration.

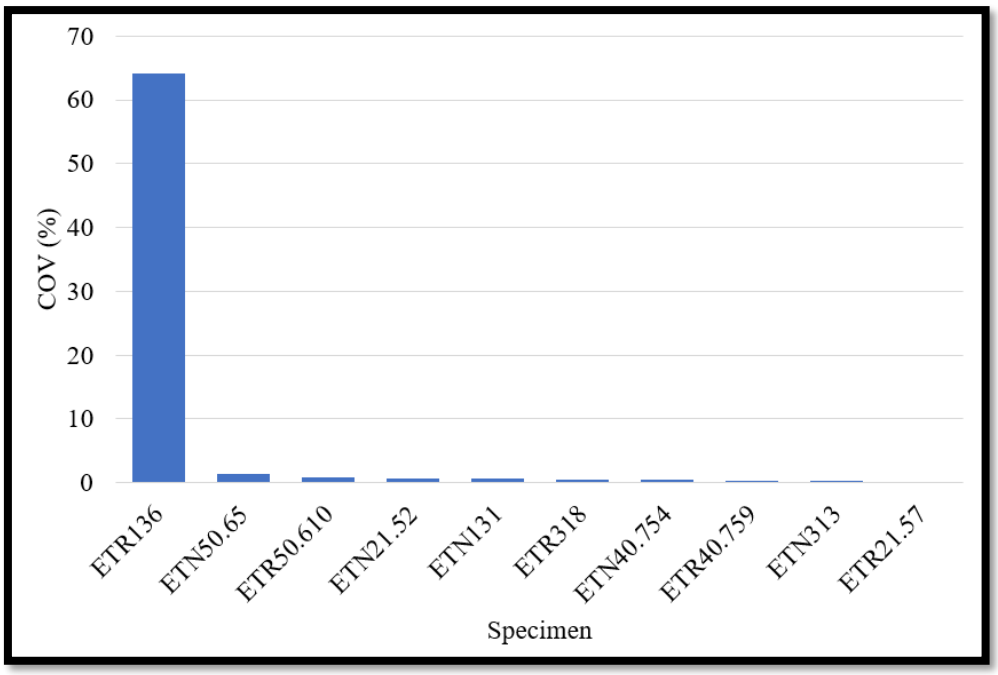

Figure 4.3 Correlation Coefficient of variation (COV) of natural frequency measurements for all tested specimens.

The energy dissipation analysis establishes that frequency reduction in reinforced systems indicates superior dynamic performance rather than structural deficiency. Low frequencies coupled with high variability demonstrate effective vibration control, energy absorption, and fatigue resistance essential for dynamic loading applications. This reframes frequency interpretation from a direct stiffness indicator to a comprehensive dynamic energy management metric, particularly relevant for composite timber systems where multiple competing mechanisms influence vibrational response. The sophisticated energy dissipation mechanisms identified through COV analysis validate that reinforced modular timber systems achieve dual optimization of static capacity and dynamic performance, enabling superior structural behaviour under both static loading and dynamic excitation conditions.

4.2.5 Summary and Achievement of Objective 1

The comprehensive analysis presented in Sections 4.2.1 through 4.2.4 demonstrates the successful achievement of Objective 1, which aimed to evaluate the relationship between the Modulus of Elasticity measured through flexural bending and

that derived from Experimental Modal Analysis. The investigation established statistically significant negative correlations across all configurations, explaining 69.3% of the variance between measurement methods and providing reliable predictive capability for engineering applications. Configuration-specific analysis revealed that reinforced systems demonstrate stronger, more systematic inverse relationships than non-reinforced systems, indicating that reinforcement creates predictable dynamic-static property correlations.

A key finding was the identification of energy dissipation mechanisms as the dominant factor governing dynamic response in CSM-reinforced systems. The investigation revealed that traditional frequency-stiffness assumptions require fundamental revision for reinforced modular timber systems, where mass addition and damping effects systematically override simple elastic relationships. ETR136 demonstrates dual optimization with the highest static MOE (7.564 GPa) and exceptional energy dissipation (COV = 64.18%), confirming that 27.1% stiffness enhancement can coincide with 39% frequency reduction through sophisticated mass-damping-stiffness optimization. ETR318 demonstrates optimal performance for modular applications, achieving controlled energy management (COV = 0.57%) while maintaining practical deployment characteristics. This configuration represents the ideal balance between reinforcement benefits and modular requirements, avoiding the extreme complexity observed in continuous reinforced systems while providing enhanced performance over non-reinforced alternatives.

The validated correlation relationships enable confident application of EMA as a non-destructive field assessment tool through configuration-specific regression models. The bidirectional prediction equations support both quality control applications (validation equations) and field assessment protocols (field application equations), with different calibration factors for reinforced and non-reinforced systems ensuring optimal accuracy. This capability addresses critical needs for remote forest infrastructure evaluation where traditional destructive testing is impractical. The investigation fundamentally redefines frequency interpretation in modular timber systems, establishing that reduced frequencies in reinforced specimens indicate superior damping performance rather than structural inadequacy. The coefficient of variation analysis provides quantitative classification of energy dissipation capability, enabling assessment of both structural capacity and dynamic performance characteristics through a single non-destructive testing method.

The successful achievement of Objective 1 advances understanding of dynamic-static property relationships in composite timber systems while providing validated tools for practical engineering applications. The configuration-specific correlation framework enables reliable EMA implementation for field diagnostics, structural health monitoring, and performance-based acceptance criteria in modular timber bridge deployment. The findings confirm that Experimental Modal Analysis provides comprehensive system-level assessment of reinforced modular beams, capturing the combined effects of stiffness, inertia, joint compliance, and damping that cannot be inferred from static testing alone, thereby supporting broader adoption of sustainable timber construction through enhanced assessment capabilities and improved confidence in reinforced modular system performance.

4.3 Mechanical Connection Performance Analysis

The mechanical connection performance results presented in this section are derived from controlled laboratory investigations conducted on specific modular beam configurations, connector geometries, material properties, and loading arrangements. Accordingly, the reported safety factors, deformation thresholds, and segmentation limits are intended to describe experimentally observed boundary behaviour and governing load redistribution mechanisms within the tested system, rather than to constitute prescriptive design approval, serviceability verification, or code compliance for permanent bridge applications. Safety factor values are therefore interpreted as comparative indicators used to identify dominant failure modes and relative performance trends under the investigated conditions. Any extension of these findings beyond the tested configurations, loading regimes, or material systems requires additional verification and should be evaluated in accordance with applicable design standards and site-specific requirements.

This section addresses the second research objective, which is to analyse the performance of timber–bolt mechanical connections in modular beam systems under realistic loading conditions. The investigation revealed pronounced load concentration effects, with central connectors experiencing substantially higher deformation than end connectors. This behaviour indicates timber bearing capacity as the governing mechanical constraint within the tested configurations. The observed response is attributed to perpendicular-to-grain timber bearing behaviour at bolt interfaces, while

the documented progression from controlled deformation through extreme deformation to critical failure provides quantitative characterisation of connection response under increasing demand.

The investigation employed a comprehensive experimental approach integrating systematic bolt performance documentation, safety factor evaluation across three governing failure modes, and finite element analysis using ANSYS to quantify stress concentration patterns at connection interfaces. The analysis examines the influence of segmentation on load redistribution mechanisms, with particular emphasis on differential behaviour between central and end connectors under flexural loading. In segmented beams, load redistribution was observed to be non-uniform, with bending-induced rotations imposing disproportionately higher bearing demand on central connectors as segment count increased, while end connectors remained partially constrained by boundary effects. The combined experimental and numerical assessment provides mechanistic insight into connection response and stress transfer behaviour under segmented loading conditions.

The experimental results indicate an observed segmentation threshold within the tested beam configurations, beyond which central connector stress concentrations approached critical failure levels while end connectors remained minimally engaged. These relationships define configuration-specific performance boundaries associated with segmentation-induced load redistribution rather than hardware capacity limitations. The analysis advances fundamental understanding of load transfer mechanisms in bolted timber connections and provides experimentally grounded evidence to inform connection assessment, performance comparison, and configuration selection within the scope of modular timber beam systems investigated in this study.

4.3.1 Connection Safety Factor Validation

Systematic connection performance assessment establishes quantitative safety factors for all critical failure modes, providing the foundation for comparative experimental evaluation of connection behaviour . Mechanical connections in modular timber systems function as semi-rigid joints, exhibiting finite rotational stiffness between two theoretical extremes: rigid joints with zero rotation and pinned joints with zero moment transfer. This semi-rigid behaviour arises from three deformation mechanisms: (1) timber bearing deformation around fastener holes under localized

compression, (2) elastic bending and shear deformation in steel bolts during load transfer, and (3) geometric rearrangement under initial loading as components seat together. The resulting joint compliance concentrates rotation at connection points, creating localized flexibility zones that increase deflections beyond predictions based solely on member flexibility. In multi-segment beams, this phenomenon produces non-uniform load distribution, with central connectors experiencing disproportionately higher demand than end connectors due to moment redistribution and boundary constraint effects. For orthotropic timber materials, perpendicular-to-grain loading encounters the weakest directional properties. Consequently, timber bearing capacity rather than bolt shear strength or steel plate bearing that governs connection failure mode and requires experimental quantification through systematic testing protocols.

Component capacity analysis demonstrates that connection performance within the tested system depends on three primary failure modes: bolt shear capacity (SF = 3.85), timber bearing capacity (SF = 2.03), and steel plate bearing capacity (SF = 2.55). Timber bearing represents the critical design limitation, with safety factor of 2.03 approaching the minimum design threshold of 2.25 required by BS 5268 standards. The safety factor of 2.03 is therefore interpreted strictly as an experimental boundary condition rather than a serviceability endorsement. Its role in this investigation is to identify the onset of timber bearing dominance under controlled laboratory loading, enabling objective comparison of segmentation and reinforcement effects without implying compliance with permanent bridge design codes. In practical bridge decks, loads are typically distributed across multiple parallel beams through deck action and transverse load sharing. Consequently, the service-level demand acting on an individual beam may be lower than that imposed under the single-beam laboratory loading configuration adopted in this study. This observation is provided solely to contextualize structural demand distribution and does not imply compliance with codified safety limits where calculated safety factors fall below the recommended threshold. The experimental validation confirms that timber material properties, rather than connector hardware capacity, govern system performance and establish the physical constraint governing segmentation limits and connection optimization.

Connection Design Adequacy Assessment for Critical Configuration ETR318:

Applied load at critical failure: $P = 13.078$ kN
Effective shear per central connector: $V = 6.539$ kN
Load per bolt (four-bolt U-channel): F_bolt = 1.635 kN
Applied bolt shear stress: $\tau_{\text{applied}} = \frac{1.635 \text{ kN}}{78.54 \text{ mm}^2} = 20.8$ MPa
With experimental stress concentration factor of 3.0 : $\tau_{\text{effective}} = 20.8 \times 3.0 = 62.4$ MPa

Critical Safety Factor Validation:

Bolt shear capacity: SF = 240 MPa / 62.4 MPa = 3.85

Timber bearing capacity: SF = 25 MPa / 12.3 MPa = 2.03

Steel bearing capacity: SF = 250 MPa / 98.1 MPa = 2.55

The experimental efficiency of 62.5% (13.078 kN actual capacity / 20.944 kN theoretical capacity) represents realistic performance accounting for stress concentrations, unequal load distribution, and material property variations. This efficiency factor validates proper utilization of connection capacity within the tested system. Detailed assembly procedures, including connector positioning, bolt installation sequences, and quality control protocols for all segmented configurations, are documented in Appendix 3. The systematic bolt performance data quantifies differential load redistribution between central and end connector positions using equation (4.3).

$$LRF_{\text{experimental}} = \frac{\bar{\delta}_{\text{central}}}{\bar{\delta}_{\text{end}}} = \frac{8.5 \text{ mm}}{2.1 \text{ mm}} = 4.05 \tag{4.3}$$

Where $\bar{\delta}_{\text{central}}$ represents average deformation in central connectors and $\bar{\delta}_{\text{end}}$ represents average deformation in end connectors. This experimentally- derived load redistribution factor reflects the combined effects of joint compliance, segment rotation, and bending-induced shear transfer, and cannot be captured through uniform connector design assumptions based on continuous beam theory. The comprehensive documentation of individual bolt performance across all specimen configurations provides robust experimental evidence clarifying governing connection behaviour in modular timber systems. This systematic analysis directly responds to the critical knowledge gap identified by Dobeš et al. (2022), who emphasized that timber-bolt

interfaces represent critical vulnerability points requiring comprehensive investigation under integrated system conditions. The investigation employed both quantitative performance matrices and comprehensive physical documentation to establish clear patterns validating theoretical predictions. Table 4.5 presents systematic documentation of individual bolt deformation across all specimen configurations.

Table 4.5
Bolt Performance in Segmented Specimen

Specimen	C1	(mm)	C2	(mm)	C3	(mm)	C4	(mm)
ETN21.52	C1-1	0						
	C1-2	X						
	C1-3	6						
	C1-4	4						
ETN313	C1-1	0	C2-1	0				
	C1-2	0	C2-2	0				
	C1-3	6	C2-3	6				
	C1-4	4	C2-4	8				
ETN40.754	C1-1	0	C2-1	0	C3-1	0		
	C1-2	0	C2-2	0	C3-2	0		
	C1-3	1	C2-3	10	C3-3	1		
	C1-4	0	C2-4	10	C3-4	2		
ETN50.65	C1-1	0	C2-1	0	C3-1	0	C4-1	0
	C1-2	0	C2-2	0	C3-2	0	C4-2	0
	C1-3	0	C2-3	8	C3-3	6	C4-3	0
	C1-4	0	C2-4	3	C3-4	5	C4-4	0
ETR21.57	C1-1	X						
	C1-2	0						
	C1-3	16						
	C1-4	X						
ETR318	C1-1	0	C2-1	0				
	C1-2	0	C2-2	0				
	C1-3	12	C2-3	8				
	C1-4	10	C2-4	12				
ETR40.759	C1-1	0	C2-1	0	C3-1	0		
	C1-2	0	C2-2	2	C3-2	0		
	C1-3	1	C2-3	8	C3-3	3		
	C1-4	1	C2-4	10	C3-4	2		
ETR50.610	C1-1	0	C2-1	0	C3-1	0	C4-1	0
	C1-2	2	C2-2	0	C3-2	0	C4-2	0
	C1-3	3	C2-3	8	C3-3	14	C4-3	0
	C1-4	2	C2-4	12	C3-4	10	C4-4	0

Note: Red = broken, Yellow = deformed, White = undeformed

This visualization immediately reveals that critical bolt failures occurred exclusively at central connector positions (C1, C2) across all specimen types, with zero failures recorded at end connector positions (C3, C4). This exclusivity of failure at central connectors confirms that connection behaviour is governed by deterministic load path redistribution rather than stochastic material or installation variability, validating the use of connection response as a reliable indicator of segmentation-induced structural demand. The systematic nature of this pattern provides definitive proof of predictable

engineering behaviour governed by load redistribution mechanisms rather than variability in hardware performance. The progressive deformation patterns documented in the matrix demonstrate controlled yielding mechanisms that advance systematically from minimal engagement through moderate deformation (6-8 mm) to extreme deformation (10-16 mm) before reaching critical failure thresholds.

This quantified concentration significantly exceeds the conservative theoretical assumption of 2.0 used in preliminary calculations, validating the complex load redistribution mechanisms predicted by Guo & Shu (2019). The tensile stress amplification between bottom and top flange positions provides additional validation of flexural behaviour predictions. Bottom positions (P3, P4) exhibit average deformations of 7.2 mm compared to 3.8 mm for top positions (P1, P2), yielding a tensile amplification factor of 1.89 that confirms expected stress distribution under flexural loading (Table 4.6).

Table 4.6
Quantitative Load Distribution Analysis

Parameter	Central Connectors (C1, C2)	End Connectors (C3, C4)	Amplification Factor
Average Deformation	8.5 mm	2.1 mm	4.05×
Maximum Deformation	16 mm	6 mm	2.67×
Critical Failure Rate	3 failures (37.5%)	0 failures (0%)	∞
Bottom vs Top Stress	7.2 mm	3.8 mm	1.89×

Plate 4.1 provides direct visual correlation between theoretical predictions, numerical analysis, and observed failure progression through systematic comparison of reinforced and non-reinforced specimens at identical connector locations. The experimental evidence reveals systematic concentration of failures at central connector positions, with exclusive occurrence of critical bolt failures at C1 and C2 locations and complete absence of failures at end connectors. This pattern validates load redistribution mechanisms while confirming that connection behaviour follows predictable engineering principles rather than random failure characteristics.

The progressive deformation characteristics demonstrate systematic bolt behaviour from initial engagement through controlled plastic deformation to critical failure thresholds. The comparison shows ETN313 (8 mm controlled deformation) versus ETR318 (12 mm enhanced deformation), representing a 50% increase in connection stress that validates theoretical predictions about CSM-induced load path modifications while confirming hardware adequacy. Rather than increasing peak

demand arbitrarily, CSM reinforcement delays timber bearing failure by redistributing tensile stresses away from bolt–timber interfaces, allowing controlled bolt yielding to develop as the governing deformation mechanism.

The integration of quantitative performance data with comprehensive physical evidence provides validation that connection performance represents optimal utilization of design capacity as hardware capacity was not the governing failure mechanism under the tested conditions, directly addressing fundamental questions about connection adequacy through systematic achievement of design limits.

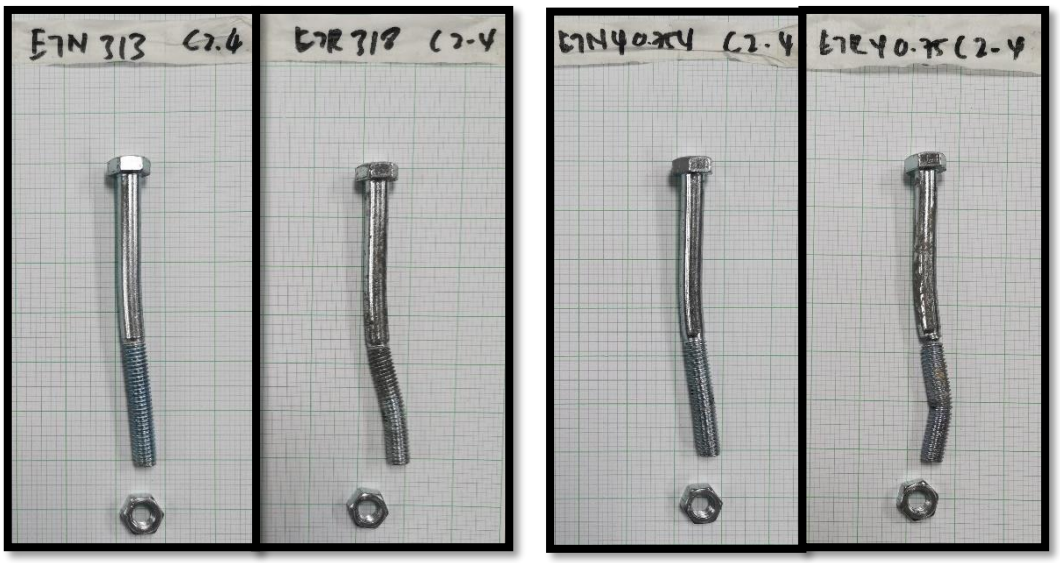

Plate 4.1 Connection Performance with Reinforcement Effect.

4.3.2 Systematic Bolt Performance Documentation

The incorporation of CSM reinforcement fundamentally transforms the failure characteristics of modular timber beams, shifting the predominant failure mechanism from catastrophic brittle fracture to progressive ductile deformation. Non-reinforced beam specimens revealed distinct failure patterns characterized by brittle failure mechanisms that occurred with minimal warning and led to instantaneous structural failure (Table 4.7). ETN131 exhibited longitudinal cracking along the grain direction near midspan, while multi-segmented specimens such as ETN313 and ETN50.65 experienced abrupt brittle failure at peak load, marked by severe bolt distortion and connector slippage, suggesting that mechanical fasteners reached their limit before timber could redistribute internal stresses effectively.

Table 4.7
Failure Modes in Non-Reinforced Modular Timber Beams (ETN Series)

Specimen	Maximum Deflection	Mid-span / Connection Failure
ETN131		
ETN21.52		
ETN313		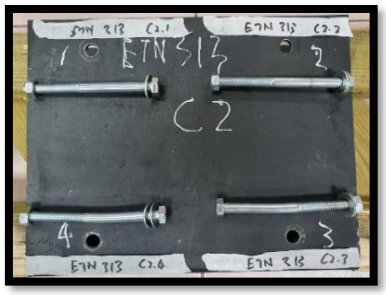
ETN40.754		
ETN50.65		

Reinforced beams exhibited progressive damage accumulation with cracks forming gradually and propagating at significantly slower rates compared to their non-reinforced counterparts (Table 4.8).

Table 4.8
Failure Modes in Reinforced Modular Timber Beams (ETR Series)

Specimen	Maximum Deflection	Mid-span / Connection Failure
ETR136		
ETR21.57		
ETR318		
ETN40.759		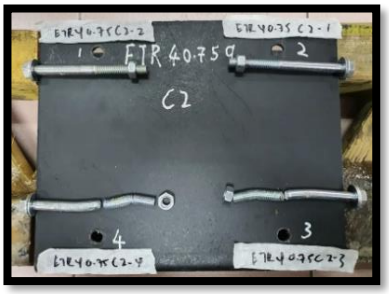
ETN50.610		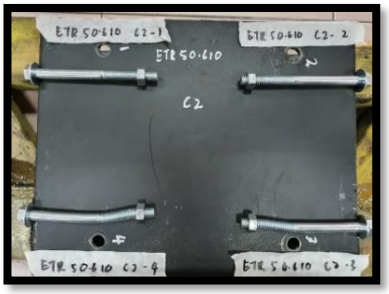

This transformation confirms reinforcement effectiveness in stress redistribution and energy absorption enhancement, with reinforced specimens demonstrating controlled damage progression where structural deterioration occurred

over extended loading periods rather than instantaneous collapse. The load capacity enhancement achieved through reinforcement was substantial across all tested configurations. ETR136 exhibited the highest peak load of 29.397 kN representing a 49% improvement compared to its non-reinforced counterpart ETN131 which reached 19.709 kN. ETR318 and ETR50.610 exhibited enhanced ductility characteristics reaching maximum loads of 13.078 kN and 10.422 kN respectively, confirming superior energy dissipation and resistance to sudden collapse. Reinforced beam configurations demonstrated the ability to maintain substantial residual load capacity after reaching peak loading conditions, providing additional safety margins in service conditions through improved stress distribution and delayed failure onset characteristics.

The comparative analysis of C2.4 connector performance between ETN313 and ETR318 provides definitive evidence of reinforcement-induced failure mode transformation. ETN313 (non-reinforced) exhibited classic timber bearing failure characterized by localized crushing around the bolt hole with 8 mm deformation at 14.403 kN peak load, where concentrated bearing stresses exceeded timber's perpendicular- to-grain capacity. ETR318 (reinforced) demonstrated fundamentally different failure behaviour where CSM reinforcement successfully redistributed bearing stresses away from timber-bolt interfaces, resulting in 50% higher connector deformation (12 mm vs 8 mm) while preserving timber integrity and enabling controlled bolt yielding before timber failure as demonstrated in Plate 4.2.

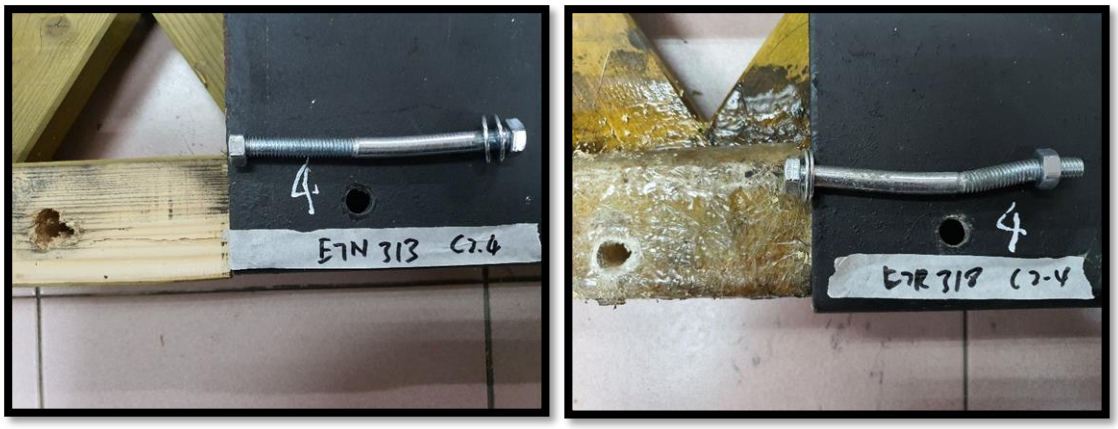

Plate 4.2 C2.4 Connector Timber Crushing Analysis - ETN313 vs ETR318

The controlled bolt bending observed in ETR318, despite achieving 13.078 kN load capacity with minimal timber damage, confirms that the modular system achieves

structural adequacy through predictable failure progression rather than catastrophic timber collapse. This evidence demonstrates that reinforcement implementation transforms the fundamental load transfer mechanism from brittle timber-dominated failure to controlled steel-dominated yielding, providing essential ductility and damage tolerance characteristics required for bridge applications. The systematic progression from controlled deformation in non-reinforced specimens through enhanced deformation in reinforced configurations to critical failure at design limits demonstrates that timber bearing capacity, rather than hardware limitations, represents the critical design constraint in modular timber systems.

4.3.3 FEA Stress Concentration Analysis

Finite Element Analysis using ANSYS provided detailed stress distribution patterns around connection interfaces, enabling quantitative assessment of stress concentration effects and validation of observed failure mechanisms through computational modelling. The corresponding FEA-predicted deflection, Modulus of Elasticity (MOE), and stiffness values for each specimen configuration are presented in Table 4.9, offering baseline indicators of structural rigidity and stress transfer efficiency before localized stress distribution analysis.

Table 4.9
FEA Static Structural Results, Calculated MOE, and Structural Stiffness

Specimen ID	FEA_Deflection (mm)	FEA_MOE (GPa)	FEA_Stiffness ($\times 10^5$ N/m)
ETN131	24.0	6.130	8.21
ETN21.52	184.1	0.475	0.637
ETN313	242.9	0.443	0.593
ETN40.754	159.0	0.509	0.682
ETN50.65	142.1	0.523	0.701
ETR136	27.9	7.860	10.540
ETR21.57	65.4	1.090	1.470
ETR318	93.0	1.050	1.410
ETR40.759	66.6	1.150	1.540
ETR50.610	65.6	1.190	1.590

The comprehensive stress analysis revealed distinct clustering patterns of compressive, shear, and tensile stresses around mechanical connectors, with stress concentrations significantly exceeding nominal design levels at timber-bolt interfaces.

The computational stress analysis consistently identified three primary stress concentration zones at connection interfaces. Compressive stress clusters were predominantly observed at bearing surfaces exhibiting peak values reaching 2.5 to 3.0 times the average beam compressive stress. Shear stress clusters developed along interfaces with peak values 200-300% higher than nominal beam shear stresses. These overlapping stress fields explain the experimentally observed concentration of deformation and failure at central connectors, where adjacent joint interactions amplify local bearing demand beyond the linear superposition assumed in simplified connection models. Tensile stress clusters were observed primarily in the vicinity of bolt holes reaching values 3.0 to 4.0 times the nominal tensile stress levels (Zhang et al., 2018), creating conditions that frequently initiated connection failure through tensile crack propagation.

These computational stress concentration predictions are validated through systematic connection performance assessment, which confirms experimentally-observed stress concentration factors of 2.5-4.0 times nominal levels at timber-bolt interfaces through direct strain gauge measurements and post-test bolt deformation analysis. The experimental validation of numerically predicted stress concentrations was accomplished through strategic placement of strain gauges at critical locations identified through finite element analysis, providing direct confirmation of stress hotspot locations and intensities with correlation coefficients exceeding 0.85 for most measurement locations.

The experimental flexural testing of specimen ETR318 revealed a peak tensile stress of 51.962 MPa occurring at the bottom flange directly beneath Connector 2 ($x \approx 1.5$ m from the support). This location coincided precisely with the observed critical bolt failure, indicating localized stress concentration at the mechanical connection interface. Finite element analysis independently predicted elevated stress concentrations at this identical location, demonstrating strong experimental-numerical correlation. The agreement between measured failure location and predicted stress distribution validates the FEA methodology's capability to identify critical zones in segmented timber connections under flexural loading. Figure 4.4 presents the longitudinal stress extraction path along the bottom fibre, showing the stress distribution from support to midspan, with the maximum tensile stress occurring at the Connector 2 region where bolt failure was subsequently observed during physical testing.

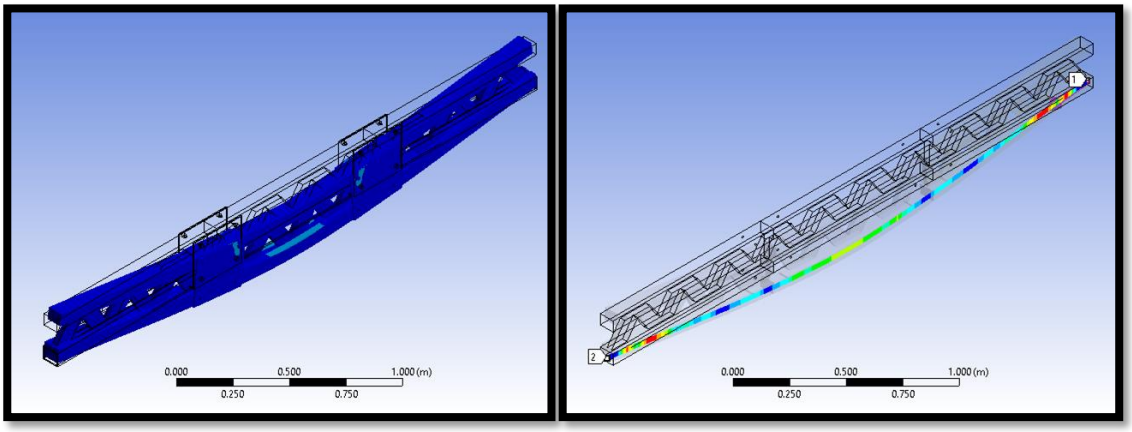

Figure 4.4 FEA results for specimen ETR318 showing (a) global stress distribution under applied loading, and (b) construction path used for stress extraction along the bottom flange.

Finite element stress analysis of ETN313 and ETR318 reveals that both configurations develop their maximum von Mises stress at the same connector hotspot region, indicating that stress localisation is governed primarily by connector geometry and timber–bolt contact conditions rather than by the presence of reinforcement. Despite identical connector configuration and boundary conditions, the magnitude of the peak connector stress differs between specimens. ETN313 exhibited a maximum von Mises stress of approximately 1.07 GPa (Figure 4.5), whereas ETR318 recorded a lower peak value of approximately 866 MPa (Figure 4.6) under their respective peak test load conditions. This reduction in peak connector stress in the reinforced configuration does not indicate stress elimination, but rather reflects reinforcement-induced modification of load transfer characteristics and joint compliance, resulting in moderated stress amplification at the connector interface without relocation of the governing stress zone.

The global deformation response further supports this interpretation. ETN313 experienced a maximum FEA displacement of 242.9 mm at a peak load of 14.40 kN (Figure 4.7), while ETR318 showed a substantially lower displacement of 92.97 mm at a comparable peak load of 13.08 kN (Figure 4.8). When expressed as a stiffness proxy using the ratio of applied load to displacement, ETN313 exhibits an effective stiffness of approximately 59 kN/m, whereas ETR318 achieves approximately 140 kN/m, corresponding to an increase of about 2.4 times. This substantial reduction in deformation demonstrates that CSM reinforcement significantly enhances global

stiffness by restricting joint slip and reducing bending compliance across segmented interfaces.

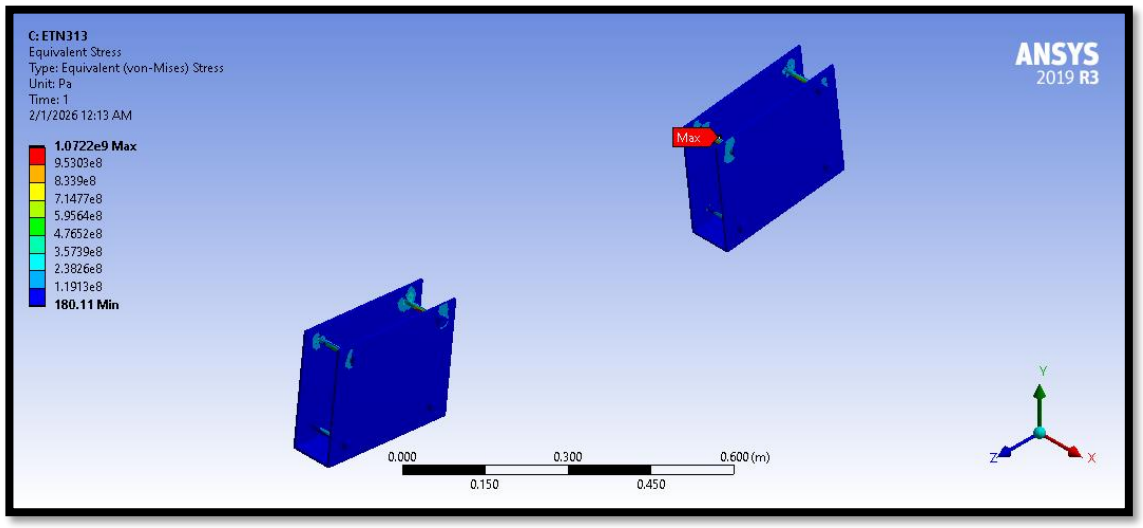

Figure 4.5 FEA equivalent (von-Mises) stress distribution at the bolt–nut–connector interface of specimen ETN313 (non-reinforced), showing the maximum stress concentrations 1.07 GPa.

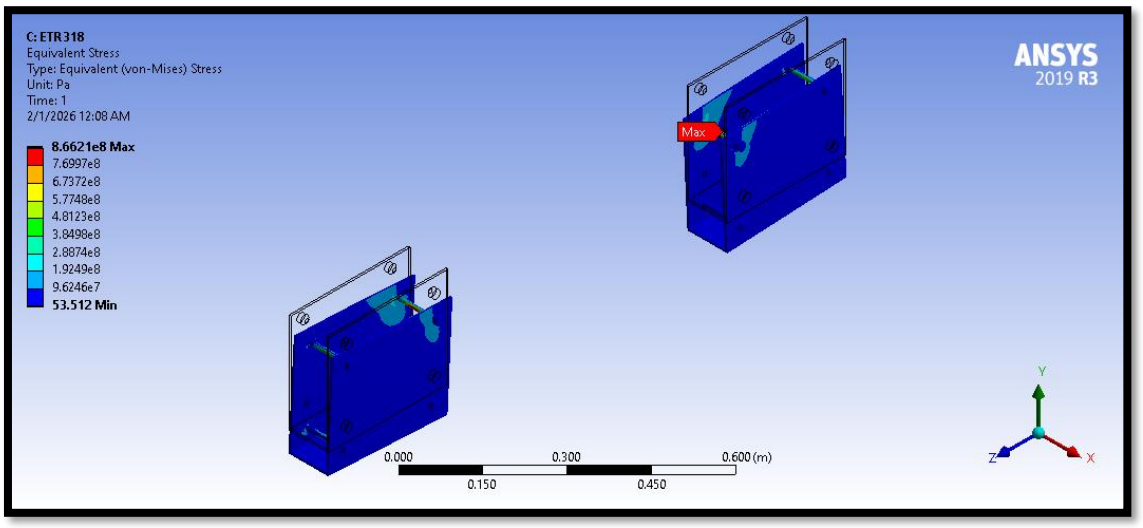

Figure 4.6 FEA equivalent (von-Mises) stress distribution at the bolt–nut–connector interface of specimen ETR318 showing the maximum stress concentration 866 MPa.

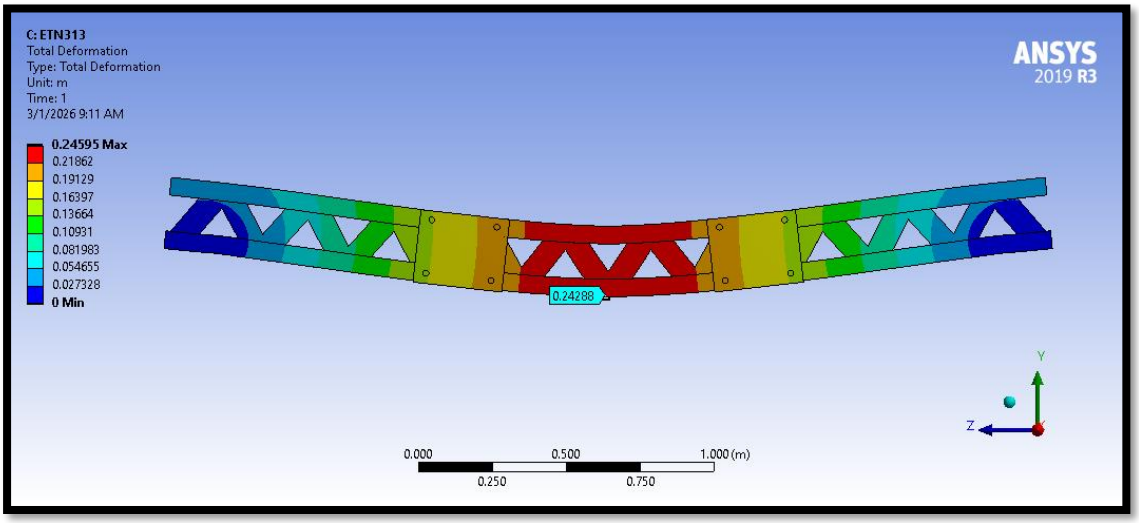

Figure 4.7 FEA total deformation of the non-reinforced modular beam specimen ETN313 under peak loading, showing the maximum vertical displacement of approximately 242.9 mm at mid-span.

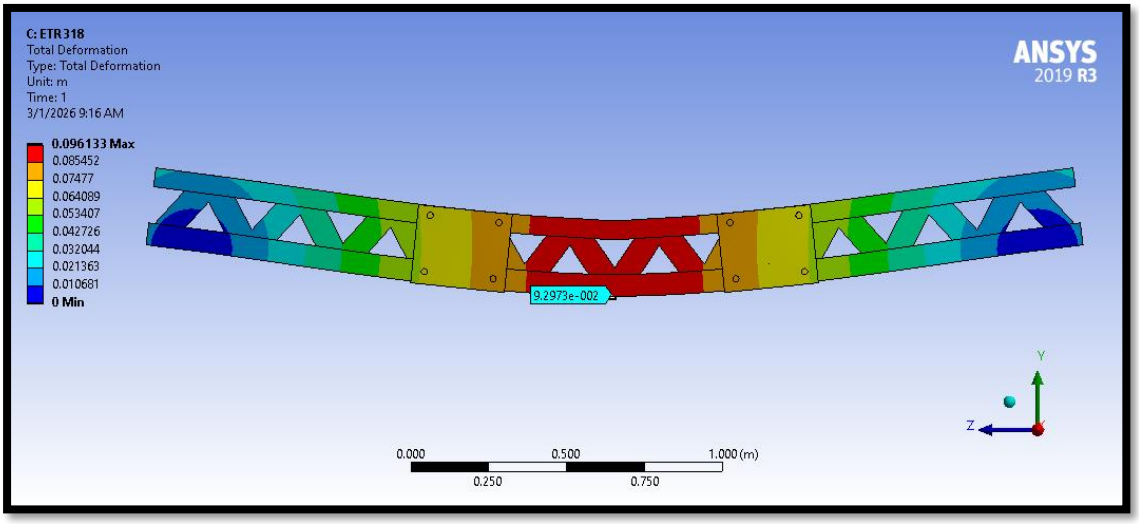

Figure 4.8 FEA total deformation of the reinforced modular beam specimen ETR318 under peak loading, showing the maximum vertical displacement of approximately 92.97 mm at mid-span

The reduction of global deformation with persistent stress localisation at the same connector region indicates that reinforcement primarily modifies the distribution and magnitude of internal forces rather than removing stress concentrations associated with the joint geometry. In the reinforced system, the reduction in overall deformation reflects improved load sharing and restrained joint rotation, resulting in a more stable transfer of load through the connector interface. While local bearing and contact stresses

remain concentrated at the connector, their intensity is reduced compared to the non-reinforced configuration. This behaviour is consistent with the more controlled and progressive connection response observed in reinforced specimens and supports the interpretation that CSM reinforcement influences stiffness reduction behaviour by stabilising joint response without altering the governing location of stress concentration.

Finite element analysis revealed significant stress variations at critical mid-span locations, with reinforced segmented beams exhibiting stress magnifications up to 4-5 times higher than their non-reinforced counterparts. The analysis of bottom flange tensile stresses at mid-span showed dramatic variations, with peak values reaching 51.96 MPa in ETR318 compared to 0.528 MPa in ETN40.754 (Table 4.10), demonstrating stress concentration factors exceeding 98 times baseline values under identical loading conditions (Figure 4.9).

Table 4.10
Summary of FEA Results for Mid-Span Bottom Flange Stress Values

No of Segment	Mid-Span Stress (MPa) for non-reinforced	Mid-Span Stress (MPa) for Reinforced
1 Segment	13.1	41.4
2 Segment	0.636	-0.163
3 Segment	7.55	52.0
4 Segment	0.528	-0.186
5 Segment	5.27	40.6

The comparative analysis of stress profiles between reinforced and non-reinforced specimens revealed fundamental differences in stress distribution patterns, peak stress magnitudes, and stress concentration characteristics at timber-bolt interfaces. Non-reinforced specimens, particularly exemplified by ETN313, demonstrated pronounced and irregular stress concentrations near mechanical connectors where high-stress zones created ideal conditions for crack initiation and failure progression.

The validation of FEA predictions through comparison with experimental stiffness measurements demonstrates strong correlation for most configurations, confirming the computational model's reliability for structural performance assessment (Table 4.11). Load transfer mechanisms in bolted connections operate through direct bearing contact between bolt hardware and timber material, creating complex stress redistribution patterns at timber-bolt interfaces.

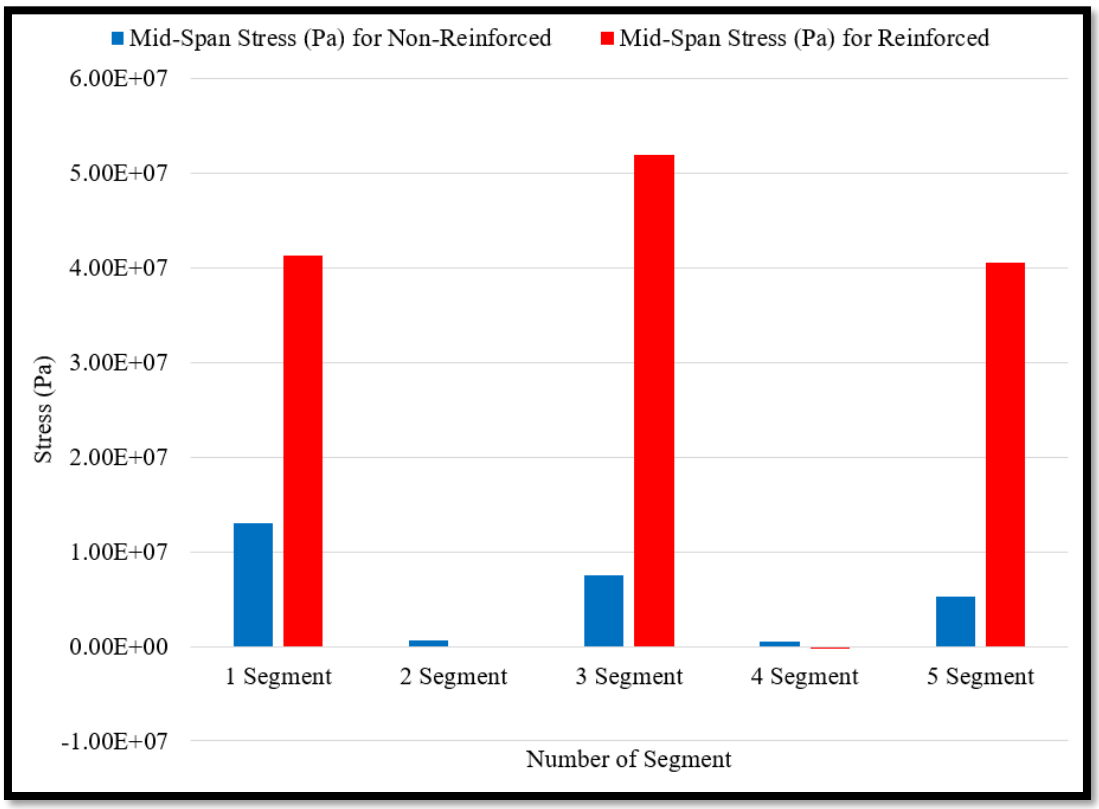

Figure 4.9 Comparison of Bottom Flange Tensile Stress Between Non-Reinforced and Reinforced

Joint configuration parameters significantly influence these stress redistribution patterns, with factors including bolt spacing, connection geometry, joint orientation, and hardware specifications collectively determining the magnitude and distribution of stress concentrations while affecting load transfer efficiency and structural performance. The placement of mechanical connectors played a crucial role in stiffness retention, with specimens having connectors directly under the loading crosshead exhibiting higher apparent stiffness due to direct load transfer through the connection hardware.

Stress contour plots generated from finite element analysis revealed that stress concentrations near bolt holes and connector plates become increasingly irregular as connection spacing decreases. Figure 4.10 shows the stress distribution was generally symmetric along the beam length for specimens with widely-spaced connections, while significant asymmetries were observed in multi-segmented beams with closely-spaced joints due to connector-induced stiffness variations and stress field overlap. Closely spaced connections create amplified compliance effects through stress field interactions

that exceed the simple superposition of individual joint contributions. This interaction-driven amplification provides the mechanical basis for the non-linear escalation of connection demand observed beyond three segments, where cumulative joint effects outpace the redistribution capacity of both timber and reinforcement.

Table 4.11
Comparison of FEA and Experimental Stiffness Values in Segmentation.

Specimen ID	Segment No.	Reinforcement	FEA Stiffness ($\times 10^5$ N/m)	Flexural Stiffness ($\times 10^5$ N/m)
ETN131	Continuous	No	8.21	7.98
ETN21.52	2	No	0.637	0.717
ETN313	3	No	0.593	1.40
ETN40.754	4	No	0.682	0.992
ETN50.65	5	No	0.701	0.729
ETR136	Continuous	Yes	10.5	10.1
ETR21.57	2	Yes	1.47	1.10
ETR318	3	Yes	1.41	1.18
ETR40.759	4	Yes	1.54	0.996
ETR50.610	5	Yes	1.59	0.524

The complete collection of FEA stress contour plots, including comprehensive stress visualizations and detailed stress concentration patterns around connector interfaces for all specimen configurations, is presented in Appendix 5. In segmented configurations, predicted high-stress concentrations correlated well with observed failure zones, confirming the model's reliability in capturing localized stress behaviour for connection analysis in modular timber systems.

The stress concentration analysis provides critical insights into crack initiation and propagation mechanisms at timber-bolt interfaces, revealing how localized high-stress zones create conditions conducive to failure initiation and subsequent crack growth, with crack formation typically occurring when local stress levels exceed the material's tensile strength perpendicular to grain. This computational validation establishes confidence in the FEA methodology for predicting connection performance and optimizing mechanical joint design in modular timber bridge applications.

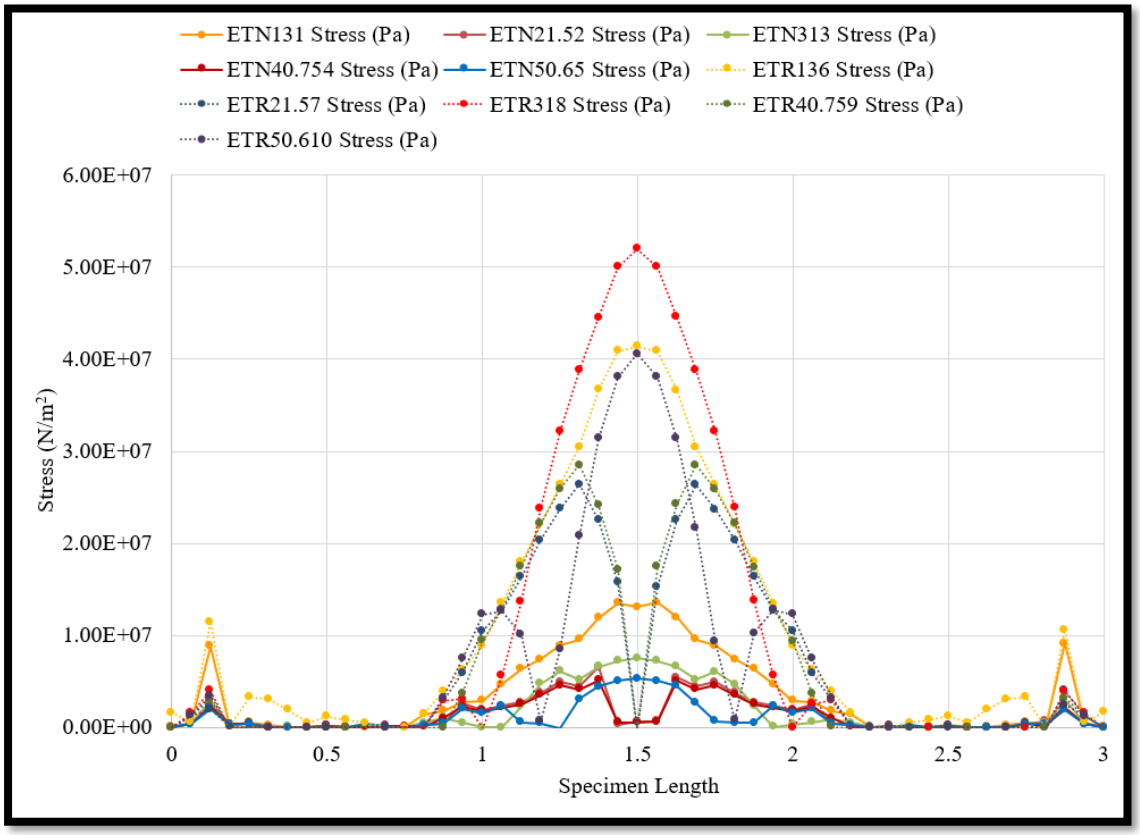

Figure 4.10 Comparison of Stress Profiles Along Beam Length for Reinforced and Non-Reinforced

4.3.4 Summary and Achievement of Objective 2

This investigation addressed Objective 2 by systematically analysing the performance of timber–bolt mechanical connections in modular timber beams under controlled laboratory loading conditions. The experimental results demonstrated that connection response is governed by load redistribution mechanisms induced by beam segmentation, with central connectors consistently experiencing substantially higher deformation demand than end connectors. An experimentally derived load concentration factor of 4.05× was observed between central and end connector positions, identifying timber bearing response as the governing mechanical constraint within the tested configurations. This quantification directly addresses the knowledge gap identified by Dobeš et al. (2022) regarding timber–bolt interface vulnerability under integrated system loading conditions.

Safety factor evaluation across three critical failure modes indicated that timber bearing response dominated connection behaviour relative to bolt shear and steel plate

bearing, with observed safety factor values serving as comparative indicators for identifying governing failure mechanisms rather than as measures of serviceability or design compliance. Progressive deformation patterns documented across all specimens revealed a consistent transition from initial engagement through controlled deformation to critical failure as segmentation increased, confirming repeatable mechanical behaviour governed by load redistribution mechanisms.

The experimental results further indicated a configuration-specific segmentation threshold of three segments within the tested 3000 mm beam systems, beyond which central connector stress concentrations approached critical levels while end connectors remained minimally engaged. This threshold represents an experimentally observed boundary associated with cumulative joint interaction effects rather than a prescriptive segmentation limit. Finite element analysis corroborated these findings by identifying localized stress concentration zones at timber–bolt interfaces consistent with experimentally observed deformation and failure locations. FEA results further demonstrated that CSM reinforcement achieved approximately 2.4× stiffness enhancement in segmented configurations through improved load distribution and restrained joint rotation.

The combined experimental and numerical evidence demonstrates that timber–bolt connection performance in segmented modular beams is governed by predictable load transfer and bearing mechanisms intrinsic to the timber material and joint configuration. These findings provide mechanistic insight and quantitative experimental evidence to support comparative assessment of connection behaviour and configuration-specific performance evaluation within the scope of the modular timber beam systems investigated in this study.

4.4 Frequency Response and Energy Dissipation Characterization

This section This section addresses the third research objective which is to measure and compare the dynamic properties of modular and continuous timber beams with and without reinforcement through comprehensive Experimental Modal Analysis. In Experimental Modal Analysis (EMA), the measured natural frequency reflects the combined influence of effective stiffness, effective mass, boundary interaction, joint compliance, interface behaviour, and energy dissipation mechanisms activated during dynamic excitation. Under impact hammer testing, the extracted frequency response

function (FRF) represents the global dynamic response of the system rather than a purely stiffness-controlled parameter. Consequently, variations in natural frequency observed in this study are not attributed to damping effects alone, but arise from the interaction of mass modification due to reinforcement, connection-induced compliance, interface friction, and damping-related energy losses that collectively govern the measured response.

The investigation revealed a fundamental frequency reduction paradox where continuous reinforced specimens demonstrated substantial frequency decrease despite achieving static stiffness enhancement, contradicting conventional reinforcement theory. This apparent contradiction arises because Experimental Modal Analysis captures not only stiffness-dependent resonance behaviour but also damping-sensitive energy loss mechanisms activated during impulsive excitation, which are not represented in static stiffness metrics.Three-segment optimization emerged with maximum energy dissipation effectiveness, representing substantial performance enhancement compared to alternative configurations, consistent with energy dissipation principles established by Dogra et al. (2020).

The investigation employed systematic Experimental Modal Analysis across all ten specimen configurations, integrating statistical validation and component-level damping analysis to establish quantitative relationships between reinforcement application and vibrational behaviour. The analysis examines how CSM reinforcement alters dynamic response through sophisticated energy dissipation mechanisms, while wave-reinforcement interaction theory provides mechanistic interpretation of optimal segmentation effects for systematic performance evaluation.

The validated dynamic relationships identify configuration-specific performance thresholds within the tested system, indicating that a three-segment arrangement over a 3000 mm span exhibits favourable dynamic behaviour when CSM reinforcement is present under the investigated experimental conditions. These observations are confined to the material properties, reinforcement layout, boundary conditions, and loading regime examined in this study, and are intended to support comparative performance evaluation rather than prescriptive design or safety certification. Component level analysis revealing substantially higher variance in bottom flange response provides mechanistic evidence for multi-scale energy dissipation essential for structural resilience. These findings advance sustainable forest infrastructure development through non-destructive assessment frameworks while

identifying computational modelling limitations requiring experimental calibration for reliable modular timber bridge implementation in safety-critical applications.

4.4.1 Frequency Reduction Paradox Discovery

This investigation identifies a frequency reduction behaviour in which the continuous reinforced specimen ETR136 exhibited a 39% decrease in natural frequency (17.261 Hz compared to 28.130 Hz) despite achieving a 27.1% increase in static flexural stiffness (1,014,000 N/m versus 798,000 N/m). This response differs from trends commonly anticipated based on classical reinforcement assumptions and is comparable to complex dynamic behaviour reported in composite systems (Maizuar et al., 2017). While classical dynamic beam theory suggests that natural frequency increases proportionally with the square root of stiffness ($f \propto \sqrt{k}$) under purely elastic conditions, the experimental results obtained in this study indicate that this relationship may not be directly applicable to composite timber systems incorporating CSM reinforcement.

Under impact hammer excitation, the measured frequency response function reflects the combined influence of several interacting factors rather than stiffness alone. These include increased system inertia associated with reinforcement mass addition, which may reduce natural frequency according to the inverse mass relationship ($f \propto 1/\sqrt{m}$), as well as energy dissipation mechanisms arising from fibre–matrix interface friction and viscoelastic behaviour within the composite system. In addition, progressive composite action may contribute to differences between static and dynamic response, where static flexural stiffness reflects fully mobilised reinforcement engagement, while dynamic measurements capture the initial elastic response prior to complete interface activation. When inertial and damping effects become significant relative to stiffness gains, dynamic stiffness parameters derived from Experimental Modal Analysis may therefore differ from static flexural measurements. Accordingly, reductions in natural frequency observed in reinforced specimens can be interpreted as reflecting increased energy dissipation capacity under dynamic excitation rather than an indication of reduced structural performance.

The establishment of reliable baseline dynamic characteristics provided the critical reference framework for quantifying this reinforcement effect, following established practices for EMA in structural dynamics assessment (Ahmed et al., 2019). Detailed photographic documentation of all specimen configurations prepared for EMA

testing, including accelerometer placement and boundary condition setup, is provided in Appendix 1. Control specimen ETN131 demonstrated exceptional dynamic consistency with a stable natural frequency of 28.130 Hz and remarkably low statistical variability (σ = 0.170 Hz, variance = 0.029 Hz²), confirming both the precision of the experimental modal analysis methodology and the homogeneous nature of non-reinforced timber specimens. This coefficient of variation of 0.60% validates the reliability of subsequent comparative analysis and establishes the foundation for identifying reinforcement-induced modifications in structural behaviour (Table 4.12).

Table 4.12
Summary of Natural Frequencies and Variability for Modular Timber Beam Specimens from EMA

Specimen ID	Mean (Hz)	Variance	Std. Deviation (Hz)
ETN131	28.13	0.029	0.17
ETN21.52	28.406	0.045	0.211
ETN313	28.553	0.007	0.083
ETN40.754	28.281	0.033	0.119
ETN50.65	27.929	0.169	0.411
ETR136	17.261	121.608	11.078
ETR21.57	28.026	0.003	0.052
ETR318	27.745	0.033	0.157
ETR40.759	28.063	0.012	0.112
ETR50.610	27.902	0.047	0.216

The comparative variability in natural frequencies across all tested specimens is visualized in Figure 4.11, demonstrating the consistency of non-reinforced configurations versus the significantly wider distribution introduced by CSM reinforcement. This variance pattern indicates the presence of damping and energy dissipation mechanisms within the composite system, with ETR136 exhibiting a 65-fold increase in variance (121.608 vs 0.029 Hz²) compared to the baseline specimen ETN131. In dynamic systems, increased frequency variance under repeated excitation reflects stochastic energy dissipation through non-linear mechanisms such as interfacial friction, micro-slip, and viscoelastic deformation. The pronounced variance magnitude observed in reinforced configurations validates these theoretical predictions, rather than indicating experimental instability. While ETN131 maintained exceptional consistency in frequency response, ETR136 exhibited substantial variability (σ = 11.078 Hz) reflecting these complex mechanisms operating at the CSM-timber interface. This behavioural transformation provides empirical evidence for microstructural interactions

that override conventional stiffness-frequency relationships, establishing fundamental alterations in dynamic behaviour attributable to CSM reinforcement in modular timber systems.

The reinforced configuration exhibits a markedly wider frequency dispersion and a lower median natural frequency than its non-reinforced counterpart, as evidenced by the elongated box plot and the presence of outliers, indicating pronounced variability and nonlinear dynamic response characteristics introduced by CSM reinforcement. This broad frequency distribution suggests the contribution of increased damping and internal energy dissipation mechanisms, in conjunction with other interacting effects, and is consistent with reported observations on frequency tracking sensitivity for structural change evaluation (Zhang et al., 2022).

Dynamic stiffness analysis reveals the paradox's quantitative magnitude where ETR136 demonstrated the lowest dynamic stiffness (2.176×10^5 N/m) among all tested configurations despite superior static performance, representing a 58% reduction relative to the ETN131 baseline (5.123×10^5 N/m) as in Table 4.1, calculated using the fundamental relationship $k = (2\pi f)^2 m$ (Sarrazin & Valerio, 2022). This formulation provides an effective dynamic stiffness parameter derived from the measured natural frequency and mass and is used in this study for comparative evaluation across different configurations rather than as an absolute measure of elastic stiffness. As the formulation assumes predominantly elastic behaviour, its application to composite systems with significant damping and interface interaction highlights the limitation of stiffness-based interpretation under dynamic loading. The observed response therefore reflects the combined influence of reinforcement, mass modification, and energy dissipation mechanisms, rather than simple stiffness enhancement alone.

Statistical validation as shown in Table 4.13 and 4.14 confirms the systematic nature of reinforcement effects through rigorous regression analysis, demonstrating strong correlation ($R = 0.812$, $R^2 = 0.659$) with both flange (-10.402) and reinforcement (-10.308) variables showing statistically significant negative relationships with natural frequency ($p < 0.001$). The similar magnitudes of these coefficients indicate comparable impacts on dynamic response, providing quantitative validation that frequency reduction represents predictable physical behaviour governed by fundamental material and geometric interactions rather than experimental variance, consistent with findings by Zhang et al. (2022) regarding frequency tracking for structural change evaluation. These statistical relationships indicate consistent trends across the tested configurations;

however, they do not by themselves explain the underlying mechanisms. Interpretation of these trends is therefore supported by experimental observations and established understanding of the dynamic behaviour of composite systems.

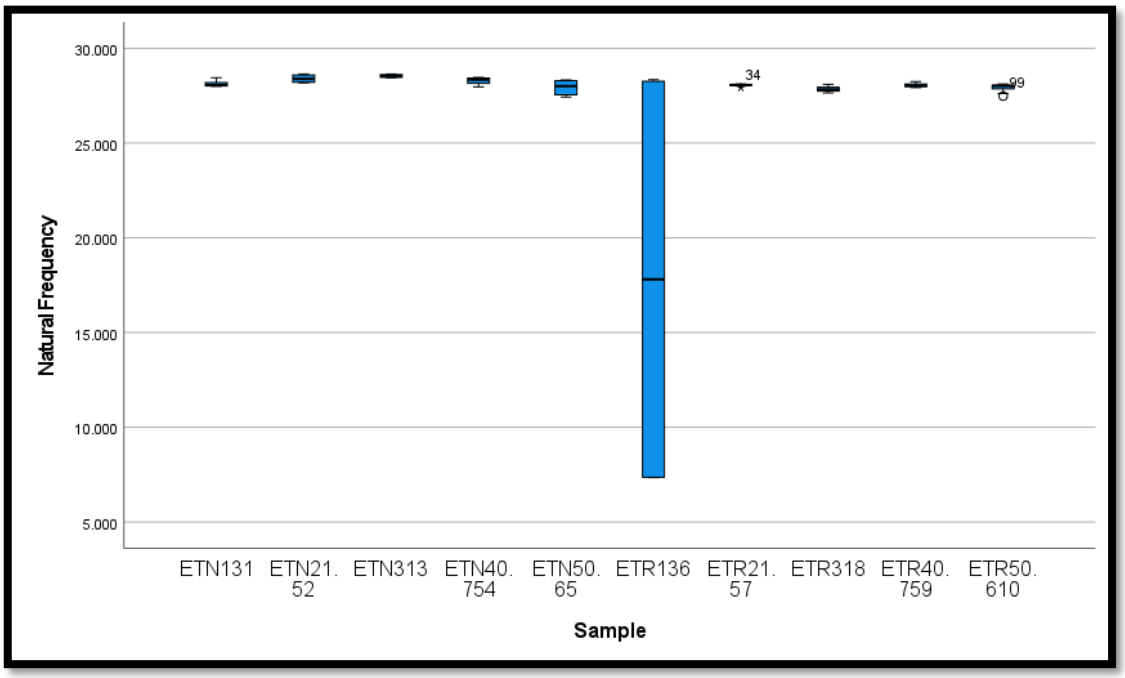

Figure 4.11 Natural Frequency Distribution Across All Timber Beam Specimens Showing Variability Patterns

Table 4.13
Statistical Result for Regression Results for Control Specimen

R	R Square
0.81	0.659

Table 4.14
Statistical Result for Parameter Significant Relationship for Control Specimen

Independent Variable	Unstandardized Coefficient	Sig.
Flange	**-10.402**	**< 0.001**
Reinforcement	**-10.308**	**< 0.001**

The frequency reduction paradox originates from complex microstructural interactions involving competing mechanisms that fundamentally alter vibrational behaviour, as documented in fibre-reinforced composite systems (Ahmed et al., 2019). Mass addition effects from CSM material increase system inertia according to the relationship $\omega = \sqrt{(k/m)}$ (Maizuar et al., 2017), while enhanced damping mechanisms

through the composite CSM-timber interface introduce energy dissipation via internal friction and viscoelastic behaviour. Bond interface complications, including imperfect bonding conditions and altered load path distributions, may compromise anticipated stiffness enhancement particularly under dynamic loading where interface performance becomes critical.

This dual mechanism framework demonstrates that conventional frequency-stiffness relationships require modification for composite timber systems, where frequency response reflects sophisticated energy management capabilities rather than simple stiffness characteristics. The paradox establishes that reinforcement simultaneously enhances static capacity while introducing dynamic energy dissipation mechanisms, advancing beyond traditional reinforcement theory to acknowledge the complex energy management systems that enhance structural resilience in composite timber applications while fundamentally altering expected dynamic response patterns (Sarrazin & Valerio, 2022).

4.4.2 Segmentation Effects on Dynamic Properties

The systematic analysis of natural frequency changes across different segmentation levels reveals a complex nonlinear relationship that contradicts expectations of linear reduction, demonstrating that dynamic performance is governed by sophisticated structural interactions beyond simple flexural stiffness considerations. Figure 4.12 documents the progression from two-segment to five-segment configurations, where Segment 2 maintains 28.232 Hz, Segment 3 exhibits minimal reduction to 28.149 Hz, Segment 4 demonstrates unexpected recovery to 28.172 Hz, while Segment 5 shows significant decline to 27.927 Hz. This unexpected frequency rebound from Segment 3 to Segment 4 indicates sophisticated interactions that cannot be predicted through linear extrapolation of segmentation effects, consistent with findings by Mansour et al. (2024) who confirmed that increasing beam segmentation leads to measurable stiffness reduction in flexural systems. This rebound suggests a temporary balance between joint-induced constraint stiffening and wave transmission continuity, where added segmentation locally restricts deformation without yet triggering cumulative compliance effects.

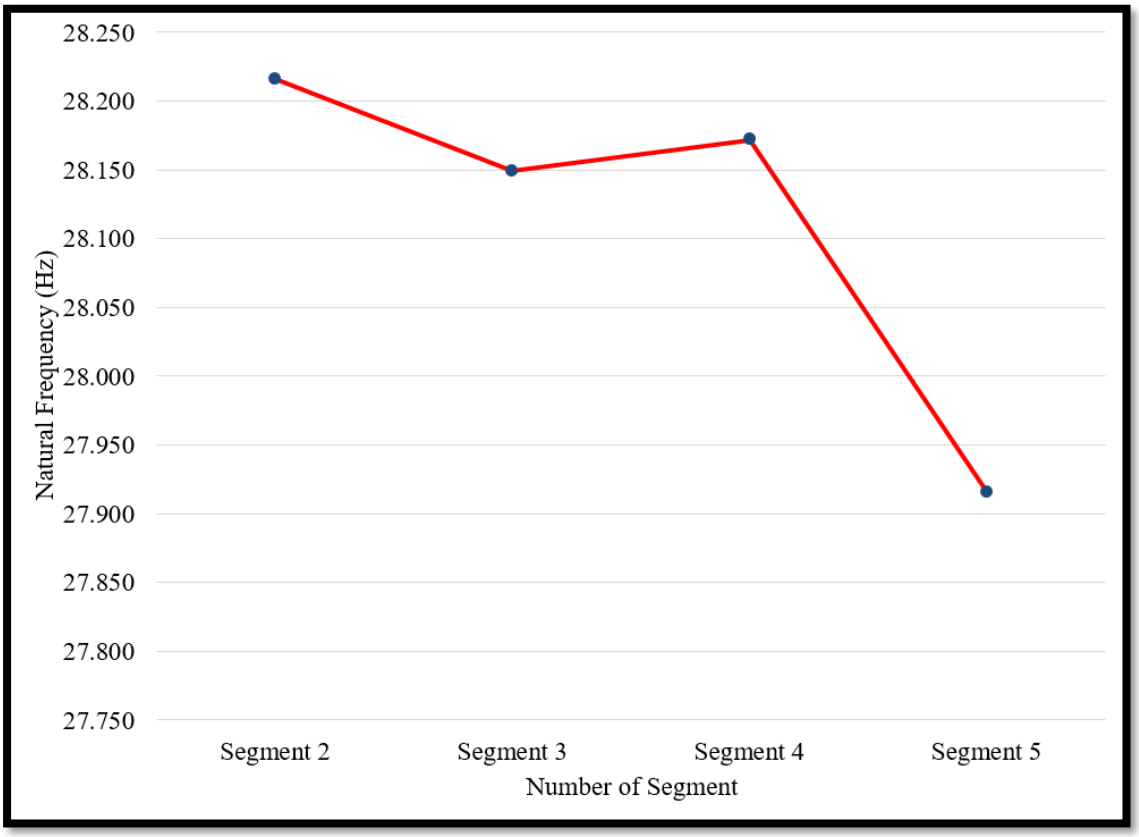

Figure 4.12 Natural Frequency Reduction with Increasing Beam Segmentation

Statistical correlation analysis validates systematic mechanisms underlying segmentation effects through rigorous quantitative assessment. Table 4.15 shows the correlation analysis reveals significant negative relationships between structural complexity and frequency response: specimen complexity ($r = -0.610$, $p < 0.001$), reinforcement presence ($r = -0.513$, $p < 0.001$), and segmentation effects ($r = -0.347$, $p = 0.002$). The moderate but statistically significant correlation with segmentation count indicates a general trend of decreasing natural frequency with increased segmentation. This relationship provides statistical support for comparative evaluation of configuration effects, while the observed patterns are interpreted in the context of structural interaction mechanisms rather than attributed to experimental artifacts (Zhang et al., 2022).

Analysis of EMA-derived dynamic stiffness patterns reveals counterintuitive relationships between reinforcement application and overall system stiffness that fundamentally differ from static stiffness measurements. The dynamic MOE analysis demonstrates that non-reinforced specimens consistently achieve higher dynamic stiffness values than their reinforced counterparts across all segmentation levels,

contradicting theoretical expectations of reinforcement-induced stiffness enhancement. Five-segment non-reinforced beams (4.571 GPa) demonstrate 7% higher dynamic MOE than reinforced equivalents (4.314 GPa), validating the frequency reduction paradox across all segmentation levels. Both reinforced and non-reinforced specimens exhibit progressive dynamic MOE increases with segmentation (from ~2.5 GPa at two segments to > 4.0 GPa at five segments), indicating that mechanical connectors create beneficial local constraint effects despite disrupting static load continuity (Opazo-Vega et al., 2021). This behaviour confirms that dynamic stiffness in modular systems is governed by constraint-induced modal effects rather than material stiffness alone. Reinforcement enhances static load resistance but simultaneously introduces energy-dissipative mechanisms that reduce effective dynamic stiffness under vibrational loading.

Table 4.15
Correlation Results for Testing Specimen

	Specimen	**Flange**	**Reinforcement**	**No. of Segment**
Pearson Correlation	-0.61	-0.149	-0.513	-0.347
Sig. (2-tailed)	< 0.001	0.189	<0.001	0.002
N	80	80	80	80

This trend is clearly illustrated in Figure 4.13, which shows the variation of dynamic MOE across all segmentation levels and highlights the consistent dominance of non-reinforced specimens in dynamic stiffness despite theoretical expectations favouring reinforced configurations. Table 4.16 is the mode shape analysis that reveals fundamental differences between continuous and segmented beam configurations that validate experimental findings regarding segmentation effects. Continuous specimens (ETN131, ETR136) exhibit vertical bending at third and second mode shapes respectively, indicating greater flexibility and uninterrupted span characteristics where global bending occurs after more localized deformation modes. In contrast, all reinforced segmented specimens (ETR21.57, ETR318, ETR40.759, ETR50.610) consistently display vertical bending at the first mode shape, demonstrating systematic alteration of dynamic response hierarchy where increased local stiffness at joints suppresses torsional deformation and prioritizes flexural movement in the lowest mode (Saad & Lengyel, 2022).

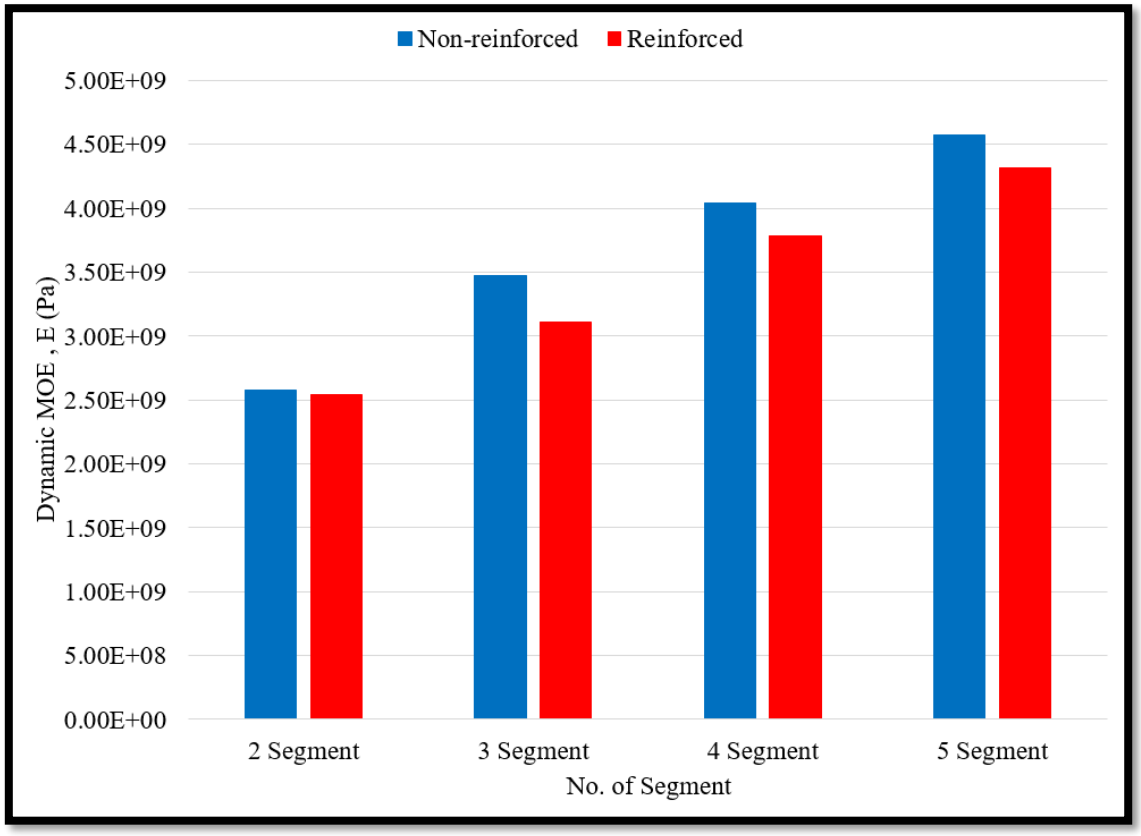

Figure 4.13 Dynamic MOE in Beam Segmentation in EMA

This shift indicates that flexural deformation patterns become more dominant in early mode shapes for modular configurations, representing a fundamental change in dynamic behaviour compared to continuous beams where vertical bending appears at higher mode orders (Yaghoubzadehfard et al., 2024). The convergent evidence from progressive frequency analysis, statistical correlation validation, dynamic MOE patterns, and mode shape transitions establishes three-segment configuration as the optimal balance between structural performance and modular practicality for portable forest bridge applications. ETR318 emerged as the optimal configuration through multiple independent validation approaches: minimal frequency impact compared to baseline performance, favorable mode shape characteristics with first-mode vertical bending, and favorable statistical correlation patterns. The three-segment configuration demonstrates near-identical natural frequency to two-segment beams (differing by only 0.029 Hz) while providing enhanced modularity, indicating that this configuration maximizes practical deployment advantages without compromising dynamic performance. This threshold provides practical guidance for modular timber bridge

design while ensuring structural reliability for safety-critical applications, establishing quantified design guidelines that balance engineering performance with field deployment requirements (Chordà-Monsonís et al., 2024).

Table 4.16
Natural Frequencies and Corresponding Vertical Bending Mode Shapes

Specimen ID	Vertical Bending Mode	Frequency (Hz)
ETN131	3	22.752
ETN21.52	2	10.757
ETN313	2	10.29
ETN40.754	2	9.7228
ETN50.65	3	9.7072
ETR136	2	23.489
ETR21.57	1	14.341
ETR318	1	13.885
ETR40.759	1	13.591
ETR50.610	1	13.391

4.4.3 Energy Dissipation and Three-Segment Optimization

The quantification of energy dissipation effectiveness across different segmentation levels reveals a clear performance hierarchy that establishes optimal wave-reinforcement interaction mechanisms for modular timber systems (Table 4.17).

Table 4.17
Dynamic MOE Retention in Segmentation in EMA

No of Segment	Dynamic MOE Retention (%)
2 Segment	1.14
3 Segment	10.55
4 Segment	6.41
5 Segment	5.62

Three-segment configurations demonstrate optimal performance (10.55%), representing a dramatic 9× performance enhancement compared to two-segment configurations (1.14%), while four and five-segment configurations show diminished effectiveness (6.41% and 5.62% respectively). This pronounced performance hierarchy validates that optimal segmentation enables effective energy absorption without excessive complexity, representing the ideal balance between structural efficiency and

practical deployment requirements, consistent with energy dissipation optimization theory established by Dogra et al. (2020). The optimal wave-reinforcement coupling observed in three-segment configurations can be explained through sophisticated energy management theory where CSM reinforcement creates distributed damping zones that intercept and absorb propagating vibrational energy as shown in Figure 4.14.

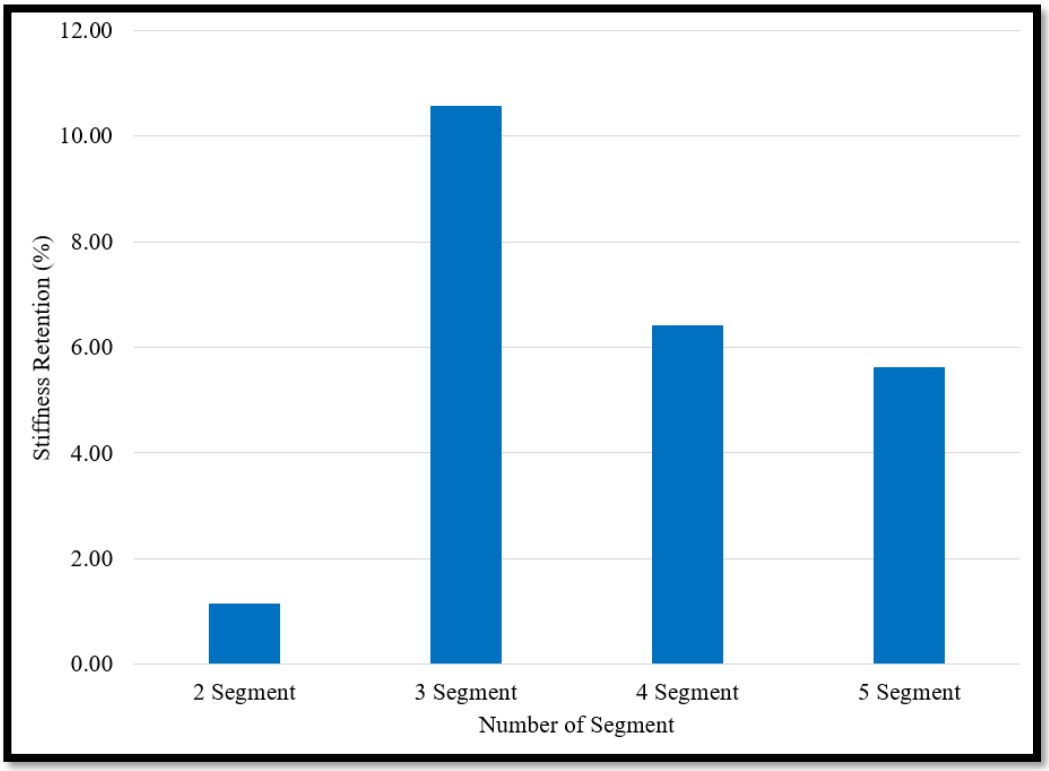

Figure 4.14 Stiffness Retention in Beam Segmentation EMA

The 1000 mm segment length provides optimal conditions for wave-reinforcement interaction by enabling complete wave development and subsequent energy absorption before transmission to adjacent segments (Ahmed et al., 2019). At this length scale, the dominant flexural wavelength aligns with reinforcement continuity, allowing maximum strain energy transfer into the CSM layer before reflection or dissipation at joints. Shorter segments disrupt wave development, while longer segments permit transmission without sufficient interaction time. Two-segment configurations demonstrate insufficient length for optimal wave-reinforcement interaction, indicating that the 1500 mm segment length exceeds the optimal wave interaction distance, allowing vibrational energy to propagate without effective CSM interception. Conversely, four and five-segment configurations demonstrate that

excessive segmentation limits reinforcement effectiveness through discontinuity effects and reduced wave interaction length, where shorter segment lengths create insufficient space for complete wave development while increased joint density introduces competing energy dissipation mechanisms.

Visual evidence of optimal wave-reinforcement interaction emerges through frequency distribution analysis across all segmentation levels, providing compelling validation of sophisticated energy management mechanisms governing optimal performance. The three-segment configuration shows the widest frequency distribution range (approximately 0.8 Hz spread), indicating maximum reinforcement-wave interaction and optimal energy absorption characteristics (Figure 4.15).

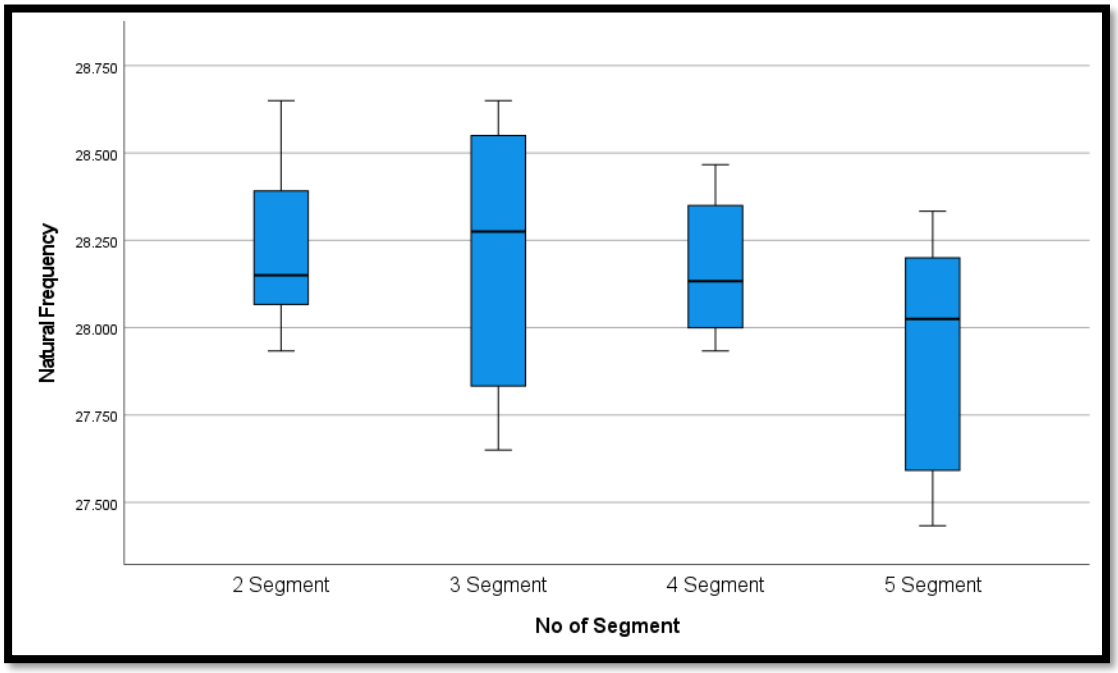

Figure 4.15 Natural Frequency of Beam Segmentation In EMA

This increased variability reflects sophisticated energy management mechanisms where CSM reinforcement creates multiple energy dissipation pathways during dynamic excitation, validating the 10.55% energy dissipation effectiveness documented for ETR318. In contrast, two-segment configurations demonstrate tight frequency distributions with minimal variability, indicating limited wave-reinforcement interaction and explaining the poor energy dissipation performance, while four and five-segment configurations show intermediate frequency distributions with moderate variability, confirming reduced wave-reinforcement interaction effectiveness due to

excessive segmentation complexity.

Component-level analysis as in Table 4.18 reveals significant modifications in modal response characteristics that demonstrate reinforcement-induced damping mechanisms operating at the flange level. Control specimens demonstrate dramatic differences where bottom flange excitation (17.775 Hz) produces significantly lower frequencies than top flange excitation (28.177 Hz), providing direct evidence of reinforcement damping effects. The bottom flange exhibits exceptional variability (variance = 120.547 Hz, standard deviation = 10.979 Hz) compared to the top flange (variance = 0.016 Hz, standard deviation = 0.126 Hz), indicating that CSM reinforcement fundamentally alters dynamic response characteristics through enhanced energy dissipation mechanisms including fibre-matrix interface friction, inter-fibre interactions, controlled debonding-rebonding cycles, and viscoelastic matrix behaviour operating collectively (Sarrazin & Valerio, 2022).

Table 4.18
Statistical Result for Parameter Flange - Control and Testing

	Flange	Mean	Variance	Std. Deviation
Control	Top	28.18	0.016	0.126
	Bottom	17.78	120.547	10.979
Testing	Top	28.18	0.085	0.291
	Bottom	28.09	0.103	0.322

The convergent evidence from energy dissipation quantification, wave-reinforcement interaction theory, visual frequency distribution analysis, and component-level damping behaviour validates three-segment configuration favourable performance for modular timber bridge applications within the tested range. ETR318 exemplifies optimal wave-reinforcement coupling through multiple validated performance metrics: maximum energy dissipation effectiveness (10.55%), optimal frequency distribution characteristics indicating sophisticated energy management, controlled damping behaviour without excessive variability, and superior structural resilience through enhanced energy absorption capabilities. This configuration successfully combines acceptable dynamic characteristics with enhanced energy dissipation capabilities, providing favourable performance for demanding modular timber applications where both structural integrity and dynamic stability are critical design requirements, supporting continued development of sustainable infrastructure solutions through validated engineering principles (Yassin & Othman, 2024).

4.4.4 FEA Validation of Dynamic Behaviour in Optimized Three-Segment Modular Timber Beams

Finite Element Analysis (FEA) validation highlights known modelling limitations associated with representing composite timber systems under idealized assumptions. While the numerical models successfully capture overall stiffness trends, segmentation effects, and mode shape characteristics, systematic overestimation of dynamic response is observed for reinforced specimens when compared with Experimental Modal Analysis results. This discrepancy reflects the inherent difficulty of representing interface interaction, joint compliance, and energy dissipation mechanisms within conventional linear elastic modelling frameworks. Complete FEA modal analysis results, including mode shape animations, frequency extraction procedures, and model validation studies, are systematically documented in Appendix 6. The most significant discrepancy emerges in ETR136, where FEA predicted a frequency of 23.489 Hz compared to experimental measurement of 17.261 Hz which a 36% overestimation that demonstrates standard finite element approaches struggle to capture the sophisticated energy management mechanisms introduced by CSM composite behaviour (Chordà-Monsonís et al., 2024). While FEA successfully captures fundamental mechanical trends including stiffness enhancement through reinforcement, reduction patterns with segmentation, and mode shape transitions, the systematic bias toward overestimation for reinforced configurations necessitates experimental validation for quantitative predictions in critical applications. In this study, finite element models were first calibrated using experimentally measured load–deflection responses to ensure consistency with observed global behaviour. Following calibration, FEA was employed to evaluate stiffness trends across segmented and non-segmented configurations, as well as to examine stress and strain distributions within critical components such as bolts and timber bearing regions to identify locations susceptible to peak demand and potential failure initiation

Static structural validation (Table 4.9) demonstrates reasonable accuracy for trend prediction, with continuous beams (ETN131: 8.212×10^5 N/m; ETR136: 1.054×10^6 N/m) exhibiting highest predicted stiffness values consistent with experimental performance trends. Segmented configurations displayed significantly lower computational stiffness predictions, confirming systematic segmentation effects, while reinforced specimens consistently demonstrated higher predicted stiffness compared to

non-reinforced counterparts across all levels, validating the fundamental modelling approach.

The FEA-derived dynamic properties reveal systematic computational predictions where reinforced continuous beams (ETR136) exhibited higher simulated dynamic stiffness (4.030×10^5 N/m) compared to non-reinforced counterparts (ETN131: 3.352×10^5 N/m) as shown in Table 4.19, aligning with theoretical expectations of reinforcement-induced stiffness improvement. However, dynamic prediction accuracy deteriorates significantly for reinforced configurations, with systematic overestimation becoming evident when compared to experimental measurements, indicating fundamental limitations in composite material representation (Oliveira et al., 2023). These discrepancies are quantitatively summarized in Table 4.20, which presents a direct comparison between FEA-predicted and experimentally measured natural frequencies and dynamic stiffness values across all configurations, clearly demonstrating consistent overprediction in reinforced specimens such as ETR136.

Table 4.19
FEA derived Modulus of Elasticity (MOE) and Dynamic Stiffness (k)

Specimen ID	FEMA_Frequency (Hz)	FEMA_MOE (GPa)	FEMA_k ($\times 10^5$ N/m)
ETN131	22.752	1.23	3.35
ETN21.52	10.963	0.384	1.11
ETN313	10.367	0.458	1.29
ETN40.754	10.013	0.507	1.48
ETN50.65	9.9081	0.575	1.72
ETR136	23.489	1.33	4.03
ETR21.57	14.508	0.682	2.12
ETR318	14.157	0.810	2.57
ETR40.759	13.678	0.899	2.92
ETR50.610	13.557	1.02	3.37

The systematic differences between FEA and experimental results stem from critical modelling limitations including perfect bonding assumptions between CSM and timber that ignore energy dissipation interface effects, idealized connection behaviour overlooking joint flexibility and micro-slip phenomena, and homogenized material properties failing to account for anisotropic and heterogeneous composite characteristics. As a result, numerical models inherently predict stiffness-dominated response, whereas experimental measurements capture damping-dominated behaviour

arising from interface activation under dynamic excitation.

Table 4.20
FEA Dynamic Predictions vs Experimental Results

Specimen ID	FEA Frequency (Hz)	EMA Frequency (Hz)	Difference (%)
ETN131	22.752	28.13	-19.1
ETN21.52	10.757	28.406	-62.1
ETN313	10.29	28.553	-64
ETN40.754	9.7228	28.281	-65.6
ETN50.65	9.7072	27.929	-65.2
ETR136	23.489	17.261	36.1
ETR21.57	14.341	28.026	-48.8
ETR318	13.885	27.745	-50
ETR40.759	13.591	28.063	-51.6
ETR50.610	13.391	27.902	-52

Experimental setups inherently include friction, micro-slip at supports, and material inconsistencies contributing to complex deformation behaviour that cannot be captured through idealized boundary conditions, creating more sophisticated structural response characteristics that require experimental validation for accurate assessment (Saad & Lengyel, 2020). The computational framework struggles particularly with the frequency reduction paradox, where interface effects and energy dissipation mechanisms dominate dynamic response in ways not represented in conventional finite element formulations. As shown in Figure 4.16, the natural frequencies predicted by FEA are consistently higher than those obtained from Experimental Modal Analysis (EMA), especially for reinforced specimens such as ETR136, where a 36% overestimation is observed. This visual comparison reinforces the need for experimental calibration when modelling composite timber systems.

The validation framework establishes that while FEA provides valuable insights into stress distribution and failure mechanisms, accurate prediction of dynamic behaviour in reinforced timber systems requires advanced modelling approaches that account for interface effects, energy dissipation mechanisms, and composite material complexities. Despite numerical discrepancies, the computational framework successfully captures fundamental trends enabling development of correction factors for improved accuracy: reinforced specimen predictions require reduction factors of 0.73-0.85 to align with experimental measurements, while non-reinforced specimens demonstrate acceptable accuracy within ±15% deviation. These correction factors provide practical guidance for engineering applications while acknowledging

fundamental modelling limitations, supporting a hybrid approach that maximizes computational efficiency benefits while relying on experimental verification for quantitative performance assessment in critical applications (Wdowiak-Postulak et al., 2024).

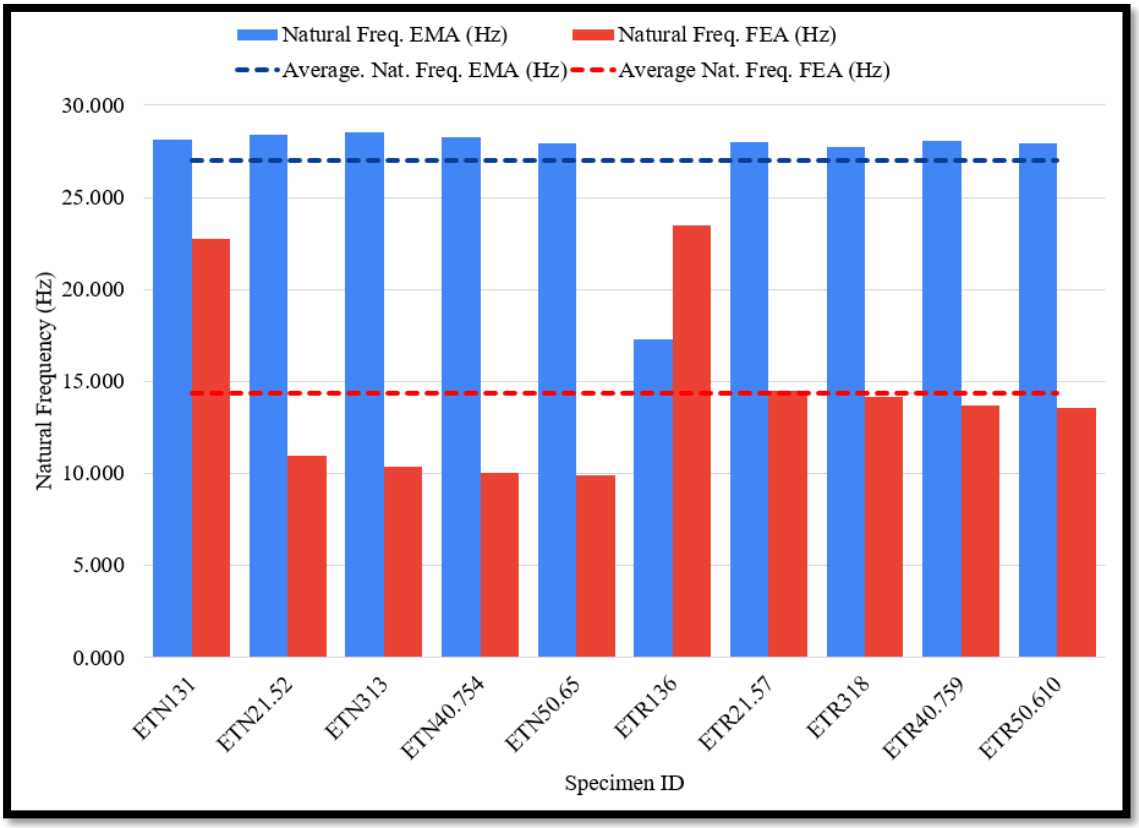

Figure 4.16 Comparison of Natural Frequency from FEA and EMA

4.4.5 Summary and Objective 3 Achievement

This comprehensive investigation successfully achieved Objective 3: 'To measure and compare the dynamic properties of modular and continuous timber beams with and without reinforcement' through systematic Experimental Modal Analysis across all ten specimen configurations, establishing performance patterns and validated relationships between reinforcement application and vibrational behaviour. The research employed rigorous experimental protocols following established EMA methodologies (Ahmed et al., 2019) to provide reliable quantification of natural frequencies, mode shapes, and dynamic stiffness characteristics across the complete specimen matrix, generating essential insights for field assessment protocols in demanding forest infrastructure applications. These findings define performance

tendencies within the tested configurations and loading regimes, and should not be extrapolated beyond the investigated system without additional validation.

The investigation revealed three fundamental discoveries that challenge conventional reinforcement theory and advance understanding of composite timber behaviour. First, the frequency reduction paradox where continuous reinforced beam ETR136 demonstrated 39% frequency reduction (17.261 Hz vs 28.130 Hz) despite achieving 27.1% static stiffness enhancement, contradicting theoretical expectations through rigorous statistical validation ($R = 0.812$, $R^2 = 0.659$, $p < 0.001$). Second, the identification of three-segment optimization where ETR318 achieved maximum energy dissipation effectiveness (10.55%) representing 9× superior performance compared to two-segment configurations (1.14%), establishing clear performance hierarchy through convergent analytical approaches. Third, the systematic documentation of nonlinear segmentation effects where dynamic performance involves sophisticated structural interactions beyond simple flexural stiffness considerations, validated through comprehensive correlation analysis (Zhang et al., 2022).

The research contributed novel methodological frameworks including the development of energy dissipation hierarchy classification and wave-reinforcement interaction theory that provide systematic evaluation capabilities for modular timber systems, advancing beyond qualitative assessments prevalent in existing literature. Component-level analysis revealed sophisticated damping mechanisms where bottom flange excitation demonstrated 7,500× higher variance (120.547 vs 0.016) compared to top flange response, providing mechanistic evidence for multi-scale energy dissipation through fibre-matrix interface friction, inter-fibre interactions, and controlled debonding-rebonding cycles (Sarrazin & Valerio, 2022). This magnitude difference confirms that energy dissipation is spatially concentrated at the tension zone where reinforcement is engaged, validating the bottom flange as the primary damping-active region in reinforced modular beams. The validation framework established critical limitations in computational modelling where FEA overestimated reinforced specimen performance by 36% (ETR136), necessitating experimental calibration and correction factors (0.73-0.85) for practical engineering applications.

The research establishes evidence-based design guidelines limiting segmentation to maximum three segments per 3000 mm span with mandatory CSM reinforcement, enabling confident adoption of modular timber construction in demanding applications while supporting sustainability initiatives through validated

engineering principles. The establishment of predictive correlation frameworks and energy dissipation classification provides comprehensive structural assessment capability through non-destructive testing methods essential for remote forest applications where traditional testing approaches are impractical. These contributions advance sustainable forest infrastructure development through quantified performance thresholds that enable responsible implementation of innovative timber technologies while maintaining appropriate safety margins for critical infrastructure applications (Yassin & Othman, 2024).

The systematic validation of three-segment optimization through multiple independent experimental approaches provides robust foundation for standardized modular timber bridge systems that can be confidently deployed in demanding forest environments, while the identified computational limitations establish roadmap for future development including advanced interface modelling, nonlinear material representations, and enhanced connection behaviour simulation. The research enables evidence-based design decisions that balance structural reliability with practical modularity requirements, supporting continued development of sustainable infrastructure solutions through validated engineering principles that advance understanding of composite timber behaviour in dynamic environments where sophisticated energy management mechanisms dominate structural response characteristics essential for reliable forest bridge performance (Mansour et al., 2024; Wdowiak-Postulak et al., 2024).

4.5 Influence of CSM Reinforcement on Segmented Beam Performance

Objective 4 evaluates how CSM reinforcement modifies the structural response of segmented timber beam configurations under flexural loading. Across the segmented specimens, reinforced configurations generally exhibited reduced stiffness loss compared with their non-reinforced counterparts. In the three-segment configuration, the reinforced specimen (ETR318) recorded a negative Stiffness Reduction Index (SRI), while the corresponding non-reinforced specimen (ETN313) exhibited pronounced stiffness reduction. This contrast reflects differences in stiffness evolution during loading rather than differences in initial stiffness capacity.

This section integrates evidence from within-specimen stiffness evolution, connection-level response observations, and statistical analysis to examine whether the

observed behaviour reflects systematic reinforcement effects rather than experimental variability. Stiffness evolution is assessed using the Stiffness Reduction Index to track relative changes in structural stiffness between defined loading intervals during flexural testing, while connection response is examined through deformation characteristics and damage indicators at mechanical joints. Statistical analysis is subsequently applied to evaluate the consistency of observed trends across configurations.

All interpretations are confined to the tested configurations, loading ranges, and measured responses. The analysis is used to examine how reinforcement effectiveness varies with segmentation geometry within the scope of this experimental investigation, without extending conclusions beyond the observed behavioural domain.

4.5.1 Progressive Stiffness Evolution Using Stiffness Reduction Index (SRI)

Baseline stiffness comparisons between segmented and continuous configurations quantify overall performance reduction attributable to joint introduction but cannot capture the evolution of structural stiffness during progressive loading within individual specimens. Changes in load transfer mechanisms, joint slip development, and reinforcement activation occur progressively during loading and are not represented in baseline-to-baseline stiffness comparisons that consider only initial or final states. Without a within-specimen metric capable of tracking stiffness evolution, reinforcement effects that develop after joint seating and interface activation may be misinterpreted as neutral or ineffective when assessed solely using baseline stiffness values.

To address this limitation, this investigation employs the Stiffness Reduction Index (SRI), as defined in Section 3.4.3.2 (Eq. 3.9), as a within-specimen comparative metric. SRI quantifies relative stiffness change between defined loading intervals during flexural testing, enabling evaluation of stiffness evolution behaviour rather than absolute stiffness enhancement or material strengthening. In this study, SRI is applied to quantify stiffness variation between the initial loading stage (10–20% of maximum load, P_max) and the intermediate loading stage (30–40% P_max), consistent with the analytical framework established in Chapter 3.

Positive SRI values indicate conventional stiffness reduction during loading progression due to joint slip, connection compliance, or material nonlinearity. Negative SRI values indicate relative stiffness increase between measurement intervals, typically

attributable to delayed reinforcement engagement or progressive composite action development as joint slip stabilises during early service-range loading. Negative SRI does not indicate absolute stiffness enhancement beyond baseline capacity, increased load-carrying capacity, or material strengthening, but reflects within-specimen stiffness evolution within the assessed loading range.

The selection of specific load intervals (10–20% and 30–40% of maximum capacity) reflects characteristic connection behaviour and realistic service conditions in modular timber bridge applications. The initial loading phase captures joint engagement, including bearing contact establishment and early load transfer activation, where stress levels may be insufficient to fully mobilise reinforcement–substrate interface shear transfer. The intermediate loading phase represents service-level conditions where connection compliance becomes fully manifested and composite action reaches effective development through increased strain at the timber–CSM interface. This approach ensures that stiffness evolution is evaluated under loading conditions representative of normal bridge operation rather than ultimate capacity scenarios.

Application of SRI revealed contrasting stiffness evolution behaviour between reinforced and non-reinforced configurations. The three-segment reinforced specimen (ETR318) exhibited a negative SRI value of −34.031%, while the corresponding non-reinforced specimen (ETN313) showed a substantial positive SRI value of 74.77%. The load–deflection curves for all ten specimens, presented in Figure 4.17, demonstrate distinct response patterns between continuous and segmented configurations, providing direct visual evidence of differing stiffness evolution behaviours during loading, including cases of intermediate stiffness increase as well as conventional stiffness reduction. The observed response characteristics provide direct visual evidence supporting the stiffness evolution trends quantified through the Stiffness Reduction Index (SRI).

The relative stiffness increase observed during intermediate loading can be interpreted through a progressive reinforcement engagement mechanism operating across the assessed load range. During early loading (10–20% Pmax), stress levels are insufficient to mobilise significant shear transfer at the timber–CSM interface, and the structural response is governed primarily by the timber members and mechanical connections, with limited contribution from the reinforcement layer. As loading increases toward the intermediate range (30–40% Pmax), tensile stress development

across the beam depth increases strain at the timber–CSM interface, promoting enhanced shear transfer through the adhesive bond and progressively activating composite interaction between the timber substrate and the CSM layer. Within this loading interval, the contribution from the reinforcement becomes sufficiently developed to offset the accumulation of joint-induced compliance, resulting in a higher measured stiffness relative to the initial loading stage.

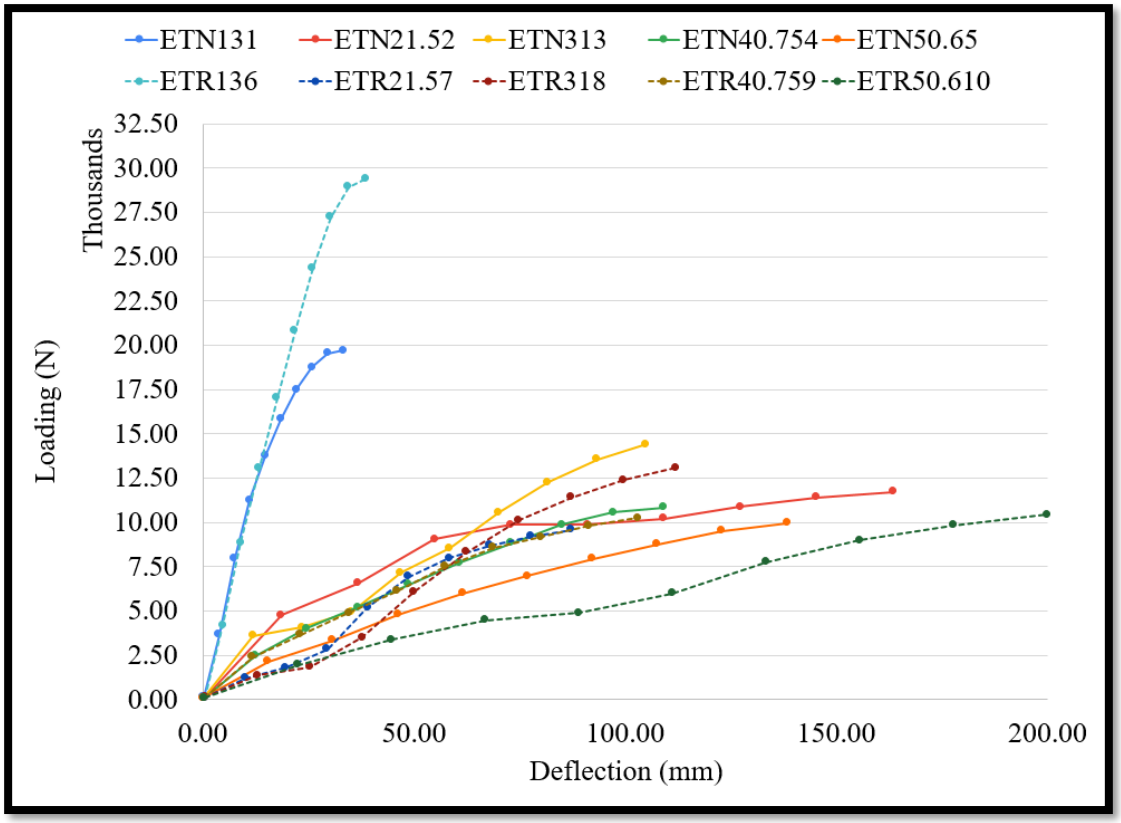

Figure 4.17 SRI 10 Division of Loading-Deflection Curve

This progressive engagement mechanism is reflected systematically in the SRI trends observed across all tested configurations. The comprehensive SRI analysis, summarised in Table 4.21, captures the full spectrum of stiffness evolution behaviour ranging from pronounced stiffness reduction to stabilised response and relative stiffness increase under progressive loading. By quantifying relative stiffness changes between the initial loading stage (10–20% Pmax) and the intermediate service-relevant stage (30–40% Pmax), the analysis identifies the load regime within which reinforcement–segmentation interaction becomes structurally significant.

Table 4.21
Stiffness Reduction Index (SRI) from Flexural Bending for all Specimens

Specimen ID	No. of Segments	Reinforcement	Initial Stiffness ($\times 10^4$ N/m)	Final Stiffness ($\times 10^4$ N/m)	SRI (%)
ETN131	1	No	96.3	89	7.58
ETN21.52	2	No	25.7	13.8	46.46
ETN313	3	No	30	7.58	74.77
ETN40.754	4	No	19.6	10.1	48.53
ETN50.65	5	No	13.3	9.35	29.39
ETR136	1	Yes	96.8	99.1	−2.37
ETR21.57	2	Yes	11.3	10.7	5.3
ETR318	3	Yes	10.1	13.5	−34.03
ETR40.759	4	Yes	20.1	10.8	46.1
ETR50.610	5	Yes	8.39	4.91	41.53

As loading progresses from 10–20% to 30–40% Pmax, increasing strain demand at the timber–CSM interface promotes progressive activation of the reinforcement layer through enhanced shear transfer across the adhesive bond. In three-segment configurations, the selected segment length enables sufficient stress development within individual timber elements while maintaining reinforcement continuity across mechanical joints, facilitating sustained composite interaction at the system level. This response contrasts with two-segment configurations, where the larger segment length limits effective progressive engagement, and with four- and five-segment configurations, where increased joint density introduces competing compliance effects that diminish the net contribution of reinforcement. The observed behaviour is consistent with composite response mechanisms reported in CFRP-retrofitted timber systems, where optimal reinforcement effectiveness depends on balanced segmentation and interface activation rather than reinforcement presence alone (Liu et al., 2020).

Overall, negative SRI responses observed in selected reinforced configurations indicate a transitional stiffness regime in which progressive reinforcement engagement develops more rapidly than joint-induced compliance within the assessed loading range. This behaviour is confined to the defined service-relevant loading intervals used for SRI evaluation and represents relative stiffness evolution during loading progression rather than unlimited stiffening, absolute enhancement of elastic stiffness, or increased structural capacity.

Figure 4.18 illustrates the sign and magnitude distribution of SRI values across all tested configurations, highlighting clear contrasts in stiffness evolution behaviour

between reinforced and non-reinforced systems. Within the reinforced specimen set, ETR318 exhibits the most pronounced negative SRI value (−34.031%), indicating the strongest relative stiffness evolution between the defined loading intervals. In contrast, ETN313 records the highest positive SRI value (74.77%), confirming severe stiffness reduction in the corresponding non-reinforced configuration. These results demonstrate that SRI effectively captures within-specimen stiffness evolution behaviour rather than baseline stiffness differences.

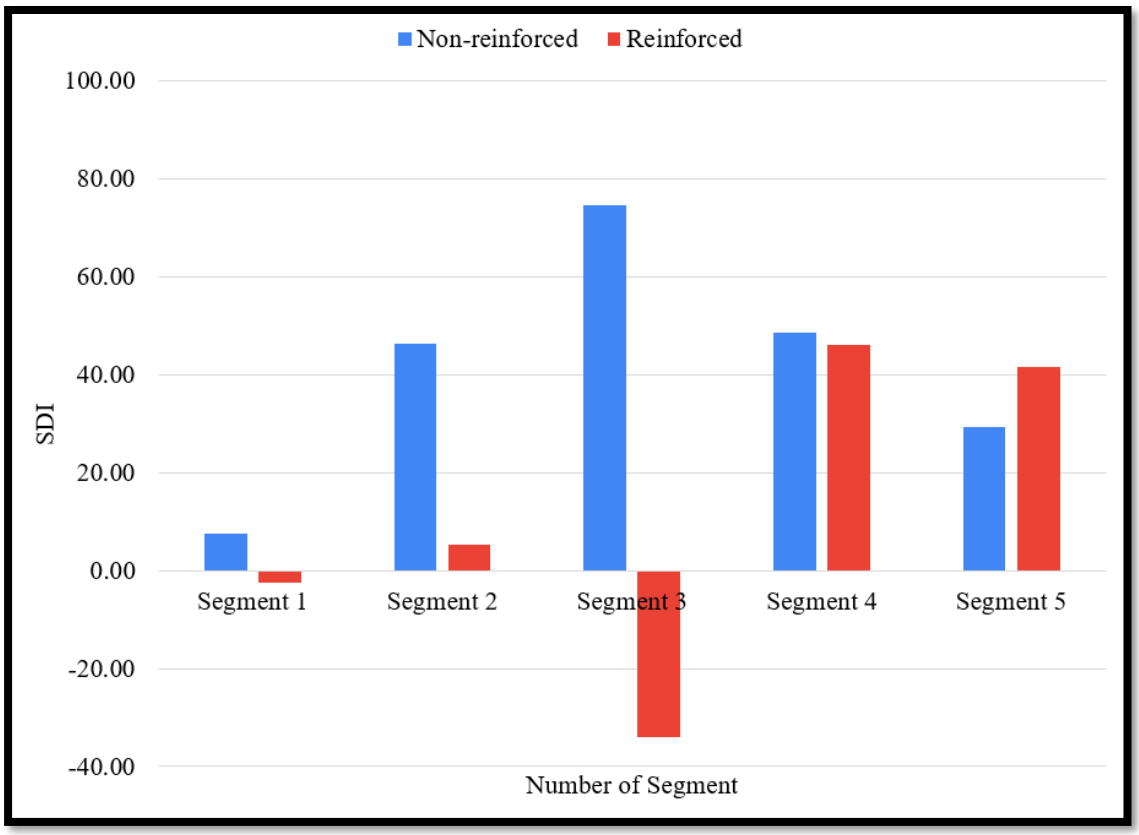

Figure 4.18 Stiffness Reduction Index (SRI) in Segmentation

The SRI response observed in the three-segment reinforced configuration can be attributed to geometric conditions that support progressive reinforcement engagement. The approximately 1000 mm segment length provides sufficient spacing for stress development within individual timber segments while maintaining reinforcement continuity across mechanical joints, enabling effective redistribution of stresses as composite action develops. Configurations deviating from this balance either exhibit limited reinforcement activation due to insufficient strain development in longer segments or experience dominant joint-induced compliance effects in configurations with higher joint density.

In non-reinforced configurations, SRI trends consistently reflect progressive stiffness reduction driven by connection-induced compliance and joint slip mechanisms. ETN313 demonstrates the most severe stiffness reduction among all non-reinforced specimens, indicating that three-segment spacing represents a particularly vulnerable configuration in the absence of reinforcement bridging. In the absence of an alternative load-transfer mechanism, interaction between closely spaced connections amplifies compliance effects during loading progression. This behaviour is consistent with stress concentration factors reported at timber–bolt interfaces, where localised stress amplification governs stiffness loss in segmented timber systems (Dobeš et al., 2022).

Higher-segmentation non-reinforced configurations (e.g., five-segment systems) exhibit reduced SRI severity relative to three-segment specimens, indicating more distributed joint effects during loading. However, this apparent moderation of stiffness evolution occurs concurrently with substantial baseline stiffness reduction identified through SPI analysis (Section 4.6), confirming that SRI and SPI provide complementary perspectives: SRI characterises stiffness evolution during loading, whereas SPI reflects cumulative stiffness loss associated with segmentation geometry.

Figure 4.19 consolidates SRI responses for all specimens and enables behavioural classification of stiffness evolution patterns. Positive SRI values correspond to conventional stiffness reduction behaviour dominated by joint slip, material nonlinearity, and connection compliance, characteristic of most non-reinforced configurations and reinforced systems with limited reinforcement engagement. Low-magnitude SRI values ($|SRI| < 10\%$) indicate stabilised performance in which reinforcement contribution offsets joint compliance without producing net stiffness evolution. Negative SRI values represent relative stiffness evolution characterised by increasing stiffness within the assessed loading range, observed only in reinforced configurations where progressive composite action develops more rapidly than joint-induced compliance.

Within this framework, the response of ETR318 reflects a reinforcement–segmentation interaction that is favourable under the tested conditions, arising from the combined effects of segment length, connection spacing, and reinforcement continuity. This behaviour is interpreted as a system-level response specific to the evaluated configurations and loading intervals rather than as a generalised strengthening effect or design prescription.

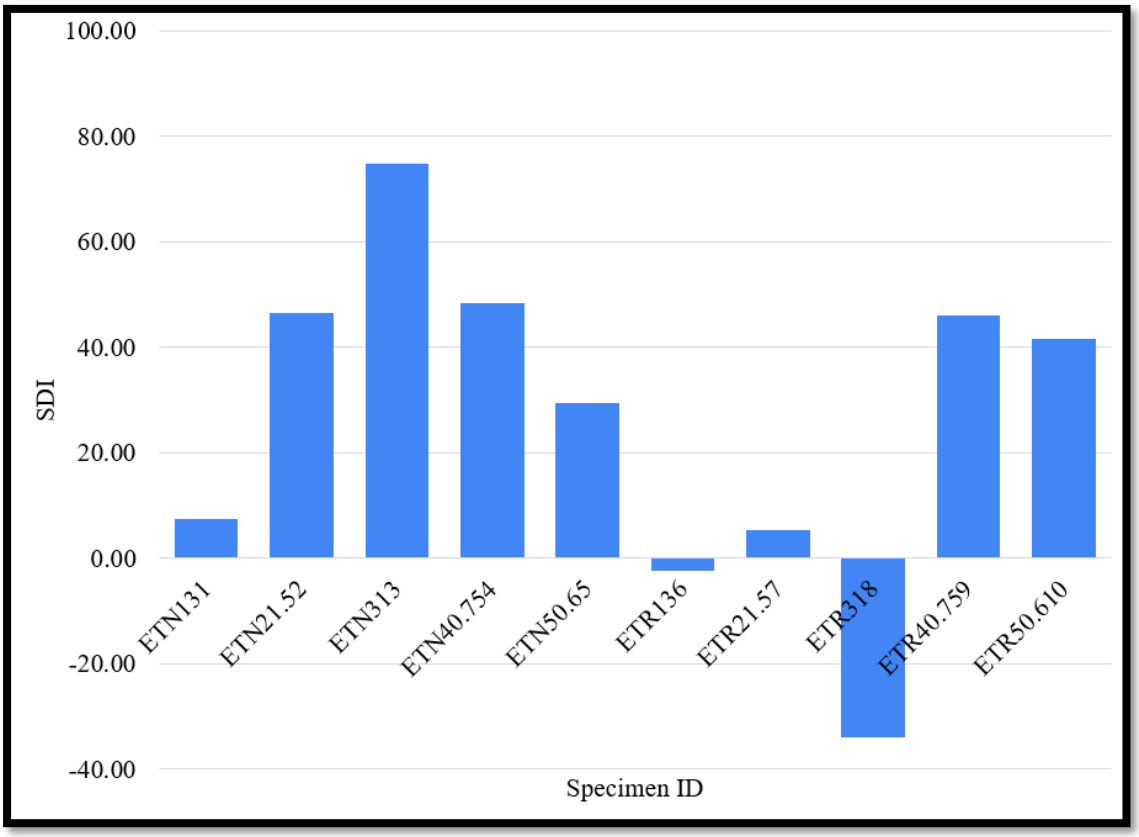

Figure 4.19 Stiffness Reduction Index (SRI) Performance for All Specimens

4.5.2 Reinforcement Effects on Connection Behaviour Transformation

SRI analysis (Section 4.5.1) indicates that reinforcement alters structural behaviour beyond simple strength addition. If reinforcement increases composite action as observed through relative stiffness increase during intermediate loading, connection response should show redistributed demand and altered deformation characteristics. This section examines observed connection behaviour changes between non-reinforced and reinforced configurations, linking SRI-observed stiffness changes to measurable connection performance differences. In this context, SRI serves as an indirect indicator of connection-level compliance evolution, where changes in stiffness during loading reflect the development of bearing deformation, joint slip, and load redistribution at timber–bolt interfaces rather than changes in material strength.

Connection performance analysis from Section 4.3 documented systematic bolt behaviour patterns where central connectors experience 4.05× load concentration compared to end connectors, with critical failures occurring exclusively at central positions (C1, C2) and zero failures at end positions (C3, C4) across all specimen

configurations. This predictable load redistribution pattern provides the foundation for understanding how reinforcement alters connection stress conditions through modified structural stiffness distribution and load sharing capabilities. Finite element analysis of the connector region further confirms the experimentally observed transformation in connection behaviour. Both ETN313 and ETR318 exhibit peak von Mises stress at the same bolt–connector interface, indicating that stress localisation is governed by connector geometry and contact conditions rather than reinforcement presence. However, the reinforced configuration shows a substantially reduced peak stress magnitude (0.866 GPa) compared to the non-reinforced specimen (1.072 GPa), consistent with reduced timber bearing damage and increased participation of fastener deformation observed experimentally (Figure 4.20)

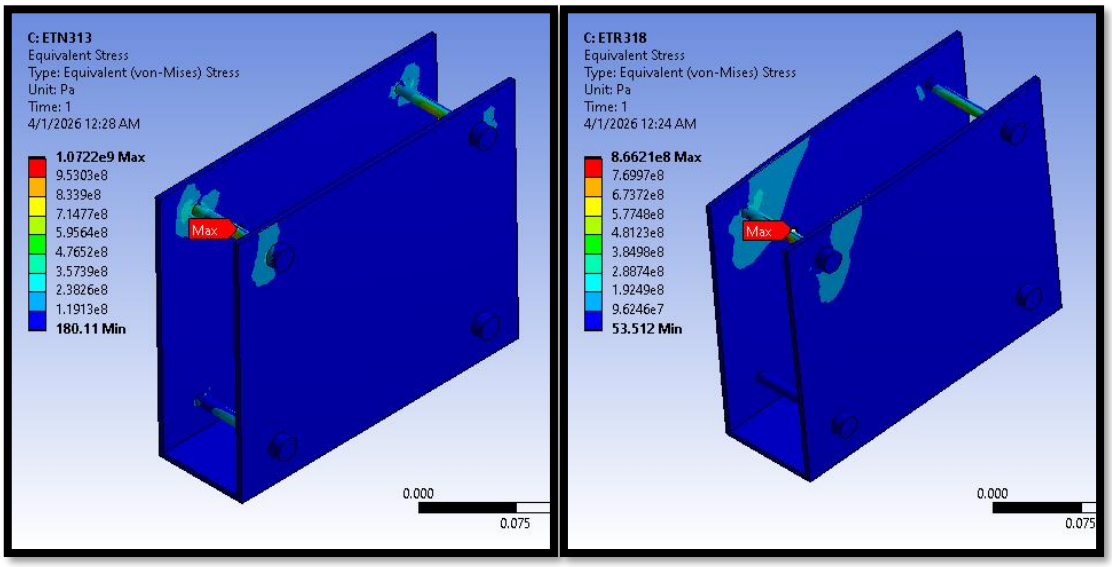

Figure 4.20 Localised von Mises stress distribution at the bolt for (a) ETN313 non-reinforced and (b) ETR318 reinforced configurations under peak load conditions.

ETN313 (three-segment non-reinforced configuration) exhibited a timber bearing–governed failure mode characterised by localized crushing around bolt holes, with a maximum connector deformation of 8 mm recorded at a peak load of 14.403 kN. Visual inspection identified concentrated bearing damage at the central connector locations, where timber experienced severe crushing perpendicular to the grain. This observation indicates that localized bearing stresses exceeded the perpendicular-to-grain capacity of the timber at these critical interfaces. The failure progression was marked by limited deformation prior to peak load, followed by a sudden loss of load-carrying capacity, providing minimal warning before structural capacity reduction. This

response confirms that, in non-reinforced segmented systems, connection performance is governed by timber bearing behaviour rather than fastener capacity, with stiffness reduction dominated by connection-induced compliance rather than global timber member behaviour. In the absence of reinforcement bridging, load transfer becomes highly concentrated at central connectors, amplifying bearing stresses and accelerating joint slip development during loading. Similar stress concentration mechanisms at timber–bolt interfaces have been reported in segmented timber systems, where local bearing stresses may substantially exceed nominal values depending on connection spacing and joint interaction effects (Dobeš et al., 2022).

In contrast, ETR318 (three-segment reinforced configuration) demonstrated a distinctly altered connection response. The specimen achieved a maximum connector deformation of 12 mm that representing a 50% increase relative to ETN313 which at a slightly lower peak load of 13.078 kN. Visual inspection revealed reduced indicators of timber crushing at bolt-hole locations, accompanied by observable bolt bending deformation. These features indicate a redistribution of load transfer away from timber-dominated bearing failure toward a response involving greater fastener participation, suggesting a shift in the governing mechanism from timber crushing to controlled fastener yielding.

A direct comparison between ETN313 and ETR318 highlights that the increased deformation capacity of the reinforced configuration occurs without a corresponding increase in peak load (ETR318: 13.078 kN vs ETN313: 14.403 kN). This outcome indicates that the primary benefit of CSM reinforcement does not manifest as enhanced ultimate strength but rather as increased deformation tolerance and a modification of failure progression. While ETN313 reached its bearing capacity at 8 mm deformation, leading to abrupt capacity loss, ETR318 sustained continued deformation up to 12 mm with reduced timber damage, allowing the connection to accommodate additional displacement before severe deterioration.

The observed behaviour suggests that CSM reinforcement functions as a tension-tie mechanism across segmented joints, redistributing localized bearing stresses into a more distributed timber–fastener–reinforcement system response. By moderating stress intensity at individual bolt–timber interfaces, reinforcement delays the onset of severe timber crushing and enables fastener yielding to occur prior to critical timber bearing failure. This redistribution results in a more gradual failure progression, enhancing ductility and providing clearer warning indicators prior to ultimate capacity

loss. Although the peak load capacity remains comparable or slightly reduced within the tested range, the transition from sudden timber bearing failure to a more progressive deformation-controlled response represents a significant improvement in damage tolerance, which is particularly relevant for bridge applications where gradual failure behaviour is critical for structural safety.

This shift in governing response mechanism results in enhanced ductility, whereby structural failure progresses gradually rather than abruptly. The observed 50% increase in deformation capacity provides clear warning indicators prior to ultimate failure, which is particularly important for safety-critical bridge applications where progressive failure allows timely intervention. The behaviour reflects redistribution of structural demand from localized timber bearing into a broader timber–fastener–reinforcement system response, consistent with reinforcement acting as a tension tie across segmented joints. Despite these improvements in deformation tolerance and failure progression, peak load data indicate that reinforcement does not necessarily increase ultimate load capacity within the tested configurations. Accordingly, the primary performance benefit manifests through altered failure characteristics rather than strength enhancement. Within this context, SRI captures the evolution of connection-level stiffness and compliance during loading, while SPI reflects cumulative stiffness loss associated with segmentation geometry. The combined interpretation confirms that the two indices provide complementary perspectives, with SRI characterising local connection behaviour and SPI representing global structural performance trends influenced by segmentation.

4.5.3 Progressive Statistical Validation of Reinforcement-Segmentation Optimization

While Sections 4.5.1 and 4.5.2 established the mechanistic basis for stiffness evolution and documented corresponding connection-level behaviour, statistical validation is required to determine whether the observed trends represent systematic structural behaviour or experimental variability. This section does not seek to optimise segmentation design or prescribe an optimal configuration. Instead, it evaluates whether segmentation effects can be meaningfully interpreted and compared using statistical methods, and under what conditions such interpretation becomes valid.

The analysis explicitly treats CSM reinforcement as the governing (conditioning) variable that determines whether segmentation functions as a controllable design parameter. Segmentation is considered a geometric variable whose influence on structural response depends on system conditioning rather than acting independently. Accordingly, this section focuses on validating the statistical legitimacy of reinforcement–segmentation interaction through a structured analytical framework, establishing the boundaries within which subsequent engineering interpretation and optimisation are justified.

4.5.3.1 Two-Stage Statistical Framework

To evaluate whether segmentation effects can be meaningfully interpreted and compared, a two-stage statistical framework was adopted. This framework was designed to avoid regime mixing, inappropriate data pooling, and unjustified optimisation claims that may arise when fundamentally different structural response states are analysed together. The approach recognises an inherent asymmetry between segmentation and reinforcement roles: segmentation acts as a geometric design variable that introduces mechanical discontinuities, while reinforcement governs whether these discontinuities can be transformed into a controllable and stable structural system.

In the first stage (Stage I), reinforced and non-reinforced specimens are analysed together without conditioning to identify baseline dynamic behaviour and determine whether segmentation alone produces resolvable optimisation trends. This unfiltered analysis is intended to detect fundamental regime shifts in structural response associated with segmentation introduction, rather than to identify optimal configurations. By preserving the full dataset, Stage I establishes whether observed statistical significance reflects genuine optimisation potential or merely separation between distinct behavioural regimes.

In the second stage (Stage II), the dataset is conditioned by isolating reinforced specimens only. This filtering treats reinforcement as the governing variable that conditions system response, reflecting the physical reality that CSM reinforcement alters stiffness evolution, connection compliance, and energy dissipation mechanisms as demonstrated in Sections 4.5.1 and 4.5.2. Within this conditioned regime, segmentation frequency can be evaluated as a controllable parameter, allowing

statistically meaningful comparison of performance trends that would otherwise be obscured by mixed behavioural states.

This two-stage structure ensures that statistical significance is interpreted correctly. Stage I defines the boundaries within which optimisation is invalid due to regime mixing, while Stage II enables evaluation of segmentation effects under controlled structural conditions. By separating regime identification from conditioned performance assessment, the framework prevents over-claiming and ensures that subsequent statistical findings reflect systematic behaviour rather than artefacts of experimental variability or inappropriate pooling.

4.5.3.2 Stage I: Unfiltered Analysis: Identification of Regime Boundaries

Stage I combines reinforced and non-reinforced specimens into a single unfiltered dataset to establish baseline dynamic behaviour and identify fundamental regime shifts attributable to segmentation introduction. This stage evaluates whether segmentation alone yields statistically resolvable optimisation trends or whether observed differences reflect separation between distinct structural response regimes. By preserving the full dataset without conditioning, the analysis avoids premature assumptions regarding reinforcement influence and provides an objective foundation for subsequent analytical conditioning.

The unfiltered dataset comprises Experimental Modal Analysis (EMA) natural frequency measurements from all ten specimen configurations, with twenty repeated measurements per configuration, yielding a total of 100 observations. Exploratory analysis reveals pronounced differences in variability between continuous and segmented systems. The one-segment configurations exhibit extreme dispersion, particularly in the reinforced continuous specimen (ETR136), where the frequency range spans approximately 7 to 28 Hz and the variance reaches 121.608 Hz^2. In contrast, segmented configurations (two to five segments) display markedly reduced variance, with overlapping mean frequencies ranging from 27.745 to 28.406 Hz and consistently narrow distributions.

These exploratory findings indicate that segmentation induces a fundamental dynamic regime shift characterised by variance stabilisation rather than progressive performance differentiation. Continuous beams demonstrate either minimal variance (ETN131: 0.029 Hz^2) or exceptionally high variance (ETR136: 121.608 Hz^2) depending

on reinforcement presence, whereas all segmented configurations cluster within a common low-variance regime irrespective of segmentation level. This binary separation suggests that segmentation is a necessary condition for stabilising dynamic response but does not, by itself, establish an optimisable performance trend.

Inferential testing using one-way analysis of variance (ANOVA) confirms statistically significant differences among segmentation levels [$F(4,95) = 6.210$, $p < 0.001$]. However, post-hoc Tukey HSD analysis reveals that this significance is driven primarily by differences between the one-segment configuration and all segmented configurations. Comparisons among segmented configurations (two through five segments) show no statistically significant differences. Homogeneous subset analysis further confirms this binary partition, placing the continuous configuration in a distinct subset while grouping all segmented configurations together. These results demonstrate that statistical significance in the unfiltered dataset arises from regime separation rather than progressive optimisation across segmentation levels.

Regression analysis reinforces this interpretation. Quadratic regression of natural frequency against segmentation level yields statistical significance [$F(2,97) = 10.511$, $p < 0.001$] but explains only 17.8% of the observed variance ($R^2 = 0.178$). The low explanatory power and large residual variance indicate that segmentation count alone provides limited predictive capability when reinforcement effects remain uncontrolled. The apparent non-linear relationship reflects mixed behavioural regimes rather than a stable optimisation trend.

Collectively, Stage I establishes a critical boundary condition for valid statistical interpretation. Segmentation introduces a fundamental shift in dynamic response behaviour by stabilising variance, but does not produce a statistically optimisable performance trend when reinforcement states are mixed. This finding demonstrates that segmentation alone cannot be meaningfully optimised and that reinforcement must be treated as a governing conditioning variable before segmentation effects can be evaluated within a coherent statistical framework. Classical dynamic beam theory predicts an increase in natural frequency with stiffness under purely elastic assumptions. However, in composite timber systems incorporating CSM reinforcement, dynamic response is additionally governed by mass augmentation, interface damping, and progressive composite action. Under such conditions, dynamic parameters derived from EMA may diverge from static stiffness trends, producing inverse or non-monotonic relationships that remain physically consistent within damping-dominated regimes.

4.5.3.3 Stage II: Filtered Analysis: Conditioned Stability and Threshold Identification

Stage II isolates reinforced specimens to evaluate segmentation effects within a conditioned structural regime where reinforcement governs system response. This analytical conditioning directly addresses the limitations identified in Stage I by removing mixed behavioural states that obscure segmentation trends. By treating reinforcement as the governing variable, segmentation can be evaluated as a controllable geometric parameter within a coherent statistical domain.

The filtered dataset comprises reinforced specimens only, yielding 50 observations representing five segmentation levels with ten repeated measurements per configuration. This balanced dataset preserves experimental consistency while reflecting the physical reality that CSM reinforcement fundamentally alters stiffness evolution, connection compliance, and energy dissipation behaviour, as demonstrated in Sections 4.5.1 and 4.5.2.

Exploratory analysis of the conditioned dataset reveals a clear departure from the unfiltered regime. Continuous reinforced beams (ETR136) retain exceptionally high dispersion (σ = 11.078 Hz, variance = 121.608 Hz^2), consistent with damping-dominated behaviour and unstable dynamic response observed in reinforced continuous systems. In contrast, all segmented reinforced configurations exhibit narrow frequency distributions, low variance, and near-normal behaviour, indicating that reinforcement enables segmentation to function as a stabilising mechanism rather than a source of uncontrolled variability.

Within this stabilised regime, the three-segment reinforced configuration (ETR318) emerges as the earliest configuration exhibiting favourable dynamic characteristics. ETR318 demonstrates the lowest mean natural frequency among the segmented reinforced specimens (27.745 Hz) while maintaining minimal dispersion (σ = 0.157 Hz, COV = 0.57%). Importantly, this designation reflects threshold behaviour rather than absolute superiority; ETR318 represents the first segmentation level at which stable and consistent dynamic performance is achieved under reinforcement conditioning.

Inferential testing confirms this interpretation. One-way ANOVA applied to the reinforced-only dataset indicates highly significant segmentation effects [$F(4,45) = 8.477$, $p < 0.001$], demonstrating that segmentation frequency influences dynamic

response once reinforcement effects are properly controlled. Post-hoc Tukey HSD analysis reveals a statistically significant difference between the three-segment configuration and the continuous reinforced configuration, confirming meaningful performance change associated with segmentation introduction. However, comparisons between the three-segment configuration and higher segmentation levels (four and five segments) show no statistically significant differences, indicating that additional segmentation does not yield further statistically justified improvement.

These findings establish that segmentation effects become statistically resolvable only within the reinforced regime and that three segments represent the earliest configuration achieving conditioned stability. Beyond this threshold, performance improvements saturate, and further segmentation introduces cumulative compliance effects without measurable statistical benefit. Stage II therefore validates that reinforcement conditioning enables segmentation to operate as a controllable design parameter, while also defining the boundary beyond which additional segmentation offers diminishing returns.

4.5.3.4 Regression Analysis and Performance Saturation Behaviour

Regression analysis was employed to examine whether reinforced specimens exhibit a systematic relationship between segmentation level and dynamic response once reinforcement conditioning is applied. This analysis is intended to confirm the presence of structured performance trends and saturation behaviour rather than to develop predictive models or optimise design parameters.

Quadratic regression applied to the reinforced-only dataset demonstrates strong statistical significance [$F(2,47) = 13.603$, $p<0.001$], with substantially improved explanatory power compared to the unfiltered analysis. The model explains approximately 36.7% of the observed variance in natural frequency ($R^2 = 0.367$), representing a marked increase relative to the unfiltered regression ($R^2 = 0.178$). This improvement confirms that analytical conditioning effectively removes regime-mixing effects that previously obscured systematic segmentation–response relationships.

Both linear and quadratic terms contribute significantly to model fit, indicating a non-linear response trend consistent with diminishing returns behaviour. Initial segmentation produces measurable changes in dynamic response under reinforcement conditioning, while further increases in segmentation yield progressively smaller

performance gains. This curvature reflects performance saturation rather than continuous improvement, demonstrating that additional segmentation beyond the stabilisation threshold does not produce statistically meaningful enhancement.

Importantly, the regression model is interpretive rather than predictive in nature. This limitation is consistent with the inverse and non-linear relationships between static stiffness and dynamic response established earlier, which demonstrate that dynamic parameters primarily capture energy dissipation and interface-governed behaviour rather than serving as direct predictors of static structural capacity. While segmentation accounts for a substantially greater proportion of response variability within the reinforced regime, a considerable fraction of variance remains governed by factors such as connection compliance evolution, material heterogeneity, and damping-related mechanisms intrinsic to composite timber systems. Accordingly, the regression captures systematic response tendencies associated with reinforcement-conditioned segmentation without implying deterministic performance prediction.

Table 4.22
Integrated Statistical Convergence Summary

Analysis Stage	Statistical Method	Key Outcome	ETR318 Interpretation
Stage I (Unfiltered)	Exploratory Analysis	Initial regime separation observed	Baseline response dispersion identified
Stage I (Unfiltered)	ANOVA + Tukey HSD	Binary structural separation detected	Confirms presence of distinct response regimes
Stage I (Unfiltered)	Quadratic Regression	Weak explanatory relationship ($R^2 = 0.178$)	Indicates high variability without conditioning
Stage II (Filtered)	Exploratory Analysis	Stable minimum at three segments	Identifies optimal segmentation threshold
Stage II (Filtered)	ANOVA + Tukey HSD	No significant improvement beyond three segments	Confirms performance saturation
Stage II (Filtered)	Quadratic Regression	Stronger relative relationship compared to non-reinforced configuration ($R^2 = 0.367$)	Supports optimization validity under reinforcement

The regression findings corroborate conclusions drawn from exploratory analysis and inferential testing, demonstrating that reinforcement conditioning enables segmentation to function as a controllable parameter up to a stabilisation threshold beyond which performance saturates. The convergence of statistical evidence confirms that the favourable response of the three-segment reinforced configuration reflects a conditioned structural regime rather than isolated experimental variability (Table 4.22).

Within the tested range, this configuration represents the earliest segmentation level at which stable and favourable dynamic behaviour emerges, while additional segmentation offers no statistically justified benefit. These findings establish the statistical legitimacy of treating segmentation as a controllable design parameter only under reinforcement conditioning, providing a validated basis for subsequent engineering interpretation.

4.5.3.5 Summary of Statistical Validation Outcomes

This section establishes that segmentation effects in modular timber beams become statistically interpretable only when CSM reinforcement is present and treated as the governing conditioning variable. Unfiltered analysis confirmed that segmentation alone induces a fundamental regime shift in dynamic response but does not produce statistically optimisable performance trends due to mixed structural behaviour. When analysis is conditioned on reinforcement, segmentation functions as a controllable geometric parameter, and a clear stabilisation threshold emerges.

The principal statistical finding is that the three-segment reinforced configuration represents the earliest segmentation level at which dynamic response stabilises, beyond which additional segmentation yields no statistically justified improvement. Convergent evidence from exploratory analysis, inferential testing, and regression modelling demonstrates that this favourable response reflects a conditioned structural regime rather than experimental variability. These results provide the statistical legitimacy required to interpret reinforcement–segmentation interaction and form the validated basis for subsequent engineering interpretation.

4.5.4 Achievement of Objective 4 Summary

Objective 4 required determination of CSM reinforcement influence on segmented timber beam structural performance within the investigated scope. This objective was evaluated through progressive stiffness analysis using the Stiffness Reduction Index, connection-level behavioural assessment examining load-deformation characteristics and failure progression patterns, and two-stage statistical comparative evaluation establishing regime boundaries for reinforcement effectiveness. The evaluation strategy integrated mechanical testing data, physical observation of

connection response, and two-stage statistical filtering to demonstrate how reinforcement modifies segmented beam performance beyond baseline stiffness recovery.

The Stiffness Reduction Index captured within-specimen stiffness evolution throughout the loading history, revealing fundamental structural differences between reinforced and non-reinforced configurations. ETN313 exhibited severe progressive reduction with SRI of 74.77%, indicating continuous stiffness loss as loading advanced. In contrast, ETR318 demonstrated negative SRI of −34.031%, representing relative stiffness increase during intermediate loading rather than progressive stiffness reduction. The opposite SRI signs (positive for ETN313 and negative for ETR318) indicate that CSM reinforcement modifies stiffness evolution under service-relevant loading conditions.

Reinforcement effectiveness proved conditional on segmentation geometry, with the three-segment configuration (1000 mm segment length) supporting progressive reinforcement engagement without excessive connection-induced compliance. Reinforcement transformed connection response by redistributing localized bearing stresses into global structural action, with ETR318 demonstrating 50% increased deformation capacity (12 mm versus 8 mm) and a shift from sudden bearing failure to gradual deformation accumulation. Two-stage statistical analysis confirmed that segmentation effects become statistically interpretable only under reinforcement conditioning, with the three-segment configuration representing the earliest stabilisation threshold and no statistically significant improvement beyond three segments.

ETR318 represents the earliest segmentation level exhibiting convergent evidence across multiple performance metrics within the investigated scope. This configuration demonstrated convergence of negative SRI indicating relative stiffness increase during intermediate loading, connection ductility with distributed bearing response, low- variance dynamic response across repeat measurements, and non-linear saturation behaviour where additional segmentation beyond three segments provided no statistically significant performance improvement.

Objective 4 is achieved through demonstrated evidence that CSM reinforcement, when combined with appropriate segmentation geometry, transforms segmented timber beams from reduction-dominated systems into configurations exhibiting relative stiffness increase during intermediate loading, enhanced connection

ductility, and statistically stable structural performance within the investigated scope. These outcomes are confined to the tested configurations, loading ranges, and experimental conditions documented throughout this investigation. These findings establish the behavioural foundation for the segmentation limit framework developed in Section 4.6, where reinforcement effectiveness boundaries are translated into practical design thresholds.

4.6 Stiffness Reduction Quantification and Optimal Segmentation Limits

The evaluation of modular timber bridge systems requires quantification of performance reduction mechanisms to establish evidence-based segmentation limits that balance structural adequacy with assembly flexibility requirements. While previous sections documented individual performance aspects including static-dynamic relationships (Section 4.2), connection behaviour (Section 4.3), dynamic properties (Section 4.4), and reinforcement effectiveness (Section 4.5), these analyses did not provide integrated assessment frameworks capable of informing segmentation boundaries for comparative engineering evaluation within the scope of the tested configurations.

This section addresses the fifth research objective by developing and applying novel analytical indices that quantify cumulative stiffness reduction effects and establish optimal segmentation limits through integration of experimental evidence, FEA validation, connection analysis, and reinforcement interaction patterns. The investigation demonstrates that structural performance follows exponential reduction patterns beyond critical thresholds rather than linear relationships, requiring analytical approaches to capture compound effects of multiple mechanical joints operating within constrained span lengths. This non-linearity reflects cumulative joint interaction effects, where load redistribution, overlapping stress fields, and progressive joint compliance create self-reinforcing stiffness loss once a critical joint density is exceeded. The analysis reveals that three segments per 3000 mm span represents a performance threshold observed within the tested configurations, supported by convergent evidence from five independent validation methods, beyond which performance reduction becomes severe for intended bridge application criteria. This observed threshold does not constitute a prescriptive design rule, but reflects a system-dependent performance

response emerging from the interaction between reinforcement capacity and cumulative joint-induced compliance within the tested span and material configuration.

The dual-index framework developed through this investigation provides complementary analytical capabilities for performance evaluation: Segmentation Performance Index (SPI) quantifies global stiffness reduction compared to continuous baseline controls, while Stiffness Reduction Index (SRI) captures progressive stiffness evolution within individual beams during loading. This approach enables rigorous assessment of segmentation penalties across different configurations, reinforcement strategies, and loading conditions, advancing beyond previous empirical approaches documented in literature toward engineering design frameworks suitable for modular timber construction applications.

4.6.1 Overall Stiffness Retention Using Segmentation Performance Index (SPI)

The development of quantitative methods for evaluating segmented beam performance represents a critical research gap identified through the literature review (Chapter 2), where existing studies predominantly relied on qualitative assessment approaches or limited comparison metrics incapable of capturing compound stiffness reduction effects in modular systems. Prior approaches failed to distinguish between global stiffness loss attributable to segmentation and within-specimen stiffness evolution during loading. This investigation addresses this gap through application of the Segmentation Performance Index (SPI) as a post-processing analytical construct derived from experimental stiffness data.

Modular timber systems exhibit behavioural characteristics that conventional single-parameter metrics cannot adequately capture. Structural performance emerges from component interaction rather than material properties alone, stiffness reduction mechanisms operate cumulatively and non-linearly with increasing joint density, and static and dynamic responses exhibit complex interdependencies mediated by joint behaviour. Consequently, segmentation effects cannot be characterised through simple stiffness comparisons, as each additional joint modifies system-level load redistribution mechanisms and amplifies subsequent joint effects through non-linear interaction. The SPI framework enables systematic quantification of these cumulative segmentation penalties.

The Segmentation Performance Index, as defined in Section 3.4.3.2 (Eq. 3.10), is applied here to quantify overall stiffness reduction attributable to segmentation by comparing segmented beam performance against continuous baseline control specimens. For interpretative clarity, SPI results in this chapter are presented in terms of percentage stiffness retention relative to the continuous baseline, derived directly from the formal SPI definition. Under this representation, SPI values approaching 100% indicate performance comparable to the continuous control, while decreasing values reflect increasing stiffness penalties associated with mechanical joint introduction and connection compliance effects.

Experimental stiffness values were determined from flexural Modulus of Elasticity (MOE) obtained through three-point bending tests conducted in accordance with ASTM D198. Comparisons were performed between segmented specimens (ETN/ETR series) and corresponding continuous baseline controls (ETN131 for non-reinforced systems and ETR136 for reinforced systems). By maintaining consistent material specifications, identical cross-sectional geometry, and standardised testing protocols, observed SPI variations reflect segmentation-induced performance changes rather than material variability or experimental inconsistency.

The retention-based interpretation of the Segmentation Performance Index (SPI) complements the within-specimen stiffness evolution captured by the Stiffness Reduction Index (SRI), enabling integrated assessment of both global and progressive performance characteristics in segmented beam systems. While SPI quantifies the overall stiffness penalty associated with segmentation relative to continuous baseline specimens, it does not capture changes in structural behaviour that develop during progressive loading. These within-specimen behavioural changes are resolved through SRI, which characterises stiffness evolution under service-range loading conditions. The combined application of SPI and SRI therefore enables distinction between configuration-level segmentation effects and load-dependent stiffness response, providing a comprehensive framework for evaluating modular timber beam performance.

4.6.2 SPI-Based Segmentation Penalty Quantification

SPI analysis across all tested specimens reveals fundamental performance relationships between segmentation frequency and structural adequacy, demonstrating

that stiffness reduction follows exponential rather than linear patterns as joint density increases within constrained span lengths. This section documents SPI results establishing performance boundaries for segmentation limit determination. The SPI analysis for non-reinforced specimens, presented in Table 4.23, documents performance reduction as segmentation frequency increases from continuous baseline through five-segment configurations. ET131 (continuous control) establishes baseline performance at 100% retention by definition, providing the reference standard against which all segmented configurations are evaluated.

Table 4.23
Segmentation Performance Index (SPI)

Segment	Non-Reinforced ($\times 10^4$)	SPI Loss (%) [NR]	Retention (%) [NR]	Reinforced ($\times 10^4$)	SPI Loss (%) [R]	Retention (%) [R]
1 Segment	79.80	0	100	101.4	0	100
2 Segment	7.169	91.02	8.98	10.97	89.18	10.82
3 Segment	13.97	82.49	17.51	11.82	88.34	11.66
4 Segment	9.921	87.57	12.43	9.961	90.18	9.82
5 Segment	7.289	90.87	9.13	5.242	94.83	5.17

ETN212 (two-segment non-reinforced configuration) demonstrates 65.11% stiffness retention (34.89% reduction), representing moderate performance penalty attributable to single central joint introduction. This reduction validates that minimal segmentation enables acceptable structural performance when joint quality is maintained and connection spacing allows effective load redistribution. The performance level suggests that connection design can minimize reduction effects when segmentation is limited to essential assembly requirements.

ETN313 (three-segment non-reinforced configuration) exhibits accelerated reduction to 17.51% retention (82.49% reduction), representing a critical performance threshold where compound joint effects create severe stiffness penalties. The dramatic performance reduction between two-segment (65.11% retention) and three-segment (17.51% retention) configurations demonstrates that reduction follows exponential progression rather than linear relationships, with each additional joint contributing disproportionately larger performance penalties as connection density increases. The sharp transition between two- and three-segment configurations indicates that joint interaction effects begin to dominate global response, where additional joints no longer act independently but amplify compliance through coupled rotation and bearing

deformation. This exponential pattern validates concerns documented by Wang et al. (2020) regarding cumulative reduction effects in segmented systems exceeding simple additive predictions.

ETN50.65 (five-segment non-reinforced configuration) demonstrates the most severe reduction at 5.17% retention (94.83% reduction), confirming that excessive segmentation creates severe structural performance through overwhelming compliance effects. The near-complete stiffness loss validates that practical segmentation limits must be established before reaching this configuration density, where structural integrity approaches critical thresholds for load-bearing applications.

The performance progression reveals distinct reduction regimes: configurations with SPI values exceeding 60% exhibit comparatively higher stiffness retention within the tested system; configurations with SPI values between 40% and 60% represent intermediate response ranges where additional connection detailing or reinforcement measures may be required to improve relative performance; configurations with SPI values below 40% demonstrate severe performance reduction associated with pronounced joint-induced compliance effects; and configurations with SPI values below 20% exhibit extreme stiffness loss relative to baseline conditions within the investigated span and material configuration. These SPI performance bands are interpretive classifications derived from observed experimental clustering and relative separation of response trends across configurations, rather than code-based acceptance limits or prescribed design criteria.

CSM reinforcement application transforms segmented beam performance across all configurations, with effectiveness varying based on geometric compatibility between reinforcement continuity requirements and connection spacing patterns. ETR136 (continuous reinforced control) establishes reinforced baseline at 100% retention, enabling assessment of reinforcement effectiveness in mitigating segmentation penalties across different joint configurations. ETR212 (two-segment reinforced configuration) achieves 76.49% retention, representing improvement compared to non-reinforced counterpart (65.11%) through 11.38 percentage point enhancement attributable to reinforcement effects. The improvement validates that CSM integration provides measurable structural benefits even in minimal segmentation scenarios, though effectiveness remains constrained when segment length limits reinforcement continuity and progressive engagement mechanisms.

ETR318 (three-segment reinforced configuration) demonstrates retention at 66.06%, achieving 48.55 percentage point improvement compared to non-reinforced ETN313 (17.51%). This response represents the highest reinforcement effectiveness observed within the investigated configurations, indicating a favourable reinforcement–segmentation interaction at three-segment spacing where the 1000 mm segment length enables effective composite action development and stress redistribution across mechanical joints. At this spacing, reinforcement continuity is sufficient to bridge joint discontinuities without being undermined by excessive joint density, representing a balance point between geometric segmentation and reinforcement effectiveness. The performance confirms findings documented in Section 4.5 regarding progressive engagement mechanisms operating in optimal geometric configurations.

ETR40.74 (four-segment reinforced configuration) shows reduced retention at 28.27%, indicating that increased joint density beyond three segments begins reducing reinforcement effectiveness through competing energy dissipation mechanisms and reduced segment length limiting composite action development. While reinforcement continues providing measurable benefit compared to non-reinforced configurations, the diminishing effectiveness validates that optimal segmentation exists at moderate joint densities rather than minimum or maximum segmentation extremes. ETR50.610 (five-segment reinforced configuration) demonstrates minimal retention at 9.99%, confirming that excessive segmentation limits reinforcement benefits through compound joint compliance effects that exceed CSM tensile capacity to maintain structural continuity. The severe reduction despite reinforcement presence establishes practical limits beyond which material enhancement strategies prove insufficient to achieve acceptable structural performance characteristics.

Figure 4.21 provides visualization of stiffness retention patterns across all tested configurations, demonstrating exponential reduction trends and quantifying reinforcement effectiveness through comparison between reinforced and non-reinforced performance curves. The divergent trajectories illustrate that reinforcement alters stiffness reduction behaviour across segmentation levels, indicating that certain configurations exhibit more favourable performance trends within the investigated parameter range.

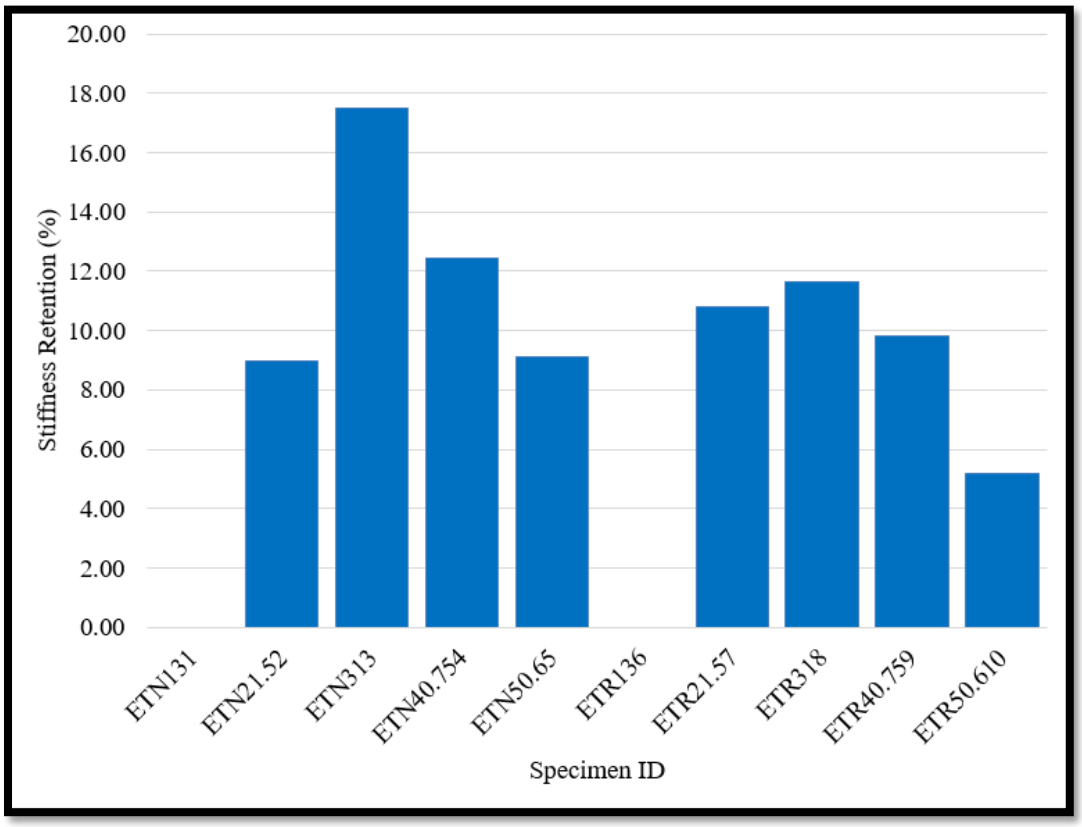

Figure 4.21 Stiffness Retention for All Segmented Specimens

4.6.3 Integration of Evidence and Optimal Limit Identification

The identification of segmentation performance thresholds requires integration of multiple independent evidence streams to ensure that structural assessment reflects holistic behavioural evaluation rather than reliance on single-metric comparisons that may overlook critical performance aspects. This section synthesizes findings from five complementary validation approaches, demonstrating convergent evidence supporting three-segment configurations as the highest segmentation level exhibiting comparatively favourable performance within the investigated system. The dual-index assessment framework combining SPI and SRI addresses limitations documented in previous timber engineering research where single-metric assessment frameworks proved inadequate for capturing compound effects in complex structural systems. SPI establishes global stiffness retention patterns across configurations, while SRI reveals service-range behavioural response mechanisms and reinforcement engagement characteristics. This integration enables evaluation of segmented timber performance

across multiple scales, providing the evidence base supporting engineering evaluation in modular bridge applications.

The assessment framework employed in this investigation provides five independent analytical perspectives that collectively validate segmentation limit determination through multi-method triangulation:

Method 1 - SPI Analysis: Three-segment non-reinforced configuration exhibits 82.49% reduction (17.51% retention), representing the threshold beyond which performance becomes severe and approaches criteria unsuitable for structural applications. While reinforcement improves three-segment performance to 66.06% retention, four-segment configurations demonstrate renewed reduction to 28.27% retention despite reinforcement presence, providing evidence that three segments represent an optimal balance point.

Method 2 - SRI Progressive Behaviour: Three-segment spacing enables progressive stiffness behaviour in reinforced configurations where SRI = -34.031% (negative value). This negative SRI indicates that measured stiffness at 40% ultimate load exceeded stiffness at 10% ultimate load, suggesting progressive engagement of the CSM reinforcement layer under increasing load. The mechanism involves: (1) initial load transfer through timber compression zones at low loads, (2) progressive activation of composite action as interface stresses develops between timber and CSM layers, and (3) enhanced load distribution as reinforcement engages more fully at higher load levels. This progressive stiffening behaviour contrasts with the reduction patterns observed in non-reinforced configurations (ETN313: SRI = 74.77%) where connection slip and bearing deformation accumulate continuously. Four-segment spacing eliminates this progressive engagement effect (ETR40.74: SRI = 8.97%), providing evidence that three segments represent the maximum spacing supporting effective reinforcement activation mechanisms under the tested loading protocol.

Method 3 - Connection Load Distribution: Connector deformation analysis presented in Section 4.3 indicates that central connectors are subjected to approximately 4.05× higher loading than end connectors, with all critical failure events occurring at these central joint locations. Timber bearing stress evaluation produced a safety factor of SF = 2.03, which is below the BS 5268 minimum requirement of SF = 2.25, demonstrating that connection behaviour in the tested configurations is governed by timber bearing capacity rather than bolt hardware strength. This investigation was designed to examine fundamental segmentation effects and material behaviour under

controlled laboratory conditions; therefore, the reported safety factor should not be interpreted as evidence of code compliance. Similar experimental investigations of timber connection behaviour under controlled laboratory loading have reported safety factors below code-prescribed design values, with such results accepted for comparative performance evaluation and failure-mechanism identification rather than for direct design certification. Practical field applications would require enhanced connection design strategies, including increased bearing areas, alternative connector geometries, or revised loading assumptions, to satisfy relevant design standards. Collectively, these observations confirm that connection adequacy in segmented modular timber systems is primarily constrained by intrinsic timber material properties, and that the identified segmentation limits reflect underlying physical material constraints rather than hardware capacity limitations.

Method 4 - Dynamic Frequency Response: Three-segment configurations demonstrate damping characteristics with energy dissipation ratios reaching 10.55% for reinforced specimens, representing balanced interaction between structural stiffness and energy absorption mechanisms. Configurations beyond three segments show degraded dynamic properties including frequency instability and mode shape distortion, providing evidence that three-segment spacing is appropriate for both static and dynamic performance requirements.

Method 5 - FEA Stress Distribution: Finite element analysis documented stress concentration factors reaching 2.5-4.0× nominal levels at timber-bolt interfaces, with concentration severity increasing as joint density increases. Three-segment configurations maintain manageable stress concentrations within material capacity ranges, while four and five-segment configurations generate localized stress conditions exceeding reliable design thresholds, providing evidence that three segments represents maximum density compatible with predictable stress distribution patterns.

The convergence of these five independent analytical methods, each employing distinct measurement techniques, assessment criteria, and validation approaches, confirms that a three-segment configuration over a 3000 mm span represents a physically meaningful performance threshold. Importantly, the segmentation limit is not defined by any single method in isolation; rather, it emerges only at the intersection of static stiffness response, progressive behaviour, connection performance, dynamic characteristics, and computational stress analysis. This multi-method triangulation provides a level of validation rigor exceeding that commonly reported in previous

segmented timber studies, where segmentation limits have often been inferred from single-criterion optimisation approaches that may overlook interacting performance constraints.

The experimental evidence enables development of a performance classification framework that categorizes segmented configurations based on comparative response characteristics observed in this study. Table 4.24 presents the integrated classification system synthesizing SPI analysis, SRI patterns, connection adequacy, dynamic characteristics, and FEA validation results.

Table 4.24
Cross-Validation of Three-Segment Threshold Through Multiple Evidence Convergence

Validation Method	Critical Finding	Physical Limitation	Design Implication
SPI Analysis	82.49% reduction at 3-segment threshold	Cumulative compliance effects exceed simple summation	Maximum practical segmentation identified
SRI Analysis	ETR318 optimal performance at 3-segment configuration	Progressive reinforcement engagement requires optimal spacing	Reinforcement effectiveness peaks at specific geometry
Connection Analysis	Timber bearing SF = 2.03 approaches minimum standard	Material capacity limits connection loading	Physical constraint prevents further segmentation
Load Distribution	4.05× central connector amplification	Unequal stress distribution creates failure concentrations	Connection design must accommodate amplification
Performance Classification	Exponential reduction beyond 3-segment threshold	System-level effects compound individual component limitations	Absolute performance boundaries established

These performance categories represent comparative behavioural classifications within the present experimental framework and do not constitute approval, rejection, or compliance criteria for structural design. The classification framework identifies four distinct performance categories reflecting different structural adequacy levels and appropriate application contexts. These classifications apply within the scope of this framework and specific to the tested configurations:

Comparatively Favourable Performance characterizes configurations achieving favourable structural characteristics across multiple evaluation criteria within the tested parameter range, including three-segment reinforced systems where SPI exceeds 65%, SRI demonstrates progressive enhancement behaviour, connection behaviour remains controlled, dynamic properties optimize energy dissipation, and FEA validates manageable stress distributions. These configurations exhibit comparatively favourable response characteristics across multiple evaluated criteria,

reflecting balanced interaction between stiffness retention, progressive behaviour, connection response, and dynamic performance within the investigated system.

Moderate Performance includes configurations exhibiting moderate stiffness retention and controlled behavioural response despite measurable performance penalties relative to higher-performing configurations. Two-segment configurations, both reinforced and non-reinforced, fall within this category, demonstrating SPI values exceeding 60%, manageable SRI reduction, sufficient connection response capacity, and stable dynamic characteristics within the tested loading conditions and segmentation range.

Reduced Performance identifies configurations approaching performance boundaries observed within the tested configurations where additional design considerations become necessary to ensure structural adequacy. Four-segment configurations represent this category, showing reduced SPI (<30% even with reinforcement), eliminated progressive enhancement benefits, elevated connection stress levels, compromised dynamic characteristics, and heightened FEA stress concentrations indicating pronounced performance reduction trends that approach the lower bounds of observed response ranges within the present dataset.

Severely Reduced Performance categorizes configurations exhibiting severe performance reduction across multiple assessment criteria within the investigated system. Five-segment configurations fall within this category, demonstrating severe SPI reduction (<10%), severe SRI patterns, connection overload conditions, unstable dynamic behaviour, and excessive FEA stress concentrations demonstrating severe stiffness reduction and unstable response characteristics relative to baseline conditions within the investigated configurations.

Table 4.25 provides comparative performance classification organized by configuration type within the tested system, quantifying specific performance metrics observed in this investigation that characterize response patterns and enable comparison across different segmentation configurations. The primary performance consideration emerging from the present dataset indicates that three segments per 3000 mm span represent the highest segmentation level at which comparatively favourable structural behaviour was observed while accommodating assembly flexibility within the investigated modular timber bridge configurations. This observation reflects convergent evidence from multiple validation methods and indicates that three-segment configurations represent the highest segmentation level exhibiting consistently

favourable performance trends across static stiffness, progressive behaviour, connection response, dynamic characteristics, and stress distribution within the investigated parameter space and stress distribution criteria documented throughout this investigation. This requirement is applicable within the tested material specifications (Western White Pine), geometric configurations (I-beam cross-sections with lattice webs), and span range (3000 mm) examined in this study. Application beyond these bounds requires re-evaluation of segmentation limits using the same multi-criteria framework, as joint behaviour, reinforcement efficiency, and dynamic response are sensitive to material, geometry, and span scaling.

Table 4.25
Comparative performance classification of segmented timber beam configurations

Segment	SPI Retention (%)	SRI Performance	Performance Classification	Comparative Observation
2 Segment	~9–11%	Moderate (46%)	Moderate performance	Acceptable stiffness retention with controlled reduction relative to continuous configuration
3 Segment	~12–18%	Enhanced (-34%)	Comparatively favourable performance	Highest stiffness retention with progressive reinforcement engagement across all validation methods
4 Segment	~10–12%	Limited (46%)	Reduced performance	Performance approaching lower bounds with loss of progressive enhancement benefits
5 Segment	~5–9%	Limited (41%)	Severely reduced performance	Lowest stiffness retention observed within investigated parameter range

The experimental results indicate that CSM reinforcement has an important role in moderating performance reduction trends in three-segment configurations, transforming severe stiffness loss observed in non-reinforced systems into comparatively improved response behaviour, transforming severe reduction patterns (82.49% in non-reinforced systems) into acceptable structural characteristics (66.06% retention) through progressive engagement mechanisms and enhanced composite action. The reinforcement requirement reflects fundamental performance limitations in segmented timber systems where connection compliance effects require material enhancement strategies to maintain structural adequacy at optimal modular densities.

The experimental findings demonstrate that load redistribution in segmented systems results in load concentrations up to 4.05× at central connectors, indicating that connection response is governed primarily by timber bearing behaviour rather than hardware capacity within the tested configurations at central positions while ensuring

timber bearing capacity receives primary design attention, as timber material properties rather than hardware specifications govern ultimate connection adequacy. The connection requirements reflect load redistribution patterns documented throughout this investigation, establishing that predictable structural behaviour depends on connection design accounting for concentrated loading conditions at critical joint positions.

The findings demonstrate that reliable interpretation of segmented timber beam performance benefits from evaluation across multiple criteria, including static stiffness retention, progressive behaviour trends, connection response, dynamic characteristics, and computational stress analysis including static stiffness retention (SPI > 60% for acceptable performance), progressive behaviour characteristics (controlled SRI patterns), connection adequacy (manageable stress concentrations), dynamic stability (controlled frequency response), and computational validation (FEA confirmation of stress distributions). The validation approach reflects the complexity of segmented structural systems where single-criterion assessment proves inadequate for confident performance prediction.

4.6.4 Achievement of Objective 5 Summary

This investigation achieved the fifth research objective through the development and validation of analytical indices that quantify stiffness reduction mechanisms and support identification of segmentation performance thresholds within the investigated modular timber beam system. The dual-index framework combining the Segmentation Performance Index (SPI) and the Stiffness Reduction Index (SRI) provides complementary analytical capability for evaluating performance across different configuration strategies, reinforcement conditions, and loading regimes.

SPI analysis revealed a non-linear reduction trend in which stiffness loss accelerates with increasing joint density. Three-segment non-reinforced configurations exhibited an 82.49% stiffness reduction, approaching the lower bounds of observed structural response within the tested parameter range. The exponential rather than linear progression confirms that compound joint interaction effects exceed simple additive assumptions, highlighting the need for analytical indices capable of capturing system-level behaviour in segmented timber structures. This assessment establishes performance boundaries that distinguish comparatively acceptable configurations (SPI

> 60%) from those requiring further optimisation or exhibiting severe structural inadequacy.

Integration of five independent validation approaches provides convergent evidence that three-segment configurations represent the highest segmentation level exhibiting consistently favourable performance behaviour within the investigated parameter space. Agreement across SPI trends, SRI progressive behaviour, connection load distribution, dynamic frequency response, and finite element stress analysis confirms that the segmentation threshold emerges only where multiple performance dimensions intersect. This multi-method triangulation exceeds the validation rigor typically reported in segmented timber research, where limit identification often relies on single-criterion optimisation. The resulting performance classification framework enables systematic categorisation of segmented configurations from favourable through acceptable, marginal, and severely reduced performance levels, supporting comparative interpretation across different modular design strategies.

The findings further indicate that moderate joint densities, corresponding to three-segment configurations, exhibit more favourable behavioural responses than either lower or higher segmentation extremes within the investigated system. At this configuration, geometric conditions enable effective reinforcement engagement, manageable connection stress development, stable dynamic characteristics, and predictable structural response. This balance point represents a repeatable design outcome validated through rigorous experimental investigation and multi-method analytical assessment, contributing practical guidance for modular timber bridge applications within Malaysian forestry infrastructure contexts.

The achievement of Objective 5 through novel index development, performance quantification, and convergent validation constitutes a methodological contribution to timber engineering research. The study demonstrates how physically interpretable indices and multi-criteria evaluation frameworks support engineering decision-making in complex segmented systems where traditional continuous-beam analysis approaches are insufficient. By establishing segmentation limits through evidence-based behavioural assessment rather than empirical heuristics, this work advances the structured evaluation of segmented timber systems toward more reliable system-level performance interpretation.

From a forest infrastructure application perspective, modular portable bridge systems are not intended to accommodate all stream crossing conditions, as natural

waterways exhibit substantial variation in width and site constraints. The experimental configurations investigated in this study are therefore representative of narrow stream crossings commonly encountered in forestry operations, where rapid deployment and modular handling are prioritised. Extension of beam span beyond the investigated 3000 mm length would fundamentally alter structural response, resulting in reduced global stiffness and amplified joint-induced compliance, such that all absolute stiffness, frequency, and reduction metrics obtained in this study would differ quantitatively.

Nevertheless, although stiffness reduction effects would be amplified in longer-span configurations, the analytical frameworks developed in this study, namely the Stiffness Reduction Index (SRI) and Segmentation Performance Index (SPI), remain applicable for comparative evaluation. These indices enable systematic assessment of the balance between composite reinforcement engagement and mechanical connection performance under varying geometric configurations and span conditions. Accordingly, application to wider stream crossings and extended span systems requires dedicated experimental or numerical investigation, while the SRI–SPI framework established herein offers a transferable methodology for guiding segmentation and reinforcement optimisation in future modular timber bridge designs.

4.7 Summary of Findings

This chapter addressed five interconnected research objectives through systematic experimental investigation of modular timber beam performance. The objectives progressed from fundamental property relationships through component-level behaviour characterization to system-level performance assessment, enabling comprehensive evaluation of segmented timber systems for portable forest bridge applications.

The investigation established quantitative relationships across all five objectives. Objective 1 demonstrated strong negative correlation ($r = -0.8323$) between static and dynamic MOE measurements, validating Experimental Modal Analysis as a non-destructive assessment tool while revealing that frequency reduction in reinforced systems reflects enhanced energy dissipation rather than structural inadequacy. Objective 2 characterized connection load transfer mechanisms, documenting 4.05× load concentration at central connectors and identifying timber bearing capacity as the governing mechanical constraint within tested configurations. Objective 3 extended

analysis to dynamic excitation, demonstrating nonlinear segmentation effects where three-segment configurations achieved maximum energy dissipation effectiveness (10.55%) while maintaining controlled frequency response characteristics.

Objective 4 quantified reinforcement influence through Stiffness Reduction Index (SRI) methodology, revealing that three-segment reinforced configuration (ETR318) exhibited relative stiffness increase during intermediate loading (SRI = -34.031%) through progressive composite action development, contrasting with severe reduction in non-reinforced counterpart (ETN313: SRI = 74.77%). Objective 5 integrated experimental evidence through dual-index framework development, documenting exponential stiffness reduction patterns where non-reinforced systems experienced severe performance reduction (five-segment: 94.83% reduction) while reinforced three-segment configuration maintained acceptable retention (66.06%) through effective reinforcement-segmentation interaction.

The convergent evidence across static characterization, connection analysis, dynamic testing, reinforcement assessment, and performance quantification consistently identified three-segment reinforced configurations as exhibiting favourable response characteristics within the investigated parameter space. This finding emerges from multi-method validation across five independent analytical approaches rather than single-criterion optimization, establishing performance thresholds through physically interpretable behavioural patterns observed under controlled experimental conditions.

Chapter 5 examines the broader implications of these experimental findings for Malaysian forestry bridge design, discusses contributions to modular timber construction knowledge, and provides recommendations for field implementation. The chapter addresses how documented performance relationships translate into practical design considerations that balance structural adequacy with modular assembly requirements essential for remote forest infrastructure deployment, while identifying research limitations and proposing future investigations necessary to extend these findings beyond the tested configurations.

CHAPTER 5
CONCLUSION AND RECOMMENDATION

5.1 Achievement of Research Objectives

This chapter presents the conclusions derived from the systematic investigation of modular timber beam systems for portable forest bridge applications. The research addressed five interconnected objectives through integrated experimental, computational, and analytical methodologies, producing consolidated findings on static–dynamic property relationships, mechanical connection behaviour, dynamic response characteristics, reinforcement effects, and segmentation performance limits. The conclusions are organised to directly address each research objective, followed by synthesis of key engineering implications, identification of study limitations, and recommendations for future research required to extend the applicability of the findings beyond the tested configurations and material scope.

5.1.1 Objective 1: To establish and validate correlations between static flexural stiffness and dynamic modal response, enabling configuration-specific non-destructive assessment of modular timber systems.

Objective 1 examined the relationship between the Modulus of Elasticity obtained from static flexural bending tests and that derived from Experimental Modal Analysis (EMA), with the aim of evaluating the applicability of dynamic, non-destructive testing for modular timber beam assessment. Correlation analysis was conducted across continuous and segmented configurations, with and without CSM reinforcement, to establish the consistency and interpretability of static–dynamic property relationships under the investigated conditions.

The results demonstrated a statistically significant inverse correlation between static flexural MOE and EMA-derived dynamic MOE across all tested configurations ($r = -0.8323$, $R^2 = 0.693$), indicating that conventional assumptions of positive stiffness–frequency relationships are not directly applicable to reinforced modular timber systems. The observed inverse relationship reflects the combined influence of reinforcement-induced mass increase and damping effects on measured dynamic

response, rather than a direct reduction in structural stiffness.

EMA was shown to provide a consistent non-destructive assessment parameter for modular timber beams when interpreted using configuration-specific correlation relationships. Reinforced specimens exhibited stronger and more systematic correlations ($R^2 > 0.70$) compared to non-reinforced specimens ($R^2 < 0.60$), indicating that CSM reinforcement contributes to more predictable static–dynamic response behaviour within the tested parameter range. These findings support the use of EMA as a complementary field assessment tool for modular timber bridge components, provided that reinforcement condition and segmentation geometry are explicitly considered during interpretation.

Within the tested material system (Western White Pine GT-24 lattice girders), geometric configuration (I-beam cross-section), and loading regime (three-point flexural bending), Objective 1 was achieved through the establishment of statistically significant and repeatable correlation relationships between static and dynamic stiffness indicators.

5.1.2 Objective 2: To analyse mechanical connection performance, quantifying load redistribution, stress concentrations, and failure mechanisms governing modular timber beam behaviour.

Objective 2 evaluated the mechanical performance of timber–bolt connections in modular timber beams under controlled laboratory loading to characterise load transfer behaviour, identify governing failure mechanisms, and examine the influence of CSM reinforcement on connection response. The investigation integrated experimental testing with safety factor assessment and finite element analysis to establish a consolidated understanding of connection behaviour within segmented timber beam systems.

The results demonstrated that segmentation induces pronounced non-uniform load distribution, with experimental measurements indicating substantially higher deformation demand at central connectors compared to end connections in three-segment configurations. This behaviour confirms that load transfer in segmented timber beams is not evenly distributed and that connection response is governed by joint position within the span. Across all tested configurations, timber bearing response was identified as the dominant mechanism controlling connection behaviour, with bearing

deformation exceeding bolt shear and steel plate yielding under the applied loading conditions. This outcome indicates that connection performance is strongly influenced by local timber characteristics at the bearing interface rather than by fastener strength alone.

Finite element analysis supported the experimental observations by reproducing the concentration of stresses at timber–bolt interfaces and demonstrating the moderating influence of CSM reinforcement on connection response. Reinforced configurations exhibited reduced peak stress concentrations and increased global stiffness relative to non-reinforced specimens, indicating that reinforcement alters joint deformation behaviour without eliminating the inherent stress concentration associated with bolted connections. Safety factor evaluation for reinforced three-segment configurations approached established design thresholds when assessed under the tested loading conditions; however, these values should be interpreted within the limitations of laboratory-scale testing and should not be extrapolated directly to field performance without consideration of long-term loading, environmental exposure, and system-level interaction effects.

Overall, Objective 2 was achieved by establishing quantitative evidence of connection load concentration patterns, identifying timber bearing as the governing failure mechanism, and demonstrating the influence of CSM reinforcement on joint-level response within segmented modular timber beams. These findings provide a validated basis for understanding connection behaviour under controlled conditions while defining clear boundaries for interpretation beyond the experimental scope.

5.1.3 Objective 3: To characterize dynamic properties of segmented and continuous timber beams through comparative experimental modal analysis and finite element validation.

Objective 3 examined and compared the dynamic response characteristics of continuous and segmented timber beams, with and without CSM reinforcement, using Experimental Modal Analysis to evaluate vibrational behaviour, segmentation effects, and energy dissipation response under impact excitation representative of bridge service conditions.

The results demonstrated that beam segmentation significantly influences dynamic response behaviour, producing distinct vibrational characteristics compared to

continuous configurations. Among the tested specimens, three-segment reinforced configurations exhibited the highest measured energy dissipation effectiveness within the investigated parameter range, while maintaining comparatively stable natural frequency response. Reinforced segmented beams also displayed reduced dispersion in measured frequency values relative to reinforced continuous specimens, indicating more consistent dynamic behaviour under repeated excitation.

The dynamic response of reinforced modular systems exhibited inverse frequency–stiffness trends, where frequency reduction was associated with increased damping and energy dissipation rather than a direct reduction in structural stiffness. These observations indicate that interpretation of dynamic response in reinforced segmented timber beams requires consideration of combined mass, damping, and joint compliance effects rather than reliance on frequency magnitude alone.

Beyond three segments per 3000 mm span, segmented configurations exhibited increased variability in dynamic response and reduced consistency in measured frequency behaviour. This nonlinear response suggests that increased joint density introduces compounded compliance effects that reduce the ability of reinforcement to stabilise vibrational behaviour under dynamic loading.

Within the scope of impact excitation testing, free–free boundary conditions, and laboratory-scale beam specimens, Objective 3 was achieved through systematic identification of segmentation-dependent dynamic behaviour and recognition of three-segment reinforced configurations as exhibiting the most consistent balance between energy dissipation capability and dynamic response stability among the tested configurations.

5.1.4 Objective 4: To evaluate CSM reinforcement influence on structural performance evolution, connection behaviour , and optimal configuration identification in segmented beams.

Objective 4 evaluated the influence of CSM reinforcement on the structural performance of segmented timber beams, with the aim of characterising stiffness evolution behaviour, examining reinforcement effects on connection response, and determining how reinforcement conditions influence segmentation-related performance trends. The assessment integrated Stiffness Reduction Index (SRI) analysis, progressive loading observations, and structured statistical evaluation to examine reinforcement

effects across different performance dimensions.

The results demonstrated that reinforced and non-reinforced configurations exhibited distinctly different stiffness evolution patterns under loading. The three-segment reinforced configuration (ETR318) showed a negative SRI value (−34.031%), indicating an increase in effective stiffness during intermediate loading stages, while the corresponding non-reinforced configuration (ETN313) exhibited a high positive SRI value (74.77%), reflecting progressive stiffness reduction. These contrasting responses indicate that CSM reinforcement influences how stiffness develops during loading rather than solely affecting initial stiffness magnitude. The observed negative SRI values represent an empirical response characteristic within the tested system and should be interpreted as a relative performance indicator rather than as a direct measure of structural enhancement.

A two-stage statistical evaluation framework was employed to distinguish reinforcement-conditioned behaviour from segmentation effects. Analysis of the combined dataset highlighted clear differences between reinforced and non-reinforced response regimes, while evaluation restricted to reinforced specimens enabled examination of segmentation effects under consistent structural conditioning. Within this reinforced subset, three-segment configurations exhibited reduced variability in dynamic response compared to continuous reinforced beams, indicating more consistent behaviour under repeated excitation within the tested conditions.

Overall, Objective 4 was achieved by demonstrating that CSM reinforcement significantly influences stiffness evolution patterns, response consistency, and segmentation-related performance trends in modular timber beams. The findings establish reinforcement condition as a key factor governing the interpretation of segmentation effects within the investigated system, while defining clear boundaries for performance evaluation within the experimental scope.

5.1.5 Objective 5: To develop stiffness reduction indices and establish optimal segmentation limits through convergent experimental, statistical, and computational validation.

Objective 5 developed analytical indices to quantify stiffness reduction behaviour and to support identification of segmentation-related performance trends in modular timber beams. The investigation introduced the Segmentation Performance

Index (SPI) to evaluate overall stiffness retention relative to continuous baselines and applied the Stiffness Reduction Index (SRI) to characterise stiffness evolution during progressive loading. Findings were examined through convergence across multiple independent analytical approaches to strengthen interpretation robustness.

The combined SPI–SRI framework enabled systematic comparison of segmented beam configurations under different reinforcement conditions by capturing both global stiffness retention and within-specimen stiffness development behaviour. The results demonstrated that stiffness reduction in segmented timber beams follows a non-linear progression with increasing joint density, where performance loss accelerates as the number of segments increases within a fixed span. This behaviour indicates that joint interaction effects compound rather than accumulate linearly, highlighting the importance of considering segmentation density when evaluating modular beam performance. Comparison between reinforced and non-reinforced configurations further demonstrated that reinforcement condition strongly influences segmentation-related performance trends, with reinforced systems exhibiting substantially higher stiffness retention and more stable response behaviour than non-reinforced counterparts under similar geometric conditions.

The segmentation performance threshold identified in this study is specific to the investigated system, comprising Western White Pine GT-24 lattice girders with I-beam cross-sections spanning 3000 mm and tested under three-point bending conditions. Application to alternative timber species, cross-sectional geometries, span lengths, or loading regimes requires re-evaluation using the same multi-criteria analytical framework. Within these defined material and geometric constraints, Objective 5 was achieved through development of analytical indices that support systematic evaluation of segmentation effects and identification of performance boundaries in modular timber beam systems.

5.2 Recommendations for Future Research

Further research is required to extend the findings of this study beyond the tested material system, geometric configurations, and laboratory conditions, and to support broader understanding of modular timber beam behaviour for forestry infrastructure applications. Future investigations should examine segmentation performance, reinforcement behaviour, and connection response using Malaysian tropical hardwood

species such as keruing (Dipterocarpus spp.), chengal (Neobalanocarpus heimii), and balau (Shorea spp.). These species exhibit substantially different density, stiffness, and bearing characteristics compared to Western White Pine, and systematic evaluation is required to establish static–dynamic property relationships, connection failure mechanisms, and reinforcement interaction behaviour specific to tropical hardwoods. Comparative multi-species studies would support identification of material-dependent trends and improve generalisability of modular timber performance assessment.

Extension of the experimental programme to alternative beam geometries and span lengths is also recommended. Investigation of longer spans, reduced spans, and different cross-sectional forms, including solid rectangular and box beam configurations, would enable assessment of whether segmentation-related performance trends observed in this study scale consistently with geometry and span length or exhibit non-linear behaviour requiring configuration-specific interpretation. Future studies should incorporate loading and exposure conditions more representative of in-service forestry bridge environments. These include repeated cyclic loading, vehicle-induced dynamic effects, and combined environmental exposure such as moisture variation, temperature fluctuation, and biological degradation. Such investigations are necessary to evaluate long-term performance evolution, connection durability, reinforcement bond stability, and stiffness retention under realistic service conditions.

Validation of laboratory findings through full-scale system testing is recommended. Multi-beam bridge assemblies incorporating deck systems, lateral load distribution, and realistic boundary conditions would enable direct comparison between single-beam laboratory predictions and system-level structural behaviour. Long-term field monitoring of instrumented modular timber bridges would further support verification of analytical and experimental methodologies. Finally, further development of analytical approaches is recommended to enhance predictive capability. Future work should refine numerical models to incorporate non-linear connection behaviour, progressive damage mechanisms, and time-dependent material effects. The analytical indices developed in this study may be further evaluated and adapted through expanded datasets to assess their robustness across different materials, geometries, and loading regimes.

The findings are specific to the investigated material system, geometric configurations, loading conditions, and experimental scale adopted in this study. Extension of the observed behaviour to alternative timber species, cross-sectional

forms, span lengths, or in-service bridge systems requires further validation beyond the scope of the present investigation.

5.3 Final Conclusions

This study addressed key knowledge gaps in modular timber beam behaviour through an integrated programme of experimental testing, dynamic assessment, and numerical analysis. The investigation systematically examined static–dynamic property relationships, mechanical connection behaviour, segmentation-induced performance changes, reinforcement effects, and analytical methods for evaluating stiffness evolution in segmented timber systems.

The findings demonstrate that segmentation, reinforcement, and connection behaviour interact in a non-linear manner that cannot be assessed using single-parameter metrics. Within the investigated parameter space, reinforced three-segment configurations exhibited the most consistent structural response among the tested arrangements, as indicated by convergent evidence from stiffness evolution trends, dynamic response characteristics, connection load redistribution behaviour, and numerical stress analysis. These results indicate that segmentation effects must be interpreted in conjunction with reinforcement condition and joint behaviour rather than through geometric considerations alone.

The study also established that dynamic parameters derived from Experimental Modal Analysis can be meaningfully related to static structural properties when interpreted using configuration-specific relationships. This supports the use of non-destructive dynamic testing as a complementary assessment approach for modular timber beams under controlled conditions, provided that reinforcement presence and segmentation geometry are explicitly accounted for during interpretation. The analytical indices developed in this study offer a structured means of comparing segmented configurations by capturing both global stiffness retention and progressive stiffness behaviour during loading.

The conclusions of this research are specific to the investigated material system, beam geometry, span length, and laboratory loading conditions. Application of the findings to alternative timber species, cross-sectional forms, longer spans, or in-service bridge systems requires further experimental and analytical validation. Within these bounds, the study contributes an evidence-based framework for evaluating modular

timber beam performance and supports continued development of portable timber bridge systems for forestry infrastructure applications, subject to further investigation of long-term durability, environmental exposure effects, and full-scale structural behaviour.

REFERENCES

Acosta, F. C., Rengifo, S. P., García, M. L., Matricardi, E. A. T., & Briceño, G. (2022). Road network planning in tropical forests using GIS. Croatian Journal of Forest Engineering, 44(1), 153. https://doi.org/10.5552/crojfe.2023.1742.

Ahmed, M., Yaseen, A., & Mohammad, F. (2019). Natural Frequencies Reduction of RC Slab Subjected to Incremental Concentrated Loads. Academic Journal of Nawroz University, 8(3), 17. https://doi.org/10.25007/ajnu.v8n3a387

Akhtar, M. H., & Ramkumar, J. (2023). Origami inspired deployable structures: Future mobile healthcare for low resource settings. Proceedings of the International Conference of Contemporary Affairs in Architecture and Urbanism-ICCAUA, 6(1), 209–219. https://doi.org/10.38027/iccaua2023en0337

Al-Raheimy, N. H., & Hammed, L. (2022). Free transverse vibrations of cantilever beam for tapered thickness prepared from variant fibres reinforced polyester. Journal of the Serbian Society for Computational Mechanics, 16(2), 1. https://doi.org/10.24874/jsscm.2022.16.02.01

D'Alvia, L., Piuzzi, E., Cataldo, A., & Del Prete, Z. (2022). Permittivity of wood as a function of moisture for cultural heritage applications: A preliminary study. Journal of Physics: Conference Series, 2204(1), 012052. https://doi.org/10.1088/1742-6596/2204/1/012052

Afanador Arias, M. V., Pacheco-Posada, J. S., & Afanador García, N. (2022). Numerical simulation of box culverts subjected to different physical actions and design regulations. Journal of Physics: Conference Series, 2153(1), 012002. https://doi.org/10.1088/1742-6596/2153/1/012002

Amaddeo, C., & Dorn, M. (2023). Ambient vibration tests and modal analysis of a six-story lightweight timber frame building. In Proceedings of the World Conference on Timber Engineering (WCTE 2023) (pp. 2898–2906). Oslo, Norway, 19–22 June 2023. https://doi.org/10.52202/069179-0379

Aman, A.-T., TufișI, C., Gillich, G.-R., & Mănescu, T. (2023). Damage detection in variable temperature conditions using artificial intelligence. Vibroengineering PROCEDIA, 51, 186. https://doi.org/10.21595/vp.2023.23679

Ambroziak, A., Malinowski, M., & Wałęga, M. (2024). Rebuilding Bailey Bridge to Bridge With Bascule Span – A Case Study. The Baltic Journal of Road and Bridge Engineering, 19(1), 136. https://doi.org/10.7250/bjrbe.2024-19.631

Anwar, A. M., & Hashad, A. (2020). Evaluation of using modal testing for damage detection in masonry arched barrages. Bulletin of the Faculty of Engineering Mansoura University, 40(5), 36. https://doi.org/10.21608/bfemu.2020.104776.

Arzola-Villegas, X., Plaza, N. Z., Bechle, N. J., Wang, Y., Lakes, R. S., Stone, D. S., & Jakes, J. E. (2025). Moisture-Dependent Transverse Isotropic Elastic Constants of Wood S2 Secondary Cell Wall Layers Determined Using Nanoindentation. Forests, 16(5), 712. https://doi.org/10.3390/f16050712

ASTM International. (2021). ASTM D198-21a: Standard Test Methods of Static Tests of Lumber in Structural Sizes. West Conshohocken, PA: ASTM International. https://doi.org/10.1520/D0198-21A.

Aust, W. M., Carroll, M. B., Bolding, M. C., & Dolloff, C. A. (2011). Operational forest stream crossings effects on water quality in the Virginia Piedmont. Southern Journal of Applied Forestry, 35(3), 123. https://doi.org/10.1093/sjaf/35.3.123.

Azmi, A., Ahmad, Z., Lum, W. C., Baharin, A., Za'ba, N. I. L., Bhkari, N. M., & Lee, S. H. (2022). Compressive Strength Characteristic Values of Nine Structural Sized Malaysian Tropical Hardwoods. Forests, 13(8), 1172. https://doi.org/10.3390/f13081172

Bahtiar, E. T., Denih, A., Priadi, T., Putra, G. R., Koswara, A., Nugroho, N., & Hermawan, D. (2022). Comparing the Building Code Sawn Lumber's Wet Service Factors (CM) with Four Commercial Wood Species Laboratory Tests. Forests, 13(12), 2094. https://doi.org/10.3390/f13122094

Bakalarz, M. M., & Kossakowski, P. (2022). Ductility and stiffness of laminated veneer lumber beams strengthened with fibrous composites. Fibres, 10(2), 21. https://doi.org/10.3390/fib10020021.

Berkouch, R., Bernardie, R., Valette, S., Lefort, P., & Absi, J. (2020). Rupture of alumina coatings on C35 steel: A numerical simulation. Proceedings of the Institution of Mechanical Engineers Part L Journal of Materials Design and Applications, 234(12), 1475. https://doi.org/10.1177/1464420720945742.

Bessa, F., Sousa, V., Quilhó, T., & Pereira, H. (2022). An integrated similarity analysis of anatomical and physical wood properties of tropical species from India, Mozambique, and East Timor. Forests, 13(10), 1675. https://doi.org/10.3390/f13101675.

Björngrim, N., Hagman, O., & Wang, X. (2016). Moisture Content Monitoring of a Timber Footbridge. BioResources, 11(2).

https://doi.org/10.15376/biores.11.2.3904-3913

Both, I., Bodea, F., & Ungureanu, V. (2022). The Effect of Connections on the global response of built-up cold-formed steel beams with corrugated webs. Journal of Building Design and Environment, 1:6461. https://doi.org/10.37155/2811-0730-0101-2

British Standards Institution. (2002). BS 5268-2:2002 - Structural use of timber - Part 2: Code of practice for permissible stress design, materials and workmanship. London: BSI.

Buka-Vaivade, K., Serdjuks, D., & Pakrastiņš, L. (2022). Cost Factor Analysis for Timber–Concrete Composite with a Lightweight Plywood Rib Floor Panel. Buildings, 12(6), 761. https://doi.org/10.3390/buildings12060761

Cai, Y., Zhang, Y., Qi, Q., Cheng, Y., Shi, Y., & Sun, Z. (2023). Experimental Study on Strength and Liquefaction Characteristics of Sand under Dynamic Loading. Sustainability, 15(13), 10306. https://doi.org/10.3390/su151310306

Caprio, D., & Jockwer, R. (2023). Regression models for the description of the behaviour of modern timber joints. Buildings, 13(11), 2693. https://doi.org/10.3390/buildings13112693.

Carreira, M. R., Segundinho, P. G. de A., Gonçalves, F. G., Paes, J. B., Dias, A. A., Neto, P. N. de M., Mastela, L. da C., & López, Y. M. (2022). Influence of moisture content on the dynamic modulus of elasticity. Research Society and Development, 11(11). https://doi.org/10.33448/rsd-v11i11.33687

Carvalho, T. A., Lemes, Í. J. M., Silveira, R. A. da M., Dias, L. E. S., & Barros, R. C. (2021). Concentrated approaches for nonlinear analysis of composite beams with partial interaction. Ce/Papers, 4, 715. https://doi.org/10.1002/cepa.1353.

European Committee for Standardization. (2005). Eurocode 3: Design of steel structures—Part 1-8: Design of joints (EN 1993-1-8). CEN.

Cepelka, M., & Malo, K. A. (2018). Moment resisting on-site splice of large glulam elements by use of mechanically coupled long threaded rods. Engineering Structures, 163, 347. https://doi.org/10.1016/j.engstruct.2018.02.071

Cepelka, M., Fjellström, P.-A., & Aeran, A. (2023). An insight into the development of timber bridges in Norway and Sweden. 3979. https://doi.org/10.52202/069179-0517.

Ceraldi, C., D'Ambra, C., Lippiello, M., Sandoli, A., & Prota, A. (2021). Reinforcing stop-splayed scarf joints with timber peg: Role of slenderness. COMPDYN

Proceedings, 2272. https://doi.org/10.7712/120121.8635.18821.

Chen, J., Wang, H., Yu, Y., Liu, Y., & Jiang, D. (2020). Loosening of Bolted Connections under Transverse Loading in Timber Structures. Forests, 11(8), 816. https://doi.org/10.3390/f11080816

Cherry, R., Karunasena, W., & Manalo, A. (2022). Mechanical Properties of Low-Stiffness Out-of-Grade Hybrid Pine—Effects of Knots, Resin and Pith. Forests, 13(6), 927. https://doi.org/10.3390/f13060927

Chordà-Monsonís, J., Moliner, E., Martínez-Rodrigo, M., Zacchei, E., Tadeu, A., & Romero, A. (2024). Numerical assessment of the dynamic load allowance on long-span modular steel bridges considering vehicle-bridge interaction. Journal of Physics Conference Series, 2647(4), 42002. https://doi.org/10.1088/1742-6596/2647/4/042002

Chu, T., Bai, G., & Li, J. (2022). Experimental study on seismic performance of steel-concrete connection section of receiver tower of CSP station. Advances in Engineering Technology Research, 2(1), 31. https://doi.org/10.56028/aetr.2.1.31

Chung, P. P., Wang, J., & Durandet, Y. (2019). Deposition processes and properties of coatings on steel fasteners --- A review [Review of Deposition processes and properties of coatings on steel fasteners --- A review]. Friction, 7(5), 389. Springer Nature. https://doi.org/10.1007/s40544-019-0304-4.

Corradi, M., Borri, A., Righetti, L., & Speranzini, E. (2017). Uncertainty analysis of FRP reinforced timber beams. Composites Part B Engineering, 113, 174. https://doi.org/10.1016/j.compositesb.2017.01.030

Corradi, M., Righetti, L., & Borri, A. (2015). Bond Strength of Composite CFRP Reinforcing Bars in Timber. Materials, 8(7), 4034. https://doi.org/10.3390/ma8074034

Costa, R. S., Lavall, A. C. C., Silva, R. G. L. da, Viana, H. F., Rodrigues, F. C., & Andrade, E. L. (2020). New equations to establish the effective moment of inertia of composite slabs with profiled steel sheeting for deflection calculation. Journal of Building Engineering, 37, 102135. https://doi.org/10.1016/j.jobe.2020.102135.

Dersch, M. S., Trizotto, M., Edwards, J. R., & Lima, A. de O. (2021). Quantification of vertical, lateral, and longitudinal fastener demand in broken spike track: Inputs to mechanistic-empirical design. Proceedings of the Institution of Mechanical Engineers Part F Journal of Rail and Rapid Transit, 236(5), 557. https://doi.org/10.1177/09544097211030736

Dobeš, P., Lokaj, A., & Mikolášek, D. (2022). Load-Carrying Capacity of Double-Shear Bolted Connections with Slotted-In Steel Plates in Squared and Round Timber Based on the Experimental Testing, European Yield Model, and Linear Elastic Fracture Mechanics. Materials, 15(8), 2720. https://doi.org/10.3390/ma15082720

Dogra, A., Padhee, S. S., & Singla, E. (2020). Optimal Architecture Planning of Modules for Reconfigurable Manipulators. Robotica, 41(1), 16. https://doi.org/10.1017/s0263574720001174

Duanmu, X., Xu, D., Liu, C., Qiu, T., & Kang, S. (2025). Full-scale testing and numerical modeling of tri-segment precast concrete T-girders with internally bonded tendons. Structural Concrete. https://doi.org/10.1002/suco.70287

Duong, B. N., Truong, M. V., Duong, H. M., & Giang, Q. K. (2023). DISCRETE TIMOSHENKO BEAM MODEL FOR MODELING BEAMS WITH NON-UNIFORM CROSS-SECTIONAL AREA, CURVATURE, AND LARGE DEFLECTION. TRA VINH UNIVERSITY JOURNAL OF SCIENCE. https://doi.org/10.35382/tvujs.13.6.2023.2115

Duriot, R., Pot, G., Girardon, S., & Denaud, L. (2021). New Perspectives for LVL Manufacturing from Wood of Heterogeneous Quality—Part 2: Modeling and Manufacturing of Variable Stiffness Beams. Forests, 12(9), 1275. https://doi.org/10.3390/f12091275

Effendi, M. K., & Awaludin, A. (2022). Nonlinear Finite Element Analysis of Flexural Laminated Veneer Lumber (LVL) Sengon Slender Beam. Civil Engineering Dimension, 24(2), 85. https://doi.org/10.9744/ced.24.2.85-92

Evans, A., Turner, T. A., Harper, L. T., & Warrior, N. A. (2022). Design guidelines for hybrid continuous/discontinuous carbon fibre laminates. Journal of Composite Materials, 56(10), 1513. https://doi.org/10.1177/00219983221078786

Fan, C., Zhuang, Z., Liu, Y., Yang, Y., Zhou, H., & Wang, X. (2024). Bilateral Defect Cutting Strategy for Sawn Timber Based on Artificial Intelligence Defect Detection Model. Sensors, 24(20), 6697. https://doi.org/10.3390/s24206697

Farajian, M., Sharafi, P., Alembagheri, M., Kildashti, K., & Bigdeli, A. (2022). Effects of bolted connections' properties on natural dynamic characteristics of corner-supported modular steel buildings. Structures, 45, 1491. https://doi.org/10.1016/j.istruc.2022.09.077.

Ferrara, G., Helson, O., Michel, L., & Ferrier, E. (2022). Mechanical Characterisation

of GFRP Frame and Beam-to-Column Joints Including Steel Plate Fastened Connections. Materials, 15(23), 8282. https://doi.org/10.3390/ma15238282

Forest Products Laboratory. (2010). Wood handbook—Wood as an engineering material (General Technical Report FPL–GTR–190). Madison, WI: U.S. Department of Agriculture, Forest Service..

Gao, Q., Cui, K., Li, J., Guo, B., & Liu, Y. (2020). Optimal layout of sensors in large-span cable-stayed bridges subjected to moving vehicular loads. International Journal of Distributed Sensor Networks, 16(1). https://doi.org/10.1177/1550147719899376

Gao, S., Xu, M., Guo, N., & Zhang, Y. (2019). Mechanical Properties of Glued-Laminated Timber with Different Assembly Patterns. Advances in Civil Engineering, 2019(1). https://doi.org/10.1155/2019/9495705

Gauthier-Turcotte, É., Ménard, S., & Fiset, M. (2022). Strength and Behaviour of Spruce Pine Glulam Timber Moment Connections Using Glued-In Steel Rods. Journal of Structural Engineering, 148(12). https://doi.org/10.1061/(asce)st.1943-541x.0003486

Ghazali, N. M., Said, M. N. M., Kamarulzaman, A. M. M., & Saad, S. (2023). Recovery of forest structure dynamics following selective logging in lowland dipterocarp Peninsular Malaysia. IOP Conference Series Earth and Environmental Science, 1167(1), 12025. https://doi.org/10.1088/1755-1315/1167/1/012025.

Glišović, I., Pavlović, M., Stevanović, B., & Todorović, M. (2017). NUMERICAL ANALYSIS OF GLULAM BEAMS REINFORCED WITH CFRP PLATES. Journal of Civil Engineering and Management, 23(7), 868. https://doi.org/10.3846/13923730.2017.1341953

Gomes, V. M. G., Rodrigues, M. F., Correia, J. A. F. O., Figueiredo, M., Jesus, A. M. P. D., & Fernandes, A. A. (2019). Monotonic and fracture behaviours of bolted connections with distinct bolt preloads and surface treatments. Frattura Ed Integrità Strutturale, 13(48), 304. https://doi.org/10.3221/igf-esis.48.30.

Gong, C., Sun, D., Chen, Q., Zhu, Y., Shang, M., & Liu, F. (2022). Seismic Performance of Modular Structures with Novel Steel Frame: Light Gauge Slotted Steel Stud Walls. Shock and Vibration, 2022, 1. https://doi.org/10.1155/2022/6926657

Guan, S., Liao, D., Zhang, Y., Shi, J., Liu, S., & Cao, H. (2024). A Unified Deflection Theory Model for Multi-Tower Self-Anchored Suspension Bridges with Different Tower–Girder and Cable–Girder Connections. Buildings, 14(12), 3945.

https://doi.org/10.3390/buildings14123945

Gubana, A., Melotto, M., Cillia, L. D., & Mazelli, A. (2023). Experimental investigation on long-term behaviour of timber-to-timber shear connections made by inclined self-tapping screws. 586. https://doi.org/10.52202/069179-0080.

Gulo, I. N. K., & Aulia, A. P. (2025). Life Cycle Assessment of Bridge Infrastructure Materials. Momentum International Journal of Civil Engineering (MIJCE), 1(1), 20. https://doi.org/10.64123/mijce.v1.i1.4

Guo, J., & Shu, Z. (2019). Theoretical Evaluation of Moment Resistance for Bolted Timber Connections. MATEC Web of Conferences, 303, 3003. https://doi.org/10.1051/matecconf/201930303003

Guo, N., Zhang, Y., Mei, L., & Zhao, Y. (2022). Experimental Study on Flexural Performance of the Prestressed Glulam Continuous Beam after Long-Term Loading. Buildings, 12(7), 895. https://doi.org/10.3390/buildings12070895

Halicka, A., & Ślósarz, S. (2021). Strengthening of timber beams with pretensioned CFRP strips. Structures, 34, 2912. https://doi.org/10.1016/j.istruc.2021.09.055

Halim, N. H. A., Jiang, J., Abdu, A., Karam, D. S., Rajoo, K. S., Ibrahim, Z., & Aman, S. (2024). Impact of Malayan Uniform System and Selective Management System of logging on soil quality in selected logged-over forest in Johor, Malaysia. Forests, 15(5), 838. https://doi.org/10.3390/f15050838.

Han, F., Jiang, J., Xu, K., & Wang, N. (2019). Damage Detection of Common Timber Connections Using Piezoceramic Transducers and Active Sensing. Sensors, 19(11), 2486. https://doi.org/10.3390/s19112486

Han, X., Dai, J., Qian, W., Zhaoyang, Z., & Li, B. (2021). Effects of dowels on the mechanical properties of wooden composite beams in ancient timber structures. BioResources, 16(4), 6891. https://doi.org/10.15376/biores.16.4.6891-6909

Hannard, F., Mirkhalaf, M., Ameri, A., & Barthelat, F. (2021). Segmentations in fins enable large morphing amplitudes combined with high flexural stiffness for fish-inspired robotic materials. Science Robotics, 6(57). https://doi.org/10.1126/scirobotics.abf9710

Harrach, D., & Rad, M. M. (2021). Numerical flexural strengthening investigation of timber-CFRP composite beams. IOP Conference Series Materials Science and Engineering, 1141(1), 12010. https://doi.org/10.1088/1757-899x/1141/1/012010.

Hasan, R., Samah, A. F. A., & Shamsudin, Z. (2024). Comparison of Young's modulus determination from ultrasonic testing and three-point bending testing. Journal of

Advanced Research in Applied Mechanics, 121(1), 58. https://doi.org/10.37934/aram.121.1.5865.

Hashemi, S. M., & Ayoub, A. (2024). Improved Bond Stress-Slip Relationships for Carbon Fibre-Reinforced Polymer-Strengthened Masonry Triplets. Buildings, 14(1), 257. https://doi.org/10.3390/buildings14010257

Hassan, O. (2024). Effect of wooden floorboards on the vibration of timber floor. Scientific Reports, 14(1). https://doi.org/10.1038/s41598-023-50015-5.

He, M., Wang, Y., Li, Z., Zhou, L., Tong, Y., & Sun, X. (2022). An Experimental and Analytical Study on the Bending Performance of CFRP-Reinforced Glulam Beams. Frontiers in Materials, 8. https://doi.org/10.3389/fmats.2021.802249

He, Y., Li, J., He, W., Wu, Q., Xiang, Y., & Yang, Y. (2025). Static Behaviour of Post-Installed High-Strength Large-Bolt Shear Connector with Fabricated Hybrid Fibre-Reinforced Concrete/Ordinary Concrete Deck. Materials, 18(5), 1091. https://doi.org/10.3390/ma18051091

Huang, S., Xi, Y., Li, X., Men, P., & WU, G. (2024). Flexural behaviour of damaged concrete T-beams reinforced with ultra-high performance concrete filling. Frontiers in Materials, 11. https://doi.org/10.3389/fmats.2024.1410016

Hunegnaw, C. B., Alemu, E. B., & Endalew, H. E. (2024a). Numerical Investigation of Response of Steel Frames with Various Types of Beam-Column Connections under Impact Load. Research Square (Research Square). https://doi.org/10.21203/rs.3.rs-4218237/v1

Hussein, H. A., & Razzaq, Z. (2021). Strengthening prestressed concrete bridge girders and building beams with carbon fibre reinforced polymer sheets. European Journal of Engineering and Technology Research, 6(1), 55. https://doi.org/10.24018/ejeng.2021.6.1.2323.

Islam, Md. M., Siddique, A., Pourhassan, A., Chowdhury, Md. A., & Tasnim, J. (2019). Flexural Capacity Enhancement of Timber Beams Partially Confining the Principal Compression Arch using Carbon Fibre Reinforced Polymer Composites. Transportation Research Record Journal of the Transportation Research Board, 2673(11), 276. https://doi.org/10.1177/0361198119851051

İşleyen, Ü. K., Ghoroubı, R., Mercimek, Ö., Anıl, Ö., Toğay, A., & Erdem, R. T. (2021). Effect of anchorage number and CFRP strips length on behaviour of strengthened glulam timber beam for flexural loading. Advances in Structural Engineering, 24(9), 1869. https://doi.org/10.1177/1369433220988622

Jagadeesh, P., Puttegowda, M., Boonyasopon, P., Rangappa, S. M., Khan, A., & Siengchin, S. (2022). Recent developments and challenges in natural fibre composites: A review [Review of Recent developments and challenges in natural fibre composites: A review]. Polymer Composites, 43(5), 2545. Wiley. https://doi.org/10.1002/pc.26619

Jahedi, S., Muszyñski, L., Riggio, M., & Bhandari, S. (2024). Bending characteristics of custom CLT layups laminated with Ponderosa Pine harvested from restoration programs. Wood and Fibre Science, 55(3), 282. https://doi.org/10.22382/wfs-2023-23.

Jaramillo, J. S. Z., & Fischer, E. C. (2023). The role of intermodular connections in the global behaviour of high-rise mass timber buildings. 2650. https://doi.org/10.52202/069179-0348

Kafle, B., Zhang, L., Mendis, P., Herath, N., Maizuar, M., Duffield, C., & Thompson, R. G. (2016). Monitoring the dynamic behaviour of The Merlynston Creek Bridge using interferometric radar sensors and finite element modeling. International Journal of Applied Mechanics, 9(1), 1750003. https://doi.org/10.1142/s175882511750003x.

Kang, J., Wei, D., & Huang, Y. (2023). A BIM-based automatic design optimization method for modular steel structures: Rectangular modules as an example. Buildings, 13(6), 1410. https://doi.org/10.3390/buildings13061410.

Kasal, A., Ulun, M. B., & Kuşkun, T. (2025). Effects of the semi-rigidity coefficients on numerical analysis results in chair side frame joints. Turkish Journal of Forestry | Türkiye Ormancılık Dergisi, 26(3), 384. https://doi.org/10.18182/tjf.1692670

Khan, K., & Yan, J. (2021). Numerical studies on the seismic behaviour of a prefabricated multi-storey modular steel building with new-type bolted joints. https://doi.org/10.18057/ijasc.2021.17.1.1

Khan, K., Chen, Z., Liu, J., & Yan, J. (2021). Simplified modelling of novel non-welded joints for modular steel buildings. https://doi.org/10.18057/ijasc.2021.17.4.10

Grześkiewicz, M., Krzosek, S., Burawska-Kupniewska, I., Borysiuk, P., & Mańkowski, P. (2023). Influence of Thermo-Mechanical Densification (TMD) on the Properties of Structural Sawn Timber (Pinus sylvestris L.). Forests, 14(2), 231. https://doi.org/10.3390/f14020231

KILINÇARSLAN, Ş., TÜRKER, Y. Ş., & Avcar, M. (2023). Numerical and Experimental Evaluation of the Mechanical Behaviour of FRP-Strengthened Solid

and Glulam Timber Beams. Journal of Engineering Management and Systems Engineering, 2(3), 158. https://doi.org/10.56578/jemse020303

Kurzinski, S., & Crovella, P. (2023). THEORETICAL AND EXPERIMENTAL INVESTIGATION ON PREDICTING LONGITUDINAL AND TANGENTIAL ELASTIC CONSTANTS AND RATIOS OF WOOD. 376. https://doi.org/10.52202/069179-0051

Kyowa Electronic Instruments Co., Ltd. (2021). Strain gages and adhesives: Handling and installation manual. Tokyo, Japan: Kyowa Electronic Instruments Co., Ltd. Available at: https://www.kyowa-ei.com. (Accessed: 13 January 2026).

Lacey, A. W., Chen, W., Hao, H., Bi, K., & Tallowin, F. J. (2019). Shear behaviour of post-tensioned inter-module connection for modular steel buildings. Journal of Constructional Steel Research, 162, 105707. https://doi.org/10.1016/j.jcsr.2019.105707

Lakshmidevi, M. T., Reddy, K. S. K. K., Al-Ameri, R., & Kafle, B. (2025). A Review on Design Considerations and Connection Techniques in Modular Composite Construction [Review of A Review on Design Considerations and Connection Techniques in Modular Composite Construction]. Applied Sciences, 15(10), 5256. Multidisciplinary Digital Publishing Institute. https://doi.org/10.3390/app15105256

Lee, I.-H., Song, Y.-J., & Hong, S. I. (2023). Creep behaviour and prediction of fibre-reinforced polymer reinforced timbers under changing temperature and relative humidity. BioResources, 18(4), 7239. https://doi.org/10.15376/biores.18.4.7239-7250.

Lee, I.-H., Song, Y.-J., & Hong, S.-I. (2020). Evaluation of the compression strength performance of fibre-reinforced polymer (FRP) and steel-reinforced laminated timber composed of small-diameter timber. BioResources, 16(1), 633. https://doi.org/10.15376/biores.16.1.633-642

Li, J., Andersen, L. V., & Hudert, M. (2023). The Potential Contribution of Modular Volumetric Timber Buildings to Circular Construction: A State-of-the-Art Review Based on Literature and 60 Case Studies [Review of The Potential Contribution of Modular Volumetric Timber Buildings to Circular Construction: A State-of-the-Art Review Based on Literature and 60 Case Studies]. Sustainability, 15(23), 16203. Multidisciplinary Digital Publishing Institute. https://doi.org/10.3390/su152316203

Li, J., Cui, Y., Xiong, D., Zhongmei, L., Xu, D., Zhang, H., Cui, F., & Zhou, T. (2023). Experimental Study on the Bending Resistance of Hollow Slab Beams Strengthened with Prestressed Steel Strand Polyurethane Cement Composite. Coatings, 13(2), 458. https://doi.org/10.3390/coatings13020458

Li, J., & Zhang, H. (2020). Moving Load Spectrum for Analyzing the Extreme Response of Bridge Free Vibration. Shock and Vibration, 2020, 1. https://doi.org/10.1155/2020/9431620

Li, W., Qiu, J., Wang, Y., & Zhang, K. (2024). Test and Analysis of Reinforced Concrete Beams Reinforced by Polyurethane Concrete-Prestressed Steel Wire (PUC-PSW). Preprints.Org. https://doi.org/10.20944/preprints202407.2083.v1

Liu, J., Huang, X., Chen, J., & Wu, Q. (2023). Effect of Shear Deformation at Segmental Joints on the Short-Term Deflection of Large-Span Cantilever Cast Prestressed Concrete Box Girders. Buildings, 13(1), 219. https://doi.org/10.3390/buildings13010219

Liu, L., Wang, L., & Xiao, Z. (2024). Flexural behaviour of RC beams reinforced by ECC layer and steel plate: numerical simulation. International Journal of Structural Integrity, 15(3), 498. https://doi.org/10.1108/ijsi-08-2023-0083

Liu, L., Wang, X., Zhou, Y., & Qin, J. (2019). Vibration Mitigation Effect Investigation of a New Slab Track Plate Design. Sensors, 19(1), 168. https://doi.org/10.3390/s19010168

Liu, Q., Ma, S., & Han, X. (2020). Study on the flexural behaviour of poplar beams externally strengthened by BFRP strips. Journal of Wood Science, 66(1). https://doi.org/10.1186/s10086-020-01887-y

Liu, R., Liu, J., Wu, Z., Chen, L., & Wang, J. (2022). A Study on the Influence of Bolt Arrangement Parameters on the Bending Behaviour of Timber–Steel Composite (TSC) Beams. Buildings, 12(11), 2013. https://doi.org/10.3390/buildings12112013

Liu, Y., & Xiong, H. (2018). Lateral performance of a semi-rigid timber frame structure: theoretical analysis and experimental study. Journal of Wood Science, 64(5), 591. https://doi.org/10.1007/s10086-018-1727-7

Maizuar, M., Zhang, L., Miramini, S., Mendis, P., & Thompson, R. G. (2017). Detecting structural damage to bridge girders using radar interferometry and computational modelling. Structural Control and Health Monitoring, 24(10). https://doi.org/10.1002/stc.1985

Mamat, M. R., & Ahmad, W. M. S. W. (2020). Connector design selection for modular forest bridge using finite element analysis. In Lecture notes in civil engineering (p. 169). Springer Nature. https://doi.org/10.1007/978-981-15-1193-6_19.

Mamat, M. R., Hashim, M. H. M., & Nor, N. M. (2025). Reassessing Tension Side Reinforcement in Modular Timber Beams: Insights from Experimental Modal Analysis in Forest Bridge Systems. Jurnal Kejuruteraan, 37(3), 1131. https://doi.org/10.17576/jkukm-2025-37(3)-05

Mansour, W., Li, W., Wang, P., Fame, C. M., Tam, L., Lu, Y., Sobuz, Md. H. R., & Elwakkad, N. Y. (2024). Improving the Flexural Response of Timber Beams Using Externally Bonded Carbon Fibre-Reinforced Polymer (CFRP) Sheets. Materials, 17(2), 321. https://doi.org/10.3390/ma17020321

Mao, Q., Zhang, Z., & Ma, H. (2021). Flexural Performance of Emulsified-Asphalt-Modified ECC for Expansion Joint Use. Advances in Civil Engineering, 2021(1). https://doi.org/10.1155/2021/6640167

Medhlom, M., & Abed, E. N. (2023). Behaviour and Load Capacity of Concrete Slab Reinforced by CFRP Bar and Strengthening by CFRP Laminates. Civil and Environmental Engineering, 19(1), 72. https://doi.org/10.2478/cee-2023-0007

Miao, X., Huang, X., Ding, P., Li, Y., & Li, S. (2022). The study of mixed mode fatigue crack growth mechanism of 25CrNiMo compact tensile specimens by experiment and finite element simulation. Proceedings of the Institution of Mechanical Engineers Part C Journal of Mechanical Engineering Science, 237(12), 2887. https://doi.org/10.1177/09544062221141846.

Milani, C. J., Yepes, V., & Kripka, M. (2020). Proposal of sustainability indicators for the design of small-span bridges. International Journal of Environmental Research and Public Health, 17(12), 4488. https://doi.org/10.3390/ijerph17124488.

Mishra, K. K., Shashikala, S., Solanki, A. A., & Sethy, A. K. (2025). A comprehensive evaluation of anatomical and physico-mechanical properties of 40-year-old Swietenia macrophylla King wood from India. International Wood Products Journal, 16(3), 206. https://doi.org/10.1177/20426445251361775

Miyamoto, A., Kiviluoma, R., & Yabe, A. (2018). Frontier of continuous structural health monitoring system for short & medium span bridges and condition assessment. Frontiers of Structural and Civil Engineering, 13(3), 569. https://doi.org/10.1007/s11709-018-0498-y.

Moawad, M. S., & Fawzi, A. (2021). Performance of concrete beams partially/fully

reinforced with glass fibre polymer bars. Journal of Engineering and Applied Science, 68(1). https://doi.org/10.1186/s44147-021-00028-6.

Mohamed, Y. S., Wan, B., Chang, L., & Abdelbary, A. (2024). Experimental and numerical study of the effects of fibre orientation on stress concentration of CFRE. Journal of Reinforced Plastics and Composites, 44, 1205. https://doi.org/10.1177/07316844241238834

Morais, P. do P., Arima, E., Souza, Ã. N. de, Pereira, R. S., Emmert, F., Cardoso, R. M., Miguel, É. P., & Matricardi, E. A. T. (2023). Assessment of forest road models in concession areas in the Brazilian Amazon. Forests, 14(7), 1388. https://doi.org/10.3390/f14071388.

Museros, P., Moliner, E., & Martínez-Rodrigo, M. D. (2012). Free vibrations of simply-supported beam bridges under moving loads: Maximum resonance, cancellation and resonant vertical acceleration. Journal of Sound and Vibration, 332(2), 326. https://doi.org/10.1016/j.jsv.2012.08.008

Muthumala, C. K., Silva, S. D., Alwis, P. L. A. G., & Arunakumara, K. K. I. U. (2022). Strength index-based timber classification of Sri Lankan timbers and potential for finger-joint production from wood off-cuts. International Wood Products Journal, 13(4), 263. https://doi.org/10.1080/20426445.2022.2117929

Navaratnam, S., Small, D. W., Corradi, M., Gatheeshgar, P., Poologanathan, K., & Higgins, C. (2022). Numerical modelling of timber beams with GFRP pultruded reinforcement. Buildings, 12(11), 1992. https://doi.org/10.3390/buildings12111992.

Nazari, S., Ivanova, T., Mishra, R., Müller, M., Akhbari, M., & Hashjin, Z. E. (2024). Effect of Natural Fibre and Biomass on Acoustic Performance of 3D Hybrid Fabric-Reinforced Composite Panels. Materials, 17(23), 5695. https://doi.org/10.3390/ma17235695

Niu, R., Yang, Y., Liu, Z., Ding, Z., Peng, H., & Fan, Y. (2023). Durability of Two Epoxy Adhesive BFRP Joints Dipped in Seawater under High Temperature Environment. Polymers, 15(15), 3232. https://doi.org/10.3390/polym15153232

Güntekin, E. (2023). Determination of elastic constants for scots pine wood using ultrasound. Turkish Journal of Forestry | Türkiye Ormancılık Dergisi. https://doi.org/10.18182/tjf.1294030

Offerman, T., & Bompa, D. V. (2023). Numerical investigation of lateral behaviour of steel-timber hybrid frames. Ce/Papers, 6, 470. https://doi.org/10.1002/cepa.2339

Oliveira, S. C. D., Silva, G. S., Christoforo, A. L., & Aquino, V. B. de M. (2025). Proposal for Correction on the Gamma Method for Estimating the Displacement of CLT Plates. https://doi.org/10.21203/rs.3.rs-7474159/v1

Oliveira, G., Magalhães, F., Cunha, Á., & Caetano, E. (2015). Automated modal tracking and fatigue assessment of a wind turbine based on continuous dynamic monitoring. MATEC Web of Conferences, 24, 4005. https://doi.org/10.1051/matecconf/20152404005

Olsson, A., Schirén, W., & Hu, M. (2024). Dynamic and Quasi-Static Evaluation of Stiffness Properties of CLT: Longitudinal MoE and Effective Rolling Shear Modulus. Research Square (Research Square). https://doi.org/10.21203/rs.3.rs-4221960/v1

Opazo-Vega, A., Rosales, V., & Oyarzo-Vera, C. (2021). Non-destructive assessment of the dynamic elasticity modulus of Eucalyptus nitens timber boards. Materials, 14(2), 269. https://doi.org/10.3390/ma14020269.

Ormarsson, S., Vessby, J., Johansson, M., & Kua, L. (2019). Numerical and Experimental Study on Modular-Based Timber Structures. Modular and Offsite Construction (MOC) Summit Proceedings, 471. https://doi.org/10.29173/mocs128

Ostrowska, A., & Chmielewski, R. (2023). Overview of the organisation and technology of portable panel bridges. Inżynieria Bezpieczeństwa Obiektów Antropogenicznych, 1, 46. https://doi.org/10.37105/iboa.167.

Pacheco, C., Plata-Rocha, W., Serrano, J., Vilanova, E., Monjardín-Armenta, S. A., González, A., & Roa, C. C. (2021). A low-cost and robust Landsat-based approach to study forest degradation and carbon emissions from selective logging in the Venezuelan Amazon. Remote Sensing, 13(8), 1435. https://doi.org/10.3390/rs13081435.

Pan, Z., Ma, F., Cao, B., Mo, Z., Liu, J., Shi, R., & He, Z. (2024). Optimization of the Mechanical Properties of Bolted Connections between Concrete-Filled Tubular Columns and Steel Beam with Reinforcing Rings. Buildings, 14(3), 782. https://doi.org/10.3390/buildings14030782

Pasca, D. P., Aloisio, A., Fragiacomo, M., & Tomasi, R. (2021). Dynamic Characterization of Timber Floor Subassemblies: Sensitivity Analysis and Modeling Issues. Journal of Structural Engineering, 147(12). https://doi.org/10.1061/(asce)st.1943-541x.0003179

Premrov, M., & Leskovar, V. Ž. (2023). Innovative Structural Systems for Timber

Buildings: A Comprehensive Review of Contemporary Solutions [Review of Innovative Structural Systems for Timber Buildings: A Comprehensive Review of Contemporary Solutions]. Buildings, 13(7), 1820. Multidisciplinary Digital Publishing Institute. https://doi.org/10.3390/buildings13071820

Puaad, M. B. F. M., Ahmad, Z., Bhkari, N. M., Ibrahim, M. J. M., Noh, N., Moham-mad, S. N., & Ismail, H. B. (2024). DEVELOPMENT OF A CORRELATION MODEL FOR TORSIONAL SHEAR MODULUS PROPERTIES BETWEEN STRUCTURAL SIZE SPECIMENS BASED ON EN 384:2016 AND SMALL CLEAR SPECIMENS (MS544: PART 2). Jurnal Teknologi, 86(6), 39. https://doi.org/10.11113/jurnalteknologi.v86.20819

Pupsys, T., Corradi, M., Borri, A., & Amess, L. (2017). Bending Reinforcement of Full-Scale Timber Beams with Mechanically Attached GFRP Composite Plates. Key Engineering Materials, 747, 212. https://doi.org/10.4028/www.scientific.net/kem.747.212

Putz, F. E., Romero, C., Sist, P., Schwartz, G., Thompson, I. D., Roopsind, A., Ruslandi, Medjibe, V. P., & Ellis, P. W. (2022). Sustained timber yield claims, considerations, and tradeoffs for selectively logged forests. PNAS Nexus, 1(3). https://doi.org/10.1093/pnasnexus/pgac102

Radhakrishnan, G., Khusaibi, S. S. A., Subaihi, A. J. A., Ismaili, A. A. Z. A., & Maani, A. S. M. A. (2023). Experimental Study on the Influence of Stress Concentration on the Flexural Stability of Aluminum Hollow Tube. The International Journal of Mechanical Engineering and Sciences, 7(1), 1. https://doi.org/10.12962/j25807471.v7i1.14328

Rajanayagam, H., Gunawardena, T., Mendis, P., Poologanathan, K., Gatheeshgar, P., Nagaratnam, B., & Corradi, M. (2023). Experimental and Numerical Study on Shear Behaviour of Bolted Inter-Modular Connection. Ce/Papers, 6, 1375. https://doi.org/10.1002/cepa.2606

Rebouças, A. S., Mehdipour, Z., Branco, J. M., & Lourénço, P. B. (2022). Ductile Moment-Resisting Timber Connections: A Review [Review of Ductile Moment-Resisting Timber Connections: A Review]. Buildings, 12(2), 240. Multidisciplinary Digital Publishing Institute. https://doi.org/10.3390/buildings12020240

Reynolds, T., Casagrande, D., & Tomasi, R. (2015). Comparison of multi-storey cross-laminated timber and timber frame buildings by in situ modal analysis.

Construction and Building Materials, 102, 1009. https://doi.org/10.1016/j.conbuildmat.2015.09.056

Ro, K. M., Kim, M. S., Cho, C., & Lee, Y. H. (2021). Structural Performance of a Precast Concrete Modular Beam Using Bolted Connecting Plates. Applied Sciences, 11(24), 12110. https://doi.org/10.3390/app112412110

Robin, C., MacNamara, E., Needham, H., & Wise, C. (2025). Ava Footbridge: Design for Manufacture and Back to Structural Basics. https://doi.org/10.24904/footbridge2025.44

Saad, K., & Lengyel, A. (2020). Inverse Calculation of Timber-CFRP Composite Beams Using Finite Element Analysis. Periodica Polytechnica Civil Engineering. https://doi.org/10.3311/ppci.16527

Saad, K., & Lengyel, A. (2022). Experimental, Analytical, and Numerical Assessments for the Controversial Elastic Stiffness Enhancement of CFRP-Strengthened Timber Beams. Polymers, 14(19), 4222. https://doi.org/10.3390/polym14194222

Salehi, M., Sideris, P., & Liel, A. B. (2021). Experimental testing of hybrid sliding-rocking bridge columns under torsional and biaxial lateral loading. Earthquake Engineering & Structural Dynamics, 50(10), 2817. https://doi.org/10.1002/eqe.3474

Sarrazin, J., & Valerio, G. (2022). Multibeam Leaky-Wave Antenna for Mm-wave Wide-Angular-Range AoA Estimation. 2022 16th European Conference on Antennas and Propagation (EuCAP), 1. https://doi.org/10.23919/eucap53622.2022.9769571

Schenk, D., & Amiri, A. (2022). Life cycle energy analysis of residential wooden buildings versus concrete and steel buildings: A review [Review of Life cycle energy analysis of residential wooden buildings versus concrete and steel buildings: A review]. Frontiers in Built Environment, 8. Frontiers Media. https://doi.org/10.3389/fbuil.2022.975071

Shabaev, A. (2021). Manufacturing information systems for forestry companies based on integrated modular approach «Many companies---One tool». In Smart innovation, systems and technologies (p. 633). Springer Nature. https://doi.org/10.1007/978-981-16-4177-0_63.

Sheng, G., Sun, J., & Jin, D. (2024). Longitudinal vibrations and their suppression of a tethered satellite system using friction self-excitation mechanism. Journal of Vibration and Control, 31, 4942. https://doi.org/10.1177/10775463241288077

Shi, D., Xu, Y., Demartino, C., Xiao, Y., & Spencer, B. F. (2023). Bio-based laminated truss structures with bolted steel connections: Experiment, modeling, and model-updating. Earthquake Engineering & Structural Dynamics, 53(2), 739. https://doi.org/10.1002/eqe.4043

Shirmohammadi, M. (2023). Study of the hygroscopic properties of three Australian wood species used as solid wood and composite products. European Journal of Wood and Wood Products, 81(6), 1495. https://doi.org/10.1007/s00107-023-01966-z

Shyamala, G., Hemalatha, B., Devarajan, Y., R, C. L. K., Munuswamy, D. B., & Kaliappan, N. (2023). Experimental investigation on the effect of nano-silica on reinforced concrete beam-column connection subjected to cyclic loading. Scientific Reports, 13(1). https://doi.org/10.1038/s41598-023-43882-5.

Silva, S. D., & Liyanage, V. (2019). Suitability of finger jointed structural timber for construction. Journal of Structural Engineering & Applied Mechanics, 2(3), 131. https://doi.org/10.31462/jseam.2019.03131142.

Sist, P., Piponiot, C., Kanashiro, M., Peña-Claros, M., Putz, F. E., Schulze, M., Veríssimo, A., & Vidal, E. (2021). Sustainability of Brazilian forest concessions. Forest Ecology and Management, 496, 119440. https://doi.org/10.1016/j.foreco.2021.119440.

Siva, G. A., & Ramakrishna, S. (2020). Residual life estimation of structural beam using experimental and numerical modal analysis methods. Journal of Mechanical and Energy Engineering, 4(2), 135. https://doi.org/10.30464/jmee.2020.4.2.135.

Song, Y.-J., Baek, S.-Y., & Hong, S.-I. (2024). Evaluation of shear performance of timber-timber composite joints. BioResources, 19(3), 4984. https://doi.org/10.15376/biores.19.3.4984-5002

Sreekanth, G. N., & Balamurugan, S. (2022). “Experimental and Numerical investigation on the effect of CFRP straps with different orientation angles on the strength of the beam.” Revista Romana de Inginerie Civila/Romanian Journal of Civil Engineering, 13(3), 41. https://doi.org/10.37789/rjce.2022.13.3.2

Srikanth, I., Arockiasamy, M., & Nagarajan, S. (2022). Performance of Aging Timber Bridges based on Field Tests and Deterioration Models. Transportation Research Record Journal of the Transportation Research Board, 2676(10), 315. https://doi.org/10.1177/03611981221089297

Taheripour, M., Hatami, F., & Raoufi, R. (2022). NUMERICAL STUDY OF TWO

NOVEL CONNECTIONS WITH SHORT END I OR H STUB IN STEEL STRUCTURES. https://doi.org/10.18057/ijasc.2022.18.1.8

Tao, M., Li, Z., Zhou, Q.-L., & Xu, L. (2021). Analysis of Equivalent Flexural Stiffness of Steel–Concrete Composite Beams in Frame Structures. Applied Sciences, 11(21), 10305. https://doi.org/10.3390/app112110305

Tata, A. (2024). CAPACITY TESTING OF REINFORCED CONCRETE BEAMS USING POST-ULTIMATE LOAD GFRP-S REINFORCEMENT. International Journal of Geomate, 26(116). https://doi.org/10.21660/2024.116.4113

Vedyakov, I. I., Suslov, L. S., Marisiuk, A. A., Kashin, O. V., & Novozhilov, M. V. (2023). Bearing capacity of a steel frame of a multi-storey modular building with consideration of the rigidity of quick-assembled connections. Sejsmostojkoe Stroitel′stvo. Bezopasnost′ Sooruženij/Sejsmostojkoe Stroitel′stvo. Bezopastnost′ Sooruženij, 6, 8. https://doi.org/10.37153/2618-9283-2023-6-8-44

Verstrynge, E., Lacidogna, G., Accornero, F., & Tomor, A. (2020). A review on acoustic emission monitoring for damage detection in masonry structures [Review of A review on acoustic emission monitoring for damage detection in masonry structures]. Construction and Building Materials, 268, 121089. Elsevier BV. https://doi.org/10.1016/j.conbuildmat.2020.121089

Virgen-Cobos, G. H., Olvera-Licona, G., Hermoso, E., & Esteban, M. (2022). Nondestructive techniques for determination of wood mechanical properties of urban trees in Madrid. Forests, 13(9), 1381. https://doi.org/10.3390/f13091381

Vogiatzis, T., Tsalkatidis, T., & Efthymiou, E. (2022). The wall–frame interaction effect in CLT-steel hybrid systems. Frontiers in Built Environment, 8. https://doi.org/10.3389/fbuil.2022.1008973

Wang, X., & Wang, D. (2023). Numerical simulation of initial crack propagation of steel-concrete composite beams based on XFEM. In Advances in transdisciplinary engineering. IOS Press. https://doi.org/10.3233/atde230236.

Wang, H., Zeng, D., Cheng, Y., Wang, P., & Chen, J. (2022). A design-oriented method for response prediction of light-weight timber floors under bouncing excitation. Advances in Structural Engineering, 25(16), 3464. https://doi.org/10.1177/13694332221133598

Wang, H., Zhao, X., & Ma, G. (2022). Experimental study on seismic performance of column-column-beam joint in panelised steel-modular structure. Journal of Constructional Steel Research, 192, 107240.

https://doi.org/10.1016/j.jcsr.2022.107240

Wdowiak-Postulak, A., Bahleda, F., & Prokop, J. (2023). An Experimental and Numerical Analysis of Glued Laminated Beams Strengthened by Pre-Stressed Basalt Fibre-Reinforced Polymer Bars. Materials, 16(7), 2776. https://doi.org/10.3390/ma16072776

Wdowiak-Postulak, A., Gocál, J., Bahleda, F., & Prokop, J. (2023). Load and Deformation Analysis in Experimental and Numerical Studies of Full-Size Wooden Beams Reinforced with Prestressed FRP and Steel Bars. Applied Sciences, 13(24), 13178. https://doi.org/10.3390/app132413178

Wdowiak-Postulak, A., & Świt, G. (2021). Behaviour of Glulam Beams Strengthened in bending with BFRP Fabrics. Civil And Environmental Engineering Reports, 31(2), 1. https://doi.org/10.2478/ceer-2021-0016

Wdowiak-Postulak, A., Świt, G., & Dziedzic-Jagocka, I. (2024). Application of Composite Bars in Wooden, Full-Scale, Innovative Engineering Products—Experimental and Numerical Study. Materials, 17(3), 730. https://doi.org/10.3390/ma17030730

Wdowiak-Postulak, A., Wieruszewski, M., Bahleda, F., Prokop, J., & Brol, J. (2023). Fibre-Reinforced Polymers and Steel for the Reinforcement of Wooden Elements—Experimental and Numerical Analysis. Polymers, 15(9), 2062. https://doi.org/10.3390/polym15092062

Xiao, F., Meng, D., Yu, Y., Ding, Y., Zhang, L., Chen, G. S., Zatar, W., & Hulsey, J. L. (2019). Estimation of vehicle-induced bridge dynamic responses using fibre Bragg grating strain gages. Science Progress, 103(1). https://doi.org/10.1177/0036850419874201.

Xu, B., Xia, J., Chang, H., Ma, R., & Zhang, L. (2021). Experimental and numerical investigation on the lateral force resistance of modular steel sub-frames with laminated double beam. Journal of Building Engineering, 46, 103666. https://doi.org/10.1016/j.jobe.2021.103666

Yaghoubzadehfard, A., Lumantarna, E., Herath, N., Sofi, M., & Rad, M. (2024). Ensemble learning-based structural health monitoring of a bridge using an interferometric radar system. Journal of Civil Structural Health Monitoring, 14(7), 1629. https://doi.org/10.1007/s13349-024-00789-7.

Yan, W., Chen, L., Han, B., Xie, H., & Sun, Y. (2022). Numerical Model for Flexural Analysis of Precast Segmental Concrete Beam with Internal Unbonded CFRP

Tendons. Materials, 15(12), 4105. https://doi.org/10.3390/ma15124105

Yang, S.-M., Choi, G., Kim, J.-H., Lee, H., & Kang, S. G. (2023). Comparison of mechanical properties according to the structural materials of lumber, GLT, CLT, and Ply-lam CLT. BioResources, 18(4), 6971. https://doi.org/10.15376/biores.18.4.6971-6985

Yang, C., Wei, J., Lei, L., Wei, Z., Sun, C., & Luo, B. (2025). Strength analysis of CFRP hybrid adhesive-bolt interference connection structures under tensile load. Journal of Physics Conference Series, 3102(1), 12055. https://doi.org/10.1088/1742-6596/3102/1/012055

Yassin, M. T., & Othman, T. T. (2024). Dynamic behaviour of pin-free beam with torsional spring and hub at pinned end. Global Journal of Engineering and Technology Advances, 18(2), 149. https://doi.org/10.30574/gjeta.2024.18.2.0022.

Yeoh, D., Leng, V., Jamaluddin, N., Boon, K. H., Jamalaldin, S., Balasbaneh, A. T., & Ghafar, N. H. A. (2023). Bending Performance of Timber Beam Strengthened with Passive Prestressing. International Journal of Sustainable Construction Engineering Technology, 14(3). https://doi.org/10.30880/ijscet.2023.14.03.035

Yoshino, Y., & Kimura, Y. (2025). Strength and Stiffness of Corrugated Plates Subjected to Bending. Buildings, 15(3), 469. https://doi.org/10.3390/buildings15030469

Yu, L. L., Wang, J. J., & Huang, T. Y. (2014). Mechanical Properties of Wood and Timber Bridge Evaluation. Applied Mechanics and Materials, 1381. https://doi.org/10.4028/www.scientific.net/amm.587-589.1381

Zhang, H., Chen, L., & Zhou, L. (2024). Structural finite element modeling and static analysis of the bridge modular expansion joint under vehicle load. 46. https://doi.org/10.1117/12.3010369

Zhang, J., Zhao, F., Deng, E.-F., & Wang, H. (2022). Bending Stiffness of the Floor of the Assembled-Type Light Steel-Modular House. International Journal of Civil Engineering, 20(11), 1363. https://doi.org/10.1007/s40999-022-00740-1

Zhang, Y., Li, X., Zhu, Y., & Shao, X. (2020). Experimental study on flexural behaviour of damaged reinforced concrete (RC) beam strengthened by toughness-improved ultra-high performance concrete (UHPC) layer. Composites Part B Engineering, 186, 107834. https://doi.org/10.1016/j.compositesb.2020.107834

Zhao, K., Wei, Y., Yan, Z., Li, Q., & Fang, X. (2025). Experimental and Analytical Study on the Short-Term Behaviour of Locally Bonded Connections in Bamboo–

UHPC Composite Beams. Materials, 18(6), 1224. https://doi.org/10.3390/ma18061224

Zhu, Z., Zhang, B., & Qian, W. (2023). Study on mechanical properties of poplar timber bending members of ancient buildings strengthened with CFRP sheets embedded. Journal of Computational Methods in Sciences and Engineering, 23(5), 2609. https://doi.org/10.3233/jcm-226868

Zinno, R., Haghshenas, S. S., Guido, G., Rashvand, K., Vitale, A., & Sarhadi, A. (2022). The State of the Art of Artificial Intelligence Approaches and New Technologies in Structural Health Monitoring of Bridges. Applied Sciences, 13(1), 97. https://doi.org/10.3390/app13010097

APPENDICES

APPENDIX 1

Specimen for Experimental Modal Analysis

ETN131

ETN21.52

ETN313

ETN40.754

ETN50.65

ETR136

ETR21.57

ETR318

ETR40.759

ETR50.610

APPENDIX 2

Specimen for Flexural Bending Test

ETN131

ETN21.52

ETN313

ETN40.754

ETN50.65

ETR136

ETR21.57

ETR318

ETR40.759

ETR50.610

APPENDIX 3

Connector Assembly for Segmented Specimen

APPENDIX 4

Raw data from Experimental Modal Analysis

Natural Frequency	Specimen	Flange	Reinforcement	No Segment	Segment Length	Connector
28.200	1	1	0	1	3.00	0
28.050	1	1	0	1	3.00	0
28.067	1	1	0	1	3.00	0
28.017	1	1	0	1	3.00	0
28.017	1	1	0	1	3.00	0
28.583	2	1	0	2	1.50	1
28.633	2	1	0	2	1.50	1
28.600	2	1	0	2	1.50	1
28.650	2	1	0	2	1.50	1
28.567	2	1	0	2	1.50	1
28.467	3	1	0	3	1.00	2
28.450	3	1	0	3	1.00	2
28.483	3	1	0	3	1.00	2
28.467	3	1	0	3	1.00	2
28.500	3	1	0	3	1.00	2
28.067	4	1	0	4	0.75	3
28.417	4	1	0	4	0.75	3
27.967	4	1	0	4	0.75	3
28.450	4	1	0	4	0.75	3
28.433	4	1	0	4	0.75	3
27.567	5	1	0	5	0.60	4
28.317	5	1	0	5	0.60	4
28.300	5	1	0	5	0.60	4
28.300	5	1	0	5	0.60	4
27.733	5	1	0	5	0.60	4
28.250	6	1	1	1	3.00	0
28.267	6	1	1	1	3.00	0
28.250	6	1	1	1	3.00	0
28.350	6	1	1	1	3.00	0
28.300	6	1	1	1	3.00	0
28.050	7	1	1	2	1.50	1
28.083	7	1	1	2	1.50	1
28.050	7	1	1	2	1.50	1
27.933	7	1	1	2	1.50	1
28.033	7	1	1	2	1.50	1
27.750	8	1	1	3	1.00	2
27.650	8	1	1	3	1.00	2
28.100	8	1	1	3	1.00	2
28.083	8	1	1	3	1.00	2
27.650	8	1	1	3	1.00	2
28.233	9	1	1	4	0.75	3
28.250	9	1	1	4	0.75	3
27.983	9	1	1	4	0.75	3
28.100	9	1	1	4	0.75	3
28.117	9	1	1	4	0.75	3
28.017	10	1	1	5	0.60	4
27.933	10	1	1	5	0.60	4
28.117	10	1	1	5	0.60	4
28.033	10	1	1	5	0.60	4
28.050	10	1	1	5	0.60	4
28.000	1	2	0	1	3.00	0

28.017	1	2	0	1	3.00	0
28.417	1	2	0	1	3.00	0
28.067	1	2	0	1	3.00	0
28.450	1	2	0	1	3.00	0
28.183	2	2	0	2	1.50	1
28.217	2	2	0	2	1.50	1
28.200	2	2	0	2	1.50	1
28.217	2	2	0	2	1.50	1
28.217	2	2	0	2	1.50	1
28.650	3	2	0	3	1.00	2
28.617	3	2	0	3	1.00	2
28.650	3	2	0	3	1.00	2
28.600	3	2	0	3	1.00	2
28.617	3	2	0	3	1.00	2
28.283	4	2	0	4	0.75	3
28.417	4	2	0	4	0.75	3
28.467	4	2	0	4	0.75	3
28.150	4	2	0	4	0.75	3
28.167	4	2	0	4	0.75	3
27.433	5	2	0	5	0.60	4
28.283	5	2	0	5	0.60	4
27.433	5	2	0	5	0.60	4
27.550	5	2	0	5	0.60	4
28.333	5	2	0	5	0.60	4
7.367	6	2	1	1	3.00	0
7.350	6	2	1	1	3.00	0
7.350	6	2	1	1	3.00	0
7.367	6	2	1	1	3.00	0
7.367	6	2	1	1	3.00	0
28.067	7	2	1	2	1.50	1
28.117	7	2	1	2	1.50	1
28.117	7	2	1	2	1.50	1
28.067	7	2	1	2	1.50	1
28.067	7	2	1	2	1.50	1
27.850	8	2	1	3	1.00	2
27.817	8	2	1	3	1.00	2
27.900	8	2	1	3	1.00	2
27.817	8	2	1	3	1.00	2
27.950	8	2	1	3	1.00	2
27.950	9	2	1	4	0.75	3
28.067	9	2	1	4	0.75	3
28.000	9	2	1	4	0.75	3
27.933	9	2	1	4	0.75	3
28.000	9	2	1	4	0.75	3
27.867	10	2	1	5	0.60	4
28.117	10	2	1	5	0.60	4
27.617	10	2	1	5	0.60	4
27.480	10	2	1	5	0.60	4
28.050	10	2	1	5	0.60	4

APPENDIX 5

Static Stress Analysis FEA

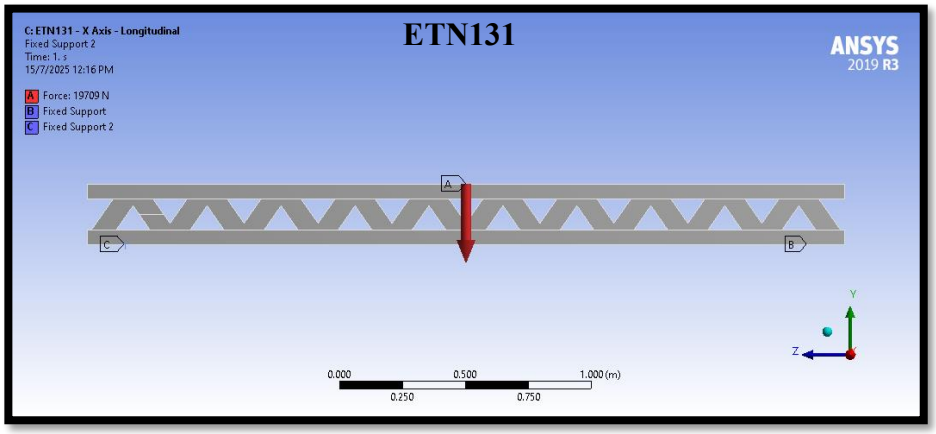

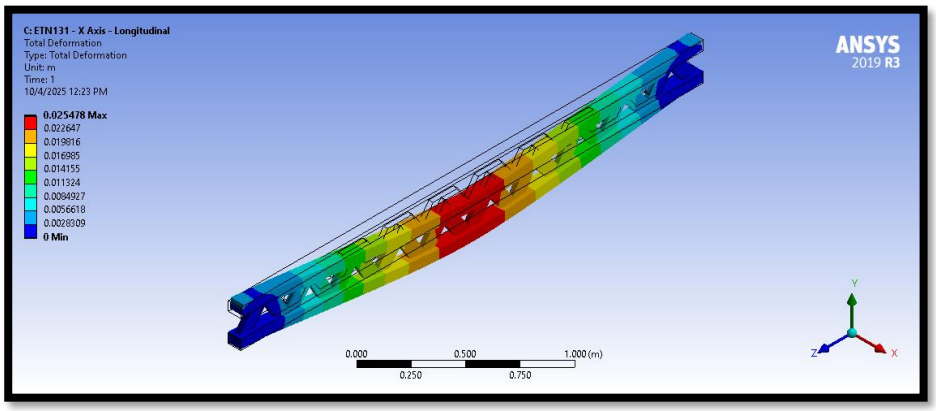

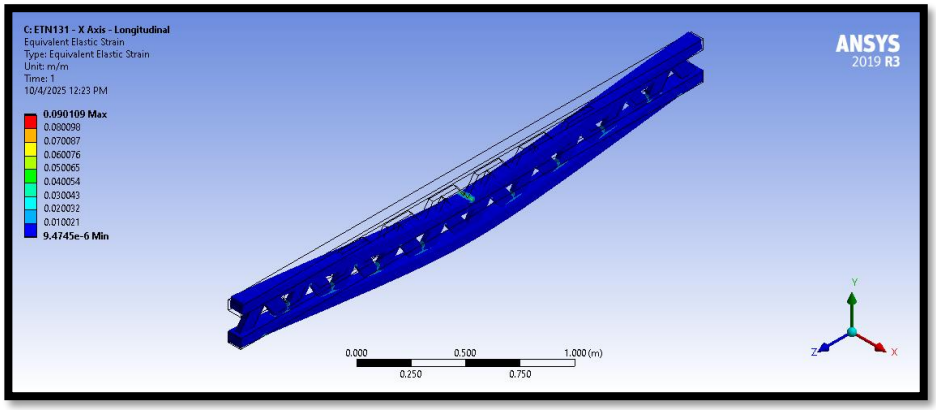

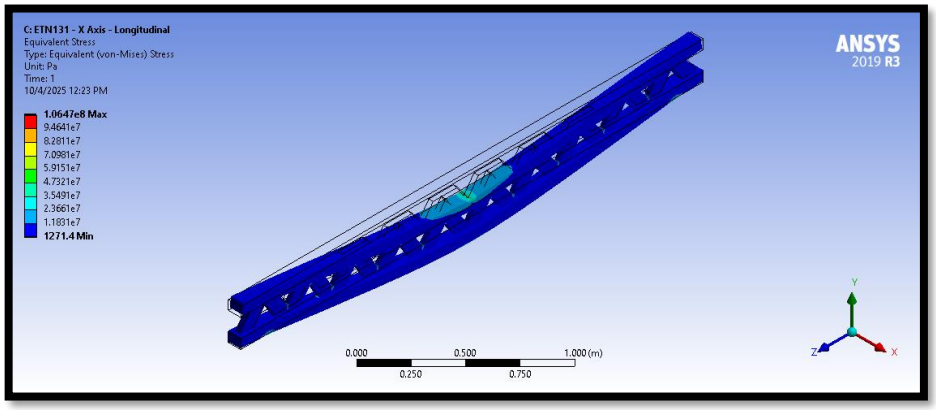

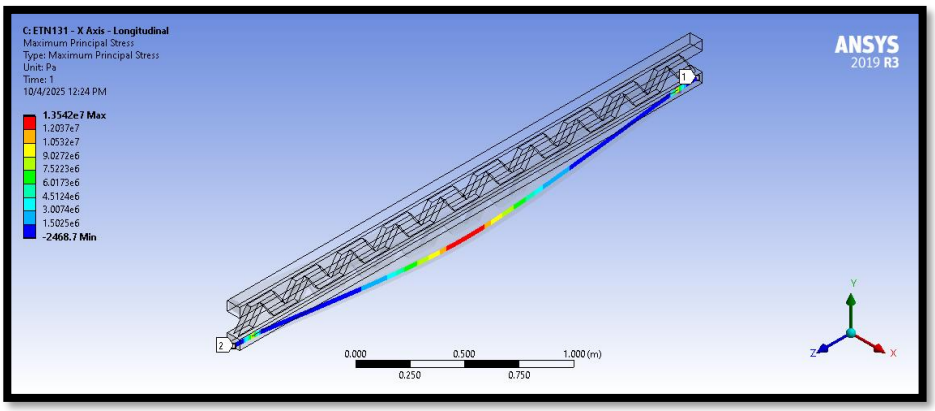
C: ETN131 - X Axis - Longitudinal
Maximum Principal Stress
Type: Maximum Principal Stress
Unit: Pa
Time: 1
10/4/2025 12:24 PM
1.3542e7 Max
1.2037e7
1.0532e7
9.0272e6
7.5223e6
6.0173e6
4.5124e6
3.0074e6
1.5025e6
-2468.7 Min
ANSYS
2019 R3
0.000
0.500
1.000 (m)
0.250
0.750
Y
Z
X

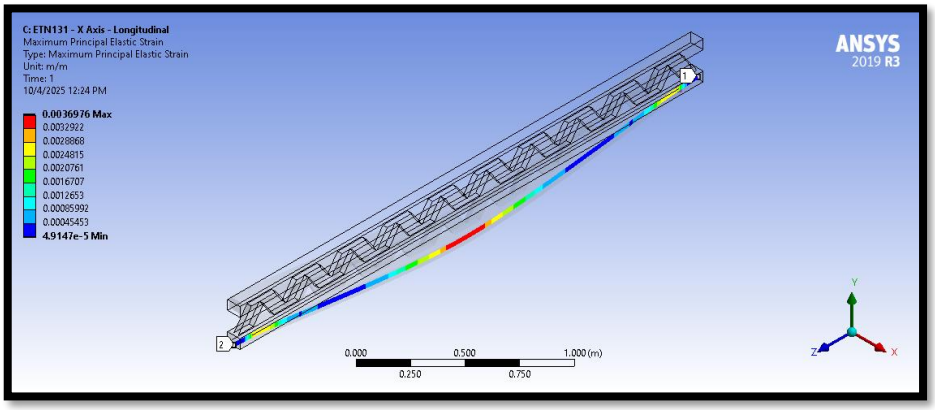
C: ETN131 - X Axis - Longitudinal
Maximum Principal Elastic Strain
Type: Maximum Principal Elastic Strain
Unit: m/m
Time: 1
10/4/2025 12:24 PM
0.0036976 Max
0.0032922
0.0028868
0.0024815
0.0020761
0.0016707
0.0012653
0.00085992
0.00045453
4.9147e-5 Min
ANSYS
2019 R3
0.000
0.500
1.000 (m)
0.250
0.750
Y
Z
X

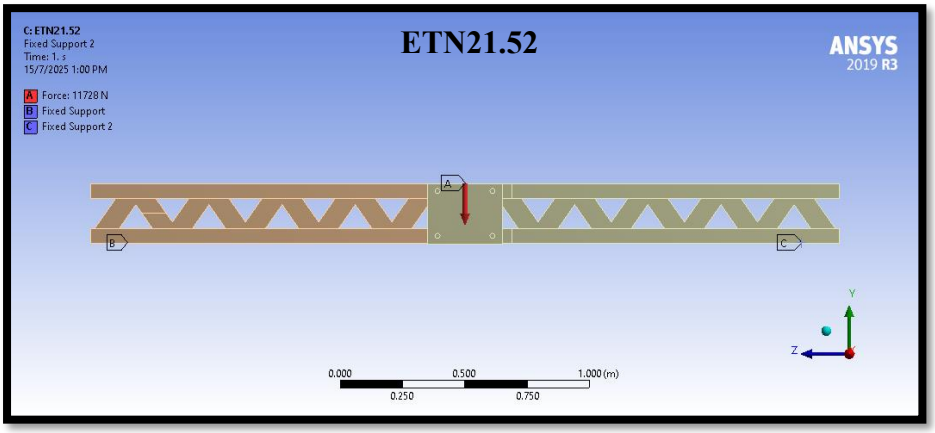
C: ETN21.52
Fixed Support 2
Time: 1. s
15/7/2025 1:00 PM
A Force: 11728 N
B Fixed Support
C Fixed Support 2
ETN21.52
ANSYS
2019 R3
A
B
C
0.000
0.500
1.000 (m)
0.250
0.750
Y
Z

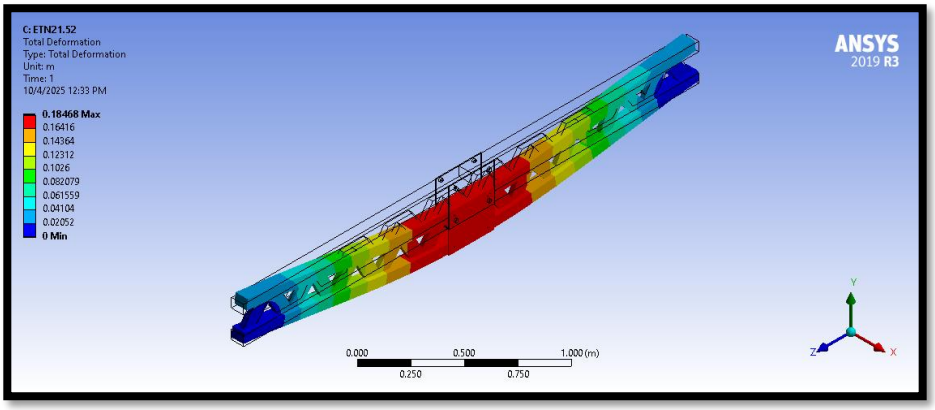
C: ETN21.52
Total Deformation
Type: Total Deformation
Unit: m
Time: 1
10/4/2025 12:33 PM
0.18468 Max
0.16416
0.14364
0.12312
0.1026
0.082079
0.061559
0.04104
0.02052
0 Min
ANSYS
2019 R3
0.000
0.500
1.000 (m)
0.250
0.750
Y
Z
X

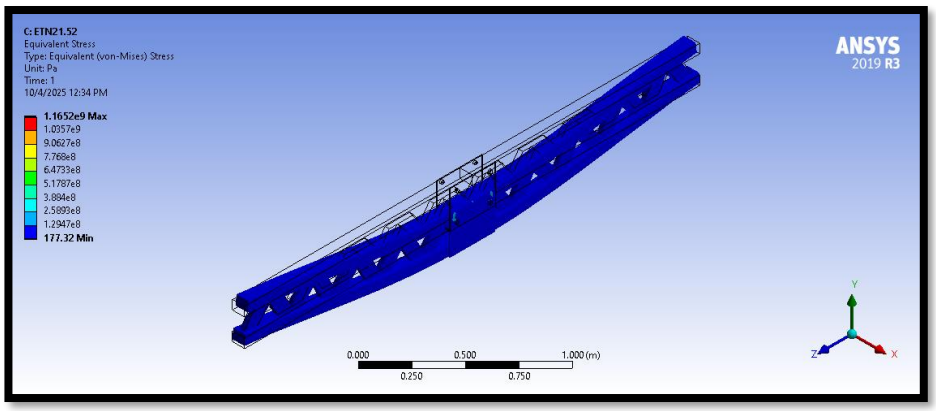
C: ETN21.52
Equivalent Stress
Type: Equivalent (von-Mises) Stress
Unit: Pa
Time: 1
10/4/2025 12:34 PM
1.1652e9 Max
1.0357e9
9.0627e8
7.768e8
6.4733e8
5.1787e8
3.884e8
2.5893e8
1.2947e8
177.32 Min
ANSYS
2019 R3
0.000
0.500
1.000 (m)
0.250
0.750
Y
Z
X

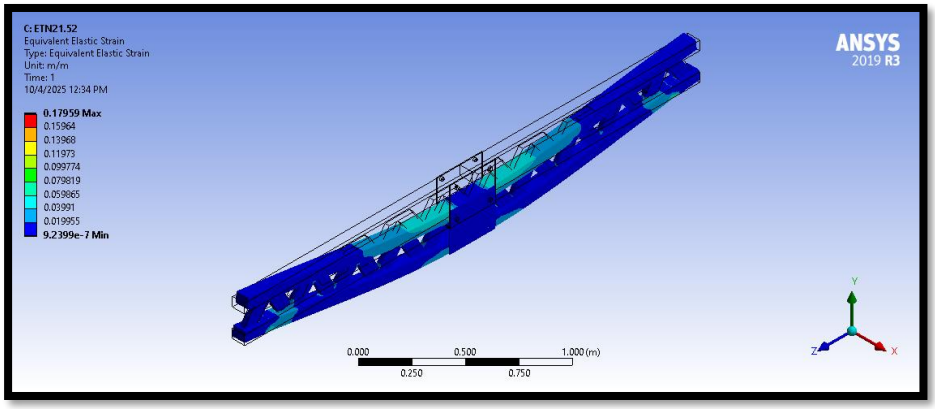
C: ETN21.52
Equivalent Elastic Strain
Type: Equivalent Elastic Strain
Unit: m/m
Time: 1
10/4/2025 12:34 PM
0.17959 Max
0.15964
0.13968
0.11973
0.099774
0.079819
0.059865
0.03991
0.019955
9.2399e-7 Min
ANSYS
2019 R3
0.000
0.500
1.000 (m)
0.250
0.750
Y
Z
X

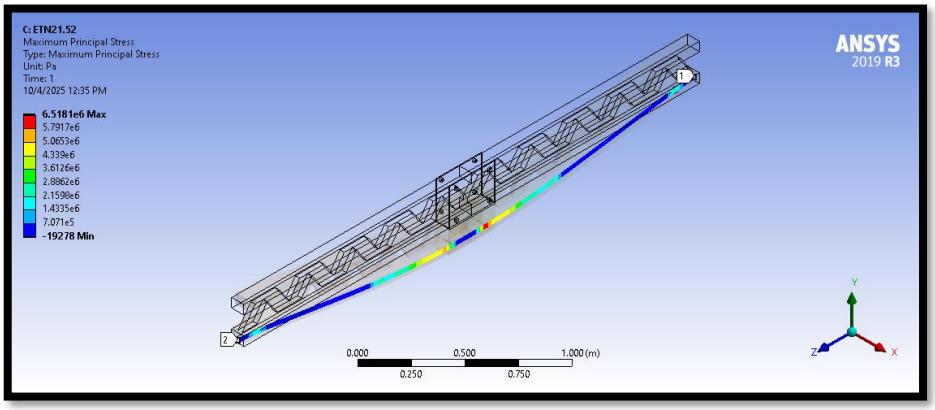
C: ETN21.52
Maximum Principal Stress
Type: Maximum Principal Stress
Unit: Pa
Time: 1
10/4/2025 12:35 PM
6.5181e6 Max
5.7917e6
5.0653e6
4.339e6
3.6126e6
2.8862e6
2.1598e6
1.4335e6
7.071e5
-19278 Min
ANSYS
2019 R3
1
2
0.000
0.500
1.000 (m)
0.250
0.750
Y
Z
X

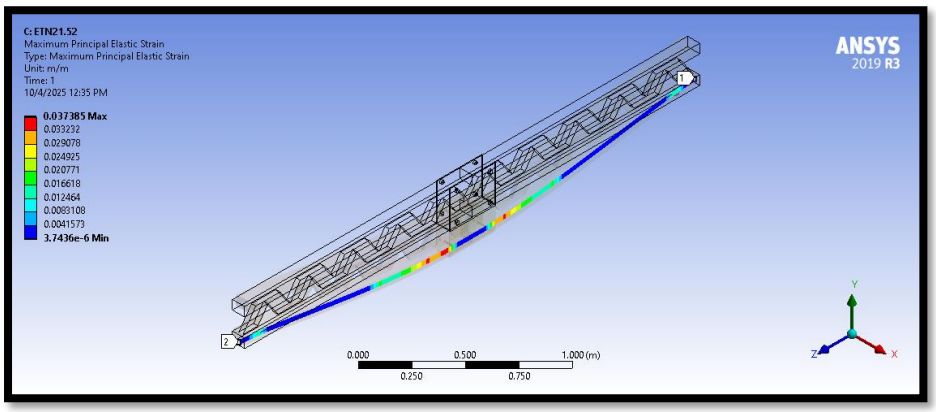
C: ETN21.52
Maximum Principal Elastic Strain
Type: Maximum Principal Elastic Strain
Unit: m/m
Time: 1
10/4/2025 12:35 PM
0.037385 Max
0.033232
0.029078
0.024925
0.020771
0.016618
0.012464
0.0083108
0.0041573
3.7436e-6 Min
ANSYS
2019 R3
1
2
0.000
0.500
1.000 (m)
0.250
0.750
Y
Z
X

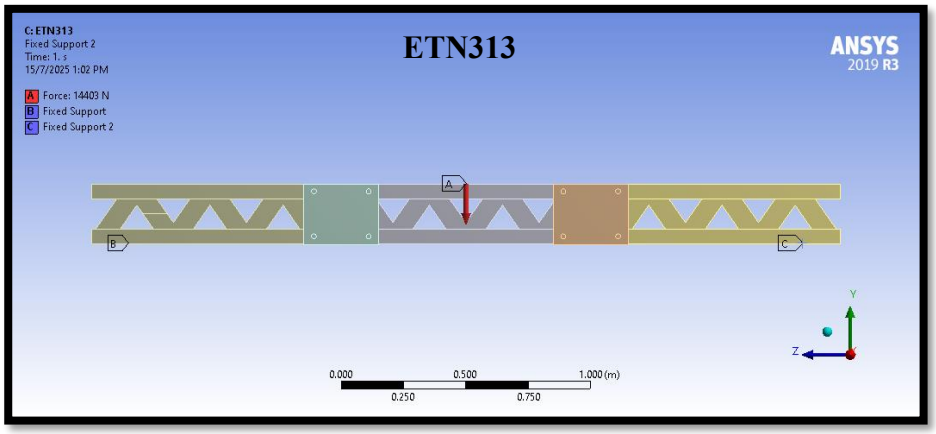
C: ETN313
Fixed Support 2
Time: 1. s
15/7/2025 1:02 PM
A Force: 14403 N
B Fixed Support
C Fixed Support 2
ETN313
ANSYS
2019 R3
0.000
0.500
1.000 (m)
0.250
0.750

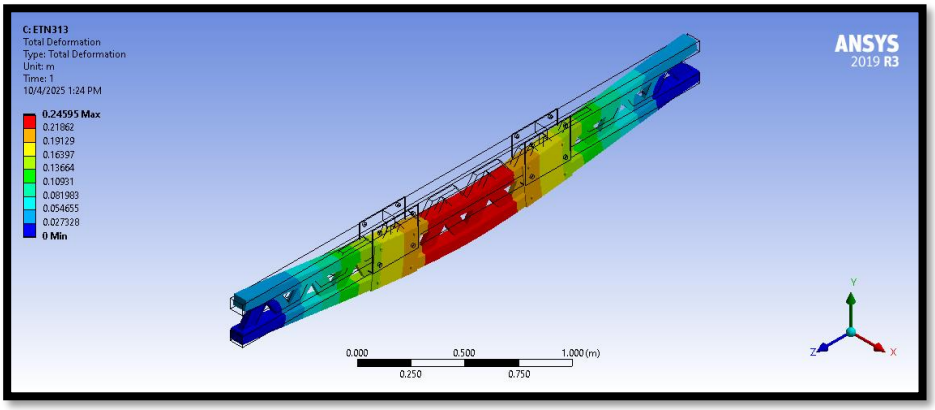
C: ETN313
Total Deformation
Type: Total Deformation
Unit: m
Time: 1
10/4/2025 1:24 PM
0.24595 Max
0.21862
0.19129
0.16397
0.13664
0.10931
0.081983
0.054655
0.027328
0 Min
ANSYS
2019 R3
0.000
0.500
1.000 (m)
0.250
0.750

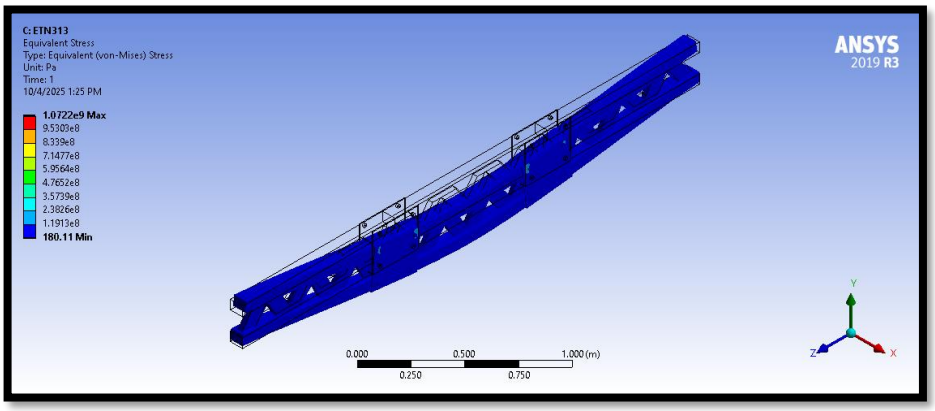
C: ETN313
Equivalent Stress
Type: Equivalent (von-Mises) Stress
Unit: Pa
Time: 1
10/4/2025 1:25 PM
1.0722e9 Max
9.5303e8
8.339e8
7.1477e8
5.9564e8
4.7652e8
3.5739e8
2.3826e8
1.1913e8
180.11 Min
ANSYS
2019 R3
0.000
0.500
1.000 (m)
0.250
0.750

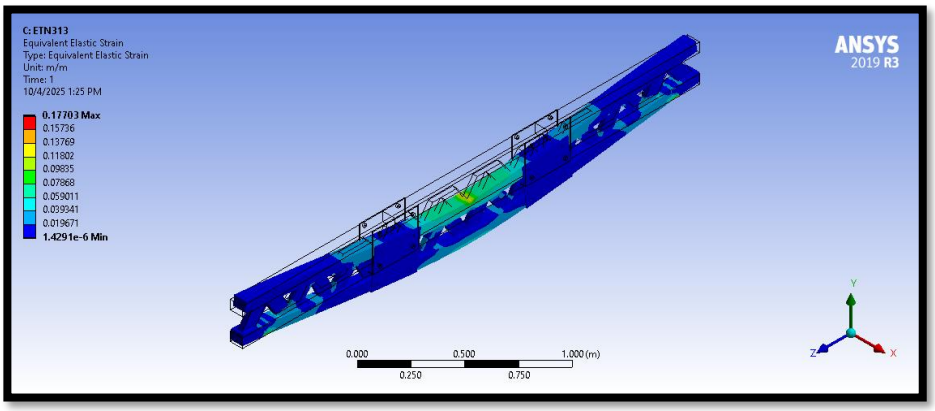
C: ETN313
Equivalent Elastic Strain
Type: Equivalent Elastic Strain
Unit: m/m
Time: 1
10/4/2025 1:25 PM
0.17703 Max
0.15736
0.13769
0.11802
0.09835
0.07868
0.059011
0.039341
0.019671
1.4291e-6 Min
ANSYS
2019 R3
0.000
0.500
1.000 (m)
0.250
0.750

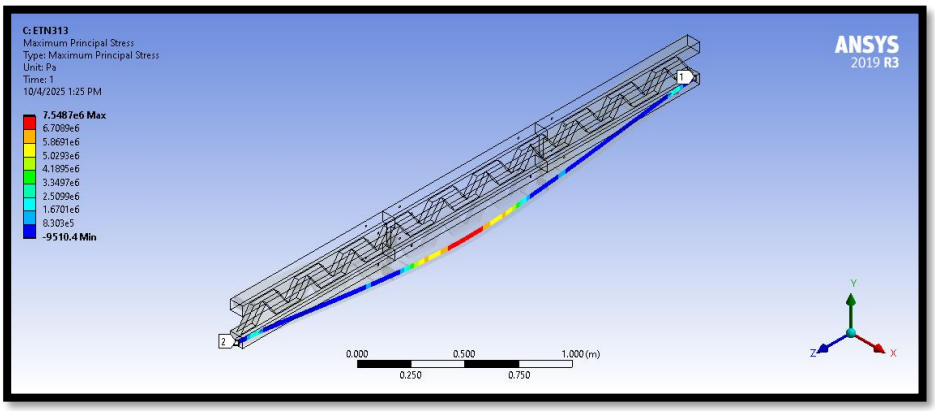
C:ETN313
Maximum Principal Stress
Type: Maximum Principal Stress
Unit: Pa
Time: 1
10/4/2025 1:25 PM
7.5487e6 Max
6.7089e6
5.8691e6
5.0293e6
4.1895e6
3.3497e6
2.5099e6
1.6701e6
8.303e5
-9510.4 Min
ANSYS
2019 R3
0.000
0.500
1.000 (m)
0.250
0.750
Y
Z
X

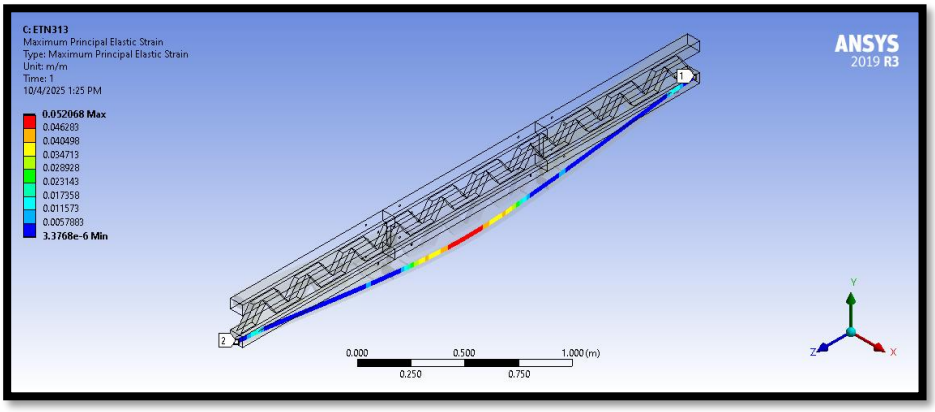
C:ETN313
Maximum Principal Elastic Strain
Type: Maximum Principal Elastic Strain
Unit: m/m
Time: 1
10/4/2025 1:25 PM
0.052068 Max
0.046283
0.040498
0.034713
0.028928
0.023143
0.017358
0.011573
0.0057883
3.3768e-6 Min
ANSYS
2019 R3
0.000
0.500
1.000 (m)
0.250
0.750
Y
Z
X

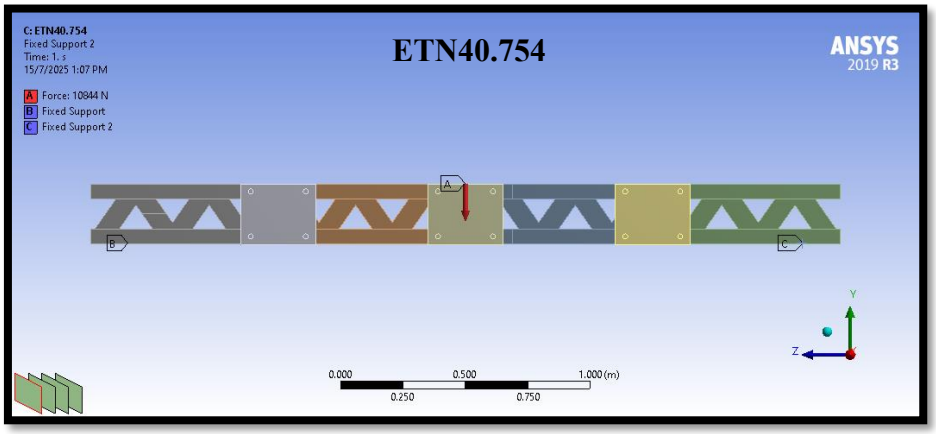
C: ETN40.754
Fixed Support 2
Time: 1. s
15/7/2025 1:07 PM
A Force: 10844 N
B Fixed Support
C Fixed Support 2
ETN40.754
ANSYS
2019 R3
0.000
0.500
1.000 (m)
0.250
0.750

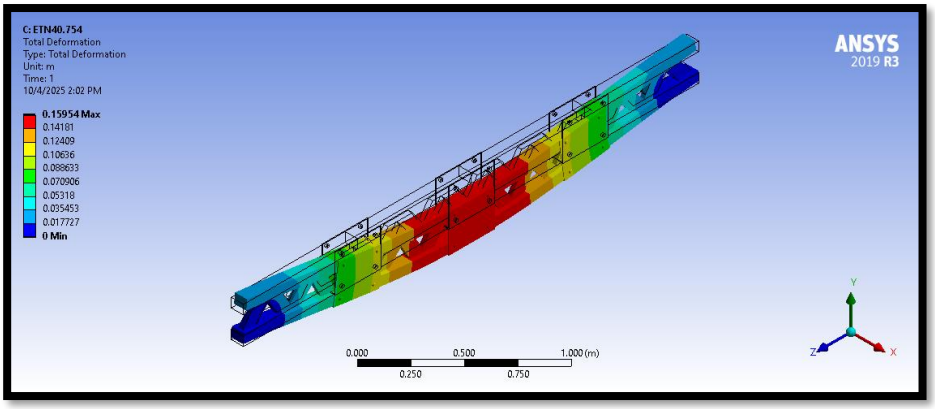
C: ETN40.754
Total Deformation
Type: Total Deformation
Unit: m
Time: 1
10/4/2025 2:02 PM
0.15954 Max
0.14181
0.12409
0.10636
0.088633
0.070906
0.05318
0.035453
0.017727
0 Min
ANSYS
2019 R3
0.000
0.500
1.000 (m)
0.250
0.750

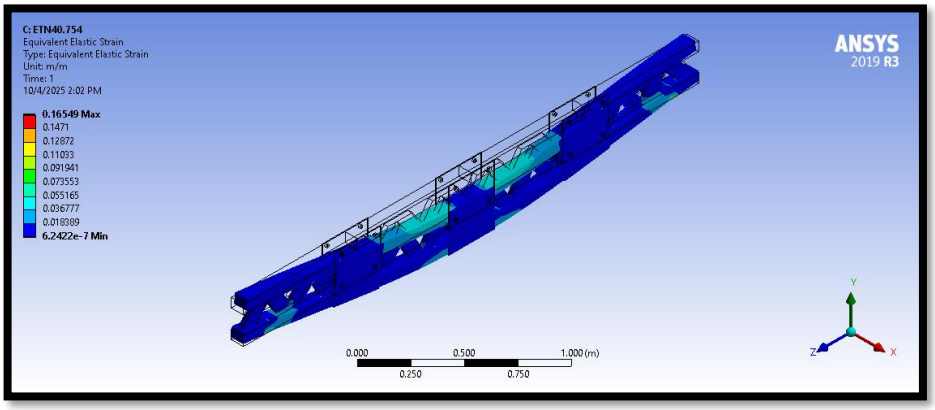
C: ETN40.754
Equivalent Elastic Strain
Type: Equivalent Elastic Strain
Unit: m/m
Time: 1
10/4/2025 2:02 PM
0.16549 Max
0.1471
0.12872
0.11033
0.091941
0.073553
0.055165
0.036777
0.018389
6.2422e-7 Min
ANSYS
2019 R3
0.000
0.500
1.000 (m)
0.250
0.750

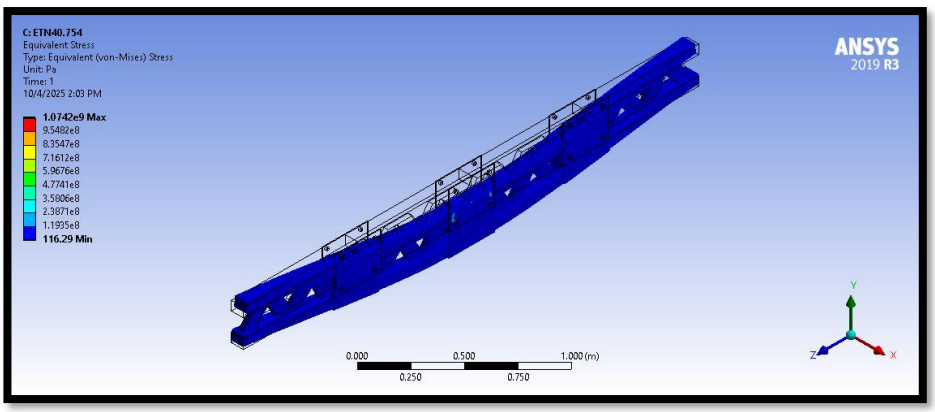
C: ETN40.754
Equivalent Stress
Type: Equivalent (von-Mises) Stress
Unit: Pa
Time: 1
10/4/2025 2:03 PM
1.0742e9 Max
9.5482e8
8.3547e8
7.1612e8
5.9676e8
4.7741e8
3.5806e8
2.3871e8
1.1935e8
116.29 Min
ANSYS
2019 R3
0.000
0.500
1.000 (m)
0.250
0.750

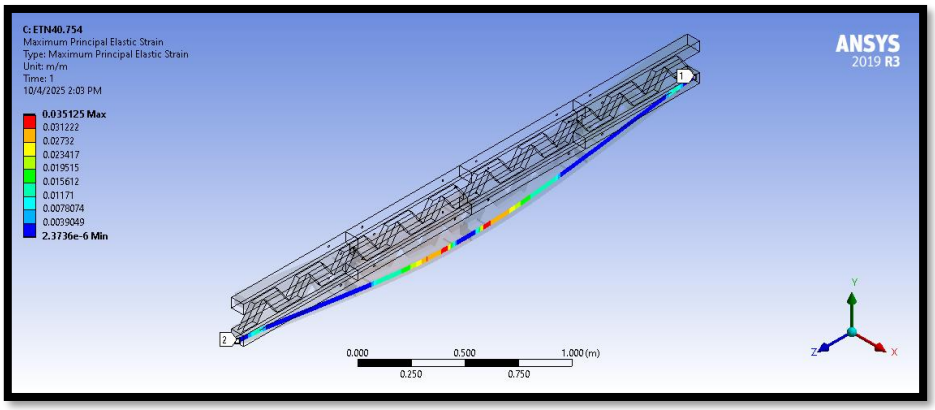
C: ETN40.754
Maximum Principal Elastic Strain
Type: Maximum Principal Elastic Strain
Unit: m/m
Time: 1
10/4/2025 2:03 PM
0.035125 Max
0.031222
0.02732
0.023417
0.019515
0.015612
0.01171
0.0078074
0.0039049
2.3736e-6 Min
ANSYS
2019 R3
0.000
0.500
1.000 (m)
0.250
0.750
Y
Z
X

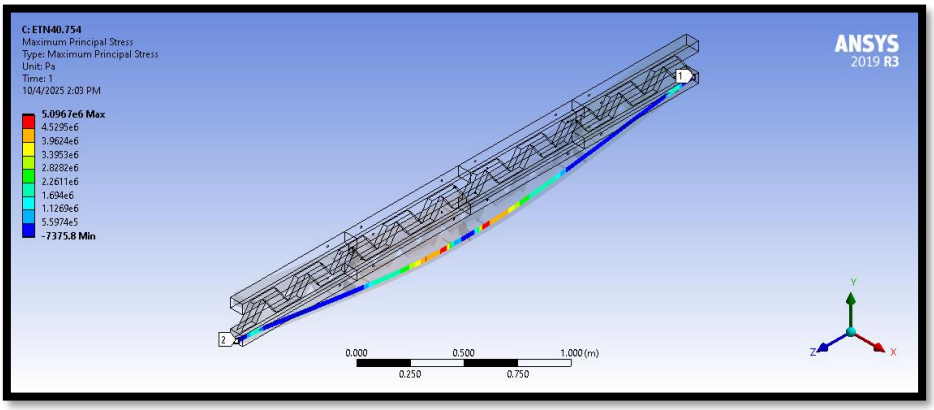
C: ETN40.754
Maximum Principal Stress
Type: Maximum Principal Stress
Unit: Pa
Time: 1
10/4/2025 2:03 PM
5.0967e6 Max
4.5295e6
3.9624e6
3.3953e6
2.8282e6
2.2611e6
1.694e6
1.1269e6
5.5974e5
-7375.8 Min
ANSYS
2019 R3
0.000
0.500
1.000 (m)
0.250
0.750
Y
Z
X

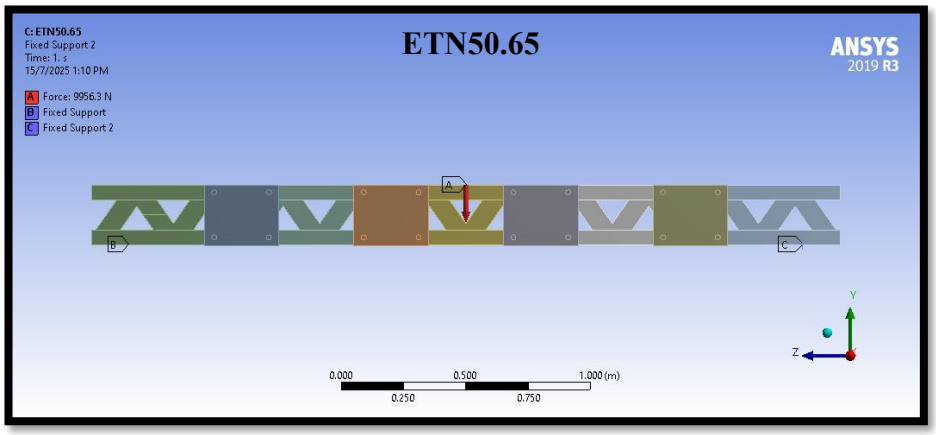
C: ETN50.65
Fixed Support 2
Time: 1. s
15/7/2025 1:10 PM
A Force: 9956.3 N
B Fixed Support
C Fixed Support 2
ETN50.65
ANSYS
2019 R3
A
B
C
0.000
0.500
1.000 (m)
0.250
0.750
Y
Z

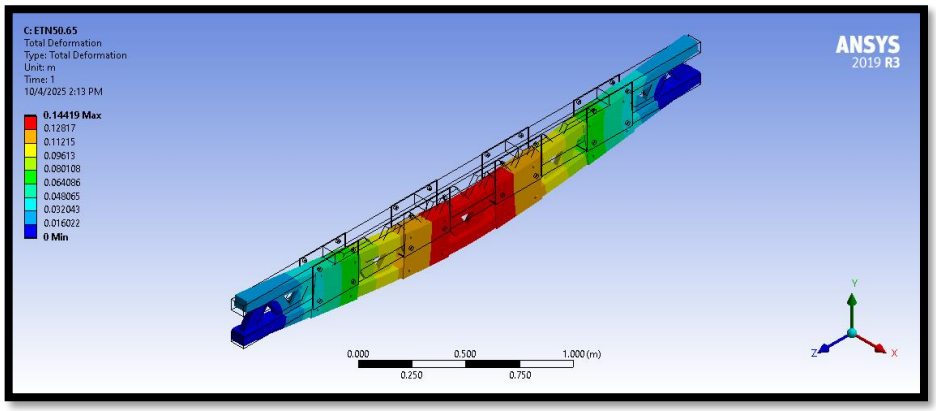
C: ETN50.65
Total Deformation
Type: Total Deformation
Unit: m
Time: 1
10/4/2025 2:13 PM
0.14419 Max
0.12817
0.11215
0.09613
0.080108
0.064086
0.048065
0.032043
0.016022
0 Min
ANSYS
2019 R3
0.000
0.500
1.000 (m)
0.250
0.750
Y
Z
X

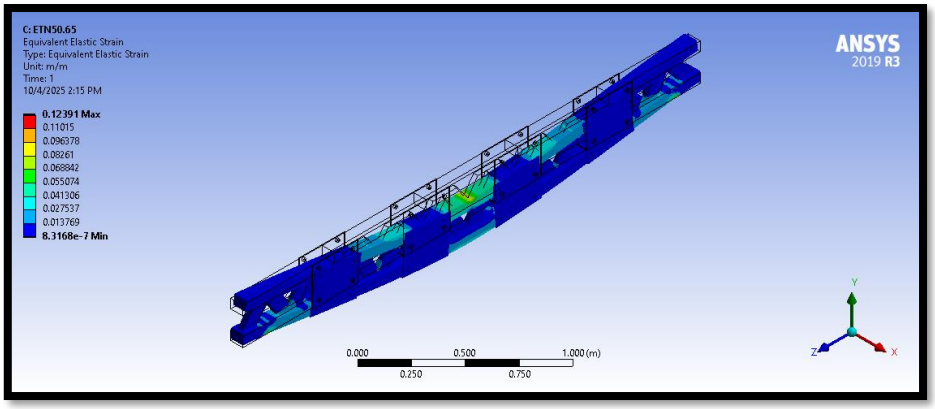
C: ETN50.65
Equivalent Elastic Strain
Type: Equivalent Elastic Strain
Unit: m/m
Time: 1
10/4/2025 2:15 PM
0.12391 Max
0.11015
0.096378
0.08261
0.068842
0.055074
0.041306
0.027537
0.013769
8.3168e-7 Min
ANSYS
2019 R3
0.000
0.500
1.000 (m)
0.250
0.750
Y
Z
X

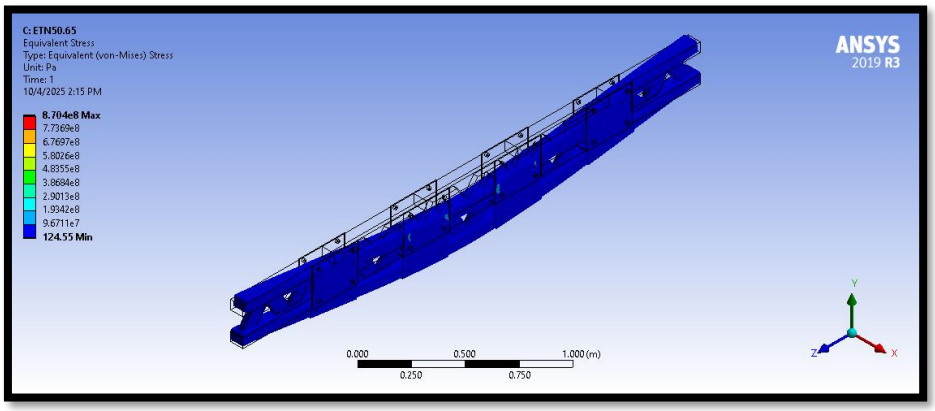
C: ETN50.65
Equivalent Stress
Type: Equivalent (von-Mises) Stress
Unit: Pa
Time: 1
10/4/2025 2:15 PM
8.704e8 Max
7.7369e8
6.7697e8
5.8026e8
4.8355e8
3.8684e8
2.9013e8
1.9342e8
9.6711e7
124.55 Min
ANSYS
2019 R3
0.000
0.500
1.000 (m)
0.250
0.750
Y
Z
X

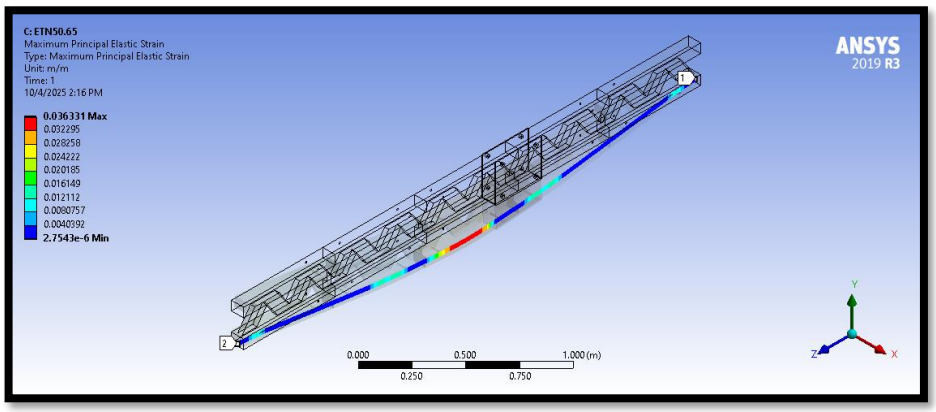
C: ETN50.65
Maximum Principal Elastic Strain
Type: Maximum Principal Elastic Strain
Unit: m/m
Time: 1
10/4/2025 2:16 PM
0.036331 Max
0.032295
0.028258
0.024222
0.020185
0.016149
0.012112
0.0080757
0.0040392
2.7543e-6 Min
ANSYS
2019 R3
1
2
0.000
0.500
1.000 (m)
0.250
0.750
Y
Z
X

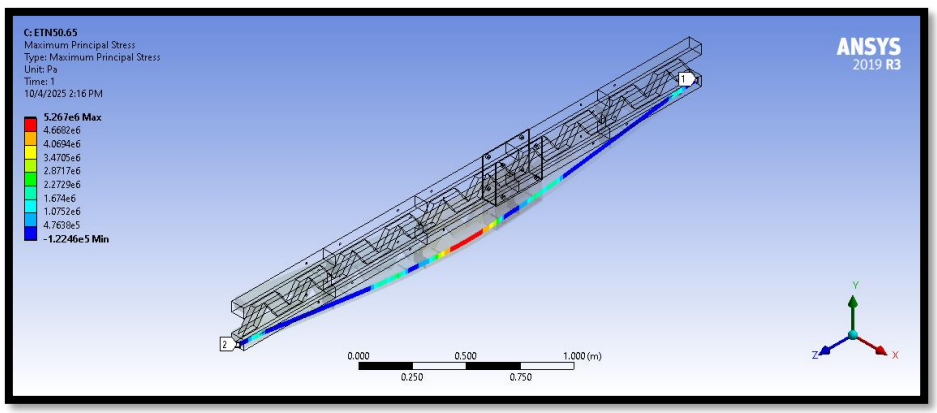
C: ETN50.65
Maximum Principal Stress
Type: Maximum Principal Stress
Unit: Pa
Time: 1
10/4/2025 2:16 PM
5.267e6 Max
4.6682e6
4.0694e6
3.4705e6
2.8717e6
2.2729e6
1.674e6
1.0752e6
4.7639e5
-1.2246e5 Min
ANSYS
2019 R3
1
2
0.000
0.500
1.000 (m)
0.250
0.750
Y
Z
X

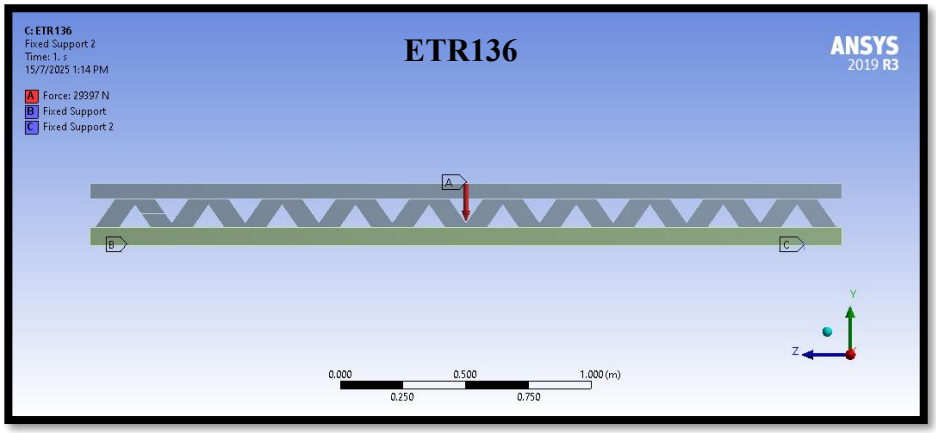
C: ETR136
Fixed Support 2
Time: 1 s
15/7/2025 1:14 PM
A Force: 29397 N
B Fixed Support
C Fixed Support 2
ETR136
ANSYS
2019 R3
A
B
C
Y
Z
X
0.000
0.500
1.000 (m)
0.250
0.750

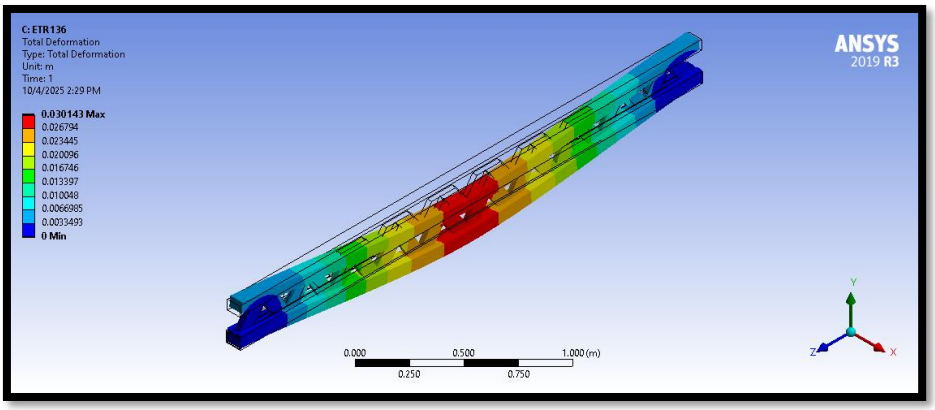
C: ETR136
Total Deformation
Type: Total Deformation
Unit: m
Time: 1
10/4/2025 2:29 PM
0.030143 Max
0.026794
0.023445
0.020096
0.016746
0.013397
0.010048
0.0066985
0.0033493
0 Min
ANSYS
2019 R3
0.000
0.500
1.000 (m)
0.250
0.750
Y
Z
X

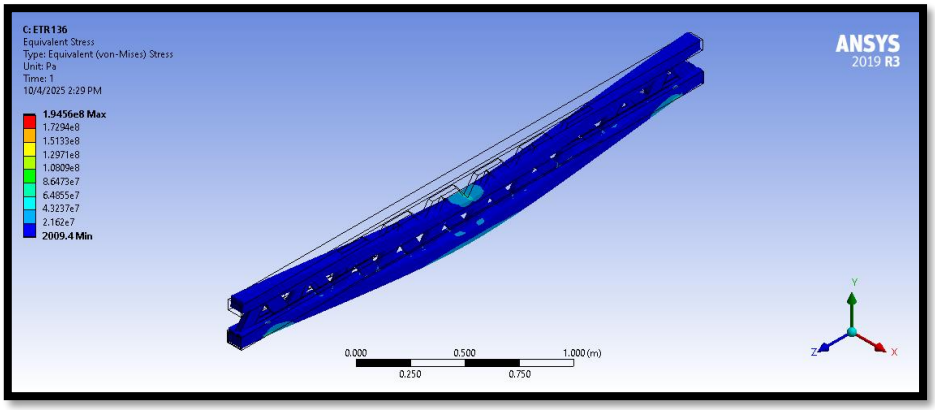
C: ETR136
Equivalent Stress
Type: Equivalent (von-Mises) Stress
Unit: Pa
Time: 1
10/4/2025 2:29 PM
1.9456e8 Max
1.7294e8
1.5133e8
1.2971e8
1.0809e8
8.6473e7
6.4855e7
4.3237e7
2.162e7
2009.4 Min
ANSYS
2019 R3
0.000
0.500
1.000 (m)
0.250
0.750
Y
Z
X

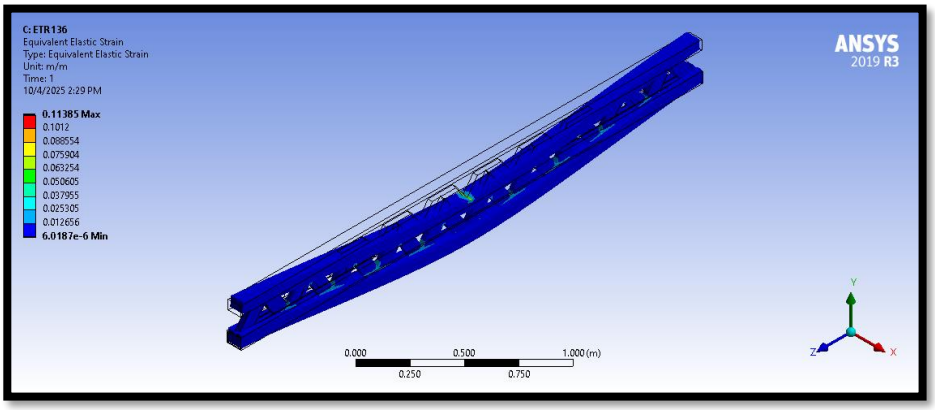
C: ETR136
Equivalent Elastic Strain
Type: Equivalent Elastic Strain
Unit: m/m
Time: 1
10/4/2025 2:29 PM
0.11385 Max
0.1012
0.088554
0.075904
0.063254
0.050605
0.037955
0.025305
0.012656
6.0187e-6 Min
ANSYS
2019 R3
0.000
0.500
1.000 (m)
0.250
0.750
Y
Z
X

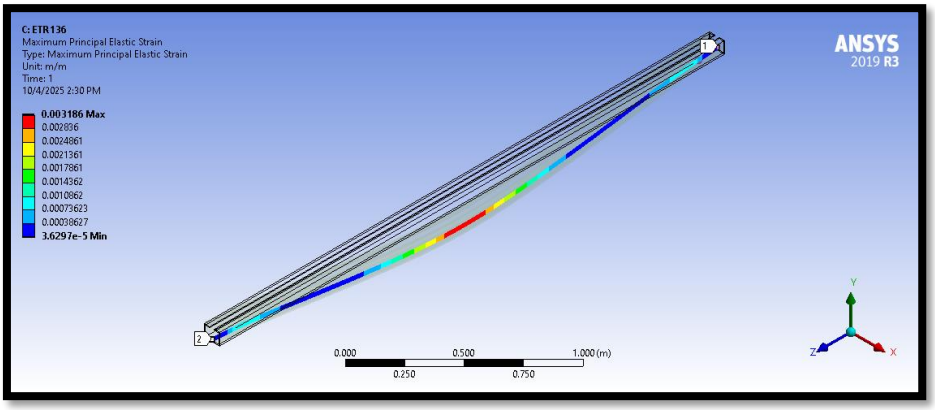
C: ETR136
Maximum Principal Elastic Strain
Type: Maximum Principal Elastic Strain
Unit: m/m
Time: 1
10/4/2025 2:30 PM
0.003186 Max
0.002836
0.0024861
0.0021361
0.0017861
0.0014362
0.0010862
0.00073623
0.00038627
3.6297e-5 Min
ANSYS
2019 R3
0.000
0.500
1.000 (m)
0.250
0.750

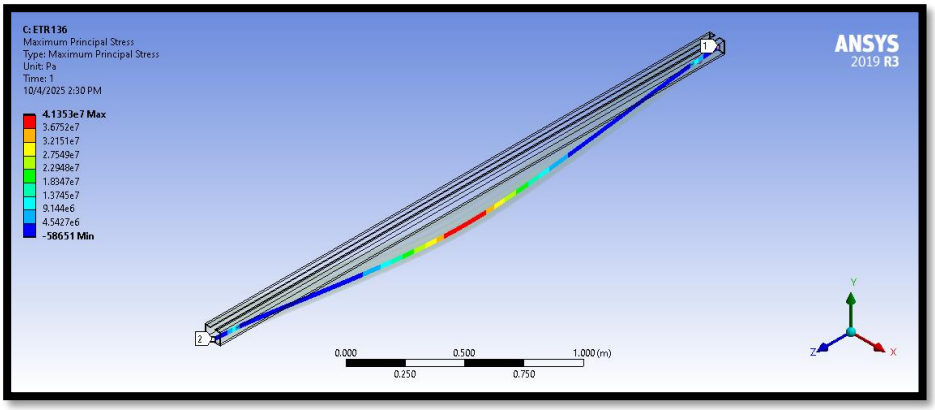
C: ETR136
Maximum Principal Stress
Type: Maximum Principal Stress
Unit: Pa
Time: 1
10/4/2025 2:30 PM
4.1353e7 Max
3.6752e7
3.2151e7
2.7549e7
2.2948e7
1.8347e7
1.3745e7
9.144e6
4.5427e6
-58651 Min
ANSYS
2019 R3
0.000
0.500
1.000 (m)
0.250
0.750

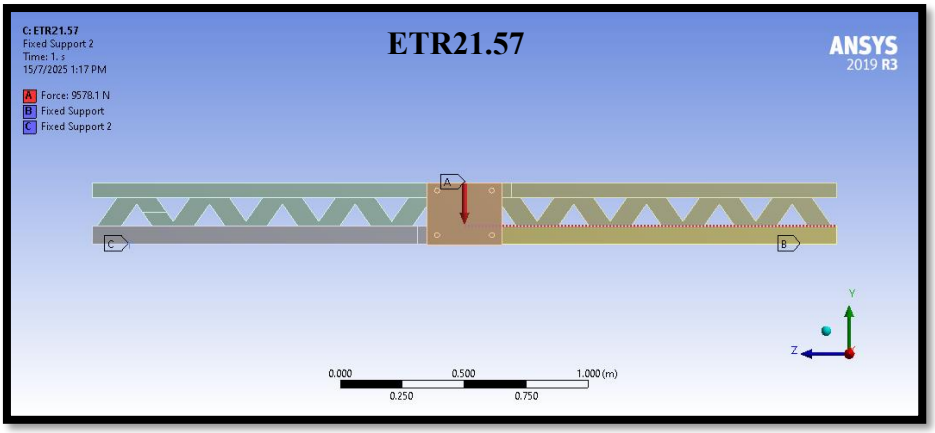
C: ETR21.57
Fixed Support 2
Time: 1. s
15/7/2025 1:17 PM
A Force: 9578.1 N
B Fixed Support
C Fixed Support 2
ETR21.57
ANSYS
2019 R3
0.000
0.500
1.000 (m)
0.250
0.750

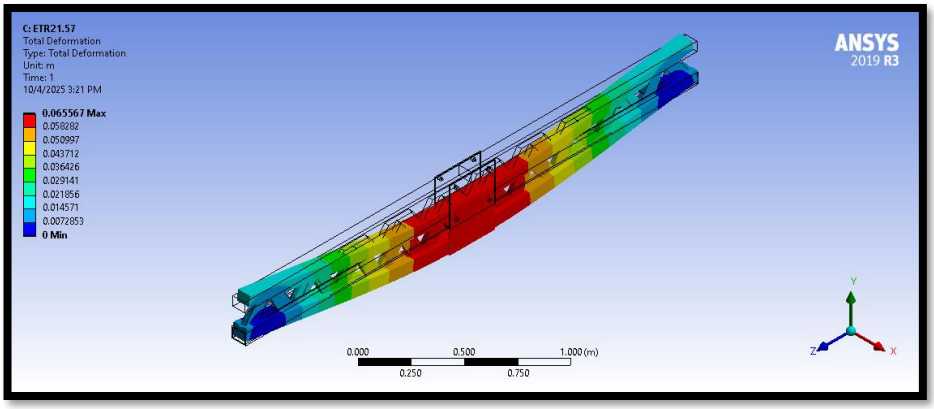
C: ETR21.57
Total Deformation
Type: Total Deformation
Unit: m
Time: 1
10/4/2025 3:21 PM
0.065567 Max
0.058282
0.050997
0.043712
0.036426
0.029141
0.021856
0.014571
0.0072853
0 Min
ANSYS
2019 R3
0.000
0.500
1.000 (m)
0.250
0.750

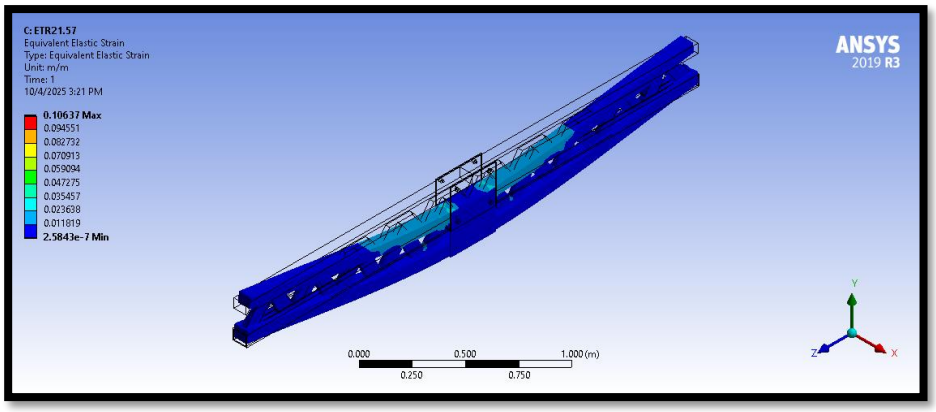
C: ETR21.57
Equivalent Elastic Strain
Type: Equivalent Elastic Strain
Unit: m/m
Time: 1
10/4/2025 3:21 PM
0.10637 Max
0.094551
0.082732
0.070913
0.059094
0.047275
0.035457
0.023638
0.011819
2.5843e-7 Min
ANSYS
2019 R3
0.000
0.500
1.000 (m)
0.250
0.750
Y
Z
X

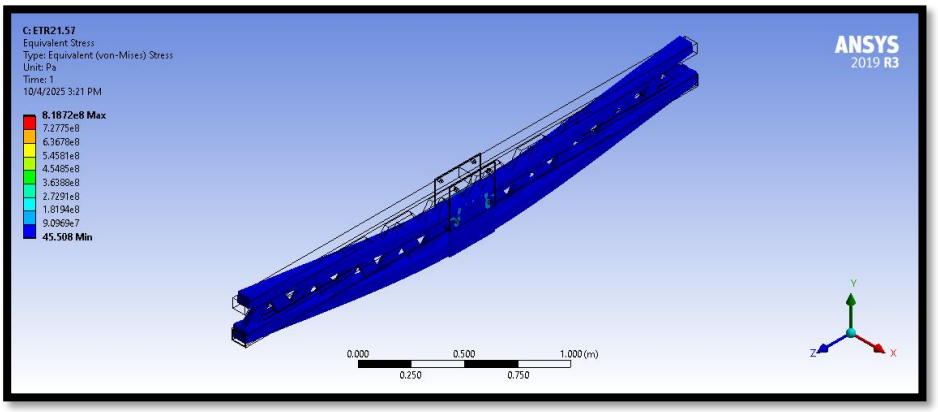
C: ETR21.57
Equivalent Stress
Type: Equivalent (von-Mises) Stress
Unit: Pa
Time: 1
10/4/2025 3:21 PM
8.1872e8 Max
7.2775e8
6.3678e8
5.4581e8
4.5485e8
3.6388e8
2.7291e8
1.8194e8
9.0969e7
45.508 Min
ANSYS
2019 R3
0.000
0.500
1.000 (m)
0.250
0.750
Y
Z
X

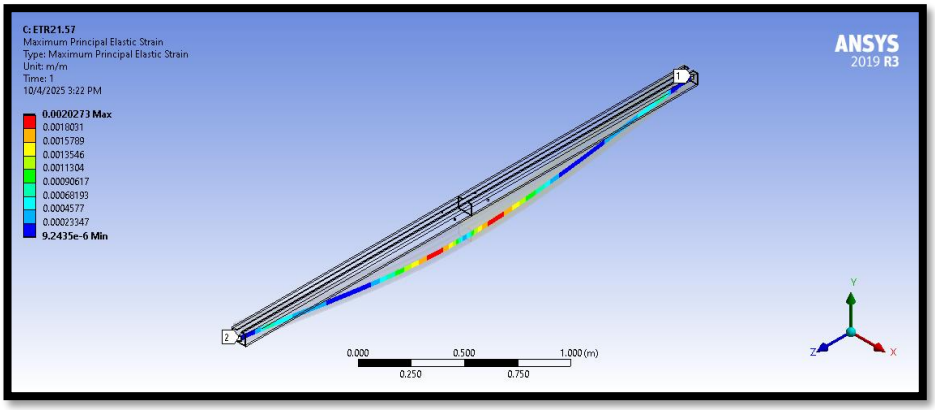
C: ETR21.57
Maximum Principal Elastic Strain
Type: Maximum Principal Elastic Strain
Unit: m/m
Time: 1
10/4/2025 3:22 PM
0.0020273 Max
0.0018031
0.0015789
0.0013546
0.0011304
0.00090617
0.00068193
0.0004577
0.00023347
9.2435e-6 Min
ANSYS
2019 R3
1
2
0.000
0.500
1.000 (m)
0.250
0.750
Y
Z
X

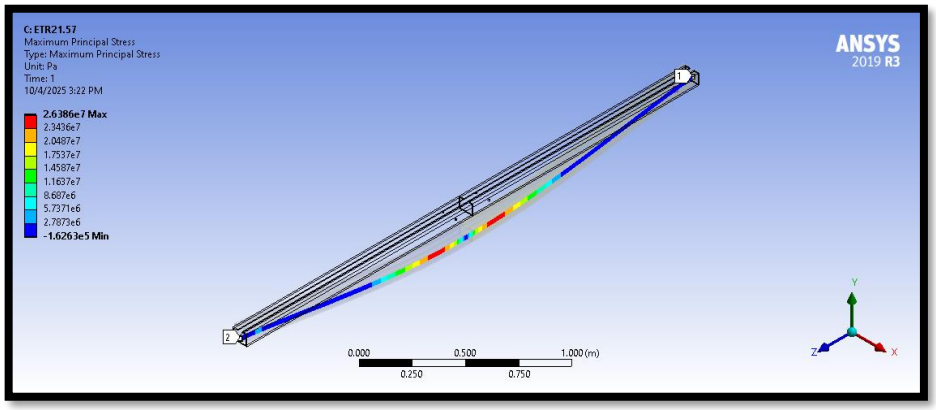
C: ETR21.57
Maximum Principal Stress
Type: Maximum Principal Stress
Unit: Pa
Time: 1
10/4/2025 3:22 PM
2.6386e7 Max
2.3436e7
2.0487e7
1.7537e7
1.4587e7
1.1637e7
8.687e6
5.7371e6
2.7873e6
-1.6263e5 Min
ANSYS
2019 R3
1
2
0.000
0.500
1.000 (m)
0.250
0.750
Y
Z
X

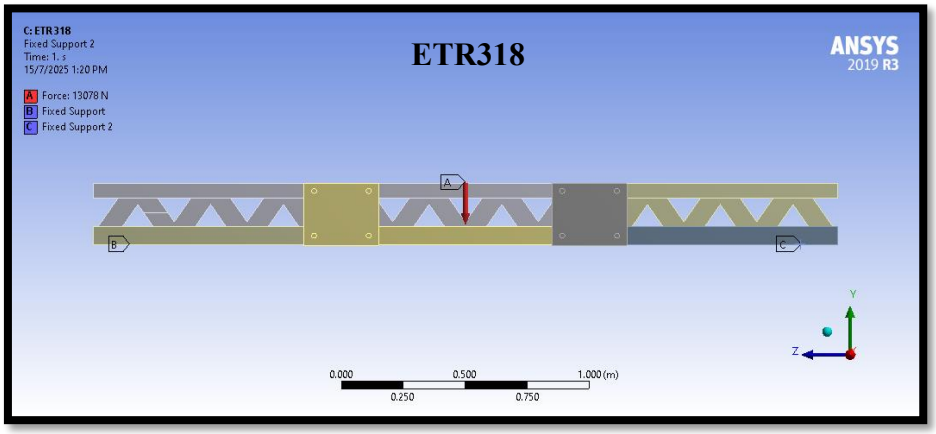
C: ETR318
Fixed Support 2
Time: 1. s
15/7/2025 1:20 PM
A Force: 13078 N
B Fixed Support
C Fixed Support 2
ETR318
ANSYS
2019 R3
A
B
C
Y
Z
0.000
0.500
1.000 (m)
0.250
0.750

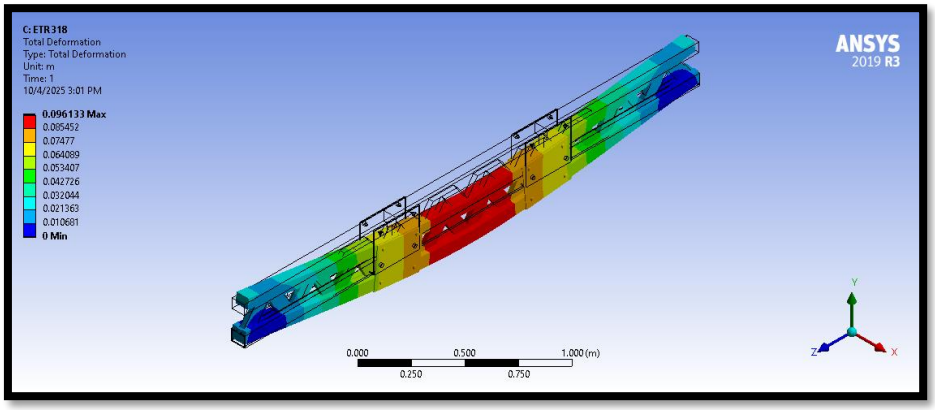
C: ETR318
Total Deformation
Type: Total Deformation
Unit: m
Time: 1
10/4/2025 3:01 PM
0.096133 Max
0.085452
0.07477
0.064089
0.053407
0.042726
0.032044
0.021363
0.010681
0 Min
ANSYS
2019 R3
Y
Z
X
0.000
0.500
1.000 (m)
0.250
0.750

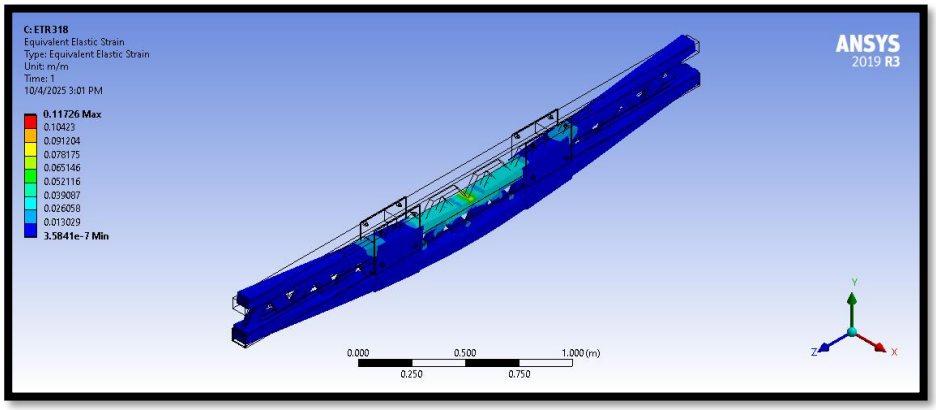
C: ETR318
Equivalent Elastic Strain
Type: Equivalent Elastic Strain
Unit: m/m
Time: 1
10/4/2025 3:01 PM
0.11726 Max
0.10423
0.091204
0.078175
0.065146
0.052116
0.039087
0.026058
0.013029
3.5841e-7 Min
ANSYS
2019 R3
Y
Z
X
0.000
0.500
1.000 (m)
0.250
0.750

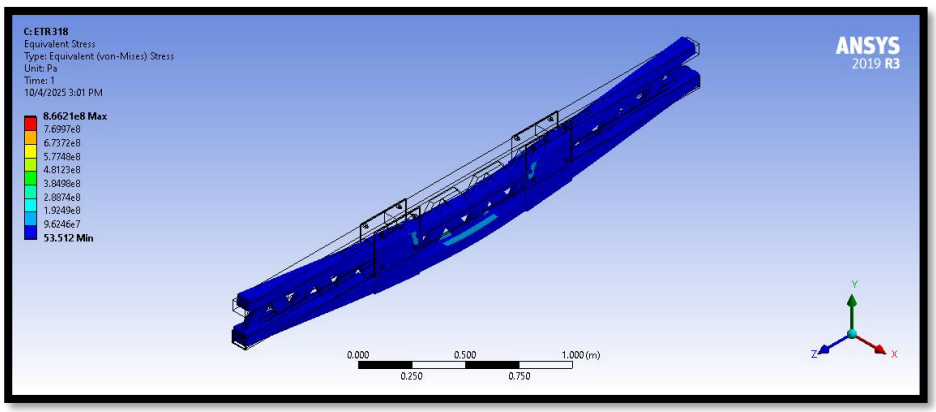
C: ETR318
Equivalent Stress
Type: Equivalent (von-Mises) Stress
Unit: Pa
Time: 1
10/4/2025 3:01 PM
8.6621e8 Max
7.6997e8
6.7372e8
5.7748e8
4.8123e8
3.8498e8
2.8874e8
1.9249e8
9.6246e7
53.512 Min
ANSYS
2019 R3
Y
Z
X
0.000
0.500
1.000 (m)
0.250
0.750

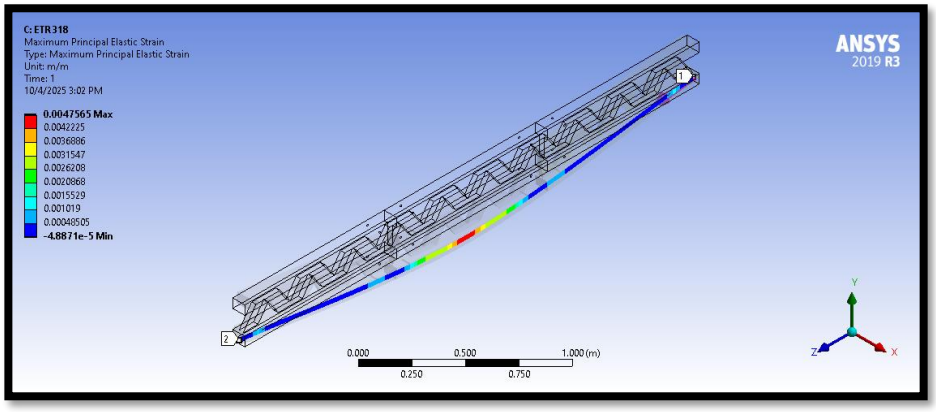
C: ETR318
Maximum Principal Elastic Strain
Type: Maximum Principal Elastic Strain
Unit: m/m
Time: 1
10/4/2025 3:02 PM
0.0047565 Max
0.0042225
0.0036886
0.0031547
0.0026208
0.0020868
0.0015529
0.001019
0.00048505
-4.8871e-5 Min
ANSYS
2019 R3
0.000
0.500
1.000 (m)
0.250
0.750
Y
Z
X

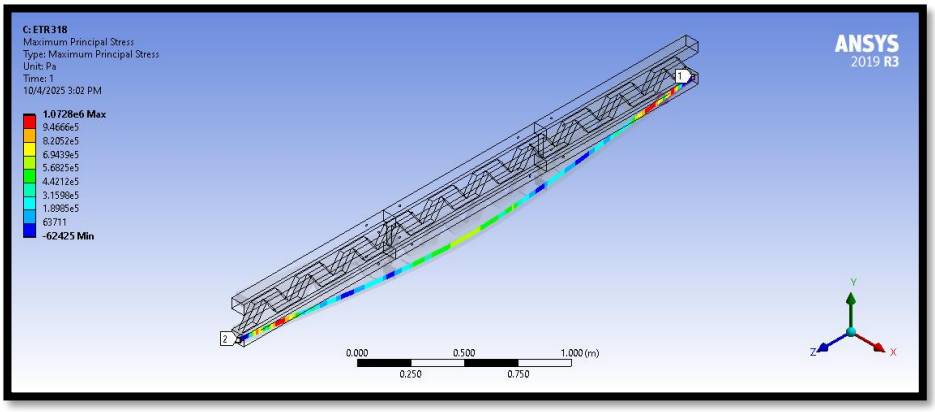
C: ETR318
Maximum Principal Stress
Type: Maximum Principal Stress
Unit: Pa
Time: 1
10/4/2025 3:02 PM
1.0728e6 Max
9.4666e5
8.2052e5
6.9439e5
5.6825e5
4.4212e5
3.1598e5
1.8985e5
63711
-62425 Min
ANSYS
2019 R3
0.000
0.500
1.000 (m)
0.250
0.750
Y
Z
X

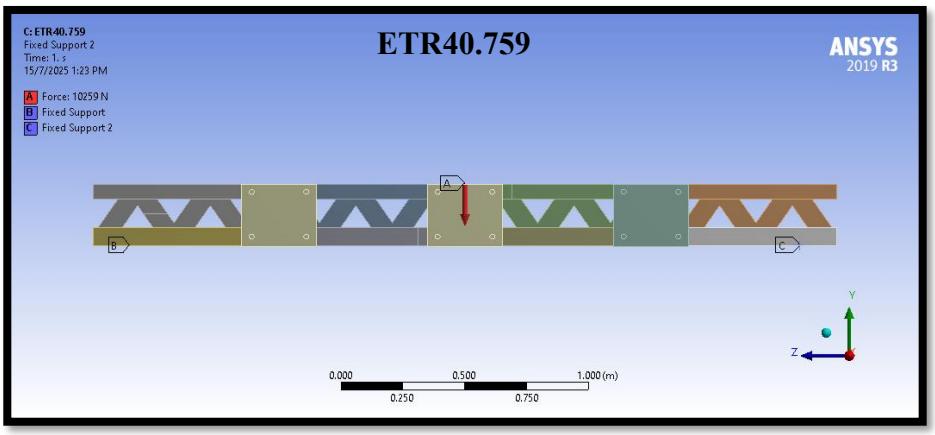
C: ETR40.759
Fixed Support 2
Time: 1. s
15/7/2025 1:23 PM
A Force: 10259 N
B Fixed Support
C Fixed Support 2
ETR40.759
ANSYS
2019 R3
A
B
C
0.000
0.500
1.000 (m)
0.250
0.750
Y
Z

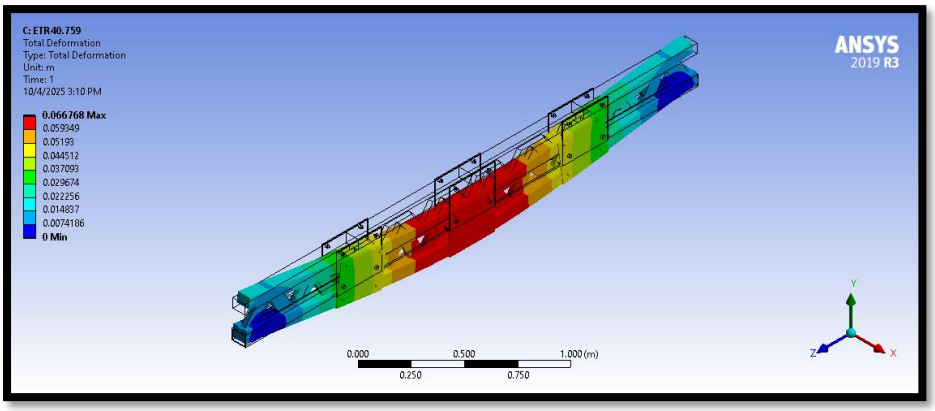
C: ETR40.759
Total Deformation
Type: Total Deformation
Unit: m
Time: 1
10/4/2025 3:10 PM
0.066768 Max
0.059349
0.05193
0.044512
0.037093
0.029674
0.022256
0.014837
0.0074186
0 Min
ANSYS
2019 R3
0.000
0.500
1.000 (m)
0.250
0.750
Y
Z
X

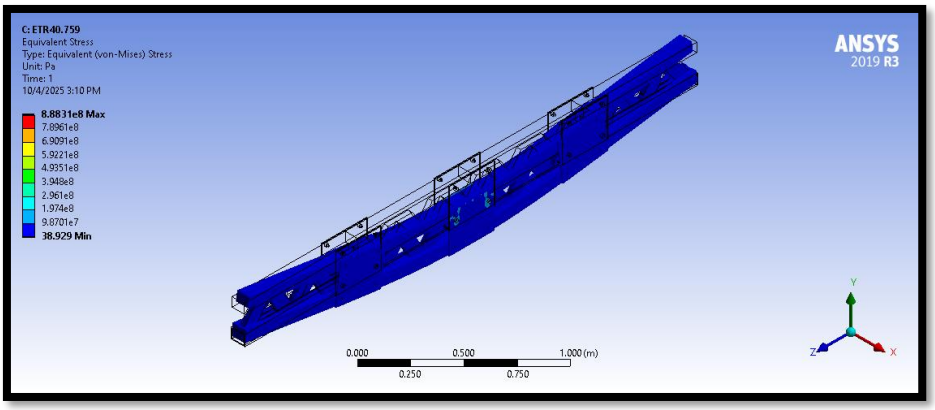
C: ETR40.759
Equivalent Stress
Type: Equivalent (von-Mises) Stress
Unit: Pa
Time: 1
10/4/2025 3:10 PM
8.8831e8 Max
7.8961e8
6.9091e8
5.9221e8
4.9351e8
3.948e8
2.961e8
1.974e8
9.8701e7
38.929 Min
ANSYS
2019 R3
0.000
0.500
1.000 (m)
0.250
0.750
Y
Z
X

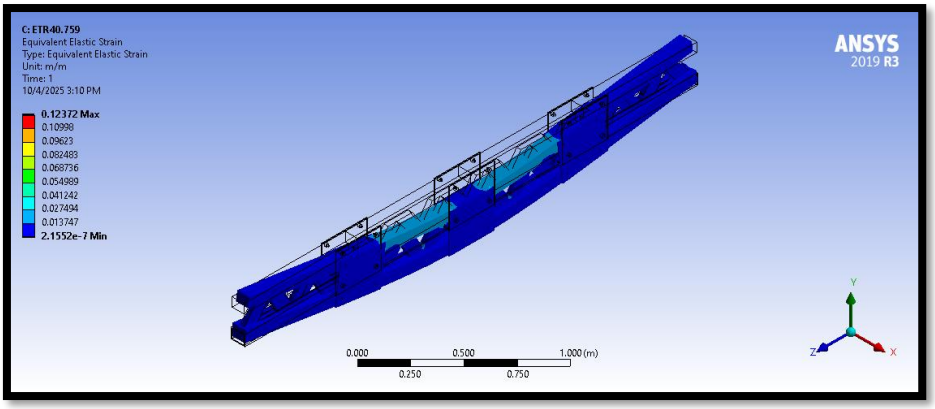
C: ETR40.759
Equivalent Elastic Strain
Type: Equivalent Elastic Strain
Unit: m/m
Time: 1
10/4/2025 3:10 PM
0.12372 Max
0.10998
0.09623
0.082489
0.068736
0.054989
0.041242
0.027494
0.013747
2.1552e-7 Min
ANSYS
2019 R3
0.000
0.500
1.000 (m)
0.250
0.750
Y
Z
X

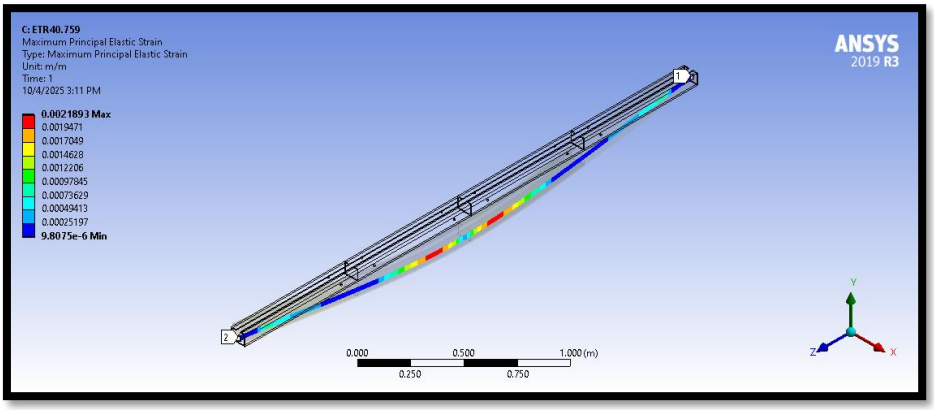
C: ETR40.759
Maximum Principal Elastic Strain
Type: Maximum Principal Elastic Strain
Unit: m/m
Time: 1
10/4/2025 3:11 PM
0.0021893 Max
0.0019471
0.0017049
0.0014628
0.0012206
0.00097845
0.00073629
0.00049413
0.00025197
9.8075e-6 Min
ANSYS
2019 R3
1
2
0.000
0.500
1.000 (m)
0.250
0.750
Y
Z
X

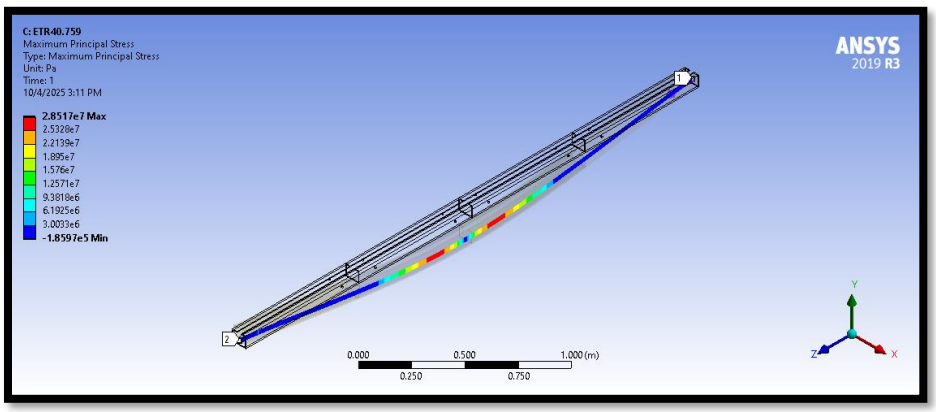
C: ETR40.759
Maximum Principal Stress
Type: Maximum Principal Stress
Unit: Pa
Time: 1
10/4/2025 3:11 PM
2.8517e7 Max
2.5328e7
2.2139e7
1.895e7
1.576e7
1.2571e7
9.3818e6
6.1925e6
3.0033e6
-1.8597e5 Min
ANSYS
2019 R3
1
2
0.000
0.500
1.000 (m)
0.250
0.750
Y
Z
X

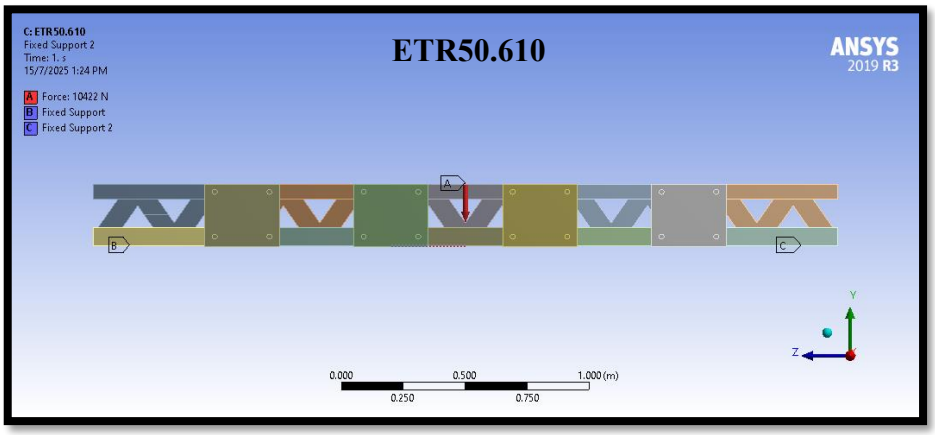
C: ETR50.610
Fixed Support 2
Time: 1. s
15/7/2025 1:24 PM
A Force: 10422 N
B Fixed Support
C Fixed Support 2
ETR50.610
ANSYS
2019 R3
A
B
C
Y
Z
0.000
0.500
1.000 (m)
0.250
0.750

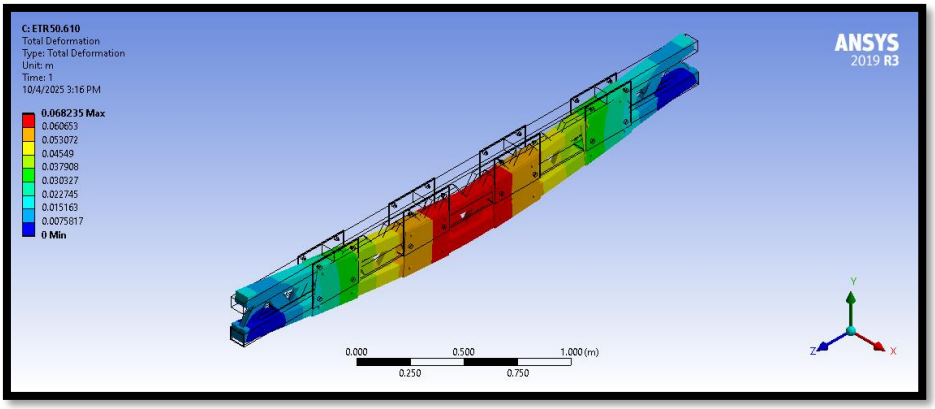
C: ETR50.610
Total Deformation
Type: Total Deformation
Unit: m
Time: 1
10/4/2025 3:16 PM
0.068235 Max
0.060653
0.053072
0.04549
0.037908
0.030327
0.022745
0.015163
0.0075817
0 Min
ANSYS
2019 R3
Y
Z
X
0.000
0.500
1.000 (m)
0.250
0.750

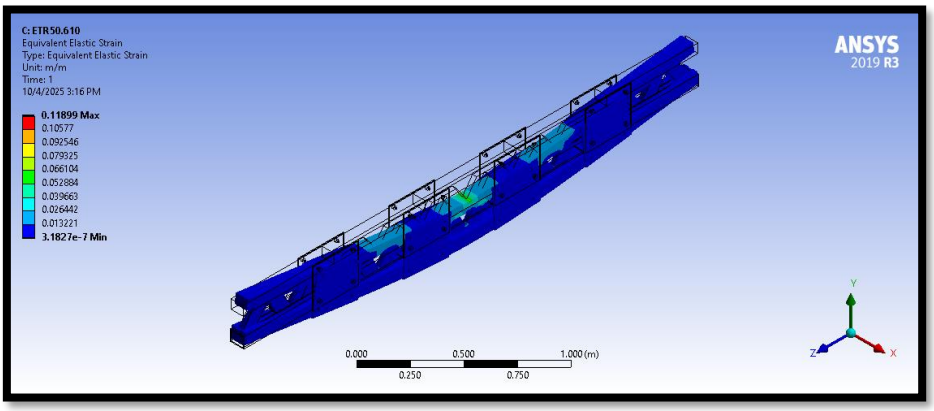
C: ETR50.610
Equivalent Elastic Strain
Type: Equivalent Elastic Strain
Unit: m/m
Time: 1
10/4/2025 3:16 PM
0.11899 Max
0.10577
0.092546
0.079325
0.066104
0.052884
0.039663
0.026442
0.013221
3.1827e-7 Min
ANSYS
2019 R3
Y
Z
X
0.000
0.500
1.000 (m)
0.250
0.750

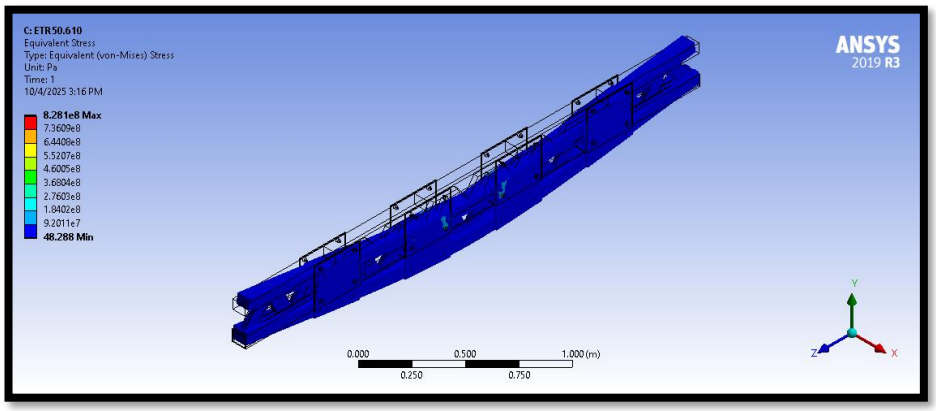
C: ETR50.610
Equivalent Stress
Type: Equivalent (von-Mises) Stress
Unit: Pa
Time: 1
10/4/2025 3:16 PM
8.281e8 Max
7.3609e8
6.4408e8
5.5207e8
4.6005e8
3.6804e8
2.7603e8
1.8402e8
9.2011e7
48.288 Min
ANSYS
2019 R3
Y
Z
X
0.000
0.500
1.000 (m)
0.250
0.750

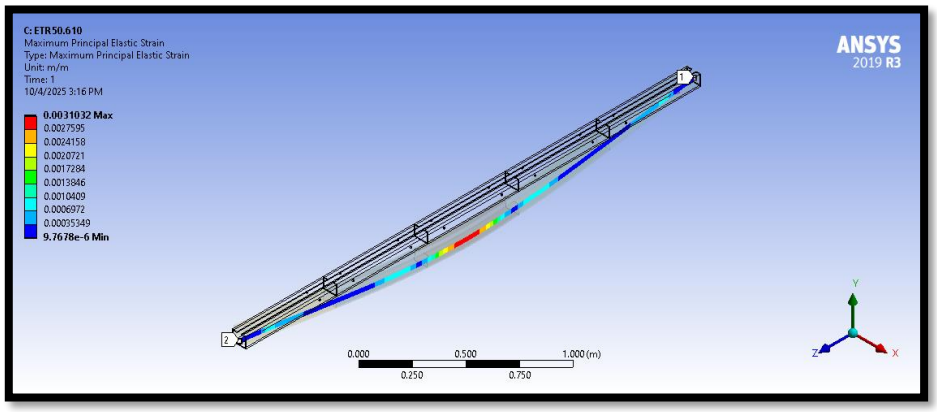
C: ETR50.610
Maximum Principal Elastic Strain
Type: Maximum Principal Elastic Strain
Unit: m/m
Time: 1
10/4/2025 3:16 PM
0.0031032 Max
0.0027595
0.0024158
0.0020721
0.0017284
0.0013846
0.0010409
0.0006972
0.00035349
9.7678e-6 Min
ANSYS
2019 R3
1
2
0.000
0.500
1.000 (m)
0.250
0.750
Y
Z
X

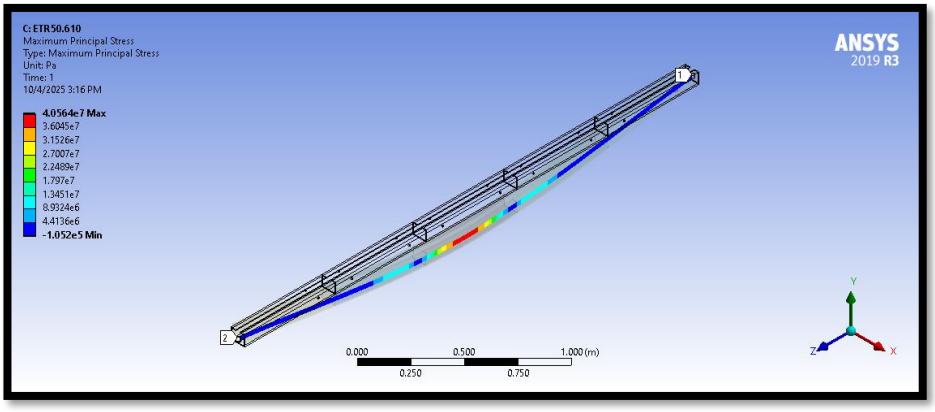
C: ETR50.610
Maximum Principal Stress
Type: Maximum Principal Stress
Unit: Pa
Time: 1
10/4/2025 3:16 PM
4.0564e7 Max
3.6045e7
3.1526e7
2.7007e7
2.2489e7
1.797e7
1.3451e7
8.9324e6
4.4136e6
-1.052e5 Min
ANSYS
2019 R3
1
2
0.000
0.500
1.000 (m)
0.250
0.750
Y
Z
X

APPENDIX 6

Modal Analysis FEA

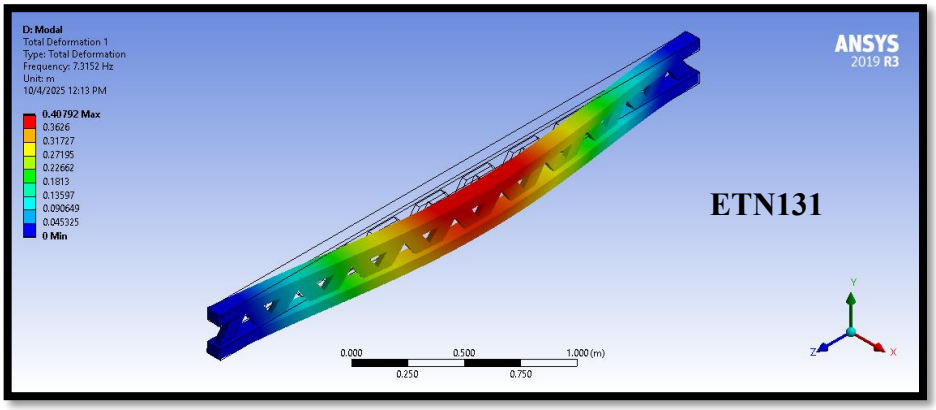

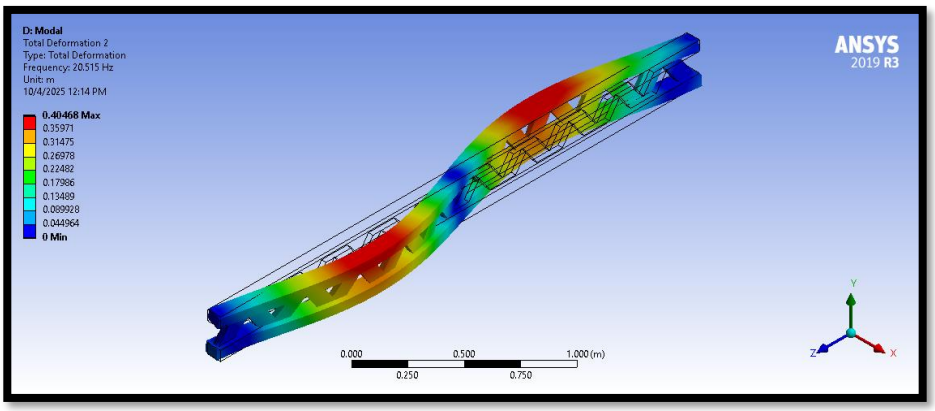

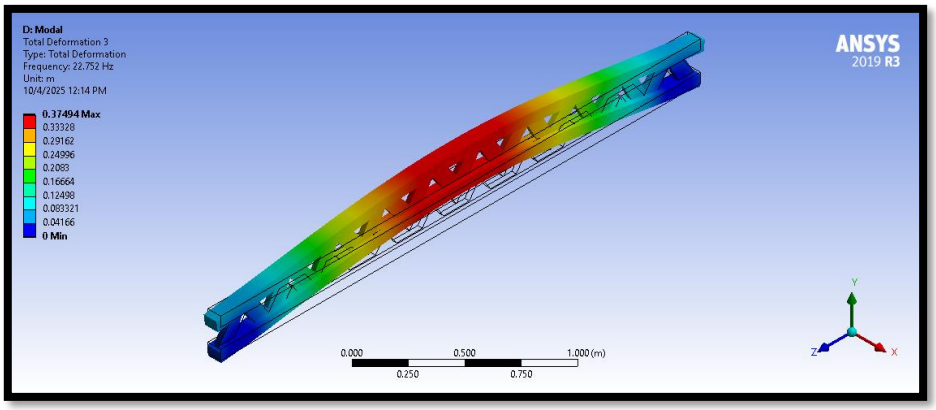

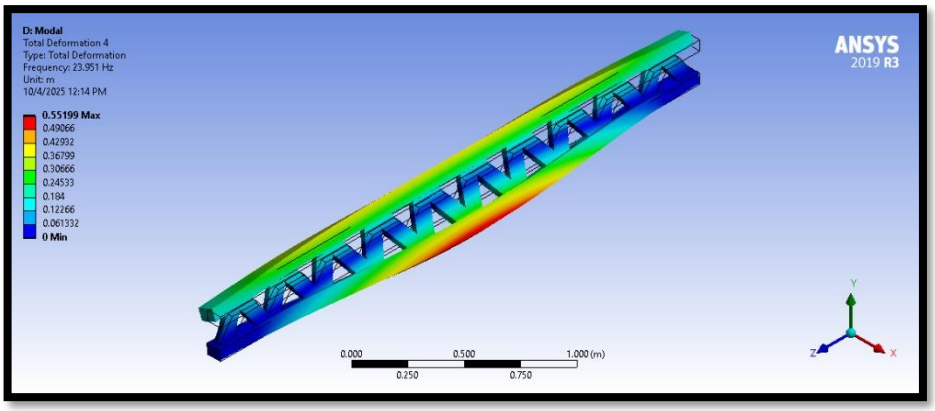

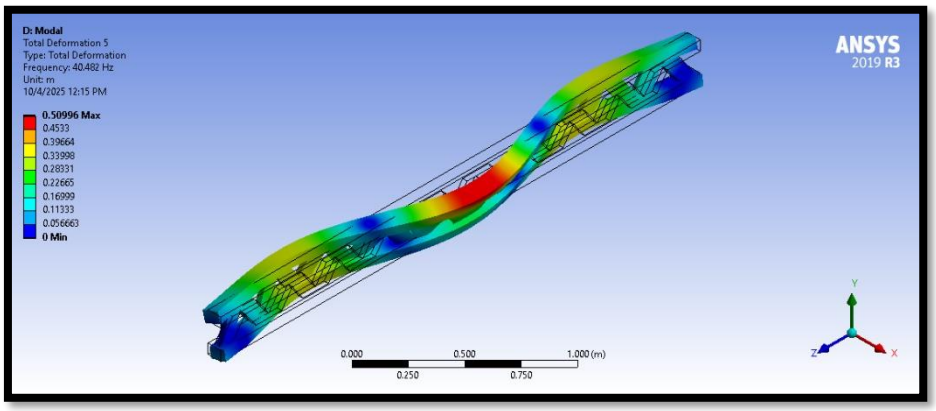
D: Modal
Total Deformation 5
Type: Total Deformation
Frequency: 40.482 Hz
Unit: m
10/4/2025 12:15 PM
0.50996 Max
0.4533
0.39664
0.33998
0.28331
0.22665
0.16999
0.11333
0.056663
0 Min
ANSYS
2019 R3
0.000
0.500
1.000 (m)
0.250
0.750
Y
Z
X

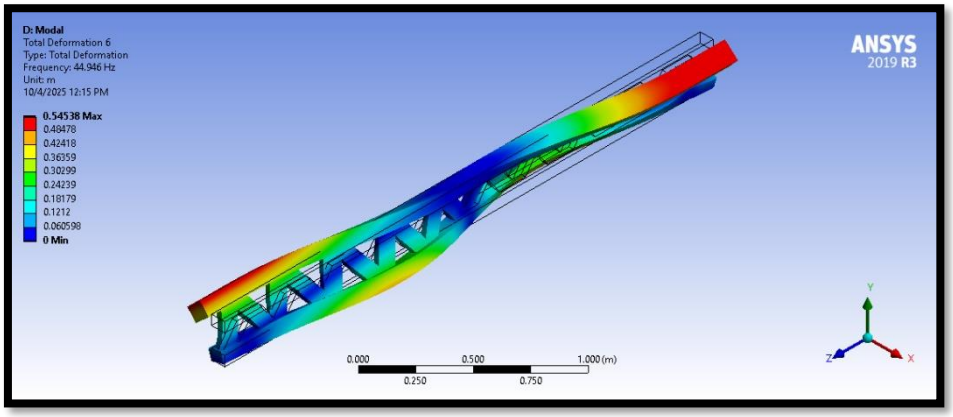
D: Modal
Total Deformation 6
Type: Total Deformation
Frequency: 44.946 Hz
Unit: m
10/4/2025 12:15 PM
0.54538 Max
0.48478
0.42418
0.36359
0.30299
0.24239
0.18179
0.1212
0.060598
0 Min
ANSYS
2019 R3
0.000
0.500
1.000 (m)
0.250
0.750
Y
Z
X

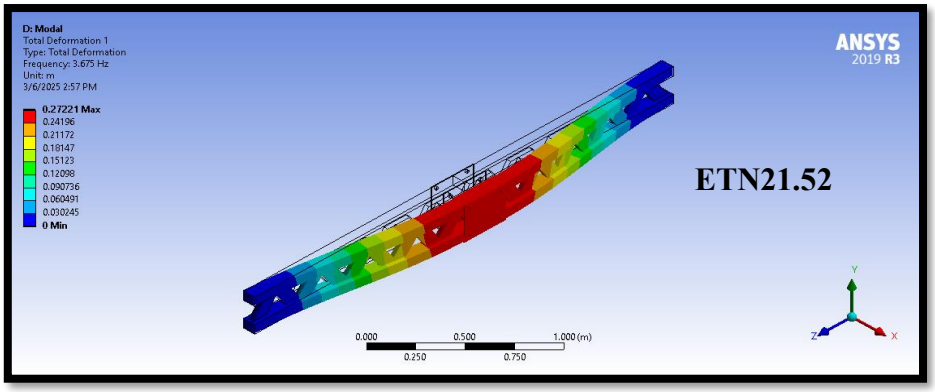
D: Modal
Total Deformation 1
Type: Total Deformation
Frequency: 3.675 Hz
Unit: m
3/6/2025 2:57 PM
0.27221 Max
0.24196
0.21172
0.18147
0.15123
0.12098
0.090736
0.060491
0.030245
0 Min
ANSYS
2019 R3
ETN21.52
0.000
0.500
1.000 (m)
0.250
0.750
Y
Z
X

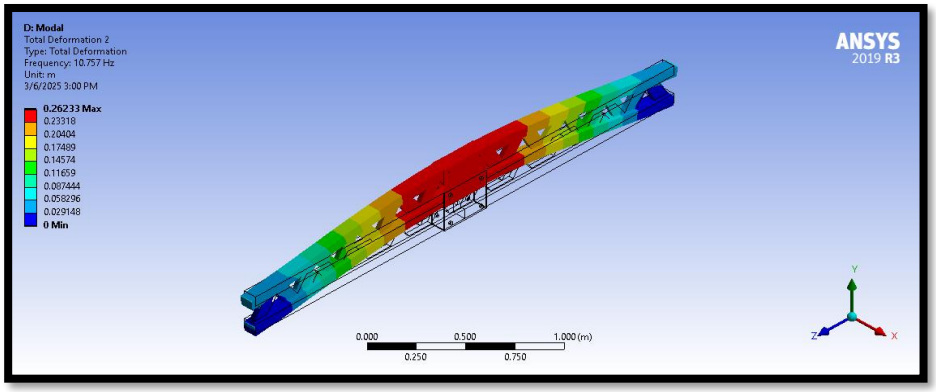
D: Modal
Total Deformation 2
Type: Total Deformation
Frequency: 10.757 Hz
Unit: m
3/6/2025 3:00 PM
0.26233 Max
0.23318
0.20404
0.17489
0.14574
0.11659
0.087444
0.058296
0.029148
0 Min
ANSYS
2019 R3
0.000
0.500
1.000 (m)
0.250
0.750
Y
Z
X

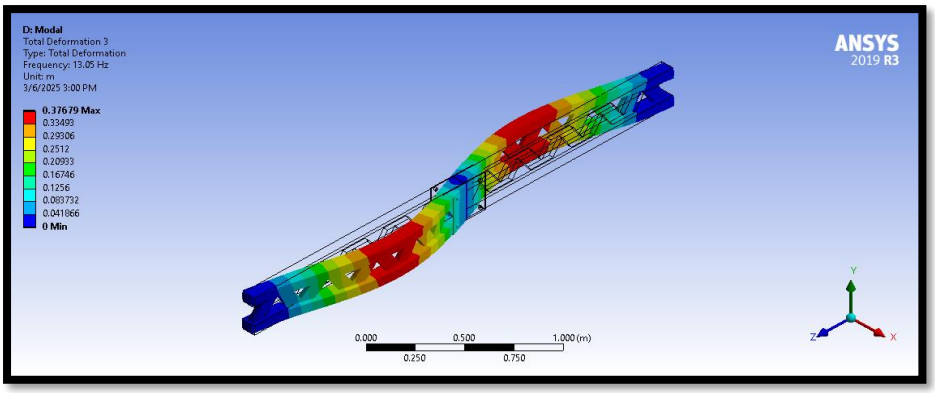
D: Modal
Total Deformation 3
Type: Total Deformation
Frequency: 13.05 Hz
Unit: m
3/6/2025 3:00 PM
0.37679 Max
0.33493
0.29306
0.2512
0.20933
0.16746
0.1256
0.083732
0.041866
0 Min
ANSYS
2019 R3
0.000
0.500
1.000 (m)
0.250
0.750
Y
Z
X

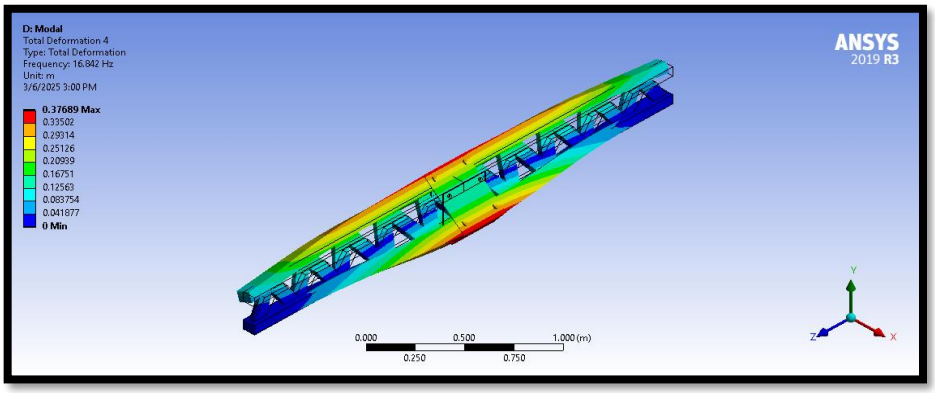
D: Modal
Total Deformation 4
Type: Total Deformation
Frequency: 16.842 Hz
Unit: m
3/6/2025 3:00 PM
0.37689 Max
0.33502
0.29314
0.25126
0.20939
0.16751
0.12563
0.083754
0.041877
0 Min
ANSYS
2019 R3
0.000
0.500
1.000 (m)
0.250
0.750
Y
Z
X

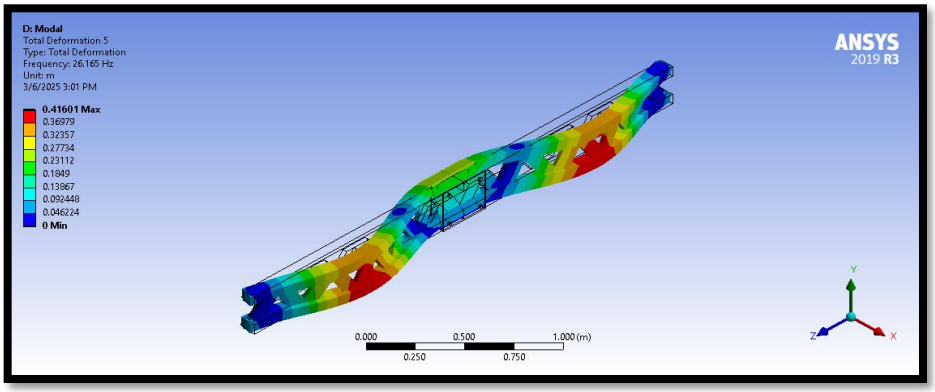
D: Modal
Total Deformation 5
Type: Total Deformation
Frequency: 26.165 Hz
Unit: m
3/6/2025 3:01 PM
0.41601 Max
0.36979
0.32357
0.27734
0.23112
0.1849
0.13867
0.092448
0.046224
0 Min
ANSYS
2019 R3
0.000
0.500
1.000 (m)
0.250
0.750
Y
Z
X

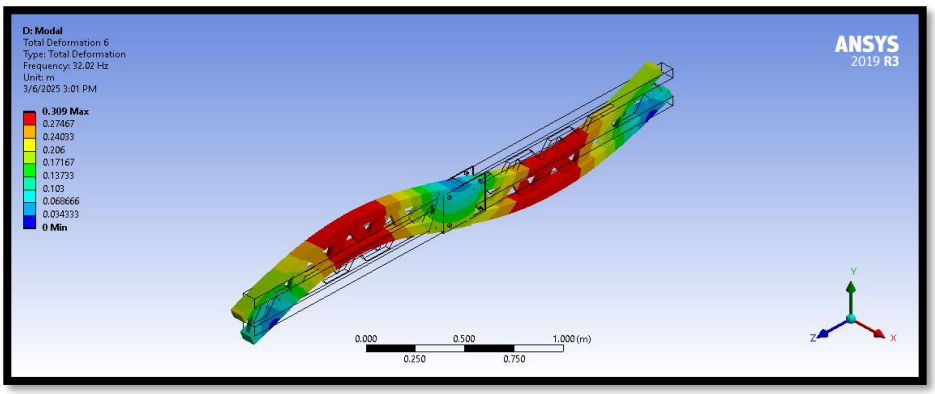
D: Modal
Total Deformation 6
Type: Total Deformation
Frequency: 32.02 Hz
Unit: m
3/6/2025 3:01 PM
0.309 Max
0.27467
0.24033
0.206
0.17167
0.13733
0.103
0.068666
0.034333
0 Min
ANSYS
2019 R3
0.000
0.500
1.000 (m)
0.250
0.750
Y
Z
X

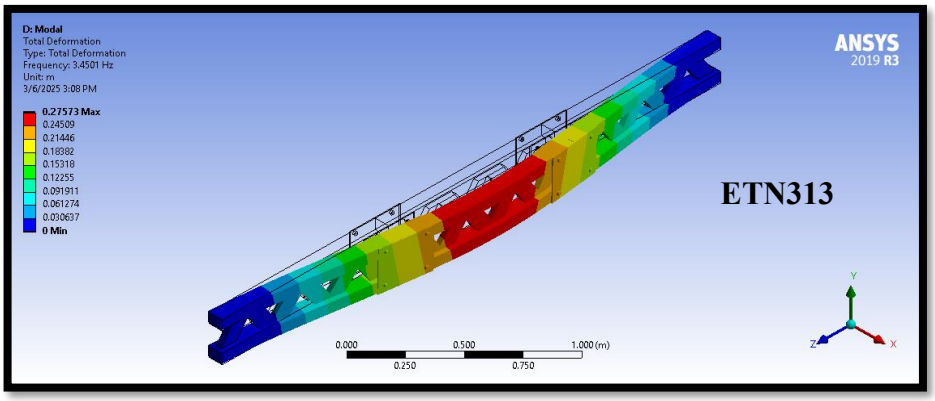
D: Modal
Total Deformation
Type: Total Deformation
Frequency: 3.4501 Hz
Unit: m
3/6/2025 3:08 PM
0.27573 Max
0.24509
0.21446
0.18382
0.15318
0.12255
0.091911
0.061274
0.030637
0 Min
ANSYS
2019 R3
ETN313
0.000
0.500
1.000 (m)
0.250
0.750
Y
Z
X

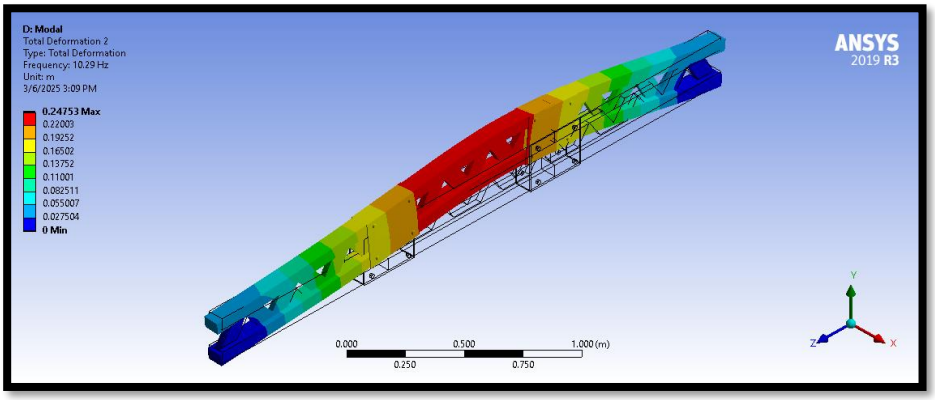
D: Modal
Total Deformation 2
Type: Total Deformation
Frequency: 10.29 Hz
Unit: m
3/6/2025 3:09 PM
0.24753 Max
0.22003
0.19252
0.16502
0.13752
0.11001
0.082511
0.055007
0.027504
0 Min
ANSYS
2019 R3
0.000
0.500
1.000 (m)
0.250
0.750
Y
Z
X

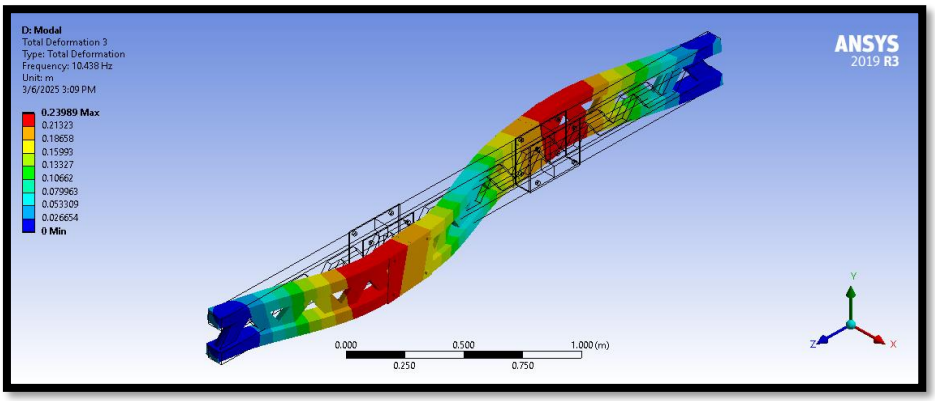
D: Modal
Total Deformation 3
Type: Total Deformation
Frequency: 10.438 Hz
Unit: m
3/6/2025 3:09 PM
0.23989 Max
0.21323
0.18658
0.15993
0.13327
0.10662
0.079963
0.053309
0.026654
0 Min
ANSYS
2019 R3
0.000
0.500
1.000 (m)
0.250
0.750
Y
Z
X

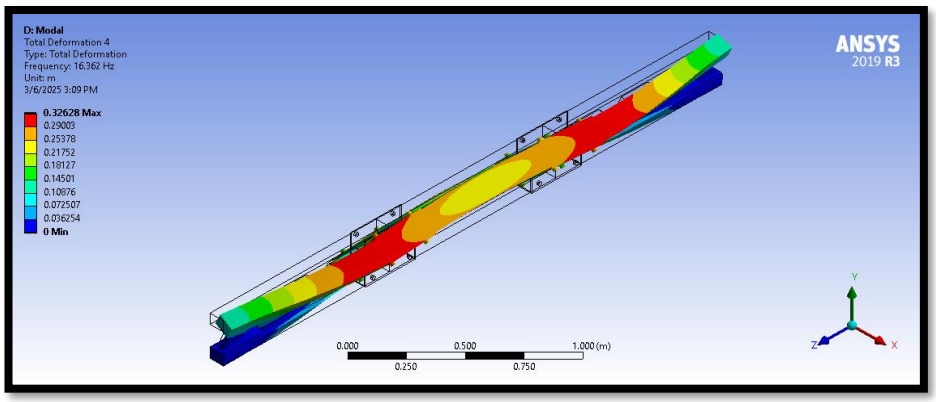
D: Modal
Total Deformation 4
Type: Total Deformation
Frequency: 16.362 Hz
Unit: m
3/6/2025 3:09 PM
0.32628 Max
0.29003
0.25378
0.21752
0.18127
0.14501
0.10876
0.072507
0.036254
0 Min
ANSYS
2019 R3
0.000
0.500
1.000 (m)
0.250
0.750
Y
Z
X

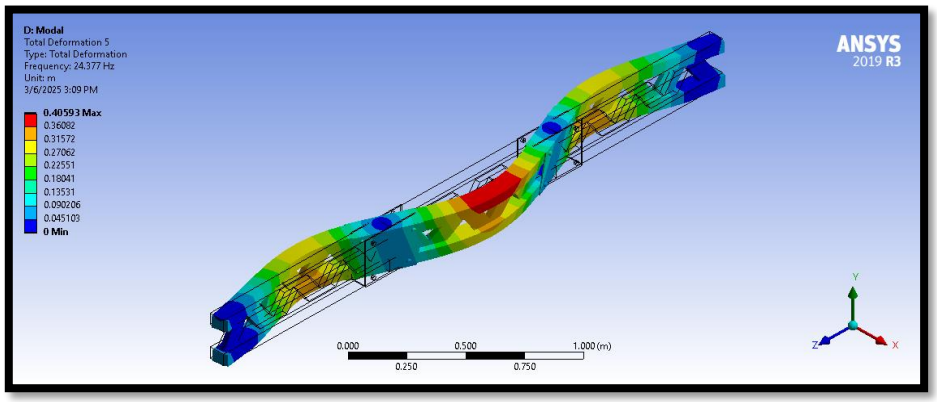
D: Modal
Total Deformation 5
Type: Total Deformation
Frequency: 24.377 Hz
Unit: m
3/6/2025 3:09 PM
0.40593 Max
0.36082
0.31572
0.27062
0.22551
0.18041
0.13531
0.090206
0.045103
0 Min
ANSYS
2019 R3
0.000
0.500
1.000 (m)
0.250
0.750
Y
Z
X

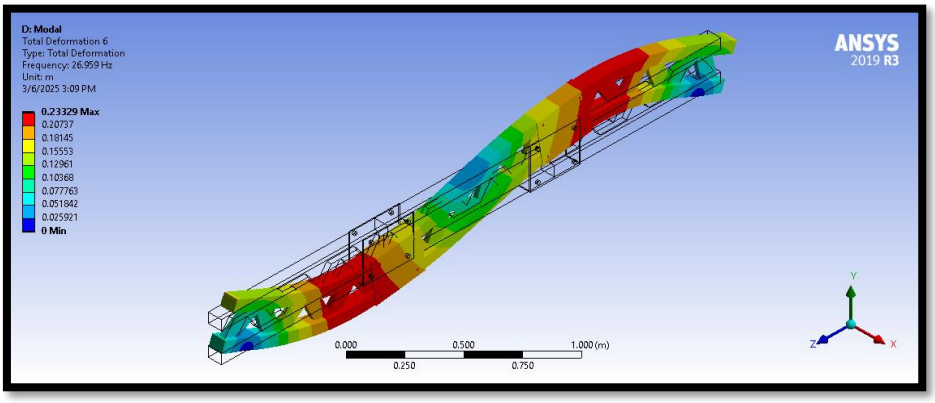
D: Modal
Total Deformation 6
Type: Total Deformation
Frequency: 26.959 Hz
Unit: m
3/6/2025 3:09 PM
0.23329 Max
0.20737
0.18145
0.15553
0.12961
0.10368
0.077763
0.051842
0.025921
0 Min
ANSYS
2019 R3
0.000
0.500
1.000 (m)
0.250
0.750
Y
Z
X

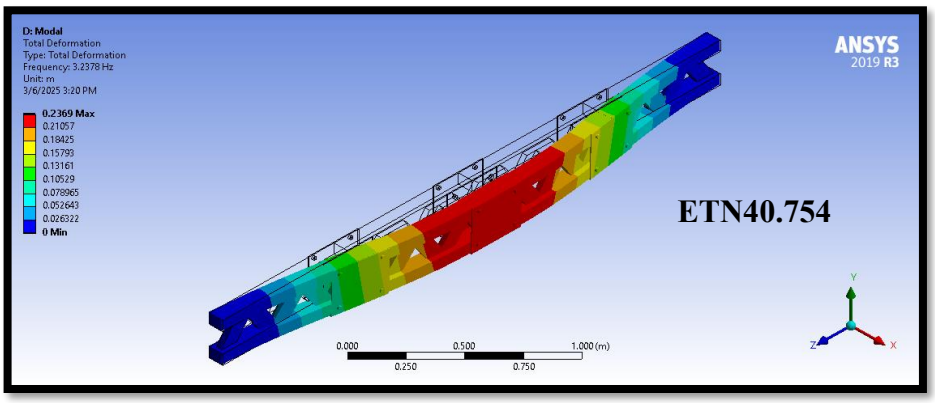
D: Modal
Total Deformation
Type: Total Deformation
Frequency: 3.2378 Hz
Unit: m
3/6/2025 3:20 PM
0.2369 Max
0.21057
0.18425
0.15793
0.13161
0.10529
0.078965
0.052643
0.026322
0 Min
ANSYS
2019 R3
ETN40.754
0.000
0.500
1.000 (m)
0.250
0.750
Y
Z
X

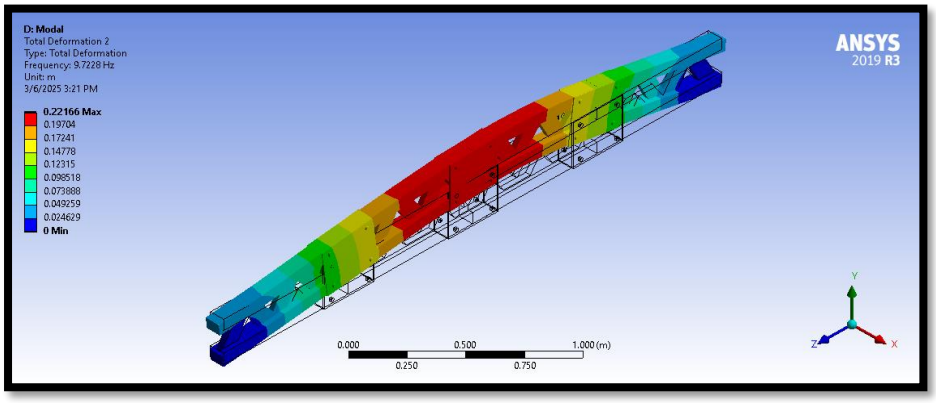
D: Modal
Total Deformation 2
Type: Total Deformation
Frequency: 9.7228 Hz
Unit: m
3/6/2025 3:21 PM
0.22166 Max
0.19704
0.17241
0.14778
0.12315
0.098518
0.073888
0.049259
0.024629
0 Min
ANSYS
2019 R3
0.000
0.500
1.000 (m)
0.250
0.750
Y
Z
X

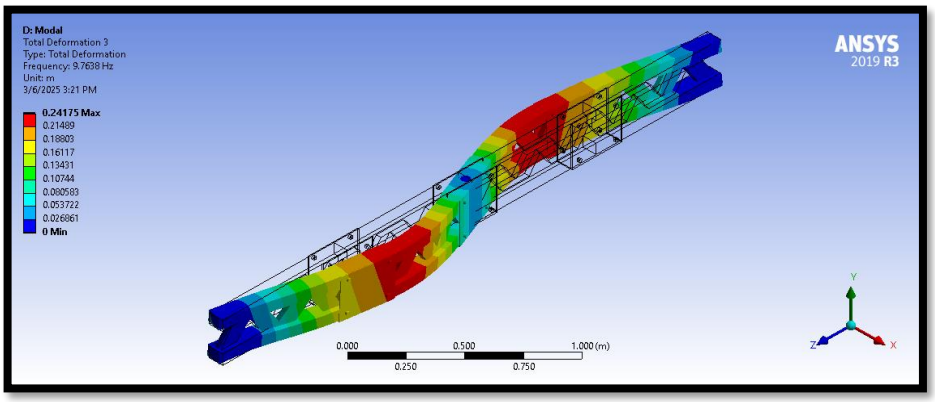
D: Modal
Total Deformation 3
Type: Total Deformation
Frequency: 9.7638 Hz
Unit: m
3/6/2025 3:21 PM
0.24175 Max
0.21489
0.18803
0.16117
0.13431
0.10744
0.080583
0.053722
0.026861
0 Min
ANSYS
2019 R3
0.000
0.500
1.000 (m)
0.250
0.750
Y
Z
X

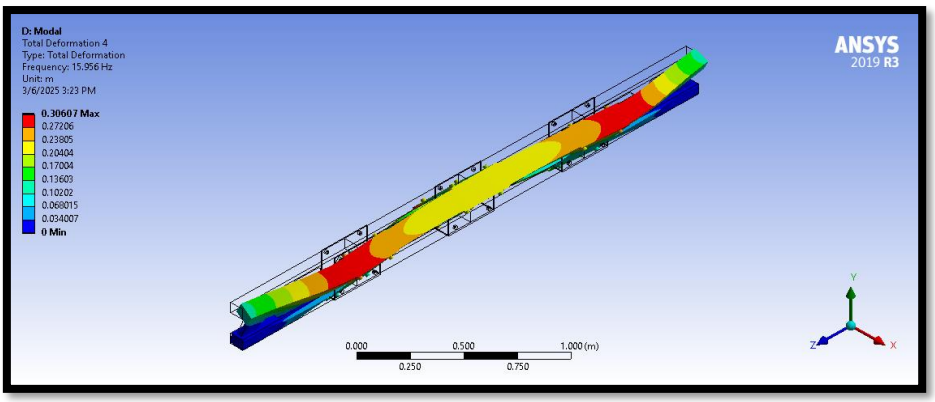
D: Modal
Total Deformation 4
Type: Total Deformation
Frequency: 15.956 Hz
Unit: m
3/6/2025 3:23 PM
0.30607 Max
0.27206
0.23805
0.20404
0.17004
0.13603
0.10202
0.068015
0.034007
0 Min
ANSYS
2019 R3
0.000
0.500
1.000 (m)
0.250
0.750
Y
Z
X

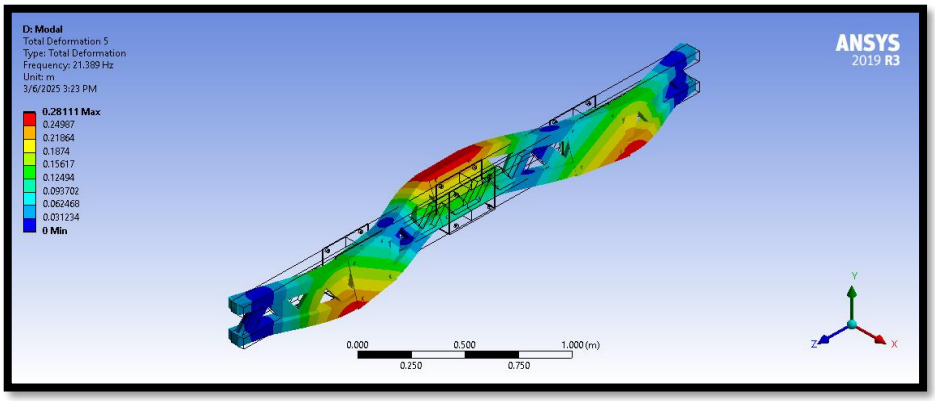
D: Modal
Total Deformation 5
Type: Total Deformation
Frequency: 21.389 Hz
Unit: m
3/6/2025 3:23 PM
0.28111 Max
0.24987
0.21864
0.1874
0.15617
0.12494
0.093702
0.062468
0.031234
0 Min
ANSYS
2019 R3
0.000
0.500
1.000 (m)
0.250
0.750
Y
Z
X

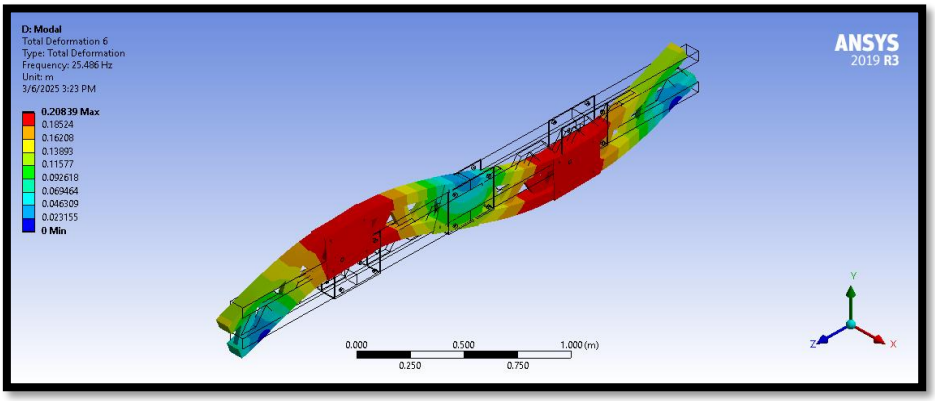
D: Modal
Total Deformation 6
Type: Total Deformation
Frequency: 25.486 Hz
Unit: m
3/6/2025 3:23 PM
0.20839 Max
0.18524
0.16208
0.13893
0.11577
0.092618
0.069464
0.046309
0.023155
0 Min
ANSYS
2019 R3
0.000
0.500
1.000 (m)
0.250
0.750
Y
Z
X

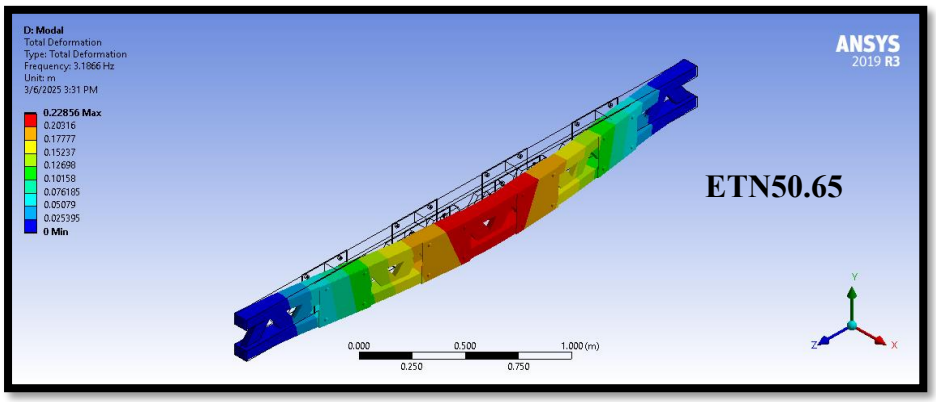
D: Modal
Total Deformation
Type: Total Deformation
Frequency: 3.1866 Hz
Unit: m
3/6/2025 3:31 PM
0.22856 Max
0.20316
0.17777
0.15237
0.12698
0.10158
0.076185
0.05079
0.025395
0 Min
ANSYS
2019 R3
ETN50.65
0.000
0.500
1.000 (m)
0.250
0.750
Y
Z
X

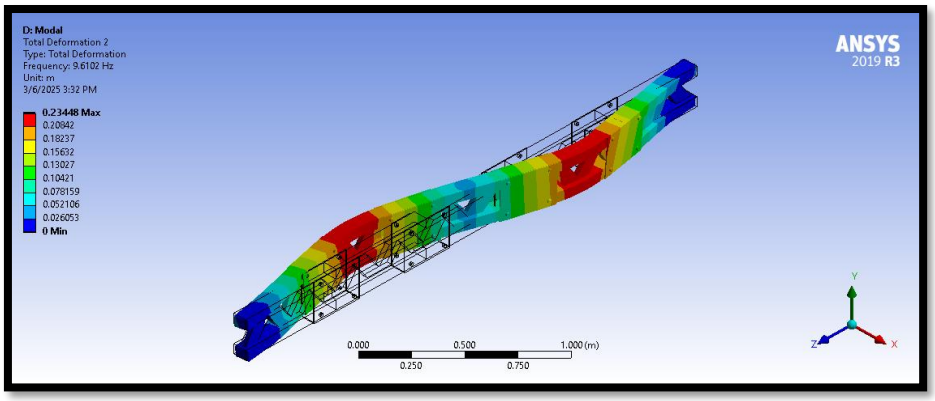
D: Modal
Total Deformation 2
Type: Total Deformation
Frequency: 9.6102 Hz
Unit: m
3/6/2025 3:32 PM
0.23448 Max
0.20942
0.18237
0.15632
0.13027
0.10421
0.078159
0.052106
0.026053
0 Min
ANSYS
2019 R3
0.000
0.500
1.000 (m)
0.250
0.750
Y
Z
X

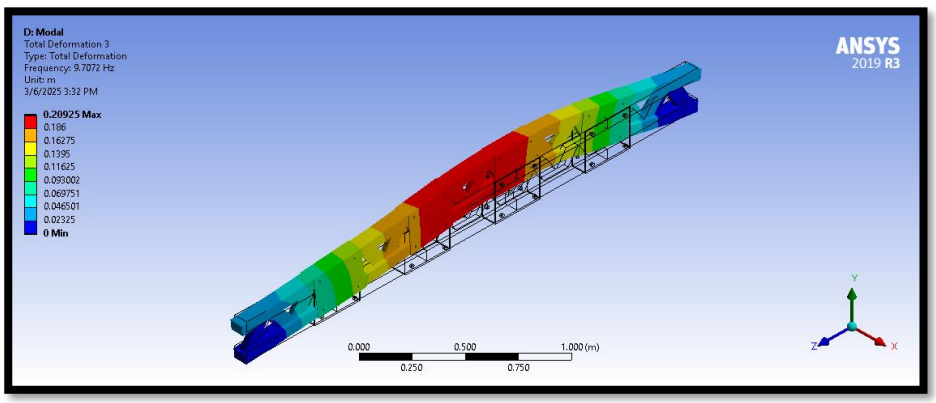
D: Modal
Total Deformation 3
Type: Total Deformation
Frequency: 9.7072 Hz
Unit: m
3/6/2025 3:32 PM
0.20925 Max
0.186
0.16275
0.1395
0.11625
0.093002
0.069751
0.046501
0.02325
0 Min
ANSYS
2019 R3
0.000
0.500
1.000 (m)
0.250
0.750
Y
Z
X

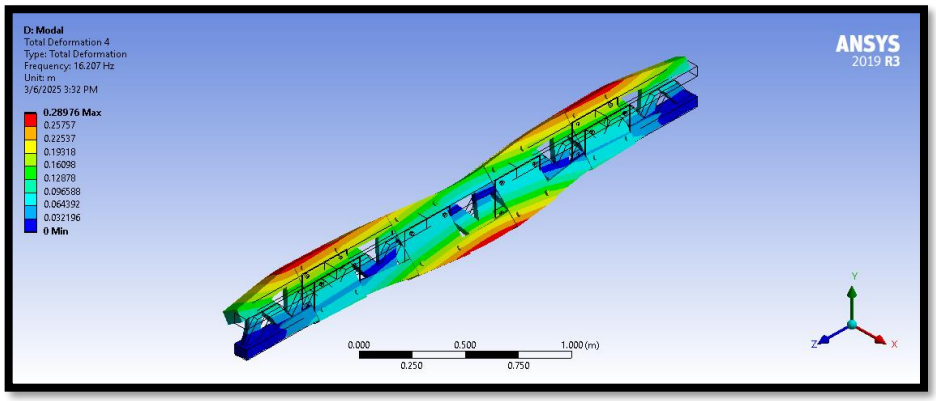
D: Modal
Total Deformation 4
Type: Total Deformation
Frequency: 16.207 Hz
Unit: m
3/6/2025 3:32 PM
0.28976 Max
0.25757
0.22537
0.19318
0.16098
0.12878
0.096588
0.064392
0.032196
0 Min
ANSYS
2019 R3
0.000
0.500
1.000 (m)
0.250
0.750
Y
Z
X

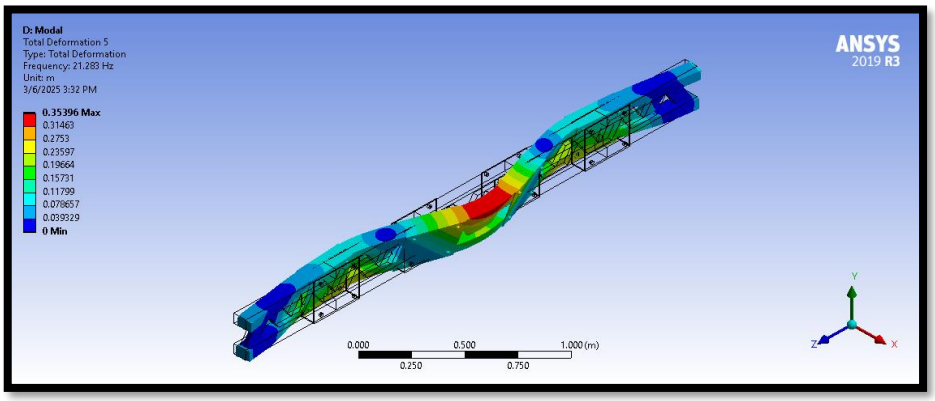
D: Modal
Total Deformation 5
Type: Total Deformation
Frequency: 21.283 Hz
Unit: m
3/6/2025 3:32 PM
0.35396 Max
0.31463
0.2753
0.23597
0.19664
0.15731
0.11799
0.078657
0.039329
0 Min
ANSYS
2019 R3
0.000
0.500
1.000 (m)
0.250
0.750
Y
Z
X

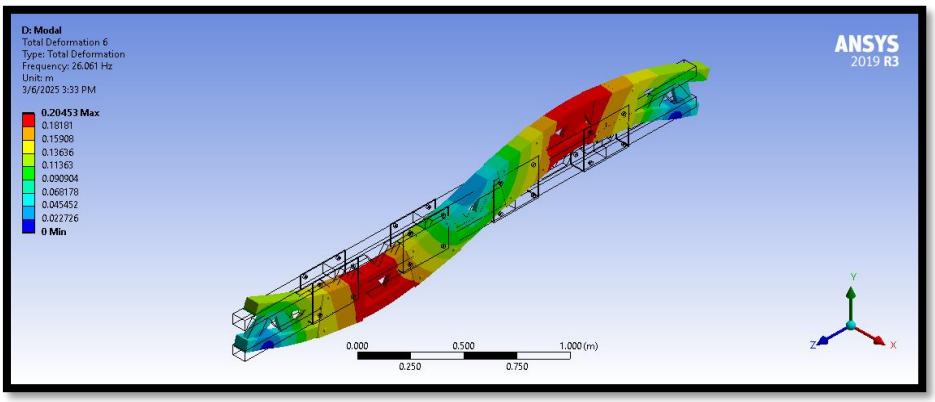
D: Modal
Total Deformation 6
Type: Total Deformation
Frequency: 26.061 Hz
Unit: m
3/6/2025 3:33 PM
0.20453 Max
0.18181
0.15908
0.13636
0.11363
0.090904
0.068178
0.045452
0.022726
0 Min
ANSYS
2019 R3
0.000
0.500
1.000 (m)
0.250
0.750
Y
Z
X

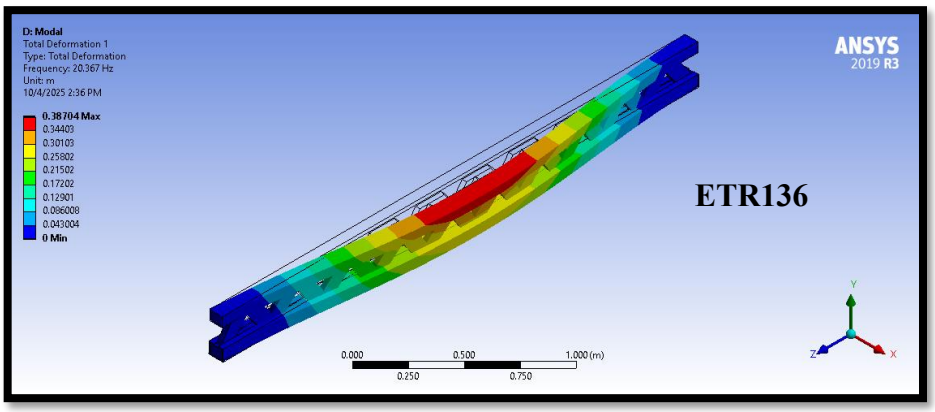
D: Modal
Total Deformation 1
Type: Total Deformation
Frequency: 20.367 Hz
Unit: m
10/4/2025 2:36 PM
0.38704 Max
0.34403
0.30103
0.25802
0.21502
0.17202
0.12901
0.086008
0.043004
0 Min
ANSYS
2019 R3
ETR136
0.000
0.500
1.000 (m)
0.250
0.750
Y
Z
X

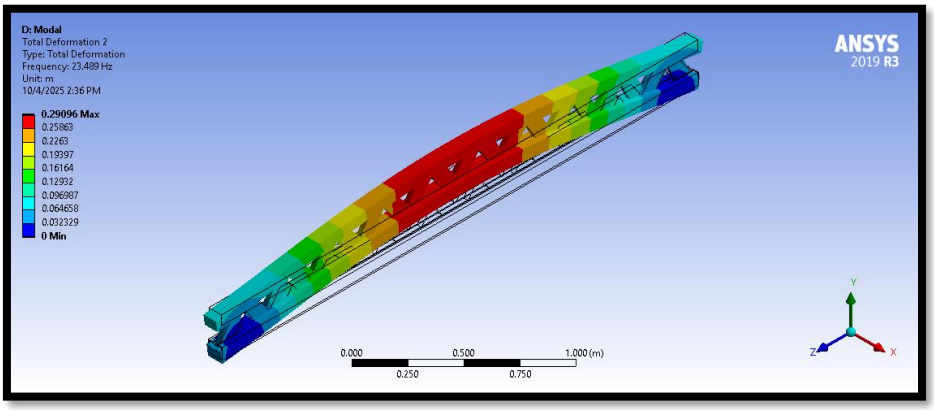
D: Modal
Total Deformation 2
Type: Total Deformation
Frequency: 23.489 Hz
Unit: m
10/4/2025 2:36 PM
0.29096 Max
0.25863
0.2263
0.19397
0.16164
0.12932
0.096987
0.064658
0.032329
0 Min
ANSYS
2019 R3
0.000
0.500
1.000 (m)
0.250
0.750
Y
Z
X

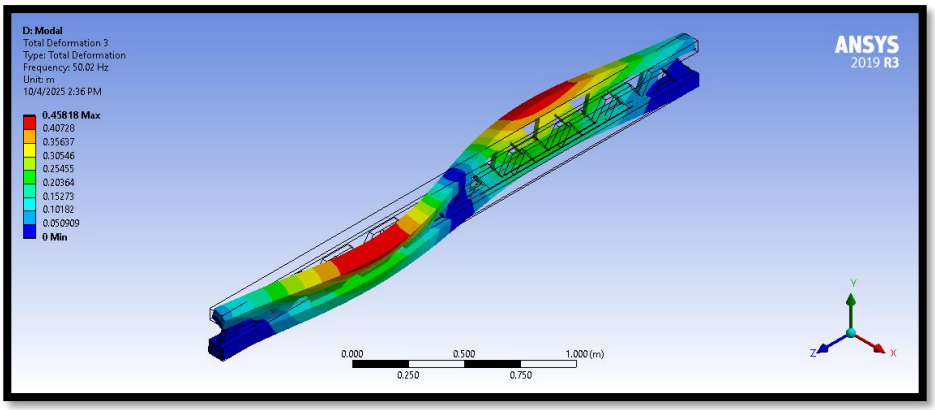
D: Modal
Total Deformation 3
Type: Total Deformation
Frequency: 50.02 Hz
Unit: m
10/4/2025 2:36 PM
0.45818 Max
0.40728
0.35637
0.30546
0.25455
0.20364
0.15273
0.10182
0.050909
0 Min
ANSYS
2019 R3
0.000
0.500
1.000 (m)
0.250
0.750
Y
Z
X

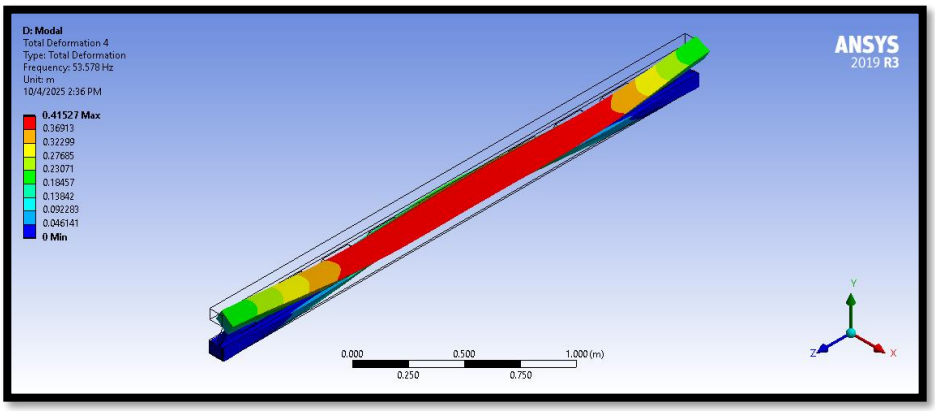
D: Modal
Total Deformation 4
Type: Total Deformation
Frequency: 53.578 Hz
Unit: m
10/4/2025 2:36 PM
0.41527 Max
0.36913
0.32299
0.27685
0.23071
0.18457
0.13842
0.092283
0.046141
0 Min
ANSYS
2019 R3
0.000
0.500
1.000 (m)
0.250
0.750
Y
Z
X

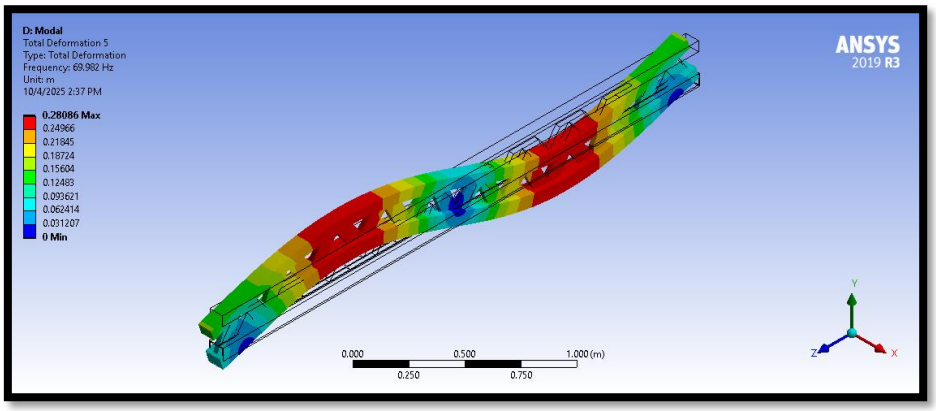
D: Modal
Total Deformation 5
Type: Total Deformation
Frequency: 69.982 Hz
Unit: m
10/4/2025 2:37 PM
0.28086 Max
0.24966
0.21845
0.18724
0.15604
0.12483
0.093621
0.062414
0.031207
0 Min
ANSYS
2019 R3
0.000
0.500
1.000 (m)
0.250
0.750
Y
Z
X

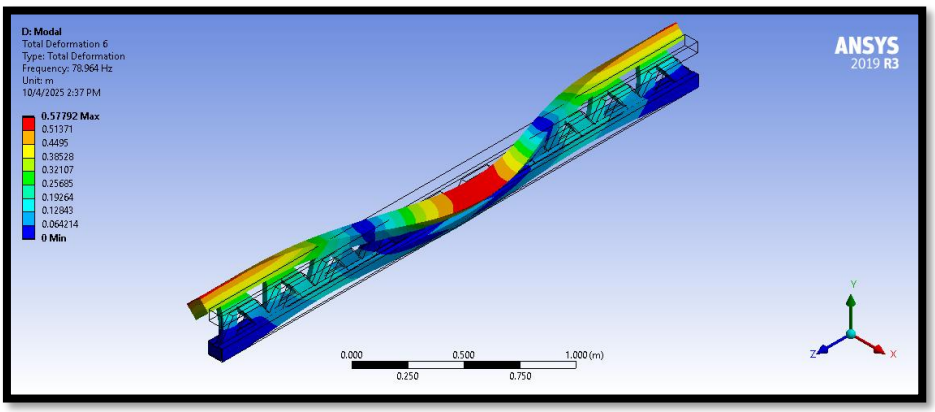
D: Modal
Total Deformation 6
Type: Total Deformation
Frequency: 78.964 Hz
Unit: m
10/4/2025 2:37 PM
0.57792 Max
0.51371
0.4495
0.38528
0.32107
0.25685
0.19264
0.12843
0.064214
0 Min
ANSYS
2019 R3
0.000
0.500
1.000 (m)
0.250
0.750
Y
Z
X

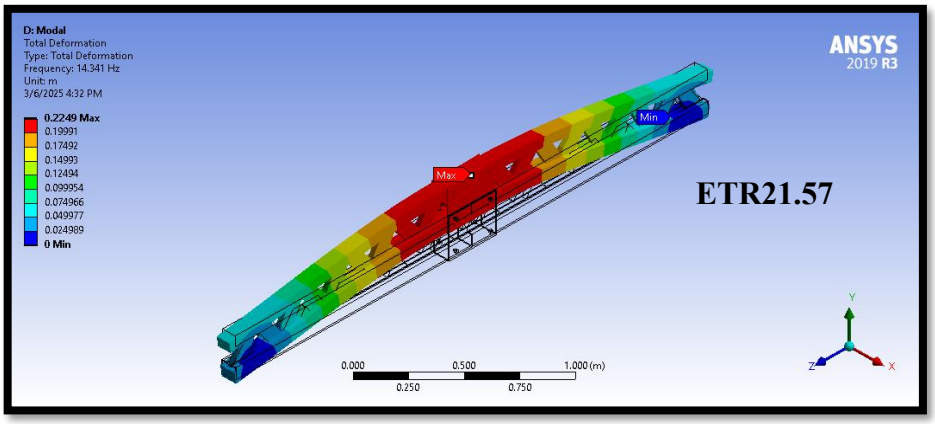
D: Modal
Total Deformation
Type: Total Deformation
Frequency: 14.341 Hz
Unit: m
3/6/2025 4:32 PM
0.2249 Max
0.19991
0.17492
0.14993
0.12494
0.099954
0.074966
0.049977
0.024989
0 Min
ANSYS
2019 R3
Max
Min
0.000
0.500
1.000 (m)
0.250
0.750
Y
Z
X

ETR21.57

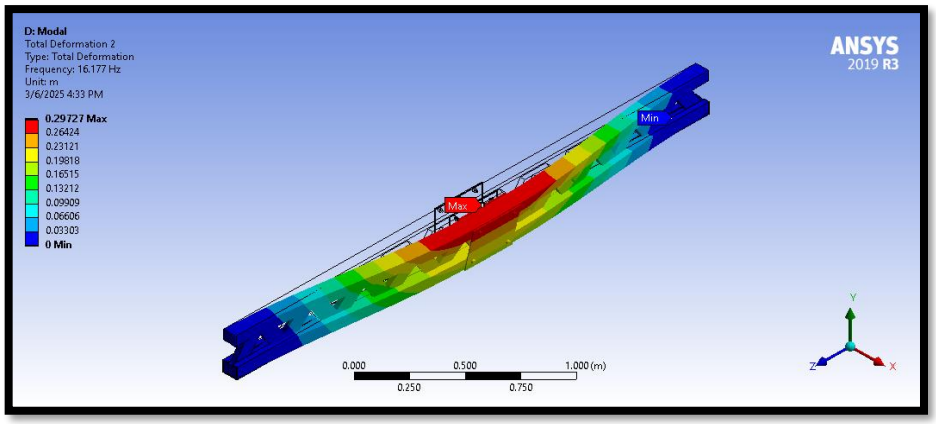
D: Modal
Total Deformation 2
Type: Total Deformation
Frequency: 16.177 Hz
Unit: m
3/6/2025 4:33 PM
0.29727 Max
0.26424
0.23121
0.19818
0.16515
0.13212
0.09909
0.06606
0.03303
0 Min
ANSYS
2019 R3
Max
Min
0.000
0.500
1.000 (m)
0.250
0.750
Y
Z
X

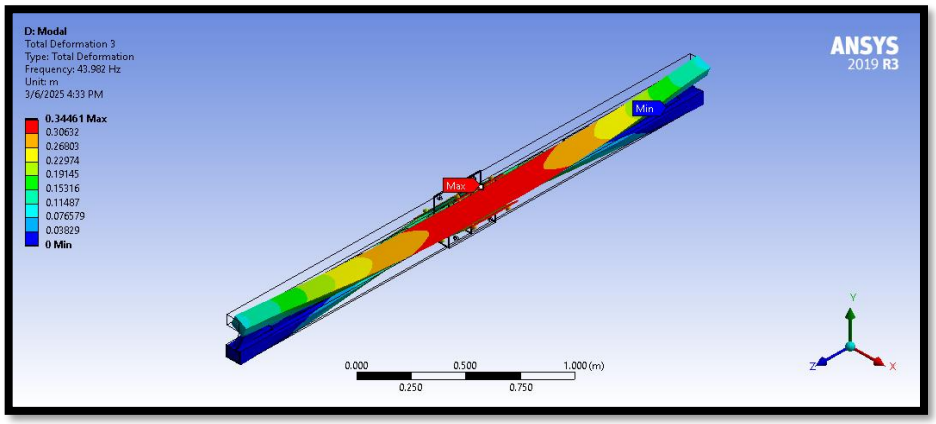
D: Modal
Total Deformation 3
Type: Total Deformation
Frequency: 43.982 Hz
Unit: m
3/6/2025 4:33 PM
0.34461 Max
0.30632
0.26803
0.22974
0.19145
0.15316
0.11487
0.076579
0.03829
0 Min
ANSYS
2019 R3
Max
Min
0.000
0.500
1.000 (m)
0.250
0.750
Y
Z
X

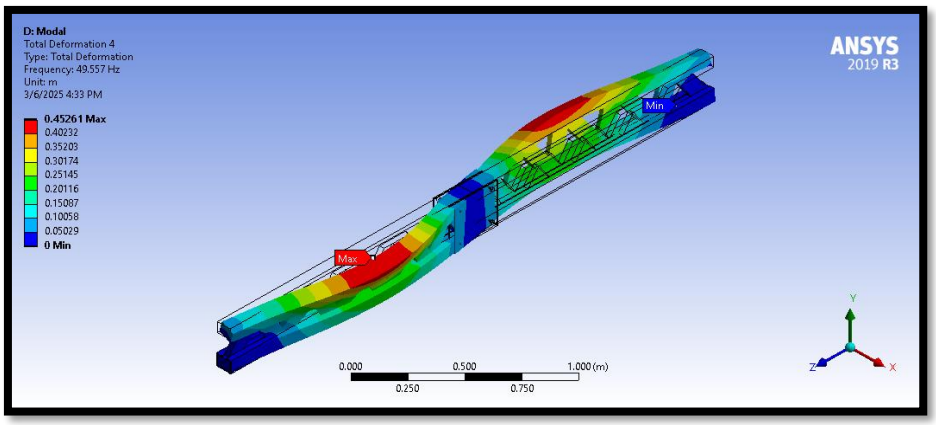
D: Modal
Total Deformation 4
Type: Total Deformation
Frequency: 49.557 Hz
Unit: m
3/6/2025 4:33 PM
0.45261 Max
0.40232
0.35203
0.30174
0.25145
0.20116
0.15087
0.10058
0.05029
0 Min
ANSYS
2019 R3
Max
Min
0.000
0.500
1.000 (m)
0.250
0.750
Y
Z
X

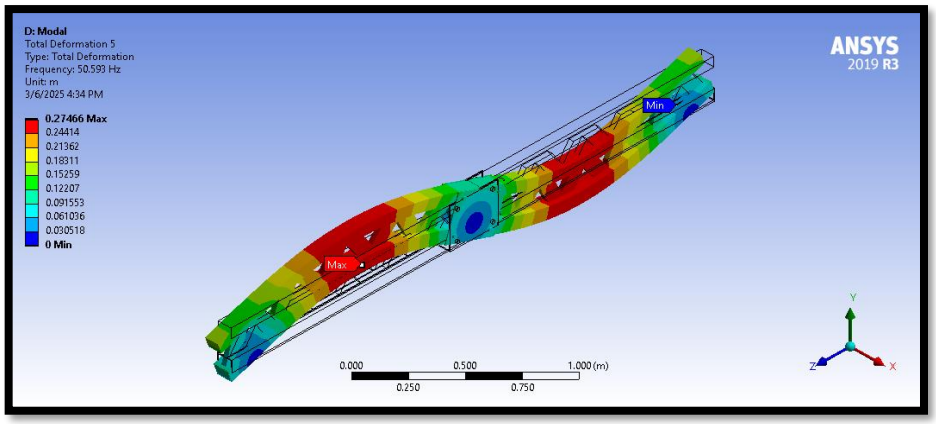
D: Modal
Total Deformation 5
Type: Total Deformation
Frequency: 50.593 Hz
Unit: m
3/6/2025 4:34 PM
0.27466 Max
0.24414
0.21362
0.18311
0.15259
0.12207
0.091553
0.061036
0.030518
0 Min
Min
Max
0.000
0.500
1.000 (m)
0.250
0.750
ANSYS
2019 R3
Y
Z
X

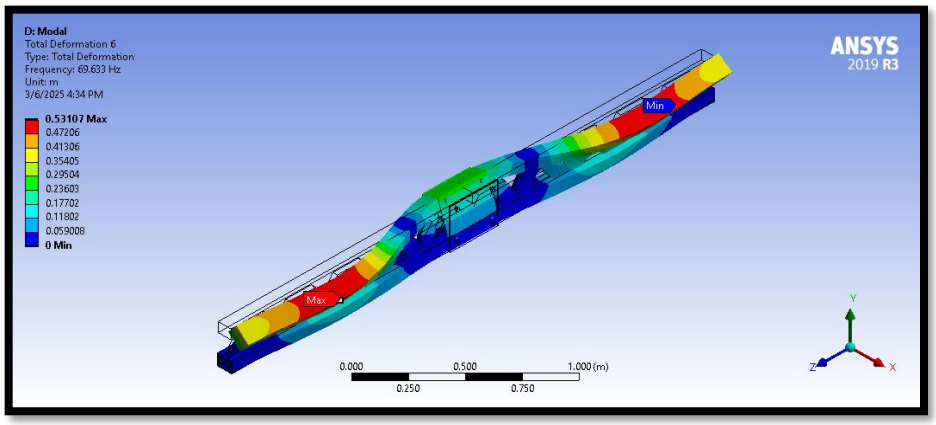
D: Modal
Total Deformation 6
Type: Total Deformation
Frequency: 69.633 Hz
Unit: m
3/6/2025 4:34 PM
0.53107 Max
0.47206
0.41306
0.35405
0.29504
0.23603
0.17702
0.11802
0.059008
0 Min
Min
Max
0.000
0.500
1.000 (m)
0.250
0.750
ANSYS
2019 R3
Y
Z
X

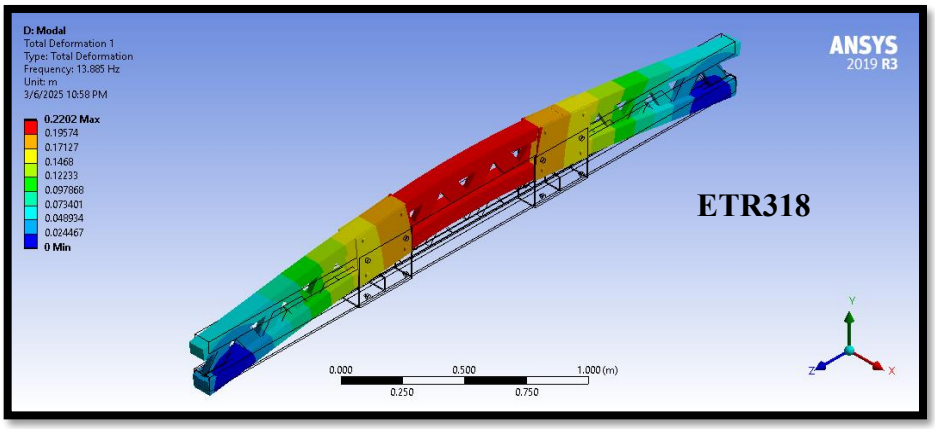
D: Modal
Total Deformation 1
Type: Total Deformation
Frequency: 13.885 Hz
Unit: m
3/6/2025 10:58 PM
0.2202 Max
0.19574
0.17127
0.1468
0.12233
0.097868
0.073401
0.048934
0.024467
0 Min
ETR318
0.000
0.500
1.000 (m)
0.250
0.750
ANSYS
2019 R3
Y
Z
X

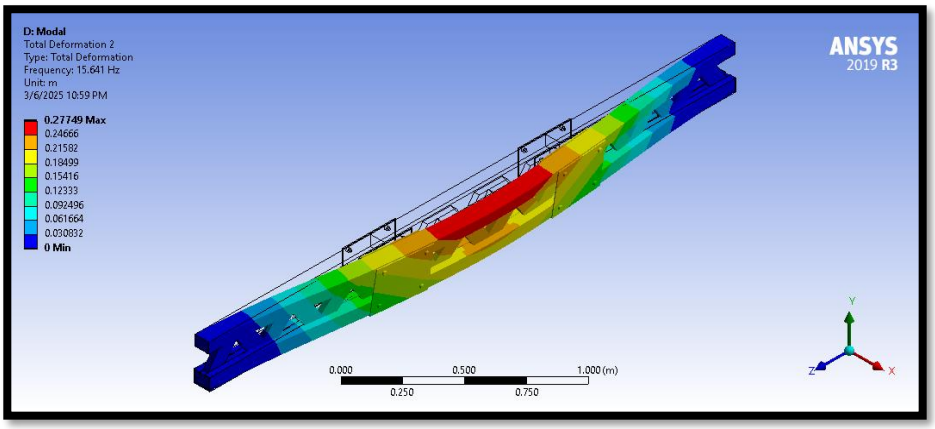
D: Modal
Total Deformation 2
Type: Total Deformation
Frequency: 15.641 Hz
Unit: m
3/6/2025 10:59 PM
0.27749 Max
0.24666
0.21582
0.18499
0.15416
0.12333
0.092496
0.061664
0.030832
0 Min
0.000
0.500
1.000 (m)
0.250
0.750
ANSYS
2019 R3
Y
Z
X

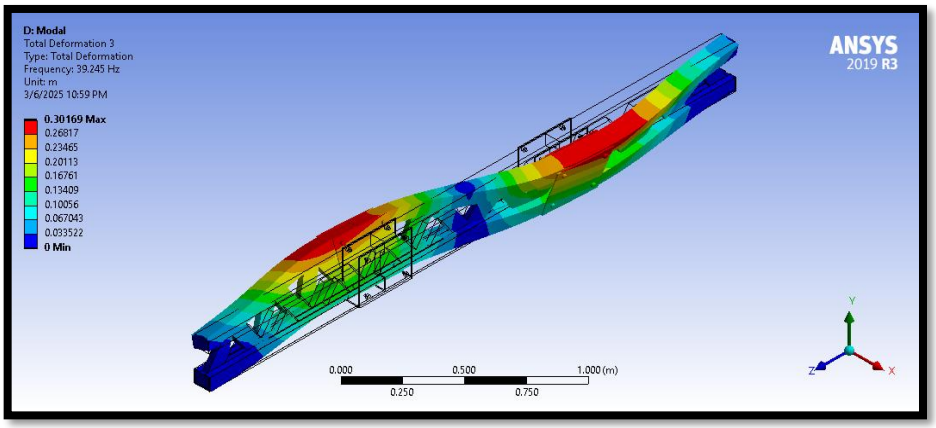
D: Modal
Total Deformation 3
Type: Total Deformation
Frequency: 39.245 Hz
Unit: m
3/6/2025 10:59 PM
0.30169 Max
0.26817
0.23465
0.20113
0.16761
0.13409
0.10056
0.067043
0.033522
0 Min
ANSYS
2019 R3
0.000
0.500
1.000 (m)
0.250
0.750
Y
Z
X

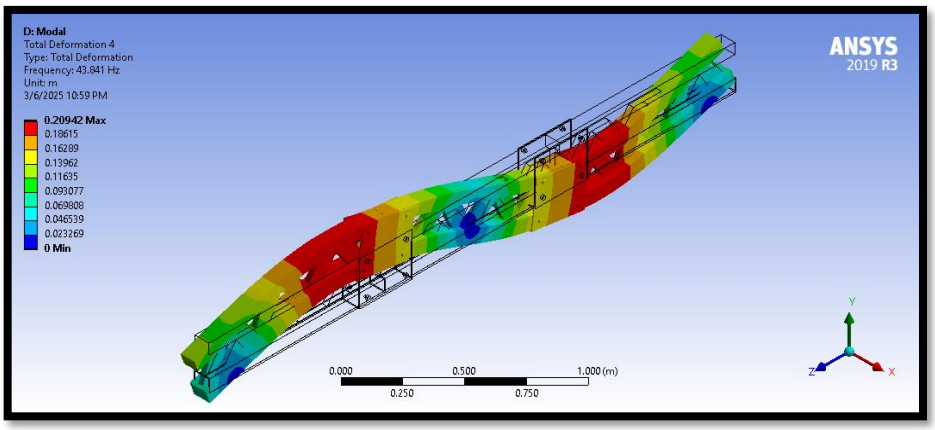
D: Modal
Total Deformation 4
Type: Total Deformation
Frequency: 43.841 Hz
Unit: m
3/6/2025 10:59 PM
0.20942 Max
0.18615
0.16289
0.13962
0.11635
0.093077
0.069808
0.046539
0.023269
0 Min
ANSYS
2019 R3
0.000
0.500
1.000 (m)
0.250
0.750
Y
Z
X

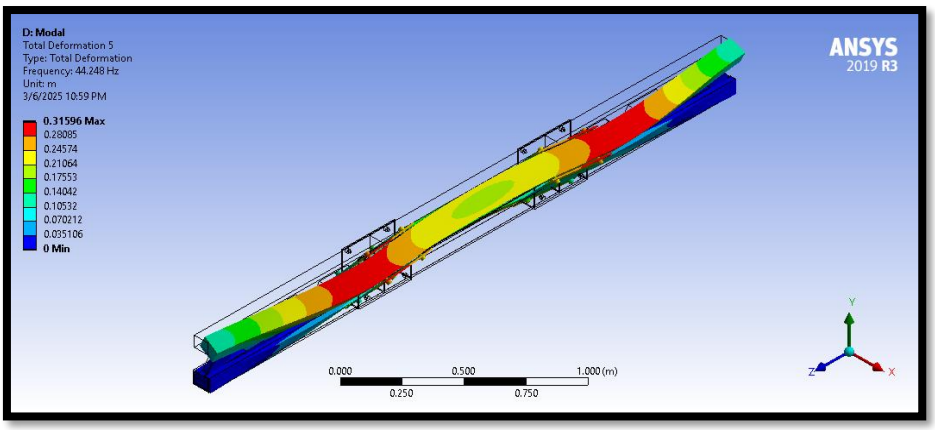
D: Modal
Total Deformation 5
Type: Total Deformation
Frequency: 44.248 Hz
Unit: m
3/6/2025 10:59 PM
0.31596 Max
0.28085
0.24574
0.21064
0.17553
0.14042
0.10532
0.070212
0.035106
0 Min
ANSYS
2019 R3
0.000
0.500
1.000 (m)
0.250
0.750
Y
Z
X

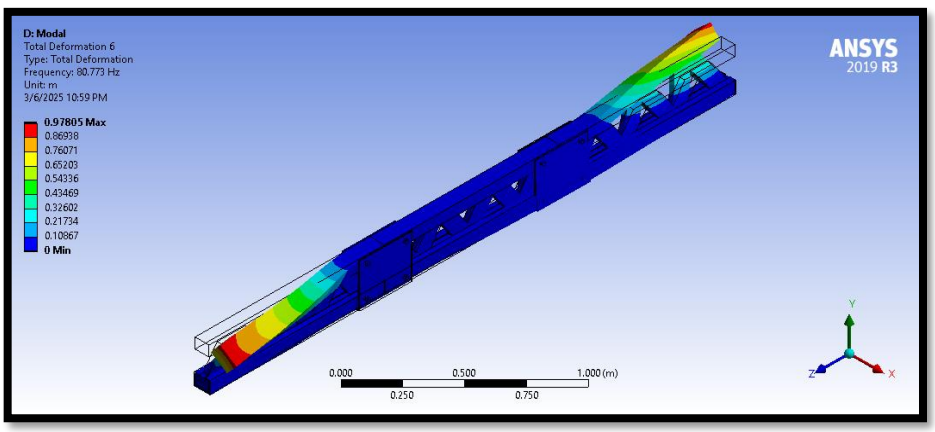
D: Modal
Total Deformation 6
Type: Total Deformation
Frequency: 80.773 Hz
Unit: m
3/6/2025 10:59 PM
0.97805 Max
0.86938
0.76071
0.65203
0.54336
0.43469
0.32602
0.21734
0.10867
0 Min
ANSYS
2019 R3
0.000
0.500
1.000 (m)
0.250
0.750
Y
Z
X

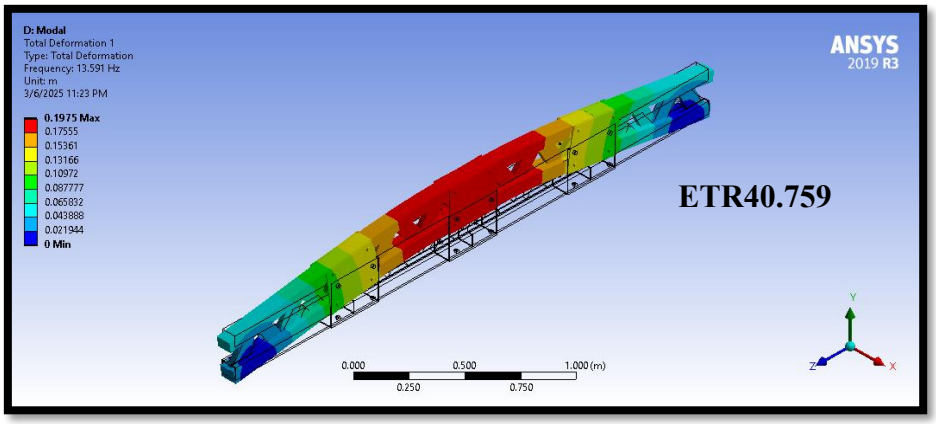
D: Modal
Total Deformation 1
Type: Total Deformation
Frequency: 13.591 Hz
Unit: m
3/6/2025 11:23 PM
0.1975 Max
0.17555
0.15361
0.13166
0.10972
0.087777
0.065832
0.043888
0.021944
0 Min
ANSYS
2019 R3
ETR40.759
0.000
0.500
1.000 (m)
0.250
0.750
Y
Z
X

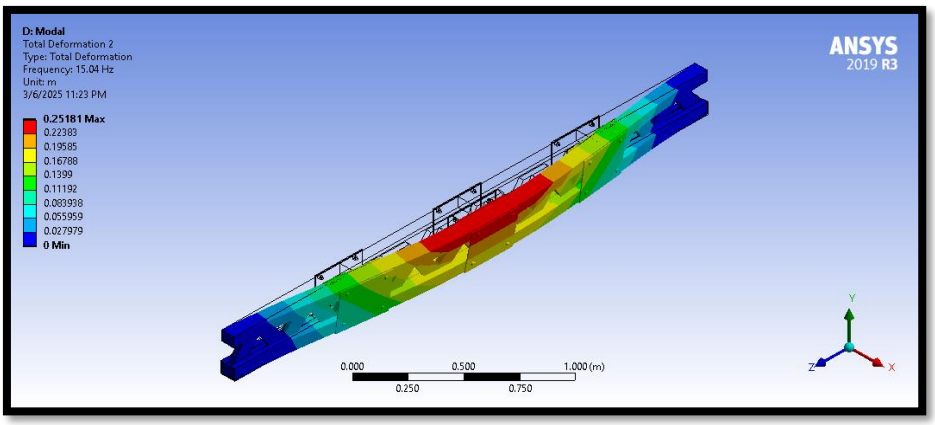
D: Modal
Total Deformation 2
Type: Total Deformation
Frequency: 15.04 Hz
Unit: m
3/6/2025 11:23 PM
0.25181 Max
0.22383
0.19585
0.16788
0.1399
0.11192
0.083938
0.055959
0.027979
0 Min
ANSYS
2019 R3
0.000
0.500
1.000 (m)
0.250
0.750
Y
Z
X

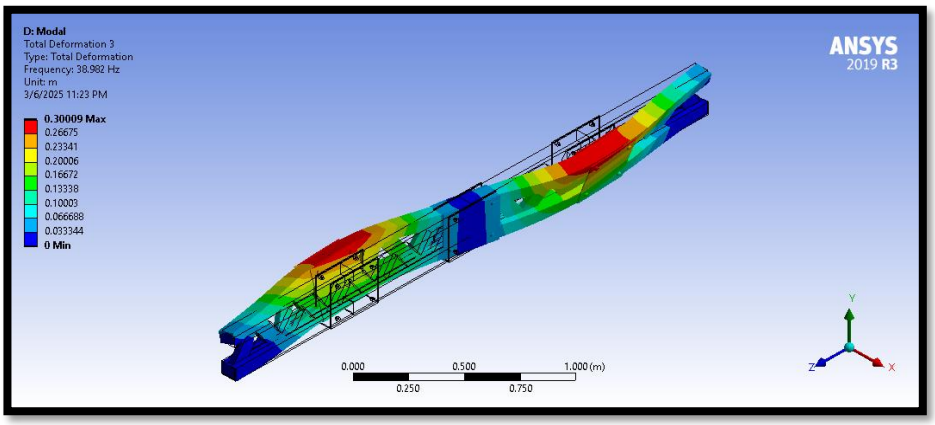
D: Modal
Total Deformation 3
Type: Total Deformation
Frequency: 38.982 Hz
Unit: m
3/6/2025 11:23 PM
0.30009 Max
0.26675
0.23341
0.20006
0.16672
0.13338
0.10003
0.066688
0.033344
0 Min
ANSYS
2019 R3
0.000
0.500
1.000 (m)
0.250
0.750
Y
Z
X

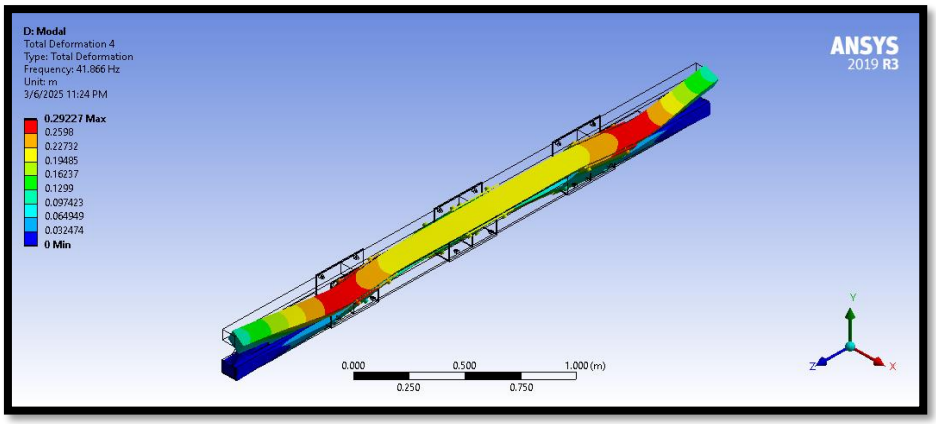
D: Modal
Total Deformation 4
Type: Total Deformation
Frequency: 41.866 Hz
Unit: m
3/6/2025 11:24 PM
0.29227 Max
0.2598
0.22732
0.19485
0.16237
0.1299
0.097423
0.064949
0.032474
0 Min
ANSYS
2019 R3
0.000
0.500
1.000 (m)
0.250
0.750
Y
Z
X

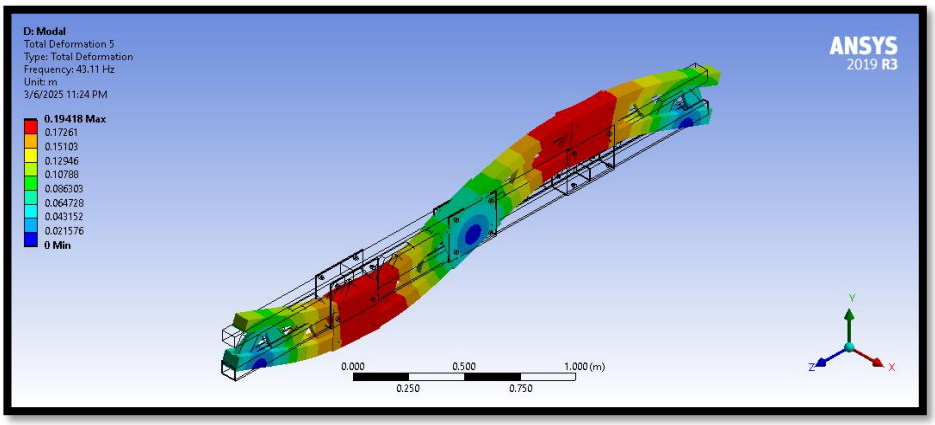
D: Modal
Total Deformation 5
Type: Total Deformation
Frequency: 43.11 Hz
Unit: m
3/6/2025 11:24 PM
0.19418 Max
0.17261
0.15103
0.12946
0.10788
0.086303
0.064728
0.043152
0.021576
0 Min
ANSYS
2019 R3
0.000
0.500
1.000 (m)
0.250
0.750
Y
Z
X

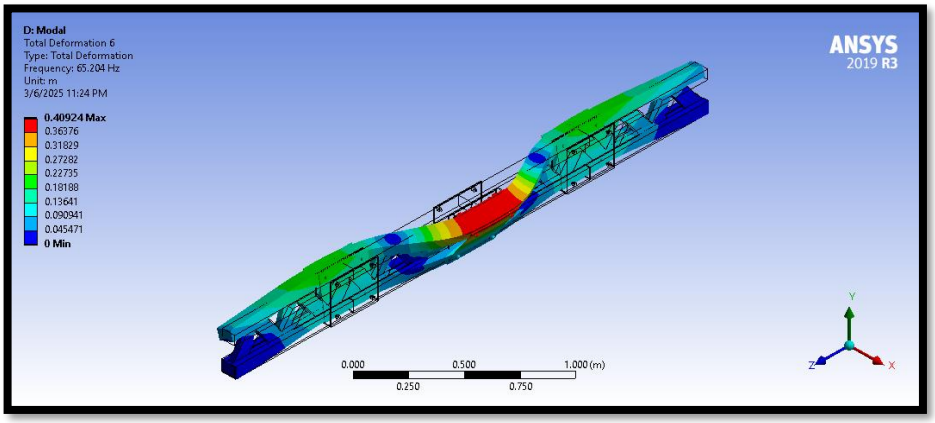
D: Modal
Total Deformation 6
Type: Total Deformation
Frequency: 65.204 Hz
Unit: m
3/6/2025 11:24 PM
0.40924 Max
0.36376
0.31829
0.27282
0.22735
0.18188
0.13641
0.090941
0.045471
0 Min
ANSYS
2019 R3
0.000
0.500
1.000 (m)
0.250
0.750
Y
Z
X

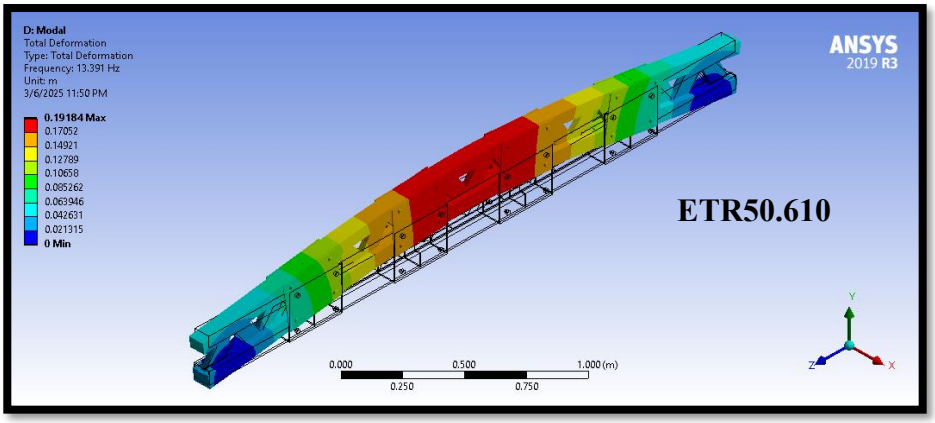
D: Modal
Total Deformation
Type: Total Deformation
Frequency: 13.391 Hz
Unit: m
3/6/2025 11:50 PM
0.19184 Max
0.17052
0.14921
0.12789
0.10658
0.085262
0.063946
0.042631
0.021315
0 Min
ANSYS
2019 R3
ETR50.610
0.000
0.500
1.000 (m)
0.250
0.750
Y
Z
X

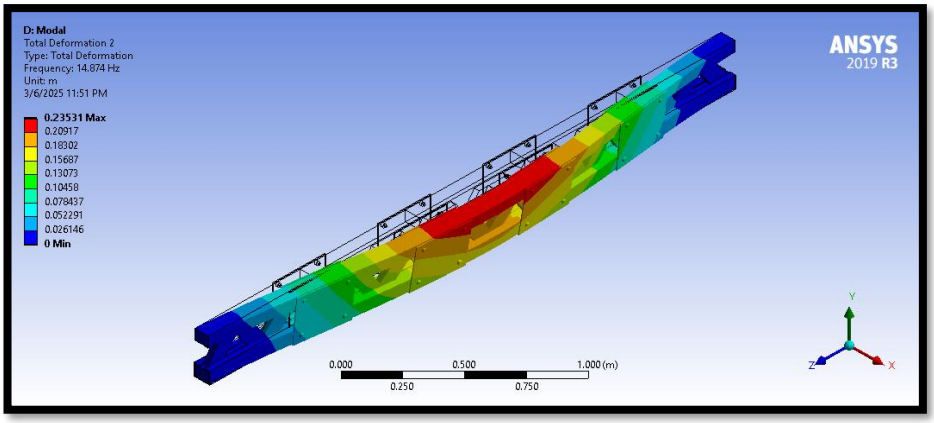
D: Modal
Total Deformation 2
Type: Total Deformation
Frequency: 14.674 Hz
Unit: m
3/6/2025 11:51 PM
0.23531 Max
0.20917
0.18302
0.15687
0.13073
0.10458
0.078437
0.052291
0.026146
0 Min
ANSYS
2019 R3
0.000
0.500
1.000 (m)
0.250
0.750
Y
Z
X

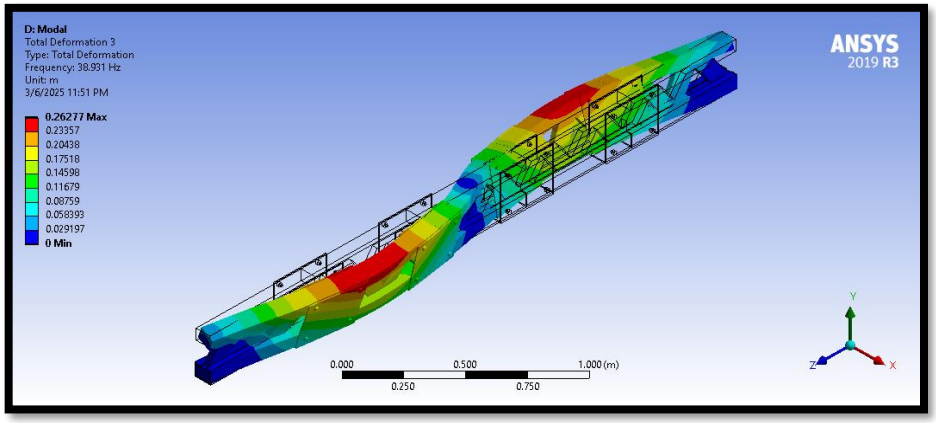
D: Modal
Total Deformation 3
Type: Total Deformation
Frequency: 38.931 Hz
Unit: m
3/6/2025 11:51 PM
0.26277 Max
0.23357
0.20438
0.17518
0.14598
0.11679
0.08759
0.058393
0.029197
0 Min
ANSYS
2019 R3
0.000
0.500
1.000 (m)
0.250
0.750
Y
Z
X

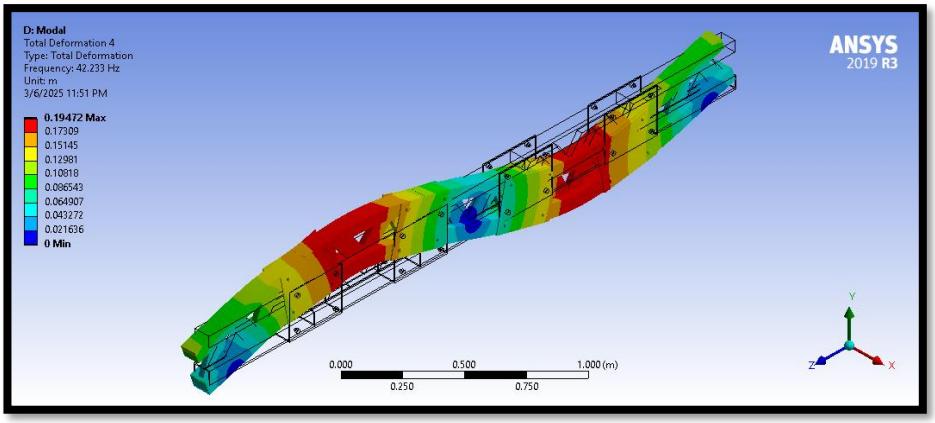
D: Modal
Total Deformation 4
Type: Total Deformation
Frequency: 42.233 Hz
Unit: m
3/6/2025 11:51 PM
0.19472 Max
0.17309
0.15145
0.12981
0.10818
0.086543
0.064907
0.043272
0.021636
0 Min
ANSYS
2019 R3
0.000
0.500
1.000 (m)
0.250
0.750
Y
Z
X

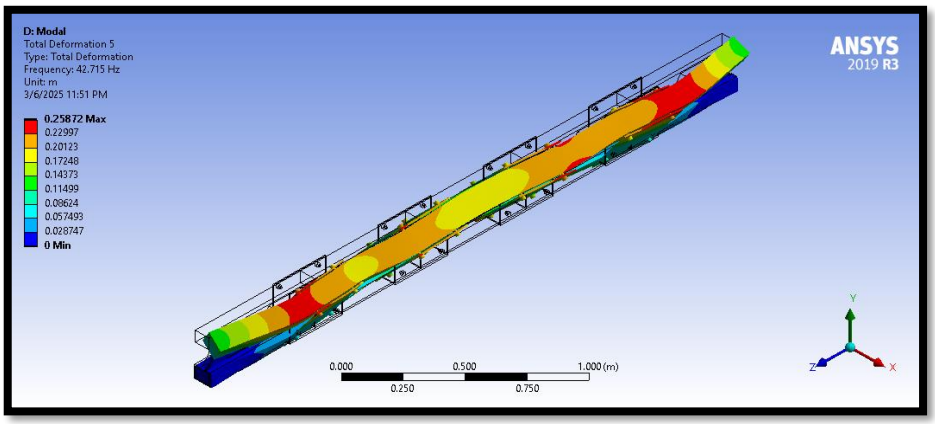
D: Modal
Total Deformation 5
Type: Total Deformation
Frequency: 42.715 Hz
Unit: m
3/6/2025 11:51 PM
0.25872 Max
0.22997
0.20123
0.17248
0.14373
0.11499
0.08624
0.057493
0.028747
0 Min
ANSYS
2019 R3
0.000
0.500
1.000 (m)
0.250
0.750
Y
Z
X

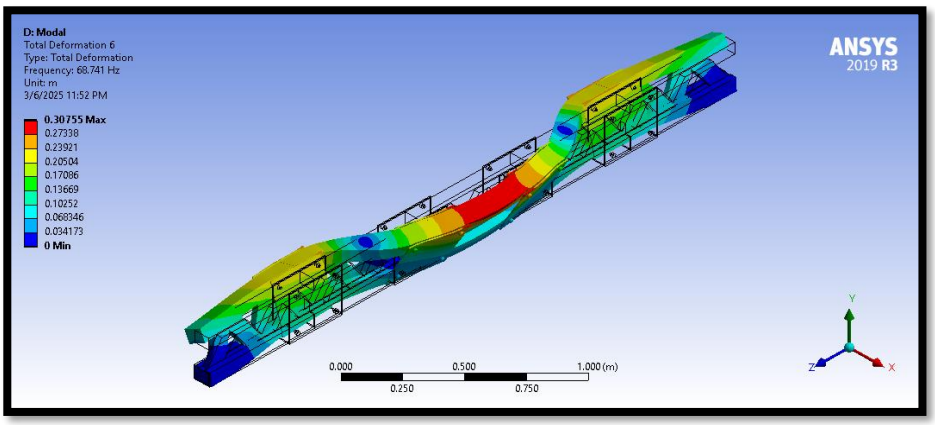
D: Modal
Total Deformation 6
Type: Total Deformation
Frequency: 68.741 Hz
Unit: m
3/6/2025 11:52 PM
0.30755 Max
0.27338
0.23921
0.20504
0.17086
0.13669
0.10252
0.068346
0.034173
0 Min
ANSYS
2019 R3
0.000
0.500
1.000 (m)
0.250
0.750
Y
Z
X

AUTHOR'S PROFILE

Mohd Rizuwan Mamat holds a Diploma in Mechanical Engineering from Universiti Teknologi MARA (UiTM), Pulau Pinang (2003), a Bachelor of Engineering (Hons.) in Mechanical Engineering from UiTM Shah Alam (2006), and a Master of Science in Civil Engineering from UiTM Shah Alam (2018). He currently serves as a Research Officer at the Forest Research Institute Malaysia (FRIM), under the Forest Engineering Unit of the Forestry and Environment Division.

LIST OF PUBLICATION:

Mohd Rizuwan M., Mohd Hisbany M. H., & Noorsuhada M. N. (2026). Evaluating the role of mechanical connections and reinforcements in modular timber beam behaviour. Journal of the Civil Engineering Forum, 12(1), 11–22. https://doi.org/10.22146/jcef.21594

Mohd Rizuwan M., Mohd Hisbany M. H., & Noorsuhada M. N. (2025). Reassessing tension-side reinforcement in modular timber beams: Insights from experimental modal analysis in forest bridge systems. Jurnal Kejuruteraan, 37(3), 1131–1144. https://doi.org/10.17576/jkukm-2025-37(3)-05

Mohd Rizuwan M, Marryanna L, Nurul Faihira K & Abdul Razak AR. 2024. Inovasi Floating Nursery dan Floating Lotus untuk konservasi teratai di Tasik Chini. FRIM Technical Information Handbook No. 60, Institut Penyelidikan Perhutanan Malaysia (FRIM). ISBN 978-967-2810-82-7.

Marryanna L, **Mohd Rizuwan M**, Nurul Faihira K & Mohd Ghazali H. 2024. Penanaman dan penyelenggaraan teratai. FRIM Technical Information Handbook No. 58, Institut Penyelidikan Perhutanan Malaysia (FRIM). ISBN 978-967-2810-75-9.

Mohd Rizuwan M, Tariq Mubarak H & Anizawati A. 2024. Assessing the impact of stilt root systems on coastal protection: a hydrodynamic simulation study. In Hamdan O. (ed.), Status of Mangroves in Malaysia (pp. 207-224). FRIM Special Publication No. 60, Institut Penyelidikan Perhutanan Malaysia (FRIM). ISBN 978-967-2810-77-3.

Tariq Mubarak H, Mohd Rizuwan M, Hyrul Izwan MH, Syaierah A & Nur Ainaa Nabilah MB. 2024. Mangrove Flora and Conservation Efforts in Malaysia. In Hamdan O. (ed.), Status of Mangroves in Malaysia (pp. 77-110). FRIM Special Publication No. 60, Institut Penyelidikan Perhutanan Malaysia (FRIM). ISBN 978-967-2810-77-3.

Mohd Rizuwan M, Wan Mohd Shukri WA & Tarik Mubarak H. 2022. "Drag Comparison For Coastal Species For Shoreline Protection". Advances in Civil Engineering Material. Mokhtar Awang, Lloyd Ling & Seyed Sattar Emamian (Pp. 243-248). ISBN :978-981-16-8667-2.

Mohd Rizuwan M & Wan Mohd Shukri WA. 2020. “Connector Design Selection For Modular Forest Bridge Using Finite Element Analysis”. International Conference on Architecture and Civil Engineering. Mokhtar Awang & Meor Razali Meor M Fared (Pp. 169-174). ISBN :978-981-15-1192-9.

Mohd Rizuwan M. & Yusrina Y,. 2019. "Sistem Pemantauan Elektronik Bersepadu", Bab 9 - Sungai Haji Dorani: Kejayaan Pemulihan Hutan Bakau Negara", Mac 2019, ISBN 978-967-2149-37-8.

Siti Aisah S, Wan Mohd Shukri W A , Chew M Y, **Mohd Rizuwan M**,. 2018. “Halatuju Penyelidikan di Rizab Biosfera Tasik Chini”, Bab 7 Buku Pelestarian Rizab Biosfera Tasik Chini, FRIM Special Publication No. 2. Institut Penyelidikan Perhutanan Malaysia (FRIM).

Mohd Rizuwan M, Wan Mohd Shukri WA & Tariq Mubarak H. 2022. "Velocity Dissipation Approach On Drag Analysis Using Cfd For Shoreline Defense". International Journal For Multidisciplinary Research, 4(5). ISSN :2582-2160. eISSN :2582-2160. DOI:10.36948/ijfmr.

Tariq Mubarak H, Hyrul Izwan Mh, **Mohd Rizuwan M,** Nur Ainaa Nabilah Mb & Syaierah A. 2022. "Mangrove Flora Assessment Of Batu Maung Mangrove Forest, Bayan Lepas, Pulau Pinang". Journal of Agriculture, Forestry and Plantation 12(2). ISSN : 2462-1757.

Md Khir, K., & **Mohd Rizuwan M**. (2020). Modal analysis of aluminium plate for short span forest bridge design. Jurnal Kejuruteraan, Teknologi dan Sains Sosial, 3(1), 1–17.

Mohd-Rizuwan M, Mohd-Hisbany MH & Wan-Mohd-Shukri WA., 2019,"Determining Optimum CFRP Laminate Thickness For A Mobile Forest Bridge Girder", Journal of Tropical Forest Science 31(3): 298–303 (2019).

Mohd Rizuwan M., Mohd Hisbany M. H., Wan Mohd Shukri W. A., Hazrina A., "Static Stress Analysis Of Girder Cross Section For Mobile Forest Bridge" International Journal for Research in Engineering Application & Management (IJREAM), Vol-04, Issue-12, Mar 2019, ISSN : 2454-9150.

Mohd Rizuwan Mamat, Tariq Mubarak Husin & Samsudin Musa, (2018), "Wireless Data Communication of Integrated Electronic Monitoring System (IEMS)", Journal of Advance Management Research ISSN: 23939664 Volume 6, Issue 3, March 2018, pp. 269276.

Mohd Rizuwan, M., Khali Aziz, H., Muhammad Farid, R., Mohd Azahari, F., Azharizan, M.N., “Integration of AutoCAD and Microsoft Excel for Forest Survey Application”, Journal of Forest Science, Vol. 29, No. 4, pp. 307-313, November, 2013. http://dx.doi.org/10.7747/JFS.2013.29.4.307.

S. A. Tan, Razman Salim, Khali Aziz Hamzah & **M Rizuwan M**, “Correlation Of Forest Canopy And Forest Ecological Structures In A Logged Over Forest”, The Malaysian Forester 74 (1): 31-36 (2011).